Crystallisation Of High-Silica Zeolites Under Ultrapure Conditions

by

James R. D. Nee (CChem, MRSC)

A thesis presented for the degree of

Doctor of Philosophy

University of Edinburgh

1993

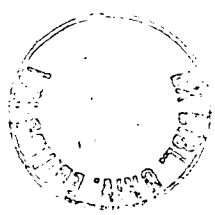

For my darling Kim...

...and for Barrie.

Barrie M. Lowe (the late)

I am very proud to have known and worked for Barrie Lowe. From the very first time we met I knew that he was quite unique. His enthusiasm and kindness were second to none. Despite difficult circumstances, he always made time for his students. That was typical of Barrie. Although I only knew him for two years, he made a dramatic impact on my life and I will be forever grateful.

Barrie Lowe was the most remarkable man I have ever met.

Abstract

The work described in this thesis is concerned with the crystallisation of high-silica zeolites under *ultrapure* conditions, that is, where rigorous attempts were made to ensure the purity of reaction mixtures and the cleanliness of reaction vessels themselves. By carrying out reactions in the absence of a particular species, information can be gained as to their role in zeolite crystallisations.

Two specific systems were examined: organic-free and alkali-free. Organic-free reactions were carried out predominantly in the potassium system. It was found that one particular composition (the *Scavenging Reaction*) was extremely sensitive to traces of seed and organic impurities. The use of this reaction to distinguish between true ZSM-5 structure-directing agents and void fillers is discussed as is its use to establish the cleanliness of a reaction vessel. Several other potential applications are described. Moreover, the work carried out in the organic-free potassium system has allowed further hypotheses to be developed on the role of sodium in the crystallisation of inorganic Na-ZSM-5 and, indeed, allows the authenticity of Na-ZSM-5 itself to be questioned. For completeness, a small number of crystallisations were carried out in the organic-free sodium system.

The crystallisation of high-silica zeolites in the absence of alkali metal impurities, where the quaternary ammonium hydroxide serves as the base and source of charge balancing cations, have been carried out. The effect of adding TMA^+ cations to these reactions is described, where the most notable effect is on the crystallisation rate of TPA-ZSM-5.

The use of diols as *synthesis modifiers* in alkali-free crystallisations is described. Their effect on the crystallisation rate and crystal size distribution is discussed and speculation made as to their role in these reactions.

Finally, work has been carried out to investigate the role of alkali metal and TMA^+ cation impurities in the synthesis of TPA-ZSM-5. The possibility that an increase in the alkali metal content of the reaction mixture may affect the crystallisation mechanism is discussed. Measurement of the alkali metal content of the solution phase during crystallisation shows that this can be used to monitor the

progress of the reaction in a similar way to pH measurements. It is possible, however, that such measurements may also give important mechanistic information.

Declaration

This thesis is of my own composition and is an accurate account of the work carried out by myself at the University of Edinburgh and ICI Chemicals and Polymers Ltd., Wilton, between March 1990 and February 1993.

James R. D. Nee

Acknowledgements

I wish to record my thanks for the help and guidance I received from my academic supervisor, (the late) Barrie Lowe. His enthusiasm and inspiration were the impetus for this work.

I wish to thank Barries' wife, Jenny, and their sons Christopher and Timothy for their kindness and patience during difficult times.

I would like to thank my industrial supervisor Dr. John L. Casci (ICI C&P Ltd., Wilton) for all his help and support. I thank him for the many valuable discussions and also for providing analytical facilities, as well as hands-on experience in a number of analytical techniques. That John was one of Barries' PhD students is not difficult to tell, as he has many of the qualities that endeared Barrie. I consider myself extremely fortunate to have been supervised by them both.

My thanks also go to Dr. C.S. Cundy for the help he has given me and the interest he has shown in my work. I also acknowledge with gratitude the support of Dr. G.S. McDougall and Dr. H.F. Leach.

I wish to thank personnel in the department's analytical group for providing CHN and AES analyses and personnel in the electronic and mechanical workshops for numerous jobs. I would particularly like to thank Stuart Mains, John Ashfield, Dr. D. McClean and Donald Palin for building the rig used for the stirred, low temperature crystallisations. My thanks also go to Graeme Cruickshank for preparing and organising XRF analysis of samples and to the Geology department for carrying out the analysis at relatively short notice.

I wish to thank members of the zeolite research group, catalysis and analytical groups at ICI C&P Ltd., Wilton for their help in providing valuable training and analysis of numerous samples. I especially wish to thank Ms. Irene Brown for chemical analyses and Mr. R. Pendlebury for XRPD analyses.

The support of my friends here in Edinburgh cannot be understated. I sincerely thank Keith, Alister, Graeme, Anne, Ian, Craig and Philip for their invaluable help with computing problems, figures, proof reading, etc. Keith deserves special mention for working through to the early hours of the morning on several occasions,

looking for word processing errors. I also wish to thank Dr. Gordon Walters for his help during the first year of my research.

I sincerely thank John Findlay (SEM unit) for his help with the SEM and for developing and processing many of the SEM photomicrographs shown in this work.

I am very grateful to the SERC and to ICI C&P Ltd. for providing a CASE studentship. I wish to thank ICI C&P Ltd. for providing analytical services and meeting expenses for visits to Wilton.

I especially wish to thank Mr. John W. Murray and Mrs. Doreen Murray (my in-laws) for generally making life much easier for Kim and I. Their kindness and generousity are immeasurable. I thank them for providing Penny (the dog) with a second home and thank them in anticipation of looking after her over the next few months.

I am grateful to my parents for their support and guidance during my school-days.

Amongst the many friends I wish to thank are Ian and Margaret Clarke, Paul and Janette McFarlane, and Steve Dewson. They have all had an impact on my life in one form or another.

Finally, I would like to thank my wife Kim for her support throughout my career. Without Kim I would not have been able to study for a PhD degree. She is quite simply, the best thing that ever happened to me.

Courses Attended:

Computers in Chemistry :Dr. K. Lawley
Dr. G.S. McDougall
Dr. R. Gould
Dr. P. Taylor
Prof. G.S. Pawley

Advances in Physical Chemistry :Dr. A. Jones
Dr. J. Tietze-Girault
Dr. S. Meach
Dr. B.M. Lowe

Catalysis : Dr. G.S. McDougall

Zeolites : Dr. B.M. Lowe

X-ray Diffraction :Dr. R. Gould
Dr. A. Blake

Surface Analysis :Dr. P. Langridge-Smith
Dr. G.S. McDougall
Dr. P. John

Aspects and Applications of NMR :Dr. I. Sadler
Dr. D. Reed

Conferences Attended:

13^{th} Annual Meeting of The British Zeolite Association, Chiselhurst, 1990

14^{th} Annual Meeting of The British Zeolite Association, Durham, 1991

15^{th} Annual Meeting of The British Zeolite Association, Southport, 1992

9^{th} Meeting of The International Zeolite Association, Montreal, Canada, 1992

Table of Contents

1. Introduction 1

1.1 General Introduction 1

1.2 Definition and Nomenclature 3

1.2.1 Structure and Classification 8

1.3 Properties and Applications 13

1.3.1 Introduction 13

1.3.2 Ion Exchange 14

1.3.3 Molecular Sieving and Sorption 15

1.3.4 Catalysis 17

1.4 Synthesis 19

1.4.1 Introduction 19

1.4.2 Development of High-Silica Zeolite Synthesis 20

1.4.3 Crystallisation Kinetics 24

1.4.4 Crystallisation Mechanism 32

1.4.5 Species in Solution 34

1.4.6 Alkali-Free Synthesis of High-Silica Zeolites 37

1.4.7 Organic-Free Synthesis of High-Silica Zeolites 38

1.4.8 The Role of Inorganic Cations in Zeolite Crystallisations - the "Templating Theory" 39

1.4.9 The Role of Organic Reagents - Template or Void Filler ? . . 40

1.4.10 Competitive and synergistic effects between inorganic and organic cations 44

1.5 This Work 45

1.5.1 Introduction 45

1.5.2 Impurities 46

1.5.3 Influence of seeding 48

1.5.4 Structure of this thesis 50

2. Experimental and Analytical Methods **52**

2.1 Experimental 52

2.1.1 Materials 52

2.1.2 Gel Preparation 55

2.1.3 Stirred Reaction Vessels 57

2.1.4 Static Reaction Vessels 67

2.1.5 Tests for Leakage 67

2.1.6 Reaction Number 69

2.1.7 Cleaning of Reaction Vessels 69

2.1.8 Separation of the Solid and Liquid Phase 71

2.2 Analytical Methods 71

2.2.1 Introduction 71

2.2.2 X-ray Powder Diffraction 72

2.2.3 Thermal Analysis 75

2.2.4 Analysis and Instrumentation 77

2.2.5 Electron Microscopy 77

2.2.6 Atomic Emission Spectroscopy (AES) 79

2.2.7 pH 81

2.2.8 CHN Analysis 82

2.2.9 Optical Microscopy (OM) 82

2.2.10 ^{13}C MASNMR 82

2.2.11 Catalysis 83

2.2.12 Sorption 83

2.2.13 X-ray Fluorescence Spectroscopy 84

3. Organic-Free Syntheses: The Potassium System **85**

3.1 Introduction 85

3.2 Experimental 87

3.2.1 Effect of Gel Aging 87

3.2.2 Effect of Sodium Cations 88

3.3 Results and Discussion 88

3.3.1 Effect of Gel Aging 101

3.3.2 Effect of Sodium Cations 103

3.4 Conclusions 104

4. The *Scavenging Reaction* **106**

4.1 Introduction 106

4.2 Experimental 107

4.2.1 Phase Separation 107

4.2.2 Procedure for Stirred Reactions 108

4.2.3 Procedure for Static Reactions;*Detection Limits* 108

4.3 Results and Discussion 110

4.3.1 Phase Separation 110

4.3.2 Discovery of the *Scavenging Reaction* 115

4.3.3 Sphere Formation 125

4.3.4 Use of the Scavenging Reaction to Detect Impurities 129

4.3.5 Effect of Gel Aging on Sensitivity to Impurities 138

4.3.6 Influence of Sodium Cations 139

4.3.7 NU-10 *Scavenging Reaction* ? 143

4.4 Conclusions 146

5. Alkali-Free Syntheses: Single Quaternary, etc. Systems 148

5.1 Introduction 148

5.1.1 Single Quaternary Systems 148

5.1.2 Mixed Quaternary and Quaternary/Amine Systems 150

5.2 Experimental 151

5.2.1 Materials 151

5.2.2 Gel Preparation 151

5.2.3 Analysis of Products 152

5.2.4 Sorption Studies 152

5.2.5 Catalytic Examination 153

5.3 Results and Discussion 154

5.3.1 Single Quaternary Reactions 154

5.3.2 Surface Area of C76 186

5.3.3 Catalytic Evaluation of C76 188

5.3.4 Other Single Quaternary Reactions 188

5.3.5 Mixed Quaternary Reactions 196

5.4 Conclusions 215

6. Alkali Metal-Free Syntheses: Quaternary/Diol System 216

6.1 Introduction 216

6.2 Experimental 217

6.3 Results and Discussion 217

6.3.1 TMA/Diol System 217

6.3.2 Other Quaternary/Diol Systems 239

6.3.3 Low Temperature Beta Syntheses 245

6.3.4 Role of Diols in Alkali-Free Systems 248

6.3.5 Effect of Alkali Metal Cations on Diol/Quaternary Reactions 250

6.4 Conclusions 253

7. Effect of Alkali Metal Cations on the Crystallisation of ZSM-5 255

7.1 Introduction 255

7.2 Experimental 256

7.2.1 Analysis of Products 256

7.3 Results and Discussion 256

7.4 Conclusions 278

8. Overall Conclusions and Further Work 279

8.1 General Comments 279

8.2 Organic-Free Syntheses 280

8.3 Alkali-free syntheses 283

APPENDIX: Organic-Free Syntheses; Sodium System 287

References 291

Chapter 1

Introduction

1.1 General Introduction

Zeolites are an important class of crystalline aluminosilicate materials, whose unique properties have made them valuable in a number of industrial applications, including catalysis, ion exchange and sorption processes. They derive their name from the Greek: *Zeein* - to boil and *Lithos* - stone. This was based on an observation made by the Swedish mineralogist Cronstedt [1] in 1756, where the mineral now known as stilbite appeared to boil on heating. This ready removal of water demonstrates one of the fundamental properties of zeolites, reversible dehydration.

Zeolites are ubiquitous in nature and are found in a number of environments where there is a ready supply of silicon, aluminium and mineralising agents, such as alkali and alkaline earth metal salts. The pH of the crystallising mixture is typically above pH 9 and is often pH 11-13.

Natural zeolites fall into two main classes:
i) igneous zeolites - these usually consist of large well defined crystals, sometimes several centimetres in length, which are formed by the action of alkaline solutions in cavities and vugs in basalt. Deposits are quite well scattered which makes industrial exploitation uneconomic.
ii) sedimentary zeolites - these comprise of aggregates of very small crystals with often ill-defined morphology. Deposits are large and localised which make their recovery for industrial application commercially viable.

Sedimentary zeolites are mainly found in two environments:
i) saline, alkaline, non-marine systems, eg. erionite and chabazite, and
ii) freshwater marine systems, eg. philipsite and clinoptilolite.
It wasn't until the discovery of large deposits of sedimentary zeolites [2] that they were recognised as being common minerals. Substantial deposits of philipsite and clinoptilolite were discovered in the bed of the Pacific Ocean by the Challenger Expedition in 1873-76 [2].

The first crystallisation of a zeolite (levynite) was reported by St Claire Deville in 1862 [3]. Other early claims are reported and have been discussed by Breck [4]. These early syntheses predated the discovery of sedimentary zeolites and consequently synthesis conditions were based on contemporary ideas on how the igneous zeolites were thought to have formed, *i.e.* high temperatures, in excess of 623 K and correspondingly high pressures. Furthermore, the composition of the reaction mixture was often very close to the stoichiometry of the mineral being synthesised.

Most of the early identification and characterisation methods were based on appearance and the effect that these materials had on light. Thus it was not until the advent of X-ray diffraction that zeolites could be reliably identified. Early claims to have synthesised new materials cannot therefore be substantiated, although the synthesis of levynite by Deville [3] is recognised. A review of syntheses carried out before 1937 is given by Morey and Ingerson [5].

It wasn't until the late 1930's that Richard M. Barrer carried out the first systematic studies into zeolite crystallisations. Barrer was the first to synthesise novel zeolites (P and Q) [6], which have no natural counterpart. Even then, however, he used very high temperatures and pressure, which resulted in the formation of relatively dense phases of little commercial value. Barrer is considered the pioneer of zeolite science; it was his early work that stimulated much interest in zeolites, both of industrialists and academics. Much of Barrer's early work is documented in two series of articles published in the Journal of the Chemical Society, entitled *Hydrothermal Chemistry of Silicates*, Parts 1-22 and *Chemistry of Soil Minerals*, Parts 1-14.

A major breakthrough in zeolite synthesis was reported in 1956 when Milton and coworkers [7] at Union Carbide announced that novel zeolite structures could be synthesised under relatively mild conditions, which resembled those under which sedimentary zeolites are formed, using reactive starting materials. The discovery of the novel zeolites, A [8], X [9], and Y [10], led to their introduction by Union Carbide as industrial sorbents in 1954. However, it was the application of zeolites X and Y in 1959 [11] as hydrocarbon conversion catalysts, that led to zeolites being recognised as commercially important materials. This *gel synthesis method* has yielded a large number of synthetic zeolites (both novel and some found in nature) as well as analogous crystalline framework structures which contain elements other than silicon and aluminium. The most notable of these are the aluminophosphates [12]. Others include the silicoaluminophosphates (SAPO), metalloaluminophosphates (MeAPO), metallosilicoaluminophosphates (MeAPSO) and the non-metallosilicoaluminophosphates (E1APSO). Structures containing framework atoms other than silicon, aluminium and oxygen and which show zeolitic properties are best referred to as *zeotypes* [13].

There are currently 54 natural zeolites known and well over 150 synthetic ones, many of which have no natural counterpart. A large number of these synthetic zeolites are not as yet fully characterised.

1.2 Definition and Nomenclature

Zeolites consist of 3-dimensional networks of $[AlO_4]^{5-}$ and $[SiO_4]^{4-}$ tetrahedra (primary building units) which link via corner oxygen atoms to four others, as illustrated in Figure 1–1. This results in very open frameworks which contain well defined channels and cavities. The incorporation of aluminium into the framework results in a net negative charge which is usually balanced by cations of group I or II. These are located in the channels and cavities together with water molecules and, because of their high degree of mobility, are easily ion exchanged. One of the fundamental properties of zeolites, as mentioned earlier, is the easy reversible

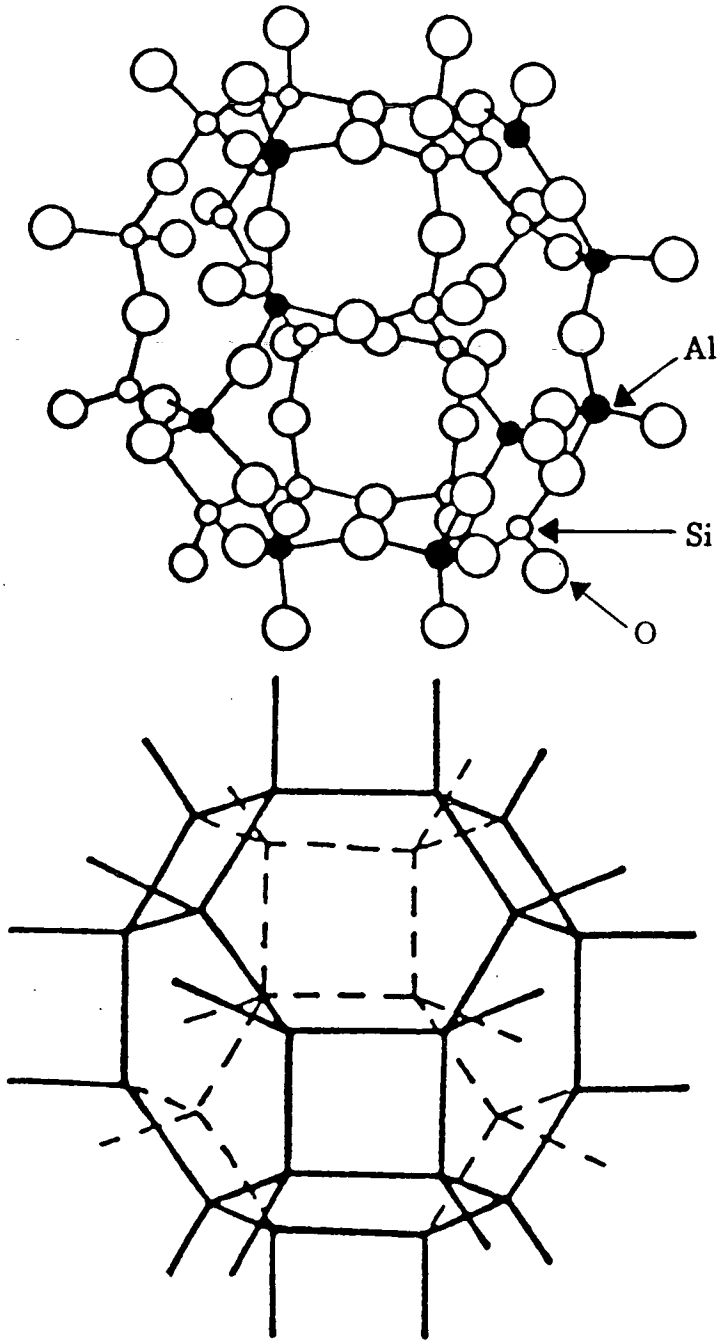

Figure 1–1: The sodalite unit showing the tetrahedral arrangement of Si and Al atoms (top) together with the framework diagram representation (bottom); the Si and Al atoms are located at the vertices and the oxygen atoms lie along the lines joining these

removal of water and other small molecules, which gives rise to their ability to act as sorbents. The framework silicon and aluminium atoms are commonly known as T-atoms (T = tetrahedral) and the rings of oxygen atoms that prescribe a pore opening are known as oxygen windows (Figure 1–2).

Zeolites and zeotypes are members of a family of materials known as *molecular sieves*, a term first coined by McBain [14] in 1932 to describe materials that could separate molecules on the basis of size and shape. The zeotypic molecular sieves such as the metalloaluminophosphates, aluminophosphates and non-aluminometallosilicates often exhibit properties similar to those of zeolites and it is not uncommon to find these properties being described as zeolitic [15]. This has led to much controversy and therefore the need for a specific definition of the term zeolite. Well before the discovery of zeotypes, Smith [16] defined a zeolite as;
"an aluminosilicate with a framework structure enclosing cavities occupied by large ions and water molecules, both of which have considerable freedom of movement, permitting ion exchange and reversible dehydration".
This definition is based on framework composition and, to some extent, the properties and structure of the material. Thus, in accordance with this definition, the all-silica analogues, non-aluminometallosilicates, aluminophosphates, *etc.*, are not classed as zeolites. On the other hand, Liebau [15] defines zeolites as:
"tectosilicates that contain tunnels or larger polyhedral cavities interconnected by windows large enough to allow ready diffusion of the polyatomic guest species through the crystal".
This definition is based only on the structure and properties of the framework silicate and does not take into account the framework composition. Thus, this definition could allow the pure silica polymorphs to be, incorrectly, described as zeolites. The definition put forward by Smith is perhaps the one that defines zeolites most adequately. A review of this subject is given by Smith [17]. A classification [18] based purely on chemical composition is shown in Figure 1–3.

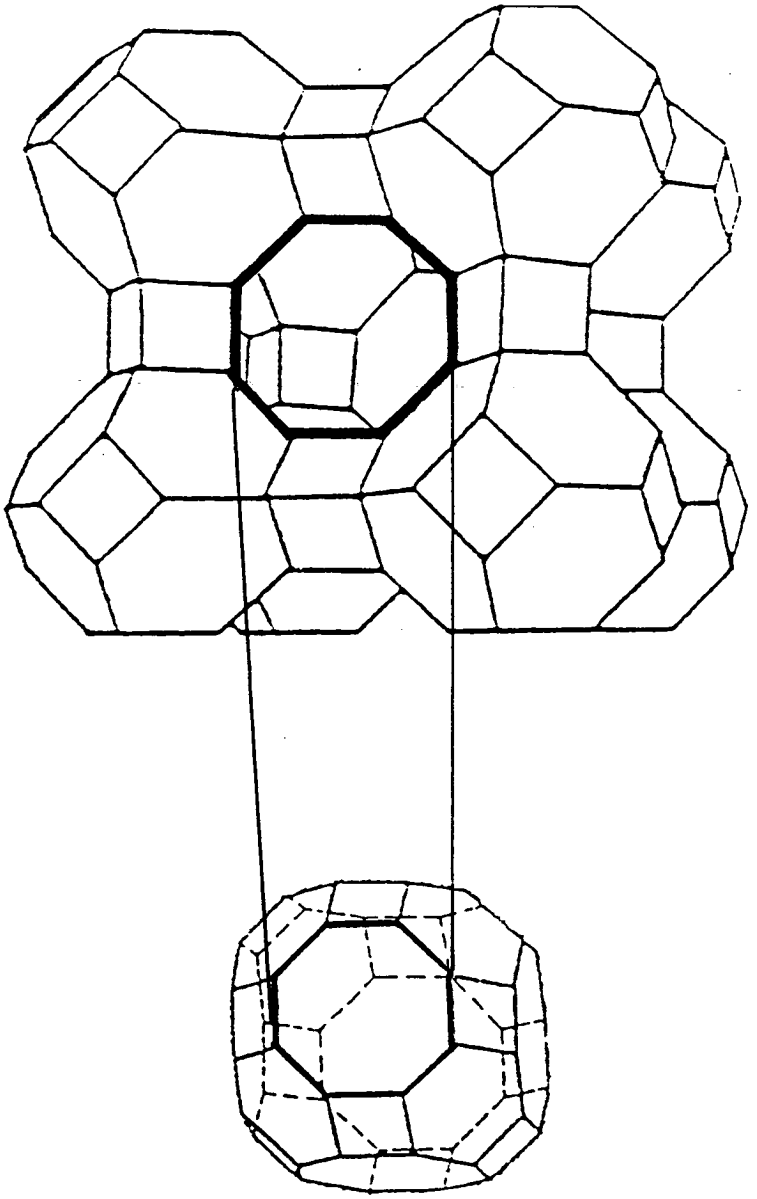

Figure 1–2: An 8-oxygen (or 8 T-atom) window prescribes the entrance to the large polyhedral cavity found in the synthetic zeolite A

Figure 1–3: Classification of molecular sieves based on chemical composition, taken from Szostak [18]

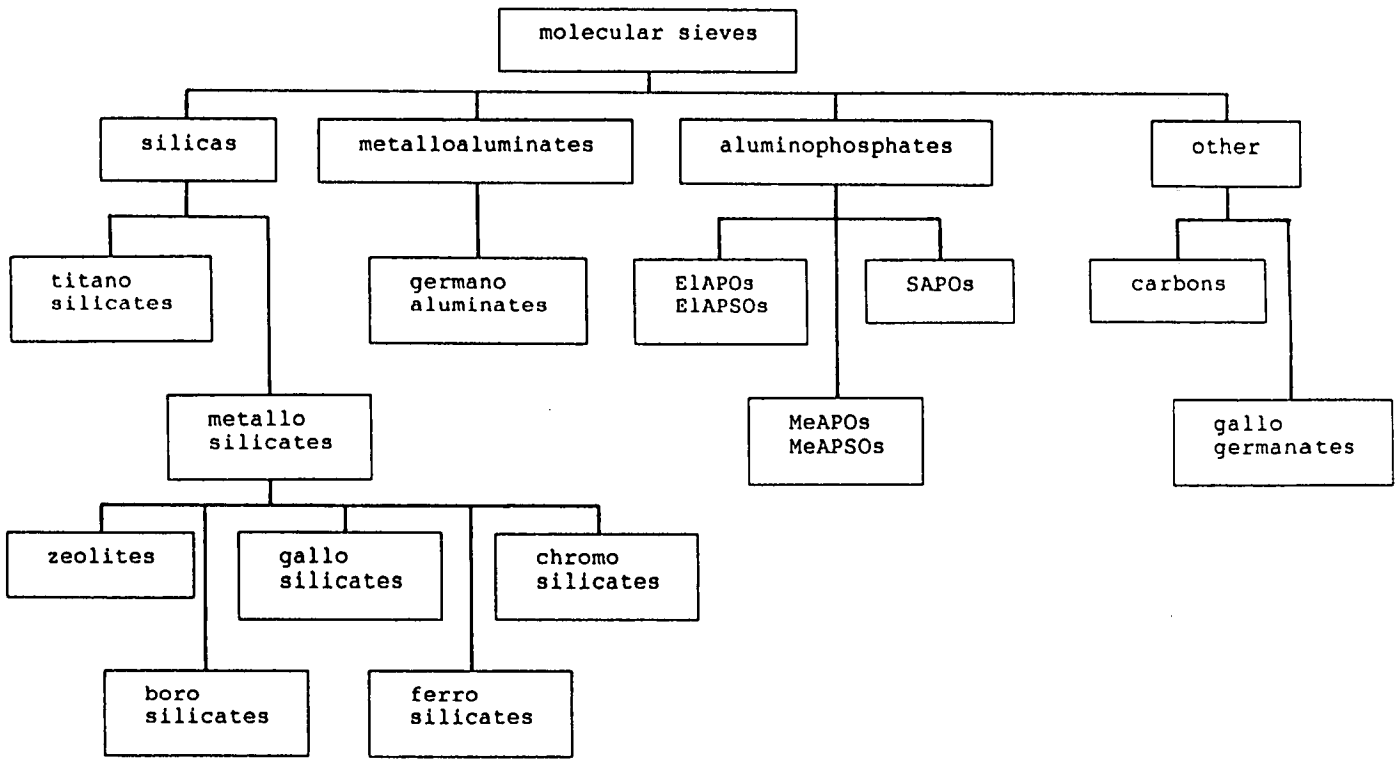

1.2.1 Structure and Classification

There are a number of ways of classifying zeolites other than that outlined above. These are primarily based on structure rather than framework composition. Smith [16] was the first to classify zeolites according to similar structural features. However, the most widely accepted method of describing and classifying framework topologies is the use of *secondary building units*, (SBU's), proposed by Meier [19]. This classification was based on the observation that all zeolite frameworks could be built up from one or more sub-units composed of small groups of linked alumina and silica tetrahedra (primary building units). Meier's classification placed zeolites in one of seven groups (later extended to nine) each named after one representative member, based on SBU's or larger polyhedral building units.

Meier reported eight SBU's which have now been extended to sixteen [20] (Figure 1–4). They show the silicon, aluminium and oxygen atom positions relative to each other but not the charge-compensating cations or water molecules. Each vertex represents a tetrahedrally coordinated silicon or aluminium atom (T-atom) and the lines joining these represent the oxygen atoms. Sometimes it is easier to describe zeolite frameworks in terms of larger polyhedral building units such as the sodalite unit (also known as the truncated octahedron or β cage). Examples of polyhedral building units are shown in Figure 1–5. The sodalite unit can be used to describe the structures of zeolites X, Y (the synthetic analogues of the rare natural zeolite faujasite) and A (Figure 1–6). It can be seen that these frameworks can also be described in terms of single 6-ring, single 4-ring, double 6-ring or double 4-ring SBU's. The use of SBU's is not restricted to zeolites but can be applied to all three dimensional silicate frameworks [21].

Each framework structure has been given a unique three letter code by the IUPAC Commission on Zeolite Nomenclature. For example, the high-silica zeolite ZSM-5 (a Mobil zeolite) has been given the structure classification MFI. The zeolites ZK-20, LZ-132 and NU-3 have similar topologies to the natural zeolite Levynite. Consequently, the structure classification is LEV.

Although species similar to these SBU's have been identified in silicate and

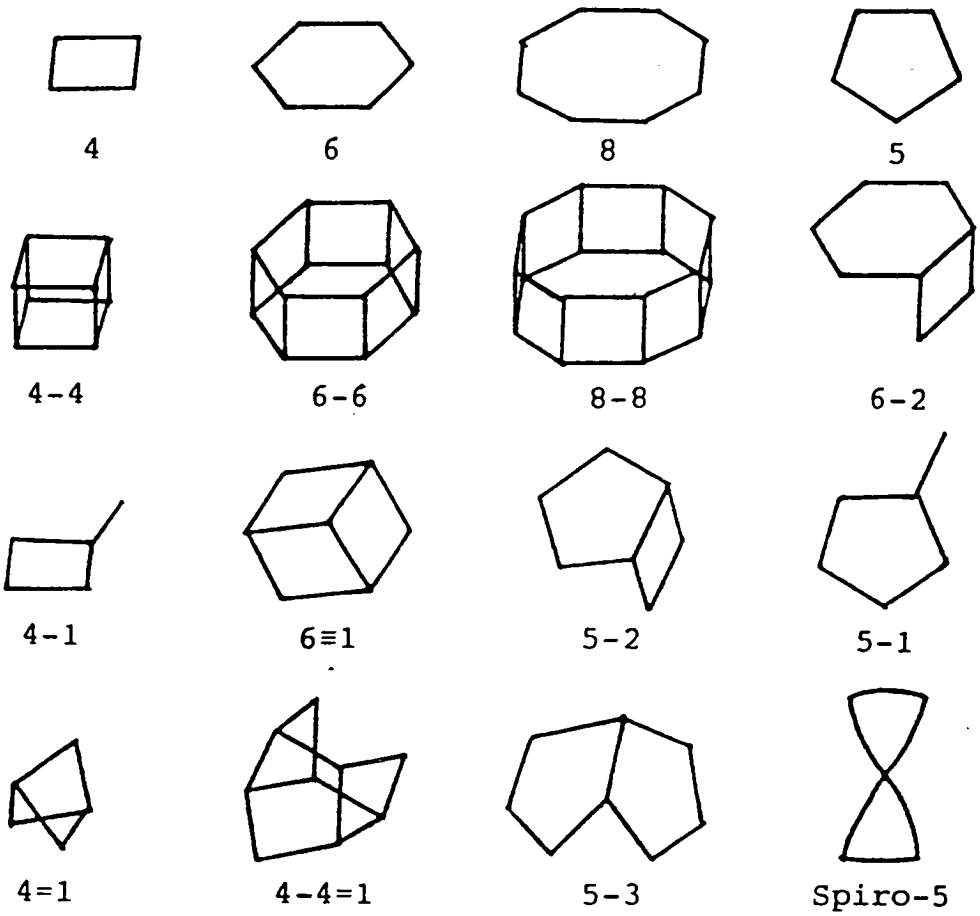

Figure 1–4: Secondary building units

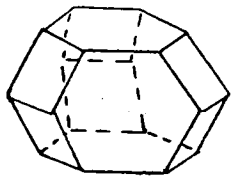

Cancrinite

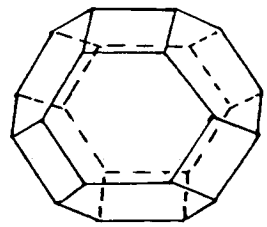

Sodalite

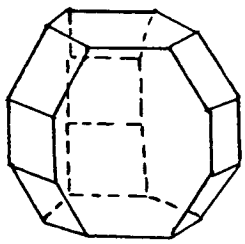

Gmelinite

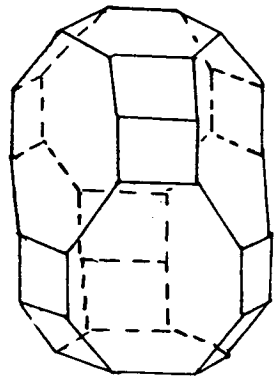

Chabazite

Figure 1–5: Polyhedral building units

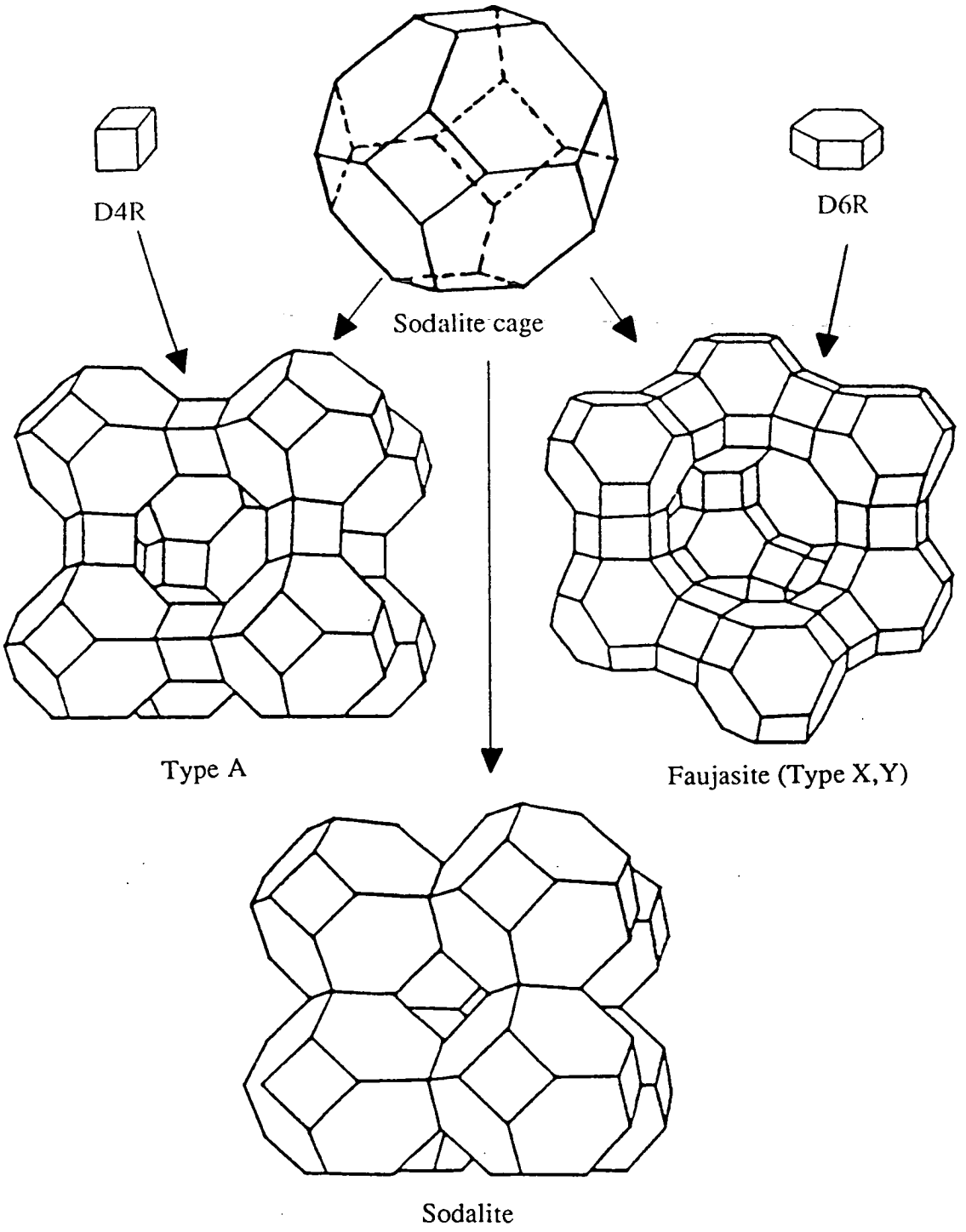

Figure 1–6: Zeolite structures based on the polyhedral sodalite (truncated octahedron) unit

aluminosilicate solutions there is no evidence for their direct participation in either nucleation or growth.

Other ways of describing zeolite framework topologies on the basis of building units are outlined in a number of notable texts [4,18,22]. Recently, van Koningsveld proposed the use of tertiary building units (TBU) to fully describe the framework topologies of more diverse structures [23].

As well as classifications based on structural sub-units that describe the framework, zeolites can be classified on the basis of their properties; this, of course, is inherently linked to their structure and composition. For example, all zeolites contain intracrystalline water which, because it can penetrate into the channels and cavities of the zeolite, can be used to give a measure of the total intracrystalline pore volume. Thus, zeolites can be classed according to pore volume. Similarly, the size of the pore opening can be used, where they are classed as small, medium or large pore. Zeolites (and other microporous materials) can also be classified according to framework density. This is essentially a measure of the openness of a structure and is measured in terms of the number of T-atoms per 1000 $\AA^3$. Such a classification, however, gives no indication as to the accessibility of the pore or channel system unlike those based on sorption properties [24,25,26,27].

Zeolites can be classed simply in terms of the framework Si/Al ratio either as low, medium or high-silica zeolites [11]. In this classification, Flanigen defines high-silica zeolites as having a Si/Al ratio greater than 150. It is further suggested that high-silica zeolites "should be susceptible to synthesis over a wide compositional range" [28].

The composition of a zeolite can be represented by the empirical formula

$$M_{2/n}O.Al_2O_3.xSiO_2.yH_2O,$$

where M = exchangeable cation and n = cation valency. Since Al-O-Al linkages are excluded [29], x must be greater than or equal to two. This is known as Lowenstein's rule and explains why, for example, the maximum substitution of silicon by aluminium in these structures is 50 %.

The size and accessibility of the channels and cavities are crucial to the application of zeolites. The channel system can be either 1-, 2-, or 3-dimensional; this is an important criterion in selecting a zeolite for a particular use, especially in catalysis. Window size, and hence the molecular sieving properties, can be altered by simply changing the number or nature of the charge balancing cation. For example, by increasing the Si/Al ratio of the zeolite, fewer charge balancing cations are required and therefore the number restricting access into the pores will be reduced. Alternatively, the pore openings can be effectively enlarged by replacing monovalent cations with smaller, divalent ones since only half the number are required to balance the framework. Not only does this lead to a change in the degree of hydration of the zeolite, but their is a small change in the unit cell parameters.

The number of molecular sieve frameworks that have been successfully synthesised is extremely small when one considers that computer simulations predict that several million frameworks are theoretically possible. Barrer [30] reflected that;
"The art of synthesising molecular sieves has developed more quickly than the chemical science which would properly account for their formation....."
Clearly then, the large discoveries that are undoubtedly yet to be made will only be achieved once the mechanism by which molecular sieves crystallise is fully elucidated. Only then will the synthesis of molecular sieves designed for specific applications be realised.

1.3 Properties and Applications

1.3.1 Introduction

The free movement of occluded charge balancing cations accounts for the ability of zeolites to undergo ion exchange and the well characterised channels and cavities allow for ready shape selective sorption of small molecules. The presence of both Bronsted and Lewis acid sites in the framework give rise to their catalytic activity.

The combination of these acid sites and the well characterised pore system accounts for their ability to behave as shape selective catalysts. The three processes; ion exchange, sorption and catalysis account for the majority of industrial applications. Although there are many zeolites, both natural and synthetic, relatively few are actually used commercially [31]. Since ion exchange, sorption and catalysis do not form the major part of this thesis, they will only be described briefly.

1.3.2 Ion Exchange

Ion exchange applications are essentially restricted to aluminous zeolites, where there is a large number of exchangeable charge balancing cations. High-silica zeolites clearly have a limited, or negligible, ion-exchange ability and ion exchange is usually limited to H^+ exchange with alkali of alkaline earth metal cations in the as-synthesised material.

Ion exchange is often carried out in order to modify the molecular sieving or catalytic properties of a zeolite. Thus, charge balancing cations located near the channel or cavity openings, which can severely affect the molecular sieving properties by restricting the effective window size, can be replaced by smaller cations, thus effectively opening the access to the pore system.

For catalytic applications, the zeolite must be in the acid form (H^+-form). Since zeolites are often synthesised in the presence of alkali or alkaline earth metal cations, the as-synthesised zeolite must be ion exchanged in one of two ways:
i) direct contact with a dilute acid, usually hydrochloric ($\sim$ 1 M), or
ii) ion exchange with ammonium cations then calcine to remove ammonia:

$$Na^+ - Z^- + NH_4^+ \rightleftharpoons NH_4^+ - Z^- + Na^+$$

$$NH_4^+ - Z^- \xrightarrow{\Delta} H^+ - Z^- + NH_3 \uparrow$$

The latter process is preferred for aluminous zeolites since the acid can leach aluminium from the framework leaving hydroxyl nests (Figure 1–7). This route has the added advantage for zeolites which contain occluded organic material,

as the organic species will be removed along with the ammonia in one single calcination step. The removal of aluminium can also occur on excessive washing of the product.

Complete exchange is rarely achieved despite using large excesses of exchanging cation, since there will be a number of cations in non-exchangeable parts of the zeolite framework. Furthermore zeolites can show a preference for cations depending on the cation size and the anion framework charge. This leads to a phenomenon known as ion sieving, which is common in zeolite ion exchange [32].

As ion exchangers, aluminous zeolites are use extensively in the detergent industry. Of particular importance is the aluminous synthetic zeolite A which is used in washing powders as a replacement for environmentally damaging polyphosphates. Their role is simply to reduce water hardness by removing calcium and magnesium cations from the wash water [33,34]. Another important application is in the treatment of nuclear effluents where, most often, the natural zeolite clinoptilolite is used to remove ^{137}Cs and ^{90}Sr from pond water [35,36,37]. Clinoptilolite is also used to remove ammonia and ammonium ions from aqueous effluents [35, 36].

1.3.3 Molecular Sieving and Sorption

McBain [14], as has already been mentioned, first coined the phrase *molecular sieve.* The high degree of selectivity afforded by zeolites in molecular separation processes was later demonstrated by Barrer [38,39].

In order to function as a molecular sieve, water and other occluded molecules must firstly be removed in order to clear the pores and channels. The size and shape of the windows giving access to the channel system is usually modified for a particular separation process by ion exchange, as mentioned in the previous section.

A number of factors can affect the molecular sieving properties, including temperature and framework composition. Zeolite frameworks are not rigid and it

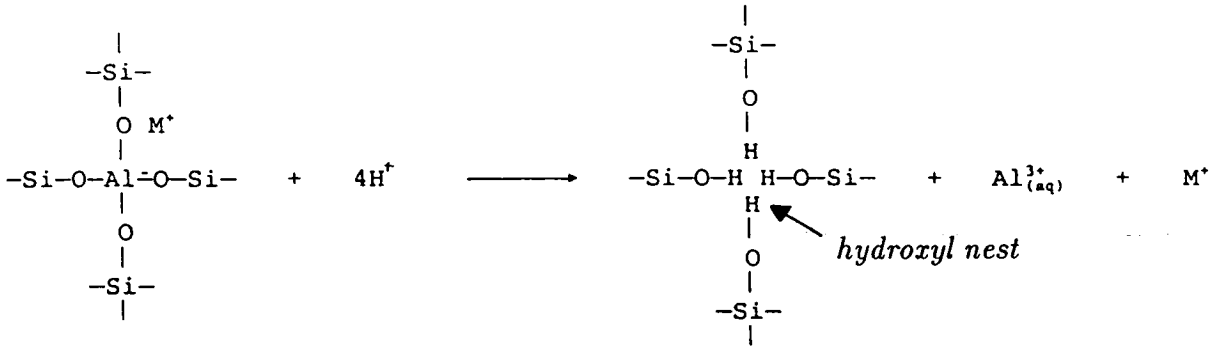

Figure 1–7: Formation of *hydroxyl nests*

has been shown that a variation in the amplitude of the lattice vibration of 10 - 20 pm is observed when the temperature is increased from 80 K to 300 K [40,41]. The temperature dependence of molecular sieving has been demonstrated in the separation of oxygen, argon and nitrogen using zeolite A [41].

The hydrophilic aluminous zeolites prefer polar molecules, whilst the hydrophobic siliceous zeolites and all-silica molecular sieves prefer non-polar, organic molecules. The aluminous zeolites strongly sorb water molecules to such an extent that the potassium form of zeolite A is often used as a dehydrating agent for organic solvents.

Industrially, there are a number of separation processes involving zeolites. These include the separation of linear hydrocarbons from branched ones using the calcium form of zeolite A [42], and the separation of para-xylene from the ortho and meta isomers for use in the synthesis of terephthalic acid, the starting material in the manufacture of polyester, using either the potassium or barium forms of zeolite Y [43,44]. All-silica molecular sieves can be used to remove traces of organics from aqueous effluents [45].

1.3.4 Catalysis

The most important application of zeolites in industry is undoubtedly in catalysis, where savings to oil companies are estimated to have run into billions of dollars. The use of zeolites in catalytic processes began in the late 1950's, when the synthetic zeolite Y was used as an isomerisation catalyst. More important however, was the introduction in 1962 of zeolite X as a potent hydrocarbon cracking catalyst [46]. These superseded the then traditional amorphous aluminosilicate catalysts, offering several orders of magnitude more activity at relatively low temperatures [47]. This discovery led the Mobil Oil Corporation to initiate an extensive research program which has essentially been the foundation for the continued research into zeolite synthesis and application.

The properties of zeolites which make them excellent catalysts are:
i) large internal surface area,
ii) well defined pore structure which can be modified to give desired products based on shape selectivity, and
iii) presence of a large number of both Bronsted and Lewis acid sites. The combination of (i) and (ii) leads to an important process known as shape selective catalysis [48]. Three types of selectivity have been identified [49]. These are:
i) reactant selectivity - molecules with dimensions larger than the pore openings will not enter the crystal structure and reach the acid sites for reaction, eg. butanol dehydration [50],
ii) product selectivity - this is based on the rate of diffusion of products from the active sites, eg. in the alkylation of toluene to para-xylene over H-ZSM-5, the para isomer diffuses much more rapidly out of the zeolite than the other isomers thus appearing as the major product, and
iii) restricted transition state selectivity - in this case, the volume available at the active site governs the size of the product intermediate. For example, in the transalkylation of meta-xylene, the least bulky transition state leads to the formation of the 1, 2, 4-trimethyl benzene and toluene.

As was mentioned in the previous section, in order to function as a catalyst,

the zeolite must be in the protonated form (H^+-form). For high-silica zeolites, this is usually achieved by direct contact with acid or an initial exchange step with ammonium cations followed by calcination as described earlier.

Zeolites contain two types of acid sites. The presence of charge balancing protons leads to Bronsted acidity (proton-donor acidity) whereas the presence of electron deficient framework aluminium gives rise to Lewis acidity (electron-acceptor acidity).

The principle requirements of a good catalyst are:
i) high activity,
ii) good selectivity and conversion, and
iii) long lifetime.
The lifetime of a catalyst is significantly reduced on coking. This results from the degradation of organics within the pore system and a subsequent build-up of carbon. Deactivation of the catalyst in this way is most significant in more open frameworks and in materials with low dimensionality (eg. EU-1, ZSM-12). However, with materials such as ZSM-5, the two sets of intersecting channels, which result in a three-dimensional channel system, make it is less susceptible to deactivation by coking.

The synthetic high-silica zeolite ZSM-5 is used in a number of catalytic applications (Table 1–1). The smaller pore openings (*cf.* X and Y) offer increased selectivity, particularly with small molecules such as methanol. Indeed, the conversion of methanol to gasoline [51,52] is a commercially important process and a plant was set up in New Zealand in 1985 specifically for this process [53]. The application of ZSM-5 as a shape-selective catalyst has been reviewed by Derouane [54].

Recent developments have been made in the use of zeolites in the production of fine chemicals and this should provide fruitful ground for further research [55]. The number of research papers and patents on the use of zeolites in catalysis is quite phenomenal and certainly makes up the bulk of the current literature. There are a number of good review articles detailing the catalytic application of zeolites in catalysis [56,57,58,59,60,61].

Table 1–1: Some industrial applications of ZSM-5[a]

Process	Product
Dewaxing	Low pour point lubes
Benzene alkylation	Styrene
Xylene isomerisation	Para-xylene

[a]Reference [31]

1.4 Synthesis

1.4.1 Introduction

The are a number of notable books [4,13,18,22] and review articles, *eg.* [62,63,64, 65] covering the synthesis of zeolites. Since this thesis is concerned only with the synthesis of high-silica zeolites and all-silica molecular sieves, aluminous zeolites and zeotypes will only be discussed where it is felt necessary for completeness. This is particularly appropriate in the next section which summarises the development of molecular sieve synthesis following the discovery of Milton's *gel synthesis method.*

Zeolites are usually crystallised from aqueous gels under hydrothermal conditions. The essential ingredients in any zeolite synthesis are silica, alumina, a mineraliser (usually an inorganic base), water and in the case of siliceous zeolites, an organic reagent. In the case of the all-silica polymorphs, aluminium is obviously not included in the reaction mixture. The gels are heated in the temperature range 373 - 473 K under hydrothermal autogeneous pressure until crystallisation is complete. The solid phase is separated from the mother liquor by filtration or centrifugation, washed with copious amounts of water (usually until the pH of the washings is pH 8 - 9), and finally thoroughly dried before characterisation.

Zeolites are metastable phases and when in contact with the mother liquor transform in time to thermodynamically more dense phases, eg. quartz. Thus, during synthesis, samples must be taken regularly in order to monitor the crystallisation and the reaction terminated well before the appearance of less desirable phases. Once the solid is isolated from the mother liquor, however, it can remain unchanged indefinitely provided it is kept in a suitable environment.

1.4.2 Development of High-Silica Zeolite Synthesis

It was soon recognised that in the synthesis of aluminous zeolites a relationship existed between the inorganic cation used in the synthesis gel and the nature of the zeolite obtained. For example, it was found that sodium ions frequently led to the formation of sodalite, gmelinite, cancrinite and faujasite-type materials whereas chabazite types were favoured by the presence of potassium ions [62,66]. This led to the so-called *templating theory* (discussed in detail in section 1.4.8) which suggested that the inorganic cation was able to promote the crystallisation of certain zeolite structures. It was this that led to the introduction of organic reagents into the synthesis recipe; the idea was that large organic molecules would create larger channels and cavities and generate new zeolite frameworks. Furthermore, there was a need to synthesise more siliceous materials, particularly for catalytic applications, since aluminous zeolites have relatively low thermal stability and poor resistance to acidic environments commonly encountered in catalysis. Thus to improve their performance under these conditions it was recognised that more siliceous zeolites would be required.

The first crystallisations of gels containing an organic component were carried out in the early 1960's [67,68]. A number of methyl-substituted ammonium compounds were examined in aluminous reaction mixtures. Those containing the tetramethylammonium (TMA) species were found to be the most successful. The result was the crystallisation of zeolite N-A (N = nitrogenous) and faujasite-type zeolites, having a slightly increased Si/Al ratio (described in the early days as *siliceous*). It is interesting to note that this was also the first attempt at an

alkali-free synthesis, *i.e.*no alkali metal was deliberately added to the synthesis gel. However, it was discovered that the products contained substantial amounts of sodium which had presumably dissolved from the glass reaction vessel. Furthermore, the silica sol used in these experiments often contained a small amount of sodium hydroxide as a stabiliser. It was subsequently shown that zeolite A would not in fact crystallise unless there was a trace of sodium present to nucleate the crystallisation and that the rate of crystallisation was dependent on the amount of sodium present [69]. This report is an excellent illustration of the effect of impurities in zeolite crystallisations.

Other *siliceous* zeolites crystallised from gels containing TMA cations include ZK-4 [70] (SiO_2/Al_2O_3 = 2 - 4) and Alpha [71] (SiO_2/Al_2O_3 = 4 - 6), both of which are siliceous versions of zeolite A. Many framework structures have since been prepared using TMA, usually in combination with alkali metal cations [63]. These are predominantly very aluminous zeolites ($SiO_2/Al_2O_3 < 10$) although one report claimed a SiO_2/Al_2O_3 ratio for mordenite of around 20 [72].

Following the success of TMA in zeolite crystallisations a number of other organic materials were investigated. One of the earliest, tetraethylammonium (TEA) hydroxide was used to crystallise what is now recognised as the first true high-silica zeolite, Beta [73], with SiO_2/Al_2O_3 ratios of up to 100 being reported.

Over several hundred different organic materials have been used in zeolite syntheses in one form or another but by far the most successful are the quaternary ammonium compounds. Perhaps the most widely known of these is the tetrapropylammonium (TPA) species which is used to synthesise the industrially important high-silica zeolite ZSM-5, first reported by Argauer and Landolt in 1972 [74]. This was followed in 1973 with the synthesis of ZSM-11 in the presence of tetrabutylammonium (TBA) cations and tetrabutylphosphonium (TBP) cations [75].

ZSM-5 and ZSM-11 are structurally very similar (Figure 1–8). ZSM-5 consists of two intersecting channel systems, one sinusoidal of near circular cross-section and the other straight with elliptical cross-section. In ZSM-11, however, both channel systems are straight and of elliptical cross-section.

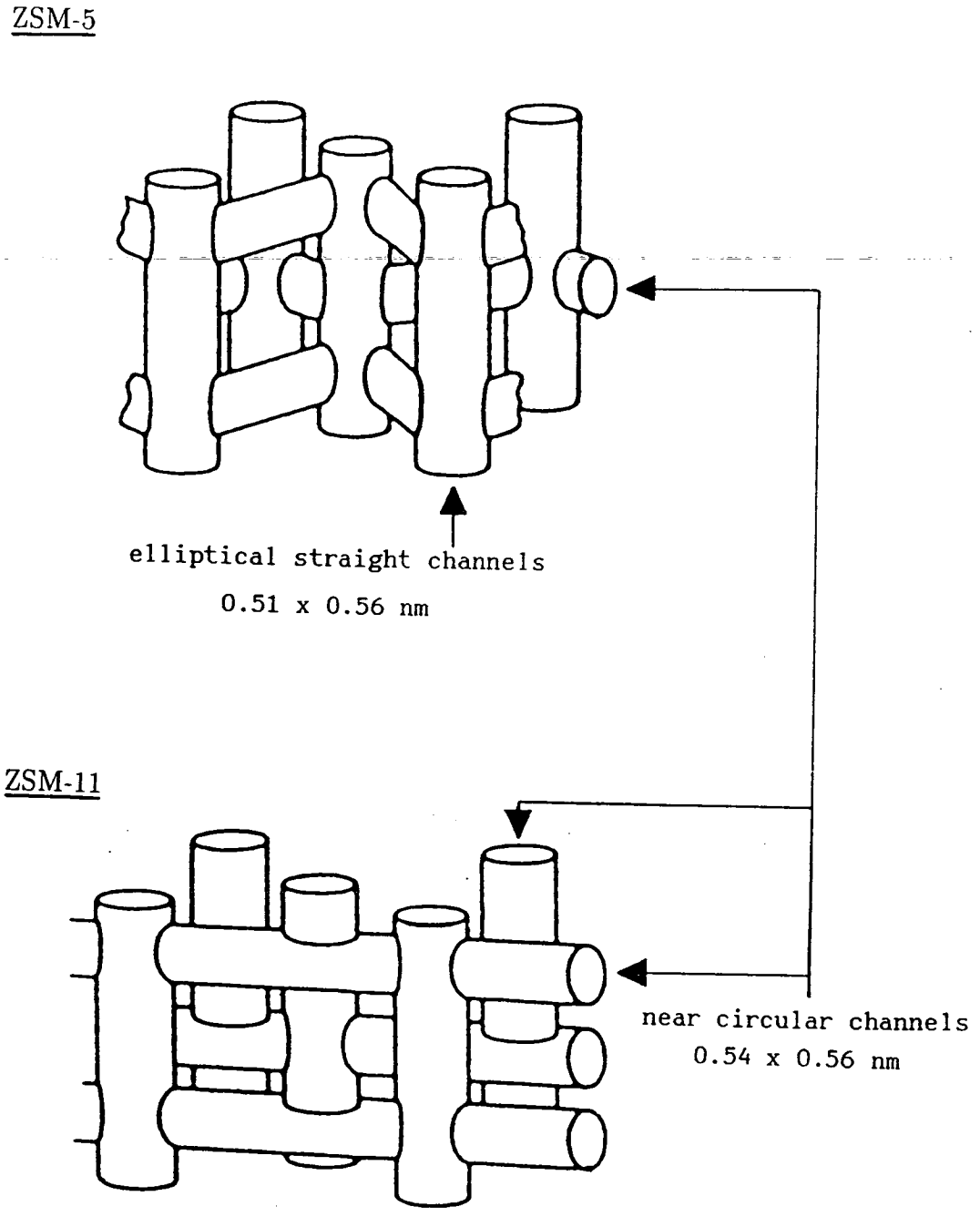

Figure 1–8: Diagrammatic representation of the channel structure of zeolites ZSM-5 (top) and ZSM-11 (bottom)

Since these structures are very similar, it is not unusual to crystallise ZSM-5/11 intergrowths [76]. In fact it is reported [77] that it is difficult to obtain a completely phase pure ZSM-11 product. Jacobs and Martens have claim that once they have used a reaction vessel to crystallise ZSM-5, they are unable to obtain ZSM-11 from subsequent reactions, despite thorough cleaning [77]. As is to be expected from the structural similarity, ZSM-5 and ZSM-11 give very similar powder X-ray diffraction patterns. These materials are in fact end members of the *pentasil* family of molecular sieves [78].

Examples of other zeolites formed in the presence of organic reagents can be found in the review by Lok *et al.* [63]. It is notable that most of these were synthesised in the presence of alkali metal cations. Furthermore, synthesis conditions are rather more demanding than those encountered with aluminous zeolites (eg. 423 - 473 K for several days).

The synthesis of ultra high-silica zeolites and pure silica molecular sieves were reported in the late 1970's [45,79,80,81]. The aluminium-free analogue of ZSM-5, silicalite was patented in 1977 [45]. This caused much controversy as Mobil, who had the patent on ZSM-5, considered Union Carbide's silicalite to be an ultra high-silica ZSM-5 and therefore violated their patent rights [82]. Mobil claim a Si/Al ratio from 10 to 4000 while Union Carbide claim that silicalite contains no framework aluminium. However, Rees [83] points out that silicalite always contains aluminium (which Union Carbide claims is an impurity) and this has been shown to be part of the framework in tetrahedral sites [84]. With this in mind its hardly surprising that there is a tendency for inventors to attempt to '... secure proprietary rights for the composition or on the synthesis of compounds which were, at the time of filing, insufficiently characterised' [85].

This dispute not only demonstrates the commercial importance of zeolite molecular sieves but also highlights once again the importance of impurities (in this case aluminium) in zeolite synthesis. It has been suggested that materials containing only adventitious amounts of aluminium should be considered as defect silicas [83].

Since TPA and TBA are used to synthesise ZSM-5 and ZSM-11 in gels con-

taining aluminium, then it comes as no surprise that, following the discovery that silicalite could be synthesised from aluminium-free TPA gels, TBA should be used to crystallise the aluminium-free analogue of ZSM-11, subsequently named silicalite II [81]. Other all-silica materials include ZSM-22 [86], silica-ferrierite [87], and silica-ZSM-48 [88]. There are also a number of other all-silica materials, for example ZSM-39 [89]. These are termed *clathrasils* since, although they contain relatively large cavities, the windows are too small to let occluded species pass through [15,90,91].

In 1982 a new class of microporous crystalline materials were reported, the aluminophosphates [12]. These have been followed by a whole host of other framework compositions, *eg.* the titanosilicates [92][1], most of which use an organic reagent as an essential component of the synthesis gel.

1.4.3 Crystallisation Kinetics

The production of crystals from an aluminosilicate gel takes place in two stages; nucleation and growth. The kinetics of zeolite crystallisations has been studied intensely. Briefly, during the nucleation stage nuclei may form and disappear until they reach a critical size at which point they are capable of supporting spontaneous crystal growth [93]. Growth is thought to take place by condensation polymerisation at the crystal surface with the elimination of water between the hydroxyl groups at the crystal surface and those on the unit being added. However, only those units with the correct size and geometry can be added [64,94]. The number of nuclei that form depends on the degree of supersaturation of the reaction mixture. At high levels of supersaturation, many nuclei are formed and consequently a large number small crystals are obtained. At low levels, a small number of large crystals are obtained. Crystal size can be controlled to a large extent by modifying the crystallisation conditions, *eg.* temperature, pH, which affects the degree of

---

[1]The importance of their work on titanosilicates was recognised at the 9th Meeting of the IZC in Montreal, where the Bellussi group received the prestigious Breck Award

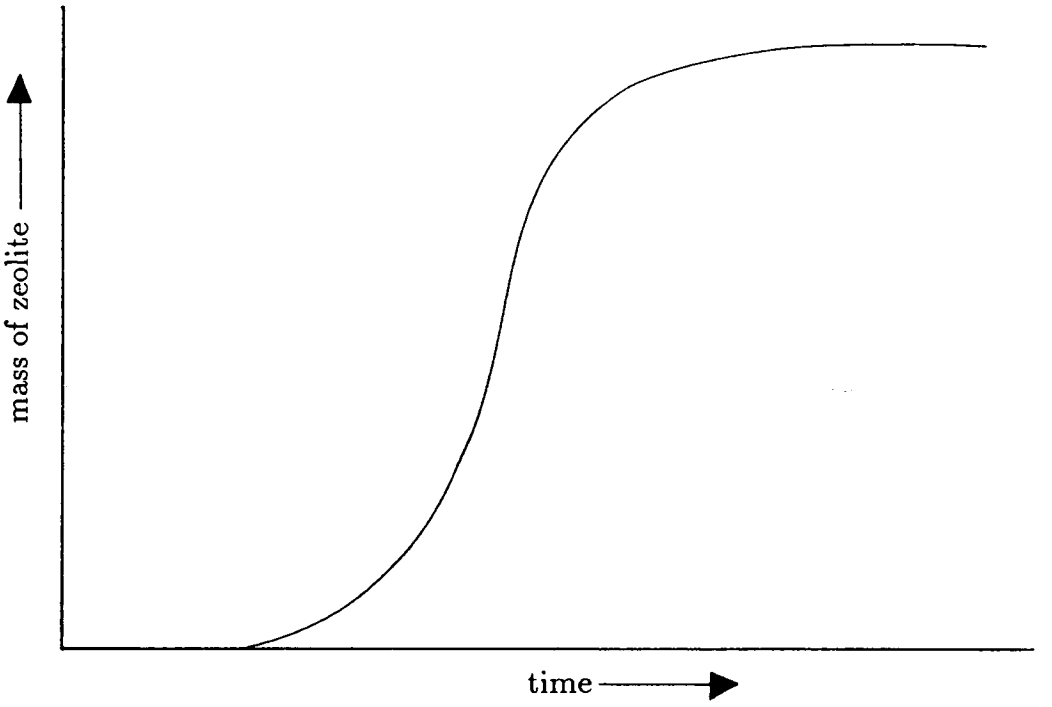

Figure 1–9: Characteristic *s - shaped* curve illustrating the crystallisation process

depolymerisation of silicate and aluminosilicate species in solution and hence the level of supersaturation.

The nucleation and growth periods are readily seen in plots of the extent of crystal growth versus time (Figure 1–9). These sigmoid or *s - shaped* curves are characteristic of zeolite crystallisations. The reciprocal of the time taken to the onset of crystallisation (*i.e.* up to the first point of inflexion on the crystallisation curve) can be used to give a measure of the nucleation rate and the steepness of the slope used to give an indication of the growth rate. The nucleation time can be reduced considerably by the addition of seed material, where growth may occur immediately.

Crystal growth is usually followed by X-ray powder diffraction (XRPD) (Chapter 2). The crystallisation curve is obtained from measurement of the degree of crystallinity of the sample, *i.e.* mass of zeolite, as a function of time. However, it is claimed that the methods used to measure the mass of zeolite produced during a crystallisation are not sufficiently sensitive to allow details of the crystallisation kinetics or activation energies to be reliably determined [95].

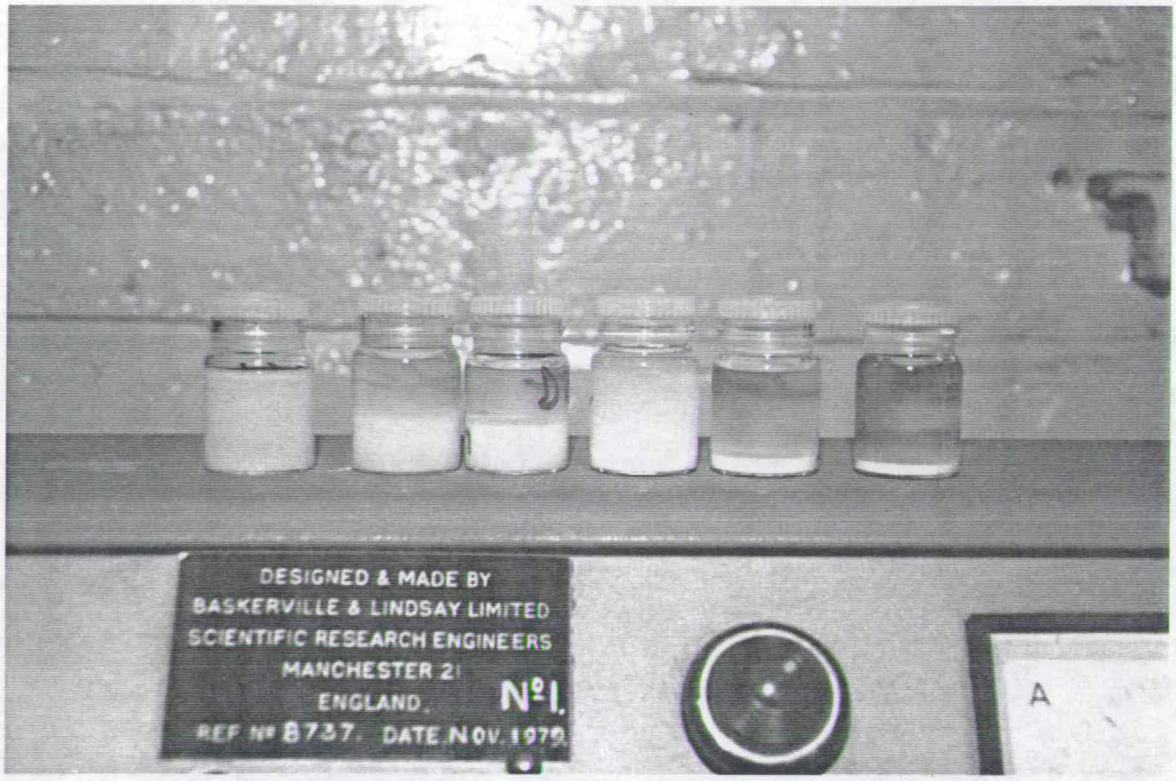

Figure 1–10: Change in sample appearance on crystallisation

Other methods used to follow the progress of a crystallisation include, infrared spectroscopy (IR) [67] and solution pH [96]. Zeolite crystallisations can also be followed visually as illustrated in Figure 1–10. As crystallisation proceeds, the denser crystals separate from the gel and settle out on standing. It is important to point out that this separation does not occur in all zeolite crystallisations. The kinetics of nucleation and growth are affected by variables such as temperature, composition, source of reagents, as well as history dependent factors such as gel aging, nature of the reaction vessel, and the order in which reagents are mixed [97,98,99,100] These will be discussed briefly in the following sections.

Effect of temperature

An increase in temperature reduces the nucleation time and increases the growth rate, which generally results in the formation of larger crystals. At high tempera-

tures zeolites may transform into denser phases. This occurs because zeolites are metastable and readily recrystallise to thermodynamically more stable phases, provided the composition of the mother liquor is suitable. These transformations are described by Ostwald's law. Specifically, since nucleation is kinetically controlled, the zeolite that crystallises first is usually the least stable thermodynamically. This will recrystallise repeatedly until the system reaches minimum entropy and the most thermodynamically stable phase is obtained. Careful control of temperature can reduce or prevent the formation of unwanted phases. These transformations are clearly also dependent on reaction time. Synthesis of high-silica zeolites carried out in the absence of an organic reagent are more likely to over-run to denser phases. Those in which an organic reagent is included in the synthesis gel do not easily over-run since the organic guest stabilises the porous framework [101]. For example, in the synthesis of ZSM-5 from a gel containing TPA cations, the TPA stabilises the metastable ZSM-5 phase sufficiently that crystallisation to the dense phase quartz is suppressed [102]. The ready interaction between quaternary ammonium cations and the silica surface effectively hinders access of OH^- ions to the surface, which reduces silica solubility [103].

Since the solubility of aluminosilicate species is dependent on temperature, the composition of the solution phase can vary quite markedly. Often, if reactions are to be run at high temperature, the alkalinity of the system is reduced in order to maintain the conditions necessary to crystallise the desired zeolite. *i.e.*the base level is reduced to decrease the reactivity of the system. This is one of the many examples of the interplay between the various parameters governing zeolite crystallisations. As well as altering the crystallisation kinetics, a change in reaction temperature for a given composition can alter the nature of the zeolite crystallised [104,105], affect crystal morphology, or even prevent crystallisation [106]. Several studies on the effect of temperature on zeolite crystallisations have allowed the calculation of apparent activation energies for both nucleation and growth [97, 107,108].

Table 1–2: Effect of composition[a] on zeolite crystallisations

Mole Ratio	Primary Influence
SiO_2/Al_2O_3	Framework composition
H_2O/SiO_2	Rate, crystallisation mechanism
OH^-/SiO_2	Silicate molecular weight, OH^- concentration
M^b/SiO_2	Structure, cation distribution
R^c/SiO_2	Structure, framework aluminium content

[a]Taken from reference [109]

[b]M = inorganic cation(s)

[c]R = organic additive(s)

Effect of gel composition

The type of zeolite crystallised depends primarily on the composition of the starting gel. The effects of the various reaction components on the nature of the zeolite crystallised and the crystallisation kinetics [109] are shown in Table 1–2. These will be outlined in the following sections:

a) SiO_2/Al_2O_3

This determines the framework composition. For example, ZSM-5 can be synthesised with a wide range of framework SiO_2/Al_2O_3 ratios from 11 to infinity (silicalite), depending primarily on the aluminium content of the reaction gel. However, it is not uncommon in zeolite synthesis to obtain a number of zeolitic and/or non-zeolitic phases on changing the SiO_2/Al_2O_3 ratio in the starting gel. A good example of this was shown by Araya and Lowe [110]. They found that the type of the zeolite obtained could be changed by merely increasing the aluminium content of the starting gel under otherwise identical synthesis conditions. Unlike ZSM-5, the crystallisation fields of other high-silica zeolites, for example zeolite Beta, can be quite narrow indeed.

The Si/Al ratio of the product zeolite is always less than that of the starting

gel since dissolved silica is always present in the mother liquor. Very little, if any, aluminium remains in solution.

The crystallisation rate can be increased by increasing the Si/Al ratio of the synthesis gel. This is attributed to the fact that the incorporation of aluminium is a disruptive process, since the resulting Al-O bond is longer than a Si-O bond which is energetically less favourable. Indeed it has been suggested that in the synthesis of ZSM-5, a silicalite-type material crystallises initially and is subsequently replaced by the aluminium-containing ZSM-5 [111].

b) OH/SiO_2

Anincrease in the alkalinity of the reaction composition has a similar effect to that of changing the synthesis temperature. An increase in alkalinity leads to several effects:

i) A decrease in the SiO_2/Al_2O_3 ratio of the crystalline product since more silica will remain in solution. This can result in the crystallisation of a different zeolite [112].

ii) A decrease in the nucleation time since a greater concentration of reactants will be in solution, resulting in more nuclei being formed as a result of collision nucleation. This will also result in smaller crystals being obtained.

iii) An increase in the rate of crystal growth since more nutrients are available in the solution phase for transport to the surface of the growing crystal.

iv) A modification in crystal morphology [113].

Inherently linked with the alkalinity of a reaction system is the yield of solid recovered. At high pH values the solution can retain much dissolved unreacted silicate species and consequently the yield will be reduced. Furthermore, since zeolites are metastable, they can redissolve and recrystallise other, usually more dense phases. Phase purity can often be controlled by careful adjustment of pH [114].

The source of hydroxide ions is usually an alkali or alkaline earth metal hydroxide, although a large number of organic bases have been used where they often serve as both the mineraliser and structure director [115]. The incorporation of silica into the framework leads to an increase in the free base level of the system.

This accounts for the increase in pH observed at the onset of crystallisation [96, 116].

c) H_2O/SiO_2

Since the base concentration of a gel changes with the water content, it is not surprising that, all things being equal, an increase in the H_2O/SiO_2 ratio reduces the nucleation and crystallisation rates. Water plays an important role in hydrolysing silicate bonds, allowing other connectivities as well as providing a medium for transport of nutrients to the growing crystal.

In aluminous systems the water is thought to play an important role in combination with the inorganic cation in determining the nature of the zeolite crystallised, where it is thought to act as a void filler [117]. In the case of high-silica zeolite synthesis, water can also have an important structure directing role. In systems containing pyrrolidine as the organic structure director, under otherwise identical conditions, an increase in the water content leads to the formation of different zeolitic phases [118].

Effect of the source of SiO_2 and Al_2O_3

There is a wide range of both silica and alumina sources. The most commonly used silica sources include CAB-O-SIL M-5 (fumed silica), water glass, Ludox, and silica gel. Aluminium is frequently added as sodium aluminate or as other soluble salts. The choice can be crucial in determining the nature of the product crystallised.

Silicates can be classed as either *active* or *inactive* [99,119]. The former include hydrated silicates while the latter include colloidal silicas. Which source is used for a particular synthesis, can determine which zeolite, if any, finally crystallises [99,119]. Furthermore, differences in particle size and consequently rates of dissolution in the alkaline medium, can influence both the rate of nucleation and growth. For example, gels containing silica with a high proportion of silicate monomer will crystallise faster than gels in which the silica is predominantly polymeric. Mostowicz and Sand have shown that the nature of the silica source

has a marked effect on the crystallisation kinetics of ZSM-5 [120]. Although pH plays a significant role in depolymerisation of silicate species, the surface area and structure of the amorphous silica are also important [121].

Alternative alumina and silica sources include other zeolites [122,123] and meta-kaolin [31]. In studying zeolite crystallisations, there are advantages in eliminating as far as possible affects due to silica and alumina sources, or at least controlling them in a reproducible manner. In Edinburgh CAB-O-SIL M-5 and aluminium wire are usually used. These are high purity materials which afford good reproducibility in zeolite syntheses. Tetraethylorthosilicate is an alternative reproducible source of silica.

Effect of gel preparation, pre-treatment and other history dependent factors

Perhaps one of the most disconcerting features of zeolite synthesis is the fact that even a change in the way in which a gel is prepared can affect the type of zeolite obtained. Thus great care must be taken to ensure that gels are prepared in exactly the same way, particularly when carrying out systematic studies. The order of mixing [124] and the extent of mixing [125] have been shown to be important factors in determining the nature of the zeolite that crystallises. Whittam [125] illustrates this in the synthesis of faujasite from mixtures which were thoroughly homogenised and ones which were not. In the former, a high yield of zeolite was obtained while in the latter the yield was poor and contaminated with other zeolitic phases [125].

Although gels are usually charged into the reaction vessel soon after preparation, occasionally quiescent aging of the gel can be useful. This can be carried out at any temperature but usually well below the synthesis temperature. It has been suggested that gel aging allows an equilibrium to be established between the heterogeneous gel and the solution phase [109]. Products with different crystallite size can be obtained by varying the period and temperature of aging [126].

Stirring the reaction mixture during the synthesis can have a dramatic effect on the crystallisation rate [127] as well as affecting the outcome of a crystallisation. It has been reported [128] that the crystallisation rate can be increased by up to three times that of the corresponding unstirred system. The nature of the zeolite obtained can also be changed by stirring the reaction mixture. Freund [99] found that the phase purity of zeolite X depended on the extent to which the reaction mixture was stirred. Furthermore, he found that the nature of the reaction vessel could also affect the crystallisation.

1.4.4 Crystallisation Mechanism

Introduction

Despite the complexity of zeolite crystallisations, great strides have been made in understanding the underlying mechanisms. Two have been proposed. These involve crystallisation in the solid phase, via a solid-solid hydrogel transformation from the amorphous to crystalline phase, or from the solution phase. The second of these is the most widely accepted mechanism. Both will be outlined in the following sections.

Solid phase transformation

The direct transformation of the amorphous gel into a crystalline product without participation of the solution phase has been claimed in several studies [129,130, 131]. Breck [132] describes a study of the synthesis of zeolite X carried out by Khatami and Flanigen where, despite separation of the gel solid from the solution phase at the end of the induction period, the solid continued to crystallise zeolite X over several weeks under ambient conditions. However, the solid phase still contained about 20 % water and it is likely that this may have promoted the crystallisation.

McNicol *et al.* [130] studied the crystallisation of a number of zeolites, which included A, X, and P, using luminescence and Raman spectroscopy. They found

that traces of Fe^{3+}, substituted for Al^{3+} in the gel, occupied a tetrahedral environment. They found no evidence for the presence of soluble aluminosilicate anions in the solution phase and concluded that crystallisation must therefore occur via a solid phase transformation mechanism.

Derouane [131] crystallised ZSM-5 via both a solid phase transformation mechanism and a solution phase mechanism, depending primarily on the gel chemistry. They suggest that the constant Si/Al ratio of the solid phase during crystallisation is indicative of a solid phase transformation mechanism. Indeed, work carried out by von Ballmoos has shown that the presence of aluminium zoning[2] is related to the synthesis mechanism [133,134]. In the case of crystallisation via a solid phase transformation, the aluminium concentration should not vary throughout the crystal.

Solution phase mechanism

Evidence for crystallisations via a solution phase mechanism has been widely reported [97,98,100,111,135,136,137,138]. These include crystallisations from clear solutions [136,138]. Kerr [135], as early as 1966, proposed that the presence of nutrients in the solution phase was vital for crystal growth. He suggested that once the zeolite nucleated the equilibrium would be disturbed in such a way that the gel would dissolve in order to provide nutrients to the growing crystal. Kerr demonstrated this by circulating sodium hydroxide through an amorphous aluminosilicate and then over zeolite A seed. All of the aluminosilicate was found to have been transported by the hydroxide and converted to zeolite A onto the seeds. Clearly, the equilibrium between the aluminosilicate in the solid and liquid phases was disturbed by the removal of nutrients from the liquid phase by the growing zeolite A crystals. To re-establish the equilibrium, more solid aluminosilicate dissolves in the hydroxide and this process continues until the supply of nutrients is exhausted.

---

[2]The aluminium concentration in the crystal can vary across its cross-section

1.4.5 Species in Solution

The nature of the silicate, aluminate and aluminosilicate species in solution has been widely studied [103,119,121,137,139,140,141,142,143] and will be briefly described here.

The nature of the species in solution will vary markedly depending on a number of factors, including the silica and alumina source, the synthesis temperature, the nature of the cation, and the solution pH. Alkaline conditions are essential in zeolite crystallisations because it is only under these conditions that tetrahedrally coordinated aluminium , as $Al(OH)_4^-$ ions, can exist. However, in sodium aluminate solutions, which contain a sufficiently large concentration of Na_2O, this ion dehydrates to give species such as AlO_2 [144]. At near neutral pH dimeric anions may form. Under acidic conditions, octahedrally coordinated aluminium dominates, *i.e.*$Al(H_2O)_6^{3+}$.

The silicate anion distribution is particularly sensitive to silicate concentration, solution pH and the nature of the organic or inorganic cation in the solution. At moderately high pH values, the solution phase can contain a whole range of oligomeric and polymeric anions. Only at very high values (pH > 11) are monomeric silicate anions abundant, together with lesser amounts of oligomeric anions [142]. The size of the inorganic or organic cation in solution can influence the silicate anion distribution. McCormick *et al.* have shown that for small silicate anions, ion pairing decreases with increasing cation size [142]. Thus with larger anions, such as the double four-ring (D4R) anion (Figure 1–11), a larger cation is preferred, eg TMA^+, which may be due to stabilisation by ion-pairing effects. Casci [143] has shown that, for aqueous silicate solutions of identical concentration at room temperature, the anion distribution is markedly different for solutions that contained TMA cations than for other tetraalkylammonium cations or alkali metal cations. It was also suggested that these differences may be due to the stabilisation of certain anions by ion-pairing [94]. Aqueous solutions of tetraalkylammonium (TAA) silicates show a smaller range of silicate anions in comparison with those of the alkali metal cations. In the case of TMA cations, the high concentration of

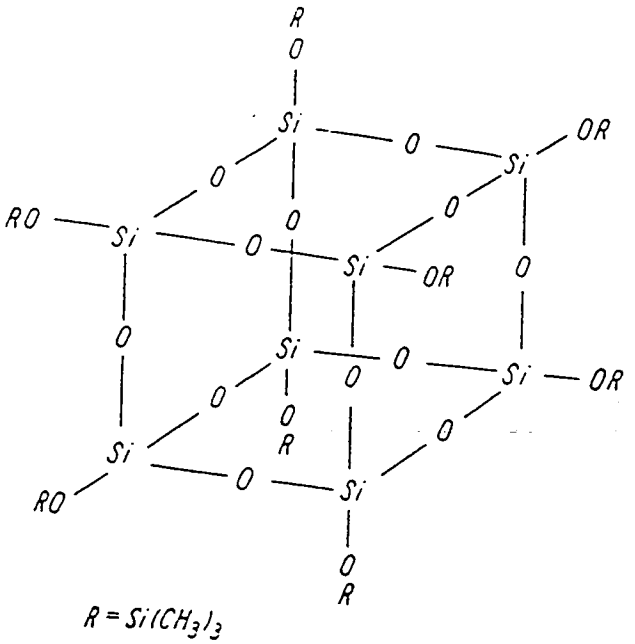

Figure 1–11: Double four-ring silicate anion trapped by the addition of $Si(CH_4)_3$

D4R's commonly found may be due to the "ordering of water and silicate anions by the TMA cations" [142]. Aiello and coworkers [145] have recently studied the influence of the nature of the cation on the properties of aluminosilicate gels and shown that sodium ions can stabilise aluminosilicate structural sub-units inside the gel matrix .

Although there is much evidence [146,147,148,149] to support the presence of silicate species in solution that resemble SBU's (*eg.*the D4R), there is none to suggest that these are the actual growth units or the precursors of zeolite nuclei. Furthermore, not all the SBU's have been observed in silicate solutions. For example, there is no evidence that the 5-1 SBU exists in solution despite the fact that many zeolite frameworks can be built from it (mordenite, ferrierite, ZSM-5). On the other hand, there is evidence that the double five-ring (D5R) unit (not an SBU) exists in solution [146,147,150] and van Santen and coworkers have shown that for a given OH/SiO_2 ratio the predominant species in solution is the D5R silicate [147]. They suggest a mechanism by which ZSM-5 forms from this precursor which involves initial ring opening by hydrolysis, followed by condensation-polymerisation (Figure 1–12). A similar mechanism was proposed by Groenen and coworkers [146].

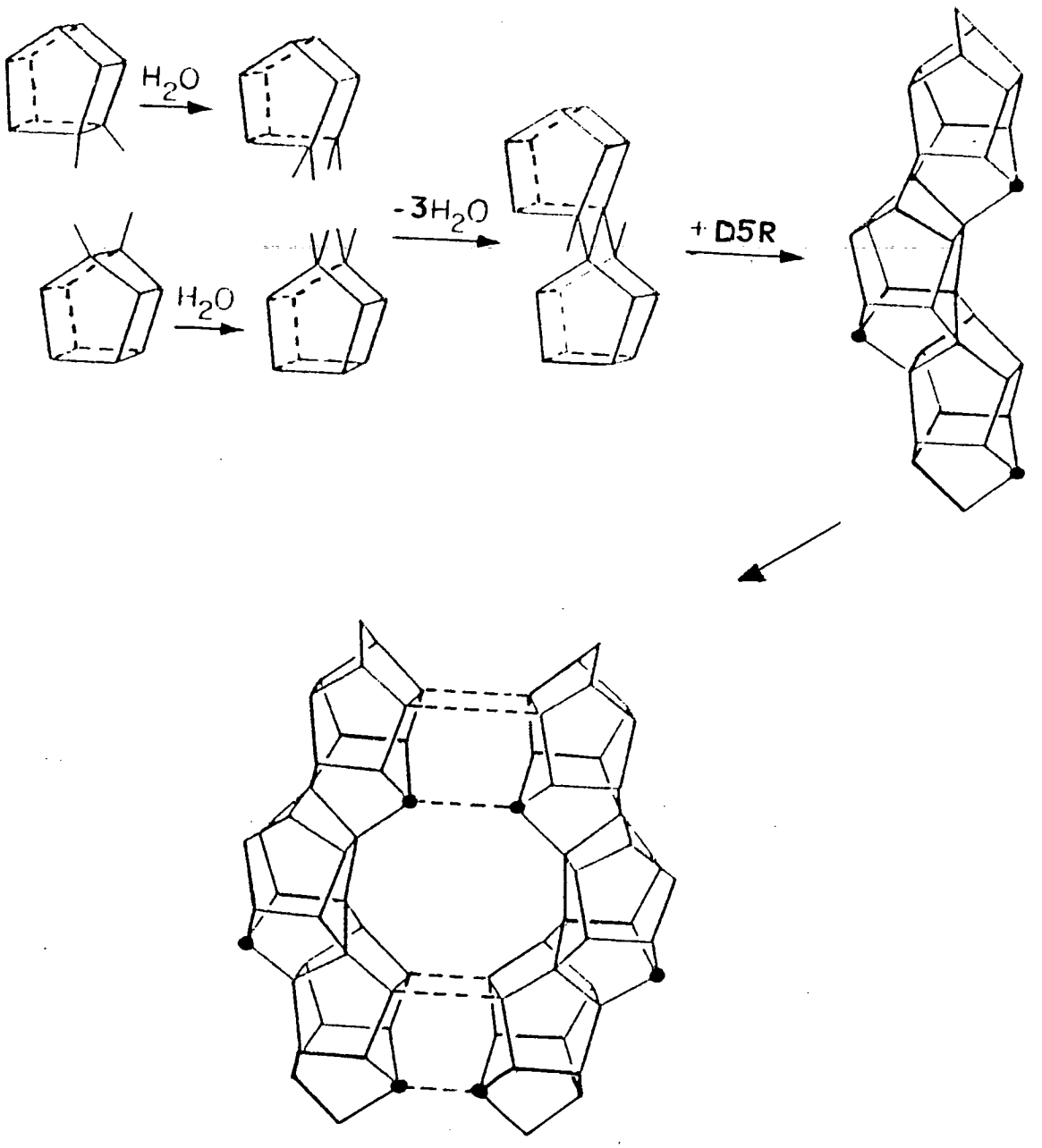

Figure 1–12: Formation of the ZSM-5 chain structure from the D5R unit, proposed by van Santen *et al.* [147]

1.4.6 Alkali-Free Synthesis of High-Silica Zeolites

One of the major drawbacks of conventional zeolite preparation, *i.e.* from systems that contain both alkali metal and organic cations, is that once crystallised (and following calcination to remove occluded organic material), the zeolite must be ion exchanged to give the H^+-form. Bibby and coworkers [151] and Dwyer and Chu [152] overcame this problem by using ammonium cations instead of alkali metal cations in the synthesis of ZSM-5 and ZSM-11. The as-synthesised products are then easily converted from the ammoniated form into the H-form by a single calcination step, the ammonia being driven off along with any occluded organic material.

There have since been a number of investigations into the synthesis of high-silica zeolites as well as all-silica molecular sieves in the absence of alkali metal cations [106,115,153,154,155,156,157,158,159,160] several of these [115,155,158] amines were used as an alternative to the quaternary ammonium salts to synthesise the MFI framework. It has been reported that amines provide good buffering and pH control [155] during the crystallisation and that the lower pH values result in increased yields [116]. An added bonus is that they are much cheaper than quaternary ammonium compounds. Alkali metal-free systems which contain an amine together with a structure directing organic species have also been reported [106,115].

In most of the alkali-free systems from which ZSM-5 has been crystallised, ammonium hydroxide was used as the source of base or mineraliser. However, it has been shown that ZSM-5 can be crystallised from aluminosilicate gels in which tetrapropylammonium (TPA) hydroxide functions both as the mineraliser and template, as well as balancing the framework charge [153,154]. This is in contrast to an early report [107] which concluded that ZSM-5 could not be made in the absence of alkali metal cations despite the presence of TPA. It should be noted that Bibby and coworkers [151] also could not crystallise ZSM-5 from gels containing TPAOH alone.

Many reports of alkali metal-free syntheses [153,154,155,156,157,159,160] do

not give information on the purity of the reagents used in the crystallisations. For example, it is widely known that quaternary ammonium hydroxides can contain a substantial amount of alkali metal impurity, particularly potassium [161]. Therefore, it is quite possible that many of these crystallisations may have been contaminated with alkali metal cations. This would have certainly affected the crystallisation kinetics, the product crystal size distribution and crystal morphology. One can only speculate as to whether the presence of these impurities may have affected the outcome of the crystallisation.

1.4.7 Organic-Free Synthesis of High-Silica Zeolites

The crystallisation of high-silica zeolites from *inorganic* gels offers several advantages. Most notable, is the obvious reduction in production costs, as the organic component is usually the most expensive. Coupled with this is the elimination of the calcination step, the expensive process by which the occluded organic material is removed by thermal oxidative degradation at temperatures usually well in excess of 773 K. Finally, the need to handle potentially toxic materials is avoided. The number of high-silica zeolites synthesised in the absence of organic reagents, however, is at present rather restricted *eg.*ZSM-5, ZSM-22-type and ferrierite-type materials. Furthermore the composition range (Si/Al, OH/Si) over which these zeolites can be synthesised is greatly reduced. For example, in the case of ZSM-5, the most notable of the high-silica zeolites that can be crystallised in the absence of organic reagents, the composition range over which it can be synthesised from inorganic gels is restricted to SiO_2/Al_2O_3 = 40 - 100 and Na_2O/SiO_2 = 0.1 - 0.2 [162].

Crystallisations from organic-free reaction mixtures tend to be slower and more likely to over-run to denser phases, than corresponding reactions in which an organic reagent is present [102]. Furthermore, it is thought that these crystallisations are sensitive to impurities such as traces of organic or seed material which may be present in the reaction vessel [163].

The work described in this section and in the previous section highlights the practical importance of carrying out crystallisations from alkali-free and organic-free reaction mixtures. These crystallisations, however, can also allow the role of the alkali metal cation and organic species be established to a large extent. It has already been mentioned that impurities may affect these crystallisations and so one cannot be entirely sure whether the observed effect may be due to the presence of these impurities rather than, say, any structure directing effect of the organic *template*. Thus it is thought that only by working under carefully controlled conditions where impurities are excluded, can the true role of these species be confidently predicted.

1.4.8 The Role of Inorganic Cations in Zeolite Crystallisations - the "Templating Theory"

It is generally recognised that cations can exert either a structure breaking (eg. Ca^{2+}) or structure forming (eg. Na^{+} , TMA^{+}) effect on the structure of liquid water and it is believed that this also occurs in aqueous gels. Furthermore, it is found that certain structural units in crystalline zeolites appear to be associated with certain (hydrated) cations [62]. In consequence, it was suggested that these hydrated cations act as templates about which the crystalline framework forms. This concept has become known as the templating theory of zeolite crystallisation and is backed by substantial experimental evidence.

The formation of a number of zeolite structures were found to have a strong cation specificity, *eg.* systems that contained sodium cations favoured the crystallisation of among others, sodalite hydrates, faujasites, and zeolite A, whereas potassium systems favoured chabazite types. In the case of high-silica zeolites the role of inorganic cations as templates is not as clear cut, since the same zeolite can be crystallised in the presence of a number of inorganic cations. There is no doubt, however, that inorganic cations can affect crystal morphology as well as the crystallisation kinetics, *eg.* [164,165,166].

Szostak [167] lists the important roles of inorganic cations. These are:

- Structure-direction
- Balancing framework charge
- Morphology
- Crystal purity
- Yield

1.4.9 The Role of Organic Reagents - Template or Void Filler ?

The reasons for using organic species in the synthesis have already been discussed. The addition of an organic reagent to a reaction mixture can cause one of three effects [168]:

i) a different zeolite is obtained,

ii) a zeolite crystallises where a reaction mixture would otherwise remain amorphous, and

iii) the same zeolite is obtained as in the absence of the organic species, but there is a change in the Si/Al ratio of the final product.

According to Rollmann [168]:, i) and ii) represent true templating effects.

The most obvious result of introducing organic reagents to the synthesis gel is that the product Si/Al ratio is usually increased. In the case of charged organic templates, the increase in Si/Al arises because fewer charge-balancing cations can be accommodated in the framework void space; this limits the anionic framework charge and hence fewer aluminium atoms are incorporated into the framework. The addition of an organic reagent can also result in the formation of more perfectly formed crystals with greatly reduced stacking faults [169] and intergrowths [170] which can be detrimental to zeolite applications.

That a number of novel high-silica zeolite frameworks have been obtained by changing the organic component of the gel has led to the idea that there is a specific relationship between the framework and the organic species. This is usually referred to as templating. Several hundred organic species have been tested

as potential templates for new frameworks but of these, relatively few have been successful.

The role of organic molecules as templates is debatable and the use of the term *template* is often misleading. Indeed, only in a very few cases does the organic species appear to behave as a true template [171,172], *i.e.*where the channels or cavities bear some relation to the shape and size of the organic molecule. The best example is TPA-ZSM-5 in which the TPA appears to fit snuggly in the channel system; the nitrogen center sits at the center of the channel intersection with the propyl groups extended into the channels. The TPA cation is too large to enter the zeolite through the 10-member ring windows of the channel system after crystallisation, therefore the framework must have been built around the organic molecule. Further evidence for the templating role of TPA in the synthesis of ZSM-5 comes from thermal analysis data, where it was shown that there are four TPA cations per unit cell, the maximum that can be accommodated by the ZSM-5 framework [131]. The use of hexamethonium cations in the synthesis of the high-silica zeolite EU-1 [173] and propellane quaternary ammonium compounds in the synthesis of SSZ-26 [174] are other examples of templating agents. In aluminous systems, a templating role has been used to describe the action of quaternary ammonium polymers on the synthesis of fault-free gmelinite and mordenite [169].

The actual mechanism by which the organic directs the zeolite structure has been the subject of much debate and is still not well understood. One thought is that the organic forms water *icebergs* around itself. These are then partially and then fully displaced by aluminosilicate anions of various configurations until the organic molecule is totally encapsulated [175]. Flanigen [62] suggests that in some cases the organic "plays a limited role in directing structure but more generally provides a source of hydroxyl ions and stabilises the formation of sol-like aluminosilicate species" [62]. The organic molecule can have a profound effect on the gel chemistry of aqueous silica solutions, *eg.* organic bases increase the solubility of aluminate and silicate species [176] which will influence the crystallisation kinetics.

A number of studies have investigated the role of organic molecules in zeolite crystallisation. For example, van der Gaag *et al.* [177] investigated the effect

of replacing TPA with a number of organic reagents in the synthesis of ZSM-5. They found that the range of gel Si/Al ratios over which they were effective varied markedly and listed them in order of increasing *potency*; eg. alcohols < amines < TPA. It should be noted that it is possible that the compositions studied would have given ZSM-5 even in the absence of these organic reagents and the role of the alcohols as structure directors is certainly debatable. In another investigation, Araya and Lowe [178] tested a number of organic reagents in a gel composition that would have given ZSM-5 even in their absence. They concluded that TPA is a true structure director, while piperazine and 1,6-hexanediamine have limited directing ability. 1,6-hexanediol, on the other hand, had no directing ability and therefore should be considered as a hydrophobic void filler rather than a structure director [178]. In the latter case, the organic stabilises the zeolite structure without having directed it's formation. Indeed Araya and Lowe [178] suggest that many of the organic species that lead to the formation of ZSM-5 are probably void fillers rather than true structure directing templates. This will be demonstrated in the work described in this thesis (Chapter 4).

As well as the range of gel Si/Al ratios over which an organic species is effective, a test of a good template is that small changes in its structure should render it ineffective. This has been demonstrated by Casci [179] and Valyocsik [180], who examined the effect of small changes in template chain length.

In a recent study by Gies and Marler [91], 61 organic species were examined in aluminium-free reaction mixtures. They found that in the majority of cases the organic species was a good fit for the particular pore system.

Although the concept of the organic template is simple and attractive, there are an overwhelming number of cases in which it is inapplicable. In some cases the composition of the gel and hence the structure crystallised determines whether the organic acts as a template. For example, TPA is used to prepare the aluminosilicate ZSM-5 and the aluminophosphate $AlPO_4$-5, both of which have completely different channel architecture. Clearly, the use of the term *template* to describe the action of the organic species in the $AlPO_4$-5 case would be inappropriate. In the synthesis of LOSOD [176] (an aluminous zeolite) from reaction mixtures that

contained bulky organic molecules, no organic was found occluded in the crystalline product. It was concluded that the organic base served only to increase the base content of the reaction mixture [176] and did not therefore act as a template. Suzuki *et al.* prepared several zeolites in the presence of pyrrolidine [118]. No obvious relationship between the geometry of the organic molecule and the type of zeolite framework crystallised was observed. However, these reactions were carried out in the presence of substantial amounts of sodium ions and it is conceivable that the pyrrolidine simply behaved as a void filler in some (or all) of the products they obtained.

Lok *et al.* [63] have listed a number of organic materials used in the synthesis of high-silica zeolites. What is clear from this list is that:
i) one organic species can direct the formation of more than one framework and these can have very different pore systems, *eg.* ZSM-5 and $AlPO_4$-5 (described above), and
ii) a specific zeolite framework can be made by the incorporation of organic species which are geometrically different. Thus there is sufficient evidence to discount a *lock and key* theory to describe the action of many organic species in zeolite crystallisations.

The role of organic and inorganic cations has recently been reviewed in a paper by Gilson [181].

It is clear that there are very few good examples in which the action of the organic can be described as a template. However, there is little doubt that they can determine the outcome of a crystallisation. Thus it is believed that they would be best described as structure directors rather than templates. The organic species can have other important functions in the reaction mixture [182]. It can:
i) act as a structure-directing agent or template,
ii) modify the gel chemistry where it can promote the formation of more siliceous products,
iii) interact chemically with other components of the gel, where they may buffer the pH of the system,
iv) modify the gelling process, solubility of the aluminosilicate species, aging char-

acteristics, transport and thermal properties, and crystallisation time, and v)act as a void filler.

1.4.10 Competitive and synergistic effects between inorganic and organic cations

Since many zeolite syntheses are carried out using gels that contain both an inorganic cation and an organic reagent, there are likely to be competitive and synergistic effects between these species. These will significantly affect the crystallisation kinetics and as well as the composition of the product zeolite. For example, TPA cations have been shown to compete with sodium cations for charge compensation of silicate and aluminosilicate framework units [183] in the synthesis of ZSM-5. In the presence of sodium ions, the rate of crystallisation of TPA-ZSM-5 is enhanced [184] which demonstrates synergism between the organic and inorganic cations. In the absence of sodium cations the crystallisation is extremely slow. Synergistic effects have also be demonstrated in the synthesis of ZSM-39 [185].

Another example of synergism arises in the synthesis of NU-10, where the addition of sodium salts increased the crystallisation rate of gels that contained tetraethylenepentamine [186]. These workers also found that the addition of sodium chloride to compositions that gave a mixture of NU-10 and ZSM-5, favoured the formation of NU-10. This leads one to question whether the sodium ion is actually a true ZSM-5 structure-directing agent, as has been proposed by Tianyou and coworkers [187].

1.5 This Work

1.5.1 Introduction

In the search for new high-silica zeolites most workers have taken the view that success lies in the choice of organic *template*. Reaction mixtures typically used to examine new organic templates have compositions closely related to that which give inorganic Na-ZSM-5. Not surprisingly, the product most frequently found is ZSM-5. Furthermore, a careful examination of results may well show that in many instances the product obtained is the one that would have formed in the absence of the organic template and that it has done no more than stabilise the product against dissolution.

In most cases sodium hydroxide has been used as the base and some workers have even used additional sodium salts. The presence of such large quantities of sodium ions may well mask any structure directing effect of the organic template. It could be that trace quantities (impurity levels) of sodium impurities could promote the formation of ZSM-5 or other common high-silica zeolites.

Many zeolite syntheses, including crystallisations from organic-free and alkali-free systems, are carried out using impure reagents and complete analyses are rarely available. Consequently, it is difficult to establish from published work whether impurities affect the course of the crystallisation or the nature of the zeolite crystallised.

The chief aim of the present work, therefore, was to investigate the influence of impurity species in the synthesis of high-silica zeolites.

1.5.2 Impurities

Introduction

An impurity may be defined as any species adventitiously present in the *ideal* composition in uncontrolled amounts. The nature of the zeolite synthesis is such that impurities in the reaction mixture can accumulate in the product zeolite and so must influence the crystallisation process in some way. For example, the incorporation of these impurities may occur systematically with some taken up earlier in the crystallisation than others. The later ones are likely to accumulate in the crystal surface. Surface ion-exchange will be an important factor here.

It may well be that certain impurities influence the crystallisation mechanism even to the extent of determining which crystal structure is formed. Furthermore, they may act catalytically, *i.e.* without themselves becoming incorporated in the product.

A good example of an impurity influencing the nature of the product obtained is given by Freund [99]. He found that under certain circumstances, Na-X would crystallise only from gels prepared from silica sources which contained an aluminium impurity (the so-called *active* silica sources). This occurred despite the large amount of aluminium used to prepare the gel.

Zeolite impurities

For a crystallographically pure zeolite impurities can be of the following types:
i) framework impurities. Isomorphous replacement of framework T-atoms occurs readily and is common in natural and synthetic zeolites. The element most likely to be introduced in this way is iron, which may come from the steel autoclave vessel or from impure reagents. The iron replaces some of the aluminium in the framework, leading to longer T-O distances [188] and a less stable framework. Some impurity framework T-atoms are easily leached out, resulting in the formation of hydroxyl nests (Figure 1–7). In the synthesis of all silica-molecular sieves, such as silicalite, the framework can readily take up aluminium impurities. These

generally originate from the use of impure reagents (discussed below).
ii) inorganic cation impurities. The most important of these are the cations of the alkali and alkaline earth groups. Transition metal cations are more likely to be incorporated into the zeolite framework or to be trapped in the channels as insoluble oxides/hydroxides. It is possible that cation impurities could become trapped during the synthesis in sites from which they cannot be removed by ion exchange. This would undoubtedly have an effect on the zeolitic properties. In the case of aluminous zeolites where there is a strong correlation between the inorganic cation and the nature of the zeolite obtained, the effects of such impurities are likely to be very significant. This study, however, is only concerned with siliceous zeolites.
iii) void filler impurities. Amines and quaternary ammonium ions usually occupy the void space in the as-synthesised zeolite as has already been described. They are incorporated during the synthesis but in hot alkaline conditions the quaternaries can degrade and the breakdown products may also be incorporated into the growing zeolite. For example, in the synthesis of zeolite Beta with tetraethylammonium (TEA) cations, the maximum practical synthesis temperature is 413 K, due to the breakdown of the quaternary via Hoffman degradation:

$$(C_2H_5)_4N^+ + OH^- \longrightarrow (C_2H_5)_3N + CH_2 = CH_2 + H_2O$$

On occasion this can affect the course of the crystallisation giving products not characteristic of the original template.

Reagent impurities

The inorganic reagents used in zeolite synthesis are rarely pure and often rich in elements that can readily be incorporated into the zeolite. For example, commercial silicas and silicates often contain significant amounts of iron and aluminium impurities. The purest form of silica available is the quartz used in the electronics industry. However, this and other forms of quartz are not sufficiently reactive for routine zeolite synthesis [147] and it is essential to use amorphous silicas or soluble silicas. As has already been mentioned (section 1.4.3) the nature of the silica

source is known to affect the rate of crystallisation and the morphology of the product zeolite. It is therefore essential to use a standard, reproducible and pure form of silica. For the present study it was decided to use a fumed silica (CAB-O-SIL M-5) which is extremely pure and has a high surface area (high reactivity). The main impurity, water, was determined for each batch by thermogravimetric analysis.

There are a number of sources of aluminium but for this study it was decided to use Analar aluminium wire. Impurities originating from the aluminium wire are likely to be insignificant, especially when one takes into account the small amounts used in a typical high-silica zeolite gel composition.

The inorganic bases can contain a large number of impurities. Wherever possible Aristar materials were used.

Many researchers have paid little attention to the purity of the organic reagent. There is some justification for this in that in many cases the most serious contaminants are unavoidable decomposition products. However, in a number of studies, in particular those carried out in apparently alkali-free systems, a quaternary ammonium hydroxide has been used as the mineraliser. These are usually contaminated with a significant amount of alkali metal cations [161] which undoubtedly affect the crystallisation kinetics and the product zeolite composition.

Some of the silica and alumina sources used in typical zeolite syntheses are summarised in Table 1–3 together with the most significant impurities [189].

1.5.3 Influence of seeding

Incomplete removal of a crystalline product from the reaction vessel can have a marked effect on the overall rate of crystallisation of the subsequent reaction. Seeds provide a *ready made* surface on which deposition can occur, leading to a reduction in the period prior to nucleation and as a result a reduction in the overall crystallisation time. The nature of the product zeolite can be different from that of the seed. Seeding is particularly important in organic-free reactions.

Table 1–3: Reagents used in zeolite syntheses together with their main impurities

Reagent	**Source**	**Impurity / ppm**
Silicon compounds		
Tetramethylorthosilicate	Merck	Na, Ca < 0.5
Tetraethylorthosilicate	"	Al < 0.2
$Na_2SiO_3.9H_2O$	'N' Philadelphia	Al < 200
	Quartz Co	Fe < 120
Water glass	"	"
Fumed Silica		
CAB-O-SIL M-5	BDH	Al < 10
Aerosil-200	Degussa	"
Colloidal Silica		
Ludox-AS-40	DuPont de Nemours	Al < 500
Aluminium compounds		
Sodium aluminate	BDH	Fe < 4
Pseudoboehemite	Vista	Ti < 40
$Al(OH)_3$	Merck	Fe < 3
Al_2O_3	Baker	Fe < 0.01

[a]Reference [189]

It would be impossible to study the effect of all impurities in zeolite crystallisations in such a short time. Therefore it was decided to limit the study to crystallisations of high-silica zeolites in two systems; the organic-free and alkali-free systems. It was argued that in the former, the most important impurities would be seed and/or traces of organic impurities and in the latter, seed and/or traces of alkali metal cations.

1.5.4 Structure of this thesis

This thesis is divided into two main sections. The first, Chapters 3 and 4, deals with crystallisations of high-silica zeolites in the potassium system under carefully controlled conditions and in the absence of organic reagents. This section also reports on the ability of trace levels of seed and organic impurities to promote ZSM-5 crystallisation within the *template-free* concentration range. It is not known whether such impurities affect the outcome of a zeolite crystallisation.

For completeness, several crystallisations were carried out in the inorganic sodium system. The results are shown in the Appendix.

In Chapters 5 and 6 an investigation of the *reverse* system is described, *i.e.* alkali-free crystallisations. The study of zeolite synthesis under ultrapure[3] conditions has not been previously reported. As was explained earlier, many of the reagents used in zeolite syntheses are substantially contaminated with impurities. Reactions carried out under ultrapure, alkali-free conditions enabled the effect of weak *templates* to be examined.

The results obtained from the work in alkali-free and organic-free systems may give more mechanistic information that may further clarify the role of inorganic and organic cations in zeolite crystallisations. Furthermore, it will be possible to study in more detail the synergistic effects between inorganic and organic species

[3]Conditions in which impurities are excluded as far as is reasonably practicable

and more importantly, synergism between different organic species in the absence of alkali metal cations. It is believed that the latter has not been widely reported.

In Chapter 7, the influence of small cations (Na^+, K^+, and TMA^+) on the crystallisation of TPA-ZSM-5 is reported. In this work, speculation is made as to the role of these cations on the crystallisation mechanism.

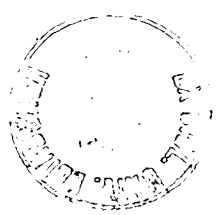

Chapter 2

Experimental and Analytical Methods

2.1 Experimental

2.1.1 Materials

The reagents used in this work are given in Table 2–1 together with the concentration of sodium and potassium impurities. A number of organic substances were used in small quantities in the work described in Chapter 4. These are shown in Tables 2–2 and 2–3. The alkali metal content was not determined for these materials. The water content of the fumed silica was determined for each batch by thermogravimetric analysis and was always found to be less than 2 %. No account of this water impurity was made when calculating reaction compositions. Ultrapure water (18 MΩ) was obtained from the department (courtesy of Dr. S.K. Chapman) and used in all stages of the gel preparation. Distilled water was only used when crystallisations from impure reagents were examined.

All quaternary ammonium hydroxides were standardised with 0.1 M hydrochloric acid using a pH meter to determine the end point. Alkali-free solutions of tetrapropylammonium hydroxide and nonamethonium hydroxide were prepared by ion exchange of the bromides with silver(I)oxide (Ag_2O) in the presence of ultrapure water as follows:
A calculated amount of the bromide was weighed into a polypropylene bottle and sufficient water added so that a 2 M solution of the hydroxide would result following ion exchange. A slight excess of the stoichiometric amount of Ag_2O was added to the bromide solution and the bottle capped. This was placed on a shaker for

Table 2–1: Reagents used together with their major impurities

Reagent	Grade	Source	Conc^n/ mg l^{-1}	
			Na	K
CAB-O-SIL M-5	-	BDH	< 40[a]	-
Potassium hydroxide (KOH)	Aristar	BDH	500[a]	-
Sodium hydroxide (NaOH)	Aristar	BDH	-	50[a]
Aluminium (wire)	Analar[b]	BDH	-	-
Tetramethylammonium hydroxide (TMAOH.5H_2O)	99 %	Aldrich	< 1	< 1
Tetraethylammonium hydroxide (TEAOH)	Pract	Fluka	670	4100
	HPLC	SACHEM	< 1	< 1
Tetrapropylammonium hydroxide (TPAOH)	Pract	Fluka	300	5750
	Purum	Fluka	250	570
	Special	SACHEM	38	2
Tetrabutylammonium hydroxide (TBAOH)	Pract	Fluka	240	8500
(TBAOH.30H_2O)	Purum	Fluka	1	< 1
(TBAOH)	HPLC	SACHEM	< 1	2
Benzyltrimethylammonium hydroxide (BzTMAOH)	Pract	Fluka	600	6300
Dibenzyldimethylammonium hydroxide[c] (DBzDMAOH)	-	-	40	nd[d]
Cetyltrimethylammonium hydroxide[c] (CeTMAOH)	-	-	3000	210
Diethylpyrrolidinium hydroxide[c] (DEP)	-	-	2	2
Methyl-n-pentylpiperidinium hydroxide[c] (MPP)	-	-	10	nd
Nonamethonium hydroxide[c] (Nona$(OH)_2$)	-	-[e]	5	nd
Hexamethonium bromide ($HexBr_2$)	Purum >99 %	Fluka	nd	nd
1,6-Hexanediamine (1,6-HXDM)	99 %	Aldrich	nd	nd
1,6-Hexanediol (1,6-HXDL)	-	Aldrich	nd	nd
2,3-Dimethyl-2,3-butanediol (2,3-DMBD)	98 %	Aldrich	nd	nd
2,4-Dimethyl-2,4-pentanediol (2,4-DMPD)	> 98 %	Fluka	nd	nd
2,5-Dimethyl-2,5-hexanediol (2,5-DMHD)	97 %	Aldrich	nd	nd
Silver (I) oxide	Purum > 99 %	Fluka	-	-

[a]Taken from suppliers specification, [b]Fe *circa* 80 mg kg^{-1}, [c]Prepared by ion exchange of the halide (made by previous students in the Department) with Ag_2O, [d]nd = non detected, [e]Supplied by ICI C&P Ltd. (ex-Lancaster synthesis)

Table 2–2: Other purum grade organic substances used in the present study; supplied by Fluka

Reagent
Tetramethylammonium bromide (TMABr)
Tetraethylammonium bromide (TEABr)
Tetrapropylammonium bromide (TPABr)
Tetrabutylammonium bromide (TBABr)
Tetrapentylammonium bromide (TPeABr)
Tetrahexylammonium bromide (THexABr)
Tetraheptylammonium bromide (THepABr)
Benzyltrimethylammonium bromide (BzTMABr)
Benzyltriethylammonium bromide (BzTEABr)
1,4-Diazobicyclo[2,2,2]octane (DABCO)
Tri-n-propylamine
n-Propylamine
Tetraethylenepentamine

Table 2–3: Reagents supplied by BDH

Reagent
Piperidine
Piperazine
1,2-Ethylenediamine
Triethylenetetramine
Glycerol

2 hours, then left to stand overnight at 298 K. The solution was carefully filtered through a 0.8 μm membrane filter and a further small amount of silver oxide added to the filtrate. The solution was again shaken and allowed to stand overnight before finally filtering it through a 0.2 μm membrane filter. The resulting hydroxide solution was standardised using 0.1 M hydrochloric acid and the alkali metal content determined by flame photometry (Section 2.2.6). The exchange efficiency was approximately 97 % (TPA) and 89 % (Nona), based on the bromide.

A number of other, potentially interesting quaternary ammonium halides were available and these too were ion exchanged using Ag_2O and standardised as above. Since there was very little of each quaternary ammonium salt available, it was difficult to carry out the ion exchange effectively. Consequently the exchange efficiencies (based on the halide) were rather low and typically of the order of 40 %. The alkali metal content of each of the hydroxides is shown in Table 2–1.

2.1.2 Gel Preparation

Since the aim of this work was to investigate crystallisations under *ultrapure* conditions, it was important to, not only use the most pure reagents available, but also to try and eliminate impurities arising from equipment used to prepare the gel. Thus for this work, new equipment was bought and care taken to ensure that equipment was used for appropriate reaction mixtures.. This included a variety of polypropylene bottles and beakers as well as a collection of hand-held electric blenders, none of which were available to any other worker in the laboratory. Thus equipment used to prepare organic-free gels were kept apart from those used to prepare alkali-free gels. It must be noted, however, that only one blender was available at the start of this work and it was not until this was found to be a major problem (Chapter 4) that more were purchased.

For all the potassium reactions (except *Scavenging Reaction* mixtures prepared later on in this work) and much of the alkali-free work, each reaction mixture was prepared in a new polypropylene bottle. However, it was found that polypropylene beakers could be repeatedly used providing they were thoroughly cleaned and

only used for appropriate reaction mixtures. Thus a separate beaker was used for *Scavenging Reaction* gels, tetrapropylammonium gels, tetraethylammonium gels, etc. After gel preparation all equipment was washed thoroughly with hot tap water followed by distilled water and finally ultrapure water. Beakers and blenders were also washed with ultrapure water just before gel preparation.

Gloves were worn at all times during the gel preparation. Although this is standard practice in any good laboratory, disposable gloves were even worn when handling the aluminium wire as a further step to limit contamination.

Care was taken to avoid contamination from zeolite dust in the laboratory area. Bench surfaces were regularly wiped down with a damp cloth well before the gel was prepared and charged into the autoclave.

Every attempt was made to carry out the reactions reproducibly and a note taken of even minor changes in the methodology.

Organic-free gels

Fumed silica was weighed into a new polypropylene bottle, A, and ultrapure water added with blending to form a slurry. Aluminium wire was added to a 50 % (wt/wt) solution of potassium hydroxide in beaker B and the solution maintained at about 318 K for several hours until the aluminium had completely dissolved. To minimise losses through evaporation, a PTFE cover-plate was placed over the beaker. In later reactions small polypropylene bottles were used instead of the beaker and cover plate. Once cooled, the clear aluminate solution was added to the silica slurry in bottle A and the contents thoroughly mixed using a hand-held blender. The remaining water was finally added to give the desired weight of gel (usually 400 g) and blending continued for a further 5 minutes.

Alkali-free gels

The procedure was much the same as described above. The quaternary ammonium hydroxide solution was weighed into a polypropylene bottle and aluminium

wire added (if required). The use of bottles in this way, reduced the possibility of CO_2 contamination of the hydroxide. Solid quaternaries were dissolved in ultrapure water before addition of the aluminium. Dissolution of the aluminium wire usually took at least 24 hours for most of the hydroxides, however, tetrapropylammonium hydroxide took longer (usually 3 days). When more than one quaternary ammonium hydroxide was used, the aluminium wire was dissolved in a mixture of the two and when gels were prepared with a quaternary ammonium hydroxide and an amine or quaternary ammonium halide, the aluminium wire was dissolved only in the hydroxide solution. The amine or quaternary ammonium halide was dissolved in ultrapure water if necessary and added to the aluminosilicate reaction mixture.

2.1.3 Stirred Reaction Vessels

Autoclaves

Four 500 cm^3 stainless-steel autoclaves (designed by Baskerville and Lindsay Ltd., Manchester), designated A, B, C and D were used throughout the present study (Figure 2–1). These were essentially identical except that the vessels had slight differences in the shape of the base and stirrers as shown in Figure 2–2. Autoclave A was constructed from stainless-steel and inconel (nickel-based alloy) and autoclaves B, C, and D from stainless-steel only. All four autoclaves were stirred by magnetically driven paddle stirrers, which throughout this work were set at 300 rpm via a dial on each of the control units. The stirrer speed was regularly checked during runs using an RS Model TM 2011 optical hand held tachometer and was found to drift by no more than +/- 5 rpm. The external heaters were controlled by Guilton-West MC36 temperature controllers and the reaction mixture temperature monitored by a thermocouple located in the thermocouple housing, which penetrated the reaction mixture (Figure 2–3). A second thermocouple located in the same housing served as the activator for the temperature trip. This was usually set 20 K above the reaction temperature. The temperature of the reaction mixture was set using the analogue meter on the control unit and checked during

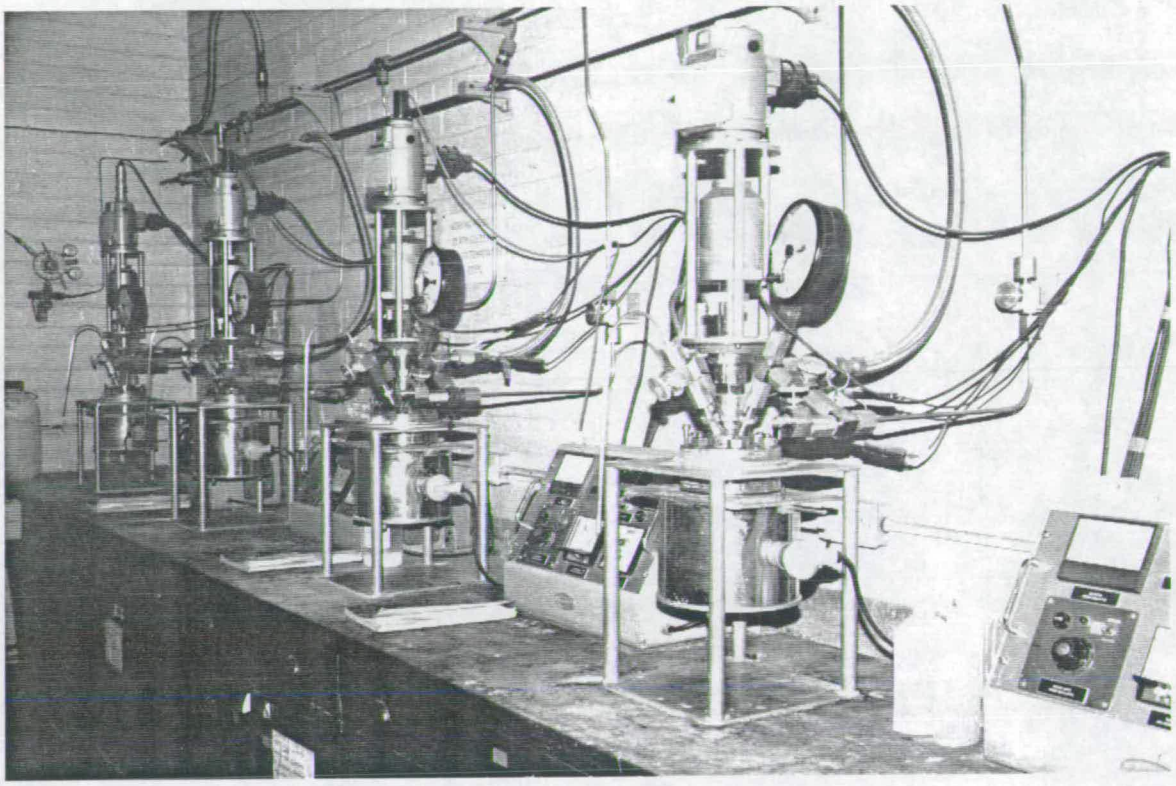

Figure 2–1: 500 cm^3 stainless-steel autoclaves (designed by Baskerville and Lindsay Ltd., Manchester)

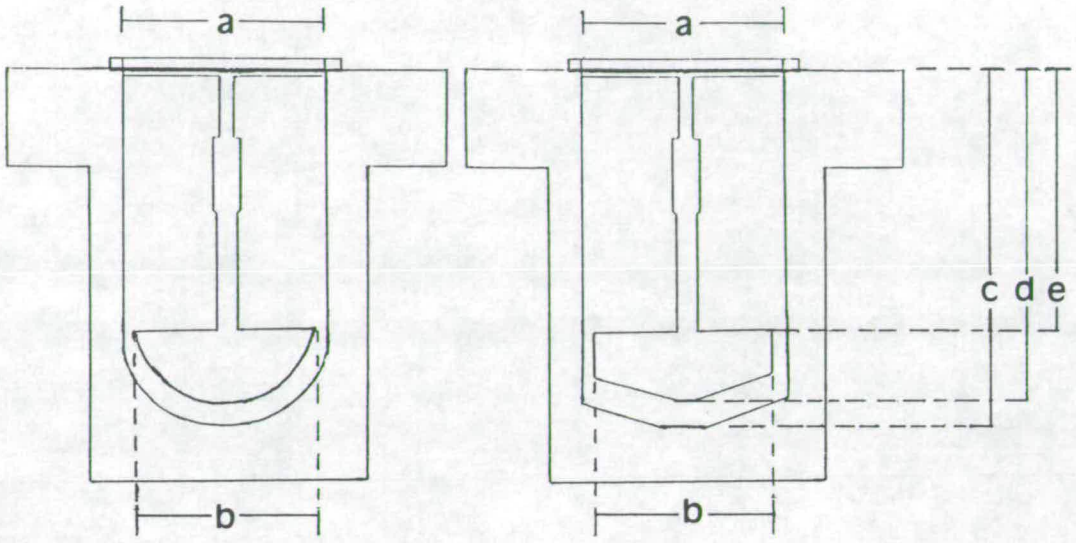

Autoclave	Dimensions / mm					
	a	b	c	d	e	c-d
A	76	67	142	116	90	26
C	76	67	142	126	100	16
B	76	69	142	126	100	16
D	76	69	142	126	100	16

Figure 2–2: Schematic of stirrer paddle and vessel geometry; left, vessels A and C, and right, vessels B and D

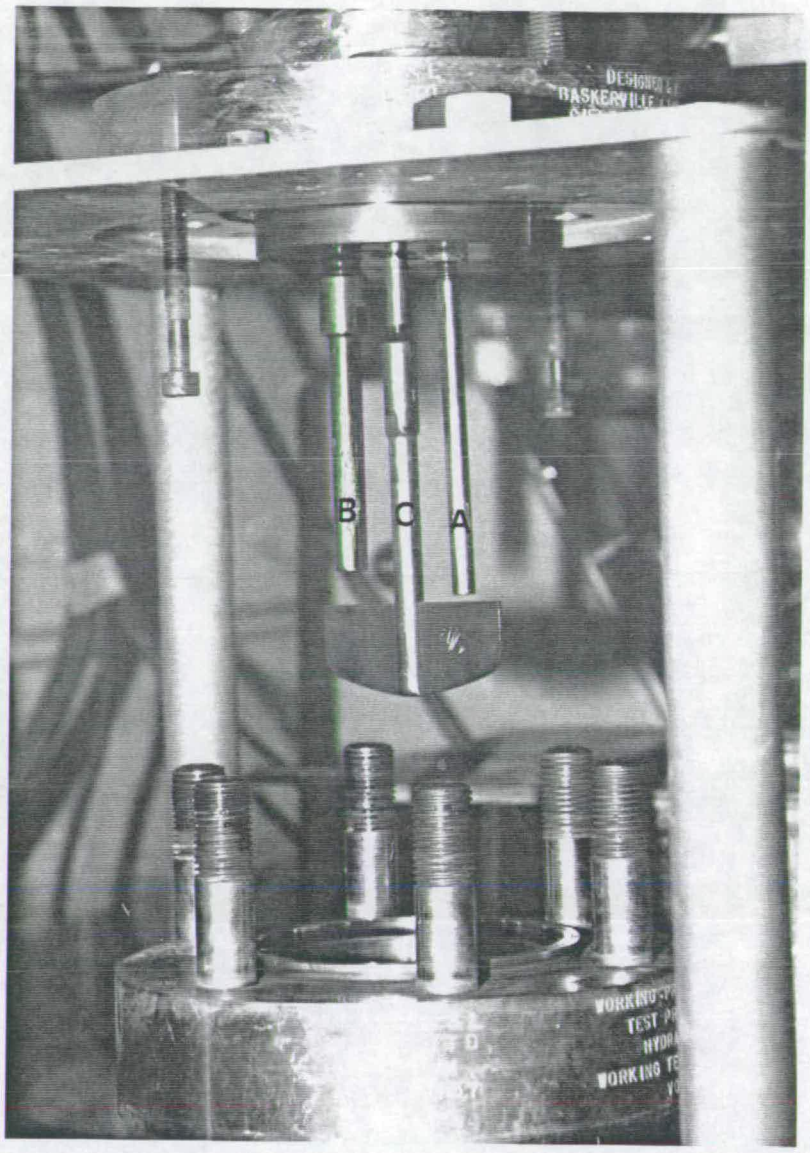

Figure 2–3: Close up of dip-tube (A), thermocouple housing (B) and stirrer paddle (C)

each run with a Comark digital thermometer 5000. The difference in the temperature between the analogue and digital readings never exceeded 2 K and was very often better than 1 K. All four autoclaves were fitted with pressure gauges which featured a pressure trip. This was activated if the pressure exceeded the pre-set value, at which point the heater was automatically switched off. The autoclaves took about 60 minutes to heat up to 423 K, and the time t_o (*i.e.* the starting time) was taken as the time at which the autoclave was switched on.

Each autoclave was fitted with a dip-tube which allowed samples to be taken during the course of the reaction without disturbing either the stirring or heating. To avoid residual material trapped in the dip-tube from contaminating the following sample, the first few cm^3 of sample were discarded. The sample size was usually 8 - 10 cm^3.

Low temperature vessels

Although the control over impurities was less than in other systems, stirred reactions (160 rpm) were carried out at 368 K using a purpose built rig (Figures 2–4 and 2–5). This consisted of four 1 litre stainless-steel reaction vessels each fitted with a flanged, glass[1] multiport lid. The broad lip at the top of the vessel was grooved to accommodate a Viton O-ring and a tensioned spring clip used to ensure an effective seal. A PTFE stirrer gland was fitted into the centre port of the lid to accommodate the stirrer. Small motors were used to drive the stirrers at a rate of 160 +/- 2 rpm. Occasionally motors had to be replaced during a run because of overheating. This usually only took about 10 minutes and it is thought that the effect on crystallisation at such low temperatures would not be significant.

Since the operating temperature was close to 373 K, it was decided to include a reflux condenser in the experimental set up. Thus, if any of the reactions were to overheat due to failure of the thermostat, there would be no build up of pressure. Thermostatting was carried out using a specially built control unit (designed and

---

[1] A probable source of impurities

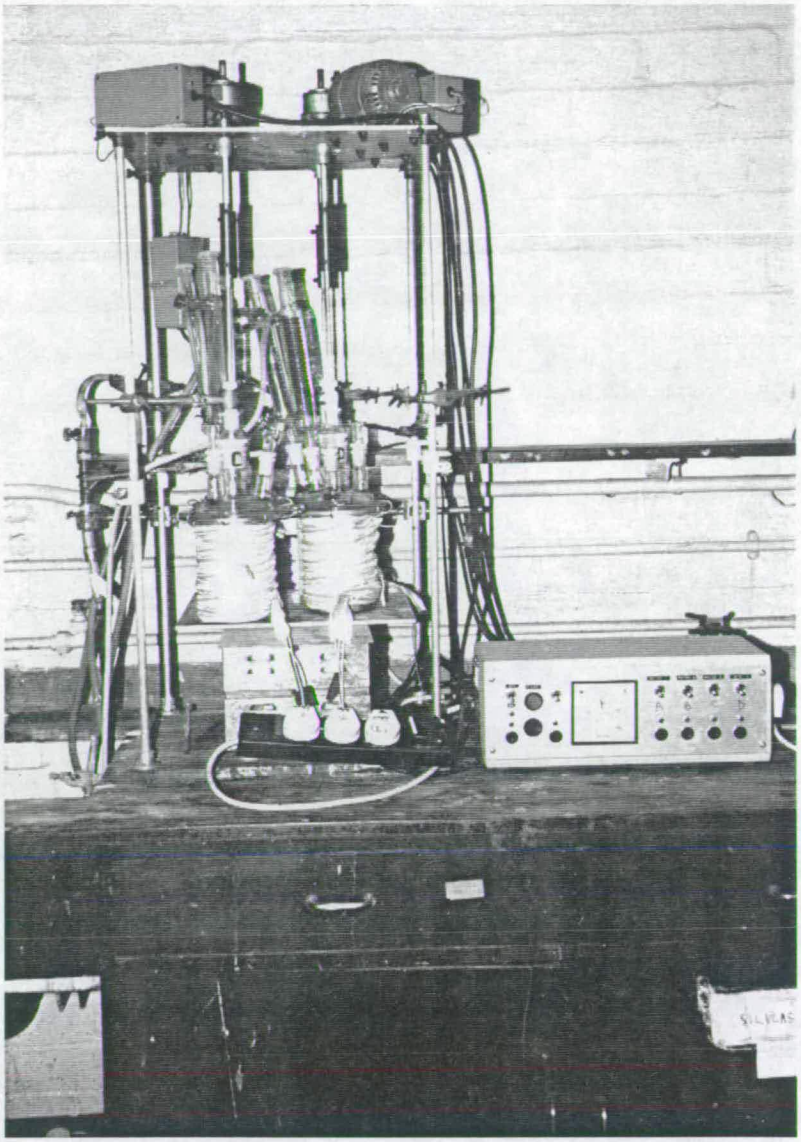

Figure 2–4: Rig used for stirred, low temperature reactions

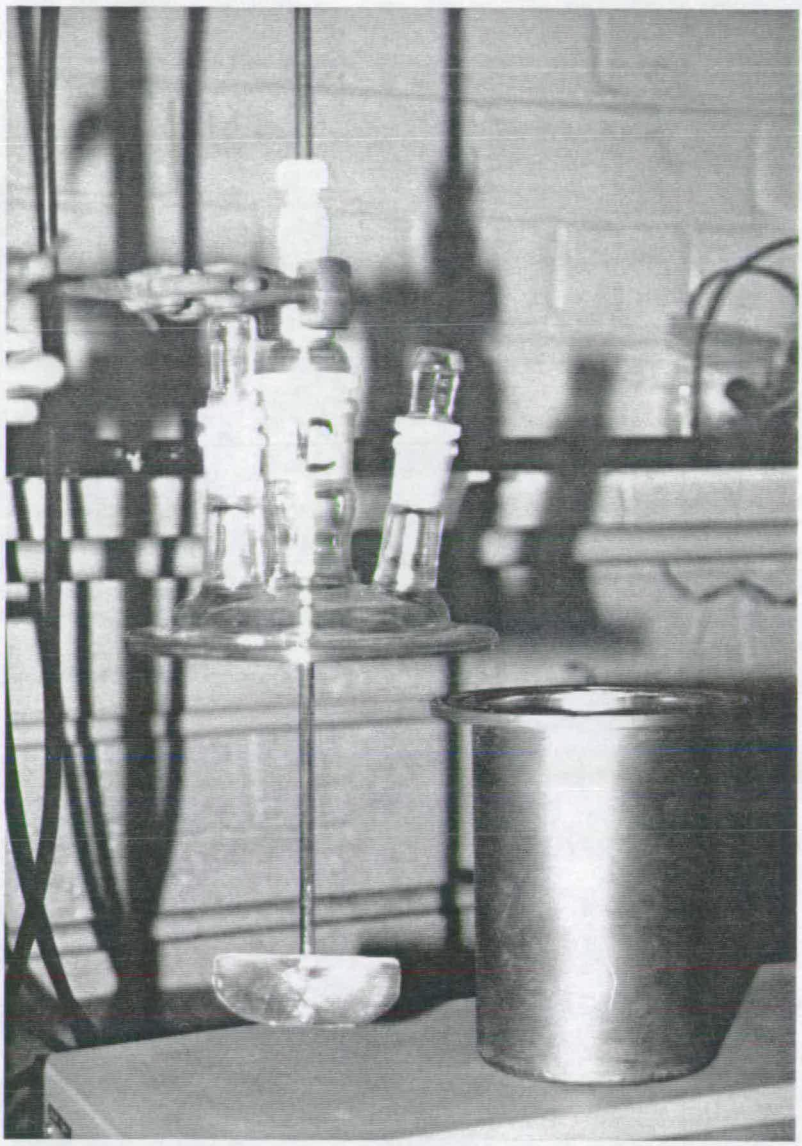

Figure 2–5: Close-up of reaction vessel and stirrer

built by personnel in the electronic workshop). This consisted of an on/off switch for each of the stirrers, a water cut-off trip (this switched off the entire rig if the flow of water to the condenser dropped below 3 l min^{-1}), a working-temperature thermocouple and an over-temperature trip. The working temperature was set using the analogue meter fitted to the control unit. The circuit diagram is shown in Figure 2–6.

The reaction vessels were heated by means of heating tapes and a hot plate. Rather than build a separate thermostatting control unit for each reaction vessel, it was decided to just use one and connect a multiblock to the output side of the control unit. Thus, in effect, the thermostatting of the four reaction vessels was controlled by thermostatting only one of them. Although this did not allow flexibility in that the four reaction vessels could not be run at vastly different temperatures, it worked remarkably well. The largest temperature difference between any two reactions was no more than 5 K and variation in the temperature throughout any one reaction was no more than 2 K (determined using the digital thermometer described above). It was felt that, since detailed kinetic studies were not required for reactions carried out in these vessels, such conditions were acceptable. Samples ($\sim$ 8 cm^3) were collected (with the stirrer switched off) through either of the other two ports using a 5 mm (i.d.) glass tube fitted to a pipette filler. Since the vessel lid was made of glass it was likely that these reactions would have contained significantly higher levels of impurities than those carried out in any of the other reaction vessels. However, the experimental set-up was such that this was difficult to avoid. It was thought that, since these low temperature crystallisations were particularly slow, turning the stirrer off during sampling would have little effect on the outcome of the reaction.

Parr bombs

Reactions carried out in Parr bombs were stirred using a magnetic stirrer / hot plate. The bomb was placed in a specially constructed steel collar (Figure 2–7) to improve thermal contact. The temperature was controlled by an over-temperature control unit (designed and built by personnel in the electronic workshop) linked by

Figure 2–6: Circuit diagram for the low temperature rig

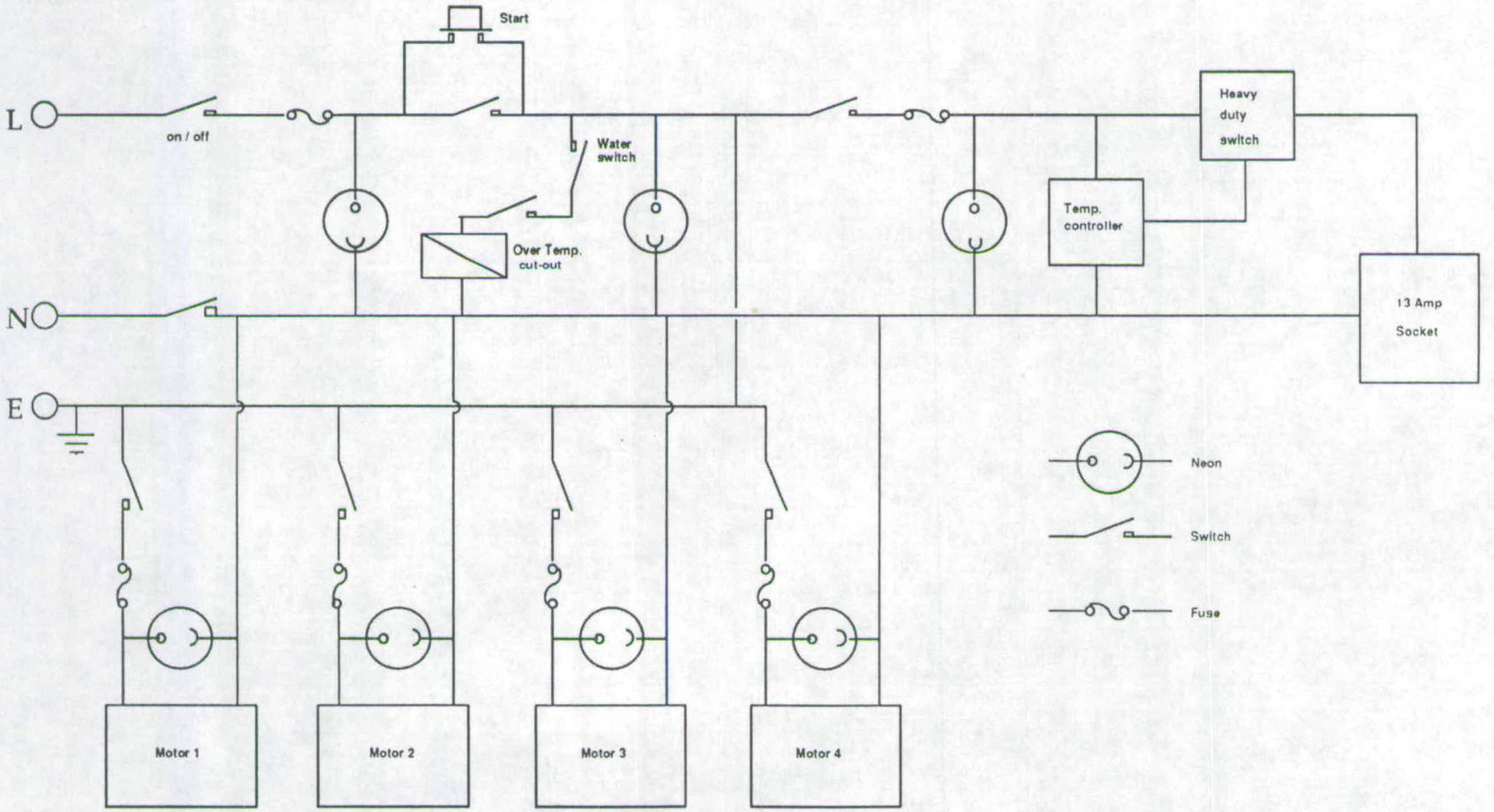

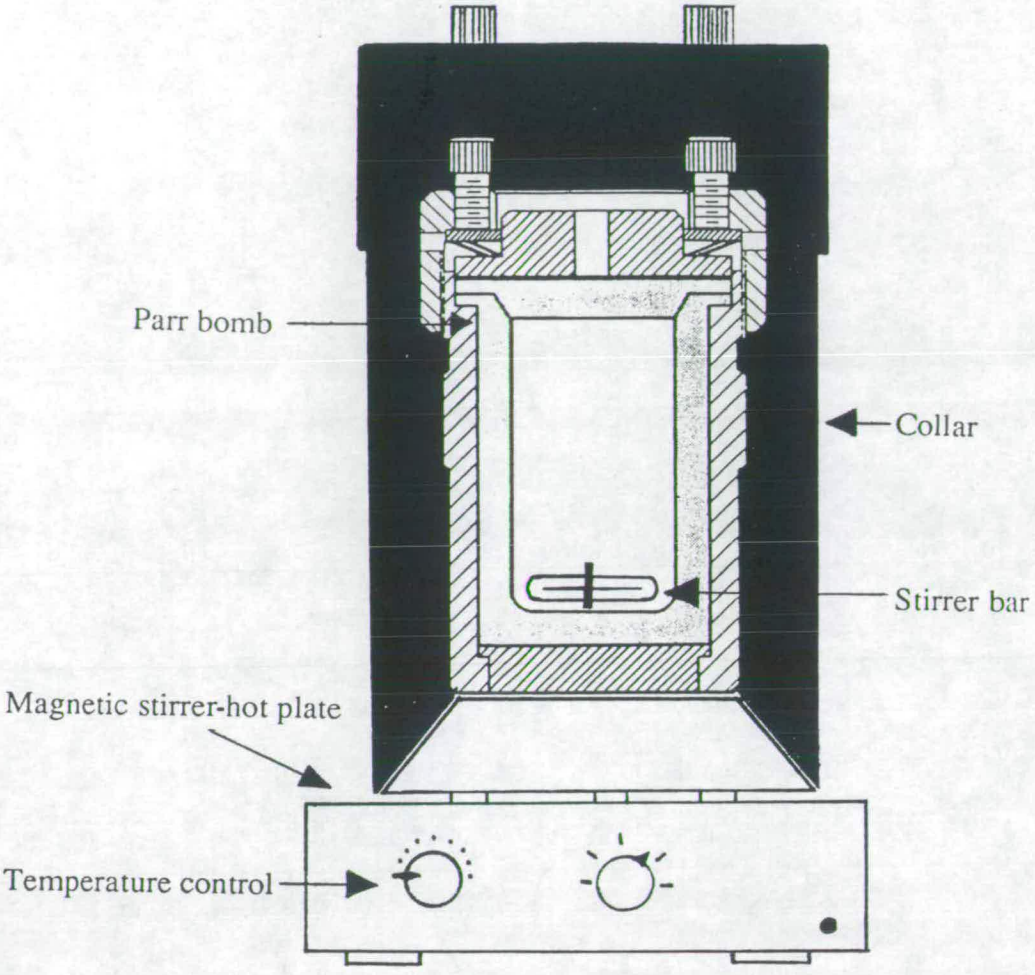

Figure 2–7: Schematic of stirred Parr bomb reactions

a thermocouple to the reaction vessel. One of the major drawbacks with this set up is that the magnetic stirrer/hot plate is not designed for continuous use for long periods and consequently it was not unusual to find that the stirrer had stopped during a reaction. When this happened the reaction was allowed to continue in the static mode and a note taken. It must be stressed that one could never be entirely sure if the reaction was being stirred, even if the magnetic stirrer was seen to be working. Consequently, results of reactions carried out in stirred Parr bombs should be treated with caution.

2.1.4 Static Reaction Vessels

Static reactions at temperatures above 373 K were carried out in 125 cm^3 teflon-lined Parr bombs, 30 cm^3 PTFE-lined bombs (designed in Edinburgh) and small, teflon-lined tubes (*TOM* reaction vessels [190] capacity approximately 1.5 g). These tubes were used primarily because they allowed a large number of reactions to be carried out with a limited amount of reaction mixture. The reaction vessels used for static reactions are shown in Figure 2–8.

Low temperature crystallisations (368 K) were carried out in 10 cm^3 polypropylene bottles, which were put into larger bottles containing water to reduce the risk of leakage. This bottle was topped up from time to time with water at 368 K.

All static reactions were carried out in pre-heated ovens set at the desired temperature. At the end of each reaction the bomb was allowed to cool naturally to room temperature.

2.1.5 Tests for Leakage

Before switching the 500 cm^3 autoclave on, the vessel was pressure-tested so that leaks could be detected. This entailed pressurising the reaction vessel, through the high-pressure inlet, with air or nitrogen to about 12×10^5 N m^{-2}, and leaving for about 15 minutes. Any major leaks were easily detected and remedial action taken.

Mass balancing was used for all reactions to check that material had not been lost during the crystallisation as a result of leakage. Specifically, this involved weighing all material sampled (including waste material collected between samples) together with the final contents of the autoclave and comparing this with the original weight of gel charged to the autoclave. For reactions carried out in the 500 cm^3 autoclaves, results are reported only for those reactions which lost no more than 5 % by weight of the original charge. However, due to the nature of the experimental set-up, a larger tolerance had to be accepted for the low temperature stirred reactions. Thus a weight loss of up to 10 % was deemed acceptable. The

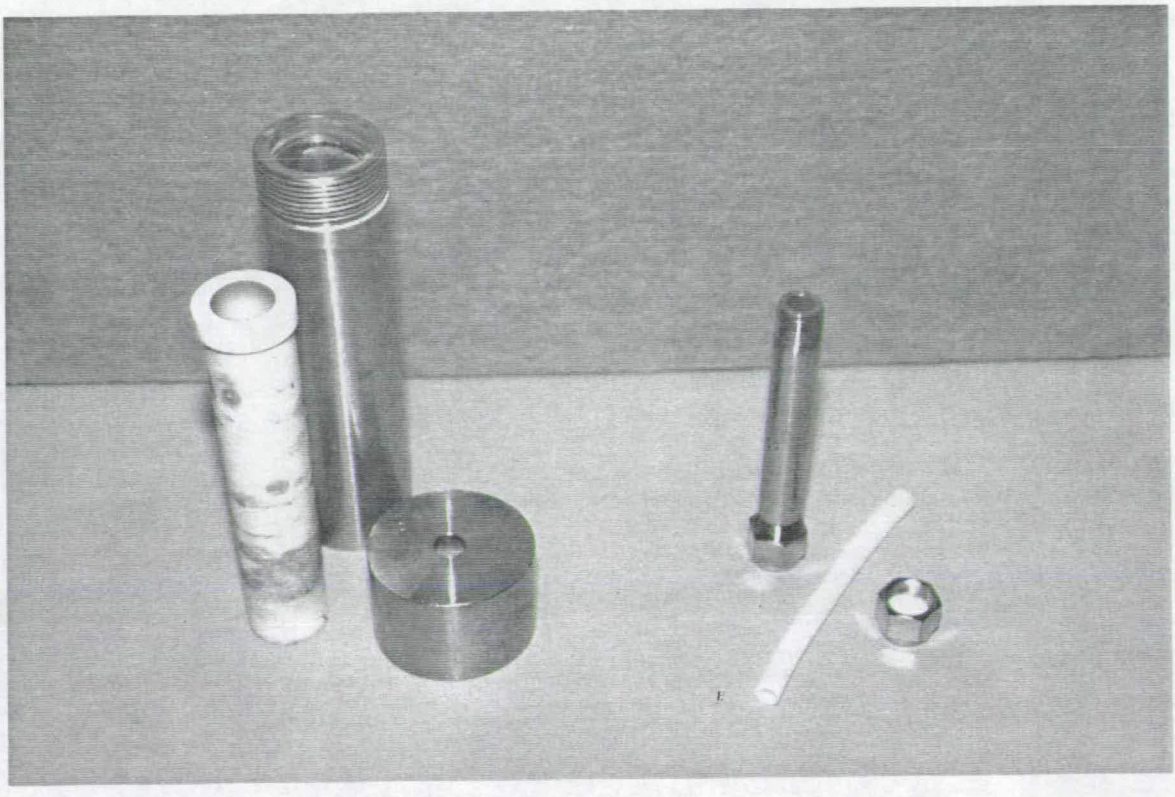

Figure 2–8: Reaction vessels used for static reactions carried out above 373 K, a) 30 cm^3 bomb and b) *TOM* reaction vessel: (Parr bomb not shown)

weight loss due to leakage form the Parr bombs and the 30 cm^3 bombs was always < 1 %. The extent of leakage from the TOM reaction vessels was not determined, although it is certain that for many of the reactions carried out at 453 K, it may have been substantial.

2.1.6 Reaction Number

The sample numbering system for reactions carried out in the 500 cm^3 autoclaves is as follows:
The letter proceeding the number identifies the autoclave in which the reaction was carried out and the number simply corresponds to the reaction number. Thus, A10 is reaction 10 carried out in autoclave A (not the 10^{th} reaction carried out in autoclave A).

Low temperature stirred reactions are similarly numbered except that the reaction vessel (A, B, C, D) is preceded by 95 to denote a low temperature reaction. Thus reaction number 95A11 is low temperature reaction 11, carried out in vessel A. Reactions carried out in Parr bombs were given the prefix P to the reaction number, *eg.* P56 denotes reaction number 56 carried out in the Parr bomb. Reactions carried out in the 30 cm^3 Edinburgh bombs were given the prefix S, *eg.* S222 is static reaction number 222. Reactions carried out in *TOM* vessels were given the prefix T, followed by the reaction number, *eg.* T3 denotes reaction number 3 carried out in a *TOM* reaction vessel.

2.1.7 Cleaning of Reaction Vessels

Autoclaves

The reaction vessel was thoroughly washed with tap water and any visible material carefully removed using a fine tungsten carbide paper (P600 grade), with the minimum of force. The dip-tube, stirrer and thermocouple housing were also cleaned with the tungsten carbide paper and rinsed with distilled water. The autoclave was then charged with a 4 % (wt/wt) solution of Aristar potassium

hydroxide and heated to 373 K (at which point the autoclave was set to trip). Hot hydroxide solution was passed through the sample delivery tube to remove any trapped material. Once the autoclave had cooled, the contents were discharged and the vessel washed with copious amounts of tap water followed by distilled water. The dip-tube, stirrer and thermocouple housing were also washed with distilled water, before cleaning the vessel at 453 K with distilled water overnight. The autoclave was again allowed to cool and the cleaning procedure repeated with ultrapure water at 453 K, each time releasing some of the contents through the dip tube. This was repeated until the alkali metal content of the washings was < 1 mg l^{-1}. Although this appears to be particularly extreme for the organic-free reactions (since alkali metal cations would be added to the reaction vessel anyway), it was argued that a standard method of cleaning would form a good base on which to carry out the present study, irrespective of the system under investigation.

It was subsequently discovered (Chapter 4) however, that, although this procedure satisfactorily reduced alkali metal impurities to a minimum, it was not sufficient to remove seed material. Thus the cleaning procedure was modified as follows:

The dip-tube was dismantled and any solid material in the dip-tube 'well' (see Figure 4-3, Chapter 4) washed away with plenty of distilled water. The dip-tube was then reconnected and a potassium hydroxide wash carried out at 373 K (3 times in succession) as described above. The water washes were repeated as described above. This cleaning procedure was shown by the *Scavenging Reaction* test to be effective at removing seed impurities (Chapter 4).

Low temperature reaction vessels

Reaction vessels and stirrers were cleaned with tungsten carbide paper and thoroughly rinsed with tap water. They were then washed with a hot 4 % (wt/wt) solution of potassium hydroxide (333 K) overnight, rinsed with tap water, scoured again with the tungsten carbide paper and finally rinsed with copious amounts of distilled water. All glassware was washed with tap water and then distilled water.

Static reaction vessels

The 30 cm^3 PTFE-lined bombs and the Parr bombs were cleaned for at least 48 hours at 423 K with the potassium hydroxide solution and thoroughly rinsed with tap water, distilled water then ultrapure water. The vessels were then cleaned with ultrapure water at 423 K until the alkali metal content of the washings was < 1 mg l^{-1}. This method of cleaning was shown by the *Scavenging Reaction* test to be effective at removing traces of seed impurity.

The teflon tube and end caps of each *TOM* reaction vessel could simply be replaced after each reaction. However, only one set of reactions were carried out.

2.1.8 Separation of the Solid and Liquid Phase

The solid phase was separated by filtration, thoroughly washed with distilled water until the pH of the washings was between 8 and 9, and dried overnight. Since the products obtained from many of the single quaternary crystallisations were composed of tiny crystallites, separation of the solid from the liquid phase had to be carried out using either a 0.2 μm membrane filter or by centrifugation. It was particularly difficult to adequately wash solids following centrifugation. These had to be resuspended in ultrapure water and centrifuged a total of three times before finally decanting the washings. The wet solid was then dried at 393 K.

A description of sample preparation and characterisation is given in the following section.

2.2 Analytical Methods

2.2.1 Introduction

The problem with many zeolite crystallisations is that the size of crystals obtained tend to be in the region 0.1 - 5 μm and are thus too small to allow full structural elucidation by single crystal analysis. However, much structural and compositional

information can be gained from X-ray powder diffraction in combination with other analytical techniques, such as thermal gravimetric analysis, magic angle spinning NMR, infrared spectroscopy, etc.

In this section only a brief account is given of the principles of each analytical technique. There is a large number of standard textbooks and review articles which give more detailed information.

2.2.2 X-ray Powder Diffraction

X-ray powder diffraction (XRPD) is by far the most widely used analytical technique in the identification and characterisation of crystalline molecular sieves. It is used predominantly as the initial means of identifying crystalline materials; each will generate a unique X-ray diffraction pattern based on the arrangement of atomic planes in the crystal. These *finger prints* allow rapid identification of a material, providing a pattern already exists in the literature. Von Ballmoos and Higgins [191] have published a collection of simulated powder patterns for most of the known zeolite and zeotype structures. Great care, however, must be taken when examining XRPD patterns, particularly if no match can be found in the literature since the presence of more than one crystalline phase in the unknown sample can lead to misinterpretation.

Although this technique can be used to give a measure of crystallinity, it can only do so if there is another phase present. This is useful when following the crystallisation of a zeolite from an amorphous gel, since there will always be two solid phases present, amorphous and crystalline until crystallisation is complete.

The use of XRPD is not restricted to the identification of a crystalline material or indeed determining crystallinity. The technique has been used in a number of studies, for example to monitor the orthorhombic to monoclinic phase transformation in zeolite ZSM-5 [192] and to estimate the SiO_2/Al_2O_3 ratio in ZSM-5 [193,194] and the synthetic faujasites [129]. Other useful information can be obtained from XRPD studies. The crystal class and unit cell parameters can often be obtained and in certain cases the space group can be determined.

The XRPD pattern can change markedly on post synthesis treatment. For example, ion exchange, de-alumination and calcination can not only modify peak intensities but also peak positions. XRPD is also sensitive to crystal size and morphology. In the former, small crystals tend to cause peak broadening. In its extreme, crystals of unit cell dimension are so much broadened that they are effectively not detected [195]. Crystals with a particularly large length to aspect ratio can give preferred orientation effects, where diffraction at certain angles occurs with unusually high intensity.

Principles

The wavelength of the X-radiation is of the same order of magnitude as the distances between scattering centres in a crystalline material; this results in diffraction of the X-rays and is described mathematically by the Bragg equation:

$$n\lambda = 2dsin\theta$$

where:

λ = the wavelength of the incident X-rays

θ = angle of incidence of the X-rays to the plane

d = distance between atomic planes

n = the reflection order, an integer

When this equation is satisfied, constructive interference occurs amongst the scattered X-rays, resulting in peaks in the plot of intensity against diffraction angle, 2θ.

Analysis and instrumentation

Samples were allowed to equilibrate in the X-ray room (humidity > 65 %) overnight before carefully grinding to a fine powder. The sample was packed into rectangular

sample holders and the exposed surface carefully pressed flat, taking care not to apply a shearing action which could lead to preferred orientation. This can lead to large errors when calculating crystallinities, particularly when comparing materials of different morphology. These errors can be minimised by avoiding the use of orientation-sensitive peaks in crystallinity calculations. For example, in ZSM-5 the peaks at 2θ = 23.0, 23.8 and 24.4° are relatively insensitive to the way in which the powder is packed [196]. In the present study very few samples showed preferred orientation effects and those that did were ZSM-5. Crystallinites were therefore calculated using the peaks at the angles mentioned above. Furthermore, care was taken to use the same weight of sample for each run. Crystallinity was determined relative to the most crystalline sample. When materials obtained from different reactions were compared, crystallinities were based on a reference sample deemed 100 % crystalline. It is estimated that the probable error in the crystallinity measurement was of the order of +/- 10 %.

Preferred orientation effects can also be reduced by simply changing the packing procedure. Front loaded samples can reduce these effects significantly. The sample is packed into the sample holder onto a glass backing plate. The holder is then placed in the diffractometer so that the X-rays penetrate the sample through the glass plate. A number of samples were analysed in this way at ICI C & P Ltd., Wilton, by Mr. R. Pendlebury.

Diffraction patterns were obtained using a Philips Powder Diffractometer equipped with an automatic sample changer (type PW1170/02). The goniometer (PW1050/80) was mounted on a highly stabilised X-ray generator (PW1730/10) which emitted Cu-K_α radiation of wavelength 154.18 pm. The scanning rate (motor control unit PW1390) used was 1° 2θ / minute with a time constant of 2 s. An AMR focusing monochromator (AMR 3-202E) was fitted in front of the detector (PW1965/60).

A silicon standard was run before and after each sample batch to allow for any variations in instrument performance. The reproducibility of the diffraction technique has been estimated at +/- 6.5 % [197] for the same sample analysed on different days.

Unless otherwise stated, the running conditions were as follows:

Tube voltage	40 kV
Tube current	30 mA
Scanning angle	40 to 4°2θ
Time constant	2 s
Range	4 x 10^3 counts s^{-1}
Step angle	1° 2θ[D min^{-1}
Chart speed	1 cm min^{-1}

2.2.3 Thermal Analysis

Introduction

In the case of high-silica zeolites, thermal analysis has been used predominantly to investigate the decomposition of occluded organic material. Both qualitative and quantitative information can be obtained. In the latter, the amount of organic per unit cell can be calculated and in combination with other techniques can allow hypotheses to be made about the templating action of these species. Thermal analysis techniques have also been used to show the presence of crystalline material in X-ray amorphous samples [131]. It is further claimed [131] that information can be obtained on the nature of the crystallisation mechanism.

The major thermal analysis techniques employed in the present study are discussed in the following sections.

Principles

Thermogravimetric analysis (tga)

This technique continuously records the weight of a sample as it is heated from ambient to typically 1173 K. The resultant thermogram can give both qualitative

and quantitative information such as the temperature at which a thermal event takes place and quantifying the weight lost. This allows decomposition pathways to be evaluated.

Differential thermogravimetric analysis (dtg)

This is simply the differential of the tga weight loss curve, and is recorded as a peak rather than a step. The derivative is useful in that it occasionally reveals information that is not readily detectable in the thermogram.

Differential thermal analysis (dta)

Endothermic and exothermic events are recorded. The sample and a reference material (usually alumina) are heated at the same rate and the temperature difference between the two is measured. In endothermic processes, such as vapourisation and sublimation, the sample becomes colder than the reference material since thermal energy is removed. Conversely, in exothermic processes, such as combustion, the sample becomes hotter due to the liberation of thermal energy. The exotherm is seen in the thermogram as a peak maximum while the endotherm shows as a peak minimum.

DTA can be used quantitatively to determine the energy involved in a particular process providing suitable calibration is carried out with standard materials of known thermal behaviour.

Thermal analysis of an as-made organic-containing zeolite will typically show an endotherm below 473 K (dehydration) and exotherms between 623 K and 873 K (combustion of organic). The combustion process usually occurs over a range of temperatures, depending on the location of the organic within the framework and the extent of its interaction with the framework.

Most samples are examined in flowing air; however, inert atmospheres such as nitrogen can be used. In this case exotherms will appear as endotherms since combustion is replaced by pyrolysis.

2.2.4 Analysis and Instrumentation

Samples were equilibrated over saturated sodium chloride ($p/p^\circ = 0.735$) overnight at 278 K. Approximately 15 mg of sample were placed in the platinum sample pan and suspended from the microbalance. Approximately 15 mg of alumina, which had been heated to 1173 K at least 3 times, was used as the reference. Runs were carried out in flowing air and the data collected on a BBC microcomputer [198].

The running conditions were as follows:

Heating rate	10 K min^{-1}
Temperature range	ambient to 1173 K
Air flow	26 cm^3 min^{-1}
Chart speed	1 cm hr^{-1}
tga f.s.d.	50 %
dta sensitivity	100, 200 or 500 μV

2.2.5 Electron Microscopy

The resolution afforded by any optical system is limited to half the wavelength of the light source (typically 0.5 μm) compared to 30 - 40 pm for accelerated electrons. This greater resolution and depth of field allows detailed surface and structural analyses to be performed. The two principal techniques used in this study were scanning and transmission electron microscopy.

Scanning electron microscopy (SEM)

This technique is used primarily to study crystal morphology, size and size distribution. At lower magnifications (x 7000), the field may contain sufficient crystals to allow crystal counting to be carried out. From the resulting crystal size distribution analysis, useful mechanistic information can be gained.

Principles

The surface of the sample is scanned with a very fine high energy electron beam in a pattern of parallel lines (raster). Low energy secondary electrons are emitted from atoms at the surface, while some incident electrons are reflected (flat surfaces will reflect more radiation than crevices and so appear as bright images). Both the secondary and reflected electrons are collected in the detector, where the signal is amplified and displayed on a cathode ray tube (CRT) screen which synchronously scans with the incident beam. Magnification is achieved by varying the ratio between the dimensions of the region of the sample scanned and those of its image on the CRT display. Resolution is increased by narrowing the electron beam and increasing the acceleration voltage. One problem with SEM, however, is the build up of electrons on the surface of a non-conducting sample. This charging causes gross image distortion and can damage the sample. A conductive layer (usually gold) is coated on the sample as a thin layer ($\sim$ 0.01 μm) in order to minimise charge build up. The gold coating also serves to improve the clarity of the image since it will usually increase secondary electron emission.

Analysis and instrumentation

A small amount of ground sample was suspended in a small amount of acetone and transferred onto an aluminium stub using a Pasteur pipette. The acetone was allowed to evaporate, leaving behind a white residue on the stub. The samples were then gold coated in an argon atmosphere before placing into the vacuum chamber of the microscope for analysis.

Scanning electron photomicrographs were obtained using a Cambridge Instruments Stereoscan 250 scanning electron microscope located in the Faculty's SEM unit. Gold coating, film processing and instrument calibration and set-up were carried out by Mr. John Findlay of the Faculty of Science SEM Unit. A number of photomicrographs presented in this work were prepared by Mr. John Findlay.

A small number of samples were analysed by Mr. R. Pendlebury at ICI C & P Ltd., Wilton.

Transmission electron microscopy (TEM)

Unlike SEM, TEM uses an illumination source, a tungsten filament. The filament emits electrons when heated which are accelerated by means of electric fields down a column under vacuum. Magnification and focusing are achieved by a series of electromagnetic lenses. The image is essentially a magnified shadow formed by areas of differing electron transparency and absorption in the sample. The image is viewed on a fluorescent screen which can be removed to permit exposure to photographic plates. TEM offers the advantage of higher magnifications than SEM allowing more detailed structural analyses to be performed. However, the technique requires a considerable amount of expertise in order to get the best results.

TEM analysis was only carried out on samples which contained crystals that were too small to be examined by SEM. This work was carried out by personnel at ICI C & P Ltd., Wilton.

2.2.6 Atomic Emission Spectroscopy (AES)

Introduction

There are a number of emission techniques including plasma and flame methods. The essential difference between these methods is the atomisation temperature. With flame methods, samples are atomised at temperatures of 2000 - 3500 K whereas with inductively coupled argon plasma (ICP), temperatures as high as 6000 - 8000 K are used. The higher temperature allows heavy elements and refractory materials to be analysed with greater sensitivity.

The instrument most commonly used for the analysis of alkali metal cations is the flame photometer. This provides a simple to use, convenient and fast method of analysis. In this study, Na and K analyses were determined in the solution phase of samples collected during crystallisations, particularly those from the alkali-free reactions. Autoclave washings were also analysed by flame photometry for alkali metal content to check the cleanliness of the reaction vessel.

Si, Al, Na, K, and occasionally Fe were determined in crystalline samples by ICP and flame AES at ICI C & P Ltd., Wilton, by Ms. Irene Brown. The detection limit for sodium and potassium was given as 0.003 % (wt).

Principles

In AES the flame or plasma acts as a source of radiation. The sample is presented as a solution and is drawn into the flame (or plasma) through a capillary tube, where it is atomised. The metallic constituents are reduced to gaseous atoms which emit characteristic radiation with wavelengths in the UV, visible and near IR regions of the electromagnetic spectrum. These arise from electronic transitions of the outer electrons. At these high temperatures, however, considerable ionisation can occur which can interfere with the analyte signal. This can be suppressed by adding materials such as caesium salts to the sample.

Analysis and instrumentation

The solution phase was analysed without any pre-treatment for sodium and potassium using a Corning type 410 digital flame photometer. Calibration standards were prepared from stock solutions of the alkali metal chlorides and the instrument calibrated. Samples were analysed at random and aspirated for at least twenty seconds or until a steady reading was displayed. Water was aspirated between samples to ensure that no cross contamination occurred. The detection limit for both sodium and potassium was approximately 0.15 mg l^{-1}.

The solid phase ($\sim$ 100 mg) was dissolved in hydrochloric and hydrofluoric acids and once dissolved, diluted with deionised water (100 cm^3). All samples were prepared and analysed by Ms. I. Brown at ICI C & P Ltd., Wilton.

2.2.7 pH

Introduction

The use of pH to follow the crystallisation of high-silica zeolites was first described by Casci and Lowe [96]. The time at which crystallisation occurs was found to be accompanied by a significant change in the pH, which was attributed to a combination of occlusion of the organic component and incorporation of silica units into the framework. On crystallisation, there is a sharp reduction in the amount of silica in the solution phase, which increases the amount of free base in the system. This is accompanied by a sharp rise in pH. It has also been suggested that pH can be used to give a measure of template strength [116]; the most effective templates give a more stable crystalline product which is consequently less soluble, giving rise to a larger pH rise.

The technique is very simple and reasonably accurate and compares favourably with other techniques used to follow the crystallisation process. However, in aluminous systems, where the pH used for crystallisations is very high, this method cannot be used with any confidence.

Analysis and instrumentation

pH measurements were taken according to the method described by Casci and Lowe [96] using a Philips type PW9422 digital pH meter fitted with an EIL type 1180/200/BNC/UKP combination electrode. The meter was calibrated before analysing samples using buffer solutions of pH 7 and 9.2. Samples were allowed to cool for at least 24 hours prior to analysis or, more usually, analysed in batches after the termination of the reaction. Measurements were made on unfiltered samples and a reading taken after 10 minutes. The electrode was rinsed thoroughly with distilled water and wiped dry with a tissue between samples. Crystallisation curves could then be constructed from plots of pH versus synthesis time, if required.

In the standardisation of quaternary ammonium hydroxide solutions, pH measurements were used to determine the end point of the titration.

2.2.8 CHN Analysis

A large proportion of this study involved the synthesis of high-silica zeolites in the presence of more than one organic component, all of which could possibly be occluded in the framework. A relatively simple way to determine the nature of the occluded species is to use CHN analysis. This gives a measure of the amount of carbon, hydrogen and nitrogen by weight (%) in the sample. Thus, C/N and C/H ratios can be used to establish whether or not more than one organic is present and also estimate the proportion of each species.

Analyses were carried out by personnel in the department of Chemistry.

2.2.9 Optical Microscopy (OM)

OM can be used as a first means of establishing whether crystallisation has occurred. However, crystal size is limited to > 5 μm. In most conventional zeolite syntheses this is not a problem, however, in this work crystal sizes were very often much smaller than this, which meant that the technique was not widely used.

Analysis and instrumentation

Samples were placed on a glass microscope slide, a drop of water added and a cover-slip placed over the top. The microscope used was a Vickers model M41 Photoplan fitted with a splitter to allow photographs to be taken.

2.2.10 ^{13}C MASNMR

A number of samples obtained from mixed quaternary and quaternary/amine systems were analysed by Ms. B. Gore at the Department of Chemistry, UMIST, Manchester. Samples were pressed into a zirconium rotar and analysed using cross polarisation. With this technique, some of the proton signal is transferred to enhance the weak ^{13}C signal.

2.2.11 Catalysis

One sample was subjected to catalytic examination under the supervision of Dr. I.S. Lake at ICI C&P Ltd., Wilton. The sample was pelletted and sieved to obtain particles within the range 0.5 - 1 mm. The sample ($\sim$ 0.2 g) was transferred to a clean stainless-steel tube, which contained a plug of glass wool and glass beads. This served to raise and support the sample bed. More glass beads were added on top of the sample and the tube plugged with more glass wool before securing it into the heating bock. The sample was calcined overnight to remove any volatile impurities before starting the run. The test reaction used was the disproportionation of ethylbenzene [199,200] (see Chapter 5).

2.2.12 Sorption

The sample was pelletted to a size of about 1 mm and calcined in an oven at 773 K to remove any occluded organic material. After calcination the sample was allowed to cool in a desiccator and transferred immediately onto the balance. The apparatus was evacuated and the sample heated to remove any sorbed water. Before the sorption process was started, the sample was again calcined to ensure that the voids were free of any water or organic species. The sorbate used in these studies was n-heptane. This was freeze-pump-thawed before use to remove any air in the system (measured using the pirani gauge). The sample was then exposed to the sorbate and the uptake and pressure recorded. From the uptake versus pressure data, an *alpha plot* was constructed to enable calculation of the surface area and micropore volume of the sample. The *alpha plot* is simply a plot of uptake versus a modified pressure and relies on the measurement of an isotherm on a reference sample of known surface area and same surface composition as the unknown sample. A full description of this technique is outwith the scope of the present work. The method is described in detail by Sing [201].

2.2.13 X-ray Fluorescence Spectroscopy

Several samples were prepared by Mr. G.D. Cruickshank and analysed by personnel at the Department of Geology. Sample preparation involved calcining the sample at 1273 K for one hour, mixing approximately 1 g of sample with a lithium borate flux and heating for 20 minutes at 1373 K in a platinum crucible. Once cooled, the mixture was reweighed and more flux added to make up for any loss of volatile components from the flux. Finally, the mixture is heated over a Bunsen burner and the liquid poured into a graphite mould. The resultant glass disc was cooled slowly then removed from the mould for analysis.

Chapter 3

Organic-Free Syntheses: The Potassium System

3.1 Introduction

There have been many investigations into the crystallisation of high-silica zeolites from organic-free reaction mixtures [63,128,147,163,178,202,203,204,205,206,207, 208,209,210,211,212]. Most of these have been carried out at relatively high temperatures with sodium aluminosilicate gels and the chief zeolitic products are Na-ZSM-5 and mordenite [63,128,147,163,178,202,203,204,205,206,207,208]. However, there have been far fewer investigations into the synthesis of high-silica zeolites from aluminosilicate gels in which potassium is the only cation in the reaction mixture [209,210,211,212].

The most notable investigations were carried out by two research groups; Nastro *et al.* [209,210,211] and Bellussi *et al.* [212]. The results reported by these groups, however, are rather conflicting. Nastro *et al.* reported that they were unable to crystallise ZSM-5 in their static systems unless considerable amounts of sodium ions were also present. They found it difficult to obtain reproducibility in their systems and did not pursue the formation of minor non-reproducible phases [209]. They concluded that ZSM-5 could not be obtained in the absence of sodium ions [209,210] and that it should be considered *sensu stricto* a sodium zeolite [210]. In contrast, Bellussi *et al.* [212] have reported the crystallisation of K-ZSM-5 in the monocationic potassium system over a limited range of reaction compositions using two different silica sources. Both groups used relatively high temperatures

(463 K [209,210,211] and 448 K [212]) which encourage the formation of dense over-run products *eg.* quartz. This may have made it difficult to detect early zeolitic products. In neither of these studies is sufficient information given to allow one to determine whether other factors, such as the purity of the reagents used or the nature and history of the reaction vessels, may have affected the outcome of the crystallisations. Furthermore, one group [209] used static systems while the other group [212] employed "shaker autoclaves", both of which are thought to be less reproducible than stirred systems, especially for large volumes.

The limited and contradictory information available on the potassium system made this an ideal system to investigate the influence of impurities on the course of zeolite crystallisations. It was believed that sodium would be one of the most important of these, in view of its ability to promote the crystallisation of ZSM-5. Therefore, great care was taken to reduce sodium impurities to a minimum.

At the outset of this work it was considered that, while a number of impurities may be present in a reaction, the most difficult to analyse for, yet most likely to have a significant effect on the outcome of a crystallisation, were traces of organic or seed material. Although the laboratory area was frequently cleaned, it is likely that the work environment contained small amounts of microscopic zeolite dust from many years efforts. Indeed, it is believed that this situation may be typical of many zeolite laboratories, both academic and industrial. Despite this, great care was taken to avoid such effects and apparently adventitious results were subjected to thorough investigation.

The 500 cm^3 stainless-steel autoclaves used in the present study had been used on a number of occasions to crystallise ZSM-5, both with and without an organic structure directing agent present. Thus before any work started, each autoclave was thoroughly cleaned with potassium hydroxide solution. Indeed, an important objective of this work was to find a method of cleaning together with a possible test reaction that would ensure that the reaction vessel was free from any organic material or seed impurity. The subsequent investigation of the inorganic potassium system under carefully controlled conditions, led to the discovery of such a test reaction, the *Scavenging Reaction*, which was found to be, among other things, a

sensitive detector of organic and seed material. This remarkable reaction will be discussed in Chapter 4.

In the present study, crystallisations were carried out from stirred reaction mixtures. A lower temperature (423 K) than has been used previously [209,210, 211,212] was employed to ensure that metastable zeolitic phases would be observed before any product over-run. It was thought that such an investigation under *ultrapure* conditions would allow for the conflicting results reported in the studies described above to be resolved.

3.2 Experimental

Reaction mixtures based on the composition:

$$y\ K_2O\ x\ Al_2O_3\ 60\ SiO_2\ 3000\ H_2O,$$

where $5 < y < 20$ and $0 < x < 2$, were prepared as described in Chapter 2. Crystallisations were carried out at 423 K in stirred autoclaves (300 rpm) and reactions terminated after 7 days, unless otherwise stated. Samples were taken during the course of each reaction and processed as described in Chapter 2.

3.2.1 Effect of Gel Aging

The composition:

$$10\ K_2O\ 1\ Al_2O_3\ 60\ SiO_2\ 3000\ H_2O,$$

was aged at 368 K for different times to establish if such pre-treatment would affect the outcome of the crystallisation.

Gels were prepared in 1 litre polypropylene bottles and placed in a pre-heated oven at 368 K with the lids slightly loose to avoid any build up of pressure as the gel was heated. After 10 minutes the lids were tightened and the bottles left

in the oven for several weeks. The bottles were weighed weekly and any weight loss made up by adding pre-heated ultrapure water. This generally amounted to a weekly addition of about 10 cm^3.

3.2.2 Effect of Sodium Cations

Since ZSM-5 has been shown [143] to crystallise readily from the composition:

$$10\ Na_2O\ 1\ Al_2O_3\ 60\ SiO_2\ 3000\ H_2O,$$

it was argued that if sodium cations were effective ZSM-5 structure directors, an increase in the amount of sodium in the corresponding potassium composition would promote the crystallisation of ZSM-5. Thus, the composition:

$$(10\text{-}y)\ K_2O\ y\ Na_2O\ x\ Al_2O_3\ 60\ SiO_2\ 3000\ H_2O,$$

where y = 1 and 3, and x = 0.667 and 1, was investigated under the reaction conditions described above.

Gels were prepared as described in Chapter 2, with the exception that the aluminium wire was dissolved in a mixture of the two hydroxides. Another hand-held blender was used for these reactions to avoid cross contamination.

3.3 Results and Discussion

The products obtained from the system

$$y\ K_2O\ x\ Al_2O_3\ 60\ SiO_2\ 3000\ H_2O,$$

where $5 < y < 20$ and $0 < x < 2$, crystallised for 7 days in stirred (300 rpm) autoclaves at 423 K are shown in Figure 3–1. Details of the reactions are given in Table 3–1 and are further summarised in Table 3–2. The sodium concentration (mg l^{-1}) in the liquid phase of samples collected during the reaction was found to be approximately equal to y/2, where:

$$Na_{soln}\ (mg\ l^{-1}) \simeq \frac{y}{2}$$

and it is thought that such low levels would not affect the outcome of the crystallisations. Indeed the [K/Na] ratio in the reaction mixture was always > 1000. For most compositions, crystallisation did not occur readily and the samples obtained were amorphous or contaminated with a substantial amount of amorphous material. At the lowest base levels ($OH/SiO_2 = 0.10$) and highest alumina content ($Al/SiO_2 = 0.067$) investigated, the mixture remained amorphous even after 8 weeks at 423 K whereas at the highest base level investigated ($OH/SiO_2 = 0.60$), a mixture with the same high alumina content gave the feldspar microcline and zeolite K-H [213], thus resembling an aluminous reaction mixture. Although zeolite K-H was present in substantial quantities after 3 days of reaction, none was detected after 6 days (Figure 3–2).

Many of the compositions gave an unknown material (designated U1) which although crystalline, was thermally unstable (Figure 3–3). It was always contaminated with amorphous material and for $OH/SiO_2 = 0.27$ - 0.31, kenyaite was also present.

Examination of U1 by SEM shows that it has a platey morphology and is likely to be a layer-lattice material (Figure 3–4). The X-ray powder diffraction pattern shows some similarities to kenyaite, a layered silicate material. The diffraction data for U1 and kenyaite are shown in Table 3–3. It is possible that this material is a collapsed form of kenyaite, which would perhaps account for the absence of the initial high basal spacing line at 1970 pm. SEM coupled with energy dispersive X-ray analysis[1] (SEM/EDX) showed U1 to have a SiO_2/Al_2O_3 ratio of approximately 40. Thus U1 is an aluminosilicate material, unlike kenyaite which is essentially all silica.

Only one aluminium-free composition ($OH/SiO_2 = 0.5$) was investigated (B37). This gave a mixture of quartz, cristobalite and the potassium silicate $KHSi_2O_5$ [214].

---

[1]Courtesy of ICI C & P Ltd., Wilton

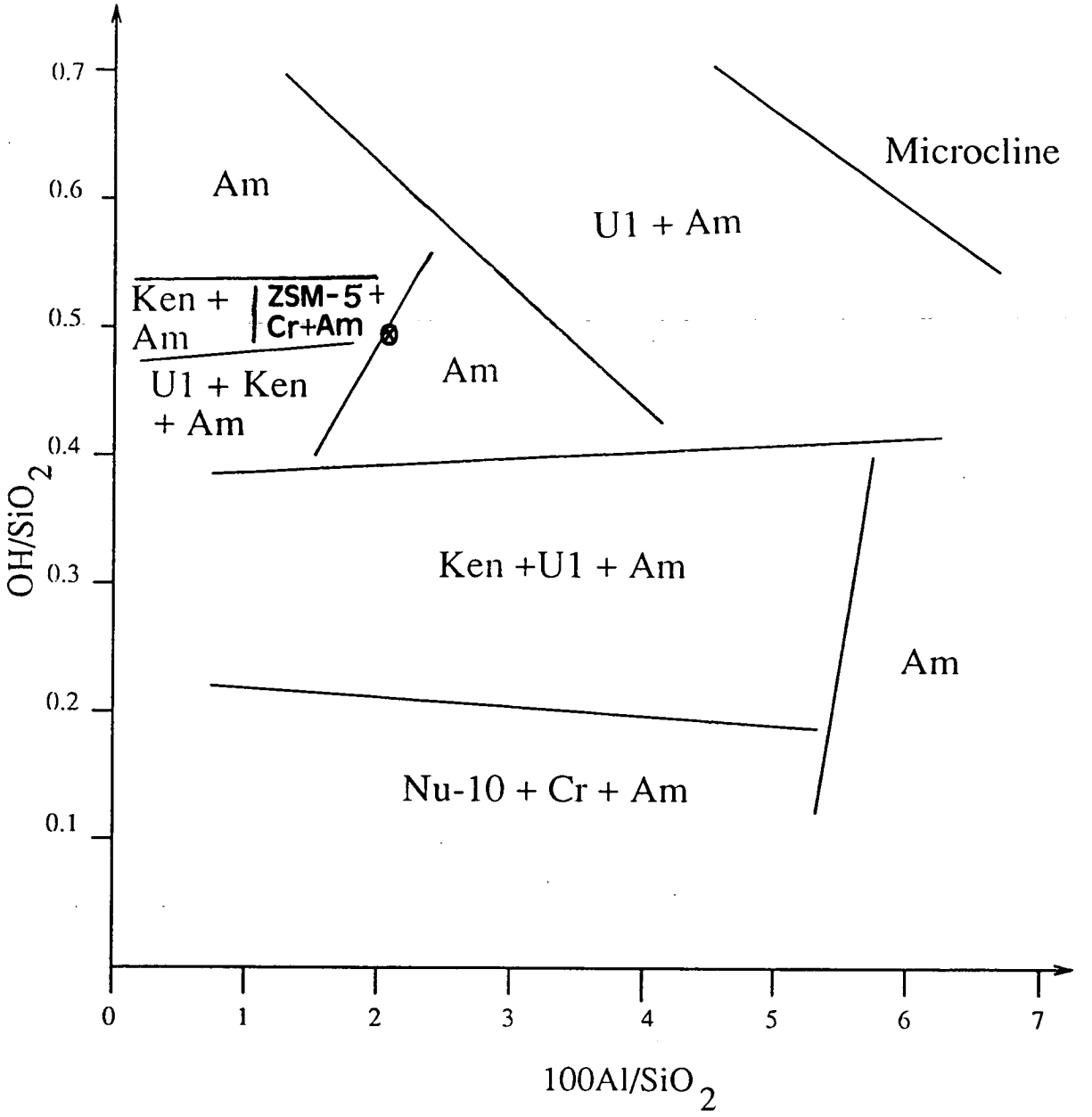

Figure 3–1: Phase diagram showing the crystallisation fields for the composition y K_2O x Al_2O_3 60 SiO_2 3000 H_2O, where $5 < y < 20$, $0 < x < 2$; (423 K, 7 d, 300 rpm)

Table 3–1: Reaction mixture compositions and products at 423 K

Run No	Molar Composition[a] y K_2O	x Al_2O_3	Run Time (h)	Products[b]
A15	5	0.667	122	NU-10 + Am
			164	NU-10 + Cr + Am
B32	5	1	168	NU-10 + Cr + Am
B33	5	2	167	Am
B52	5	2	1339	Am
A157	10	0.333	161	Ken + U1[c] + Am
A8	10	0.667	166	Ken + U1 + Am
B17	10	1	166	Ken + U1 + Am
A9	10	2	163	Am
B134	12.5	0.5	162	Am
A153	13	0.667	161	Am
B133	13	1	161	Am
A174	13.5	0.333	164	Ken + U1 + Am
B138	14	0.6	157	Am
B37	15	0	147	$KHSi_2O_5$ + α - Quartz + Cr
A41	15	0.1	167	Ken + Am
B42	15	0.2	167	Ken + Am
B27	15	0.333	162	Ken + U1 + ZSM-5 + Am
A36	15	0.5	140	ZSM-5 + Am
			171	ZSM-5 + Cr + Am
A10[d]	15	0.667	90	ZSM-5 + Am
B13	15	0.667	167	Am
A25	15	0.667	167	Am
A155	15	0.8	94	Am
A11	15	1	163	U1 + Am
A12	15	2	162	U1 + Am
A130	17	0.667	161	Am
B125	17	0.8	149	Am
A161	17	1.5	166	U1 + Am
B135	18.5	0.333	88	Am
B29	20	0.667	169	U1 + Am
B24	20	1	96	U1 + Am
			167	U1 + Microcline + Am
B31	20	2	78	Microcline + zeolite K-H
			147	Microcline

[a]Composition: y K_2O x Al_2O_3 60 SiO_2 3000 H_2O

[b]Key: Am = Amorphous; Cr = Cristobalite; Ken = Kenyaite

[c]U1 = Unidentified material, a potassium silicate probably related to kenyaite

[d]Reaction probably contaminated with a trace of seed or organic material (see text)

Table 3–2: Summary of products[a] obtained after 7 days from the potassium system

		Al_2O_3	0.500	0.667	1.000	2.000
		Al/Si	0.017	0.022	0.033	0.067
		Si/Al_2	120	90	60	30
K_2O	OH/SiO_2[b]					
20	0.667		-	U1 + Am	U1 + Microcline + Am	Microcline
15	0.500		ZSM-5 + Cr + Am[c]	ZSM-5[d] + Am	U1 + Am	U1 + Am
				Am[e]	-	-
				Am[f]	-	-
10	0.333		-	Ken + U1 + Am	Ken + U1 + Am	Am
5	0.167		-	NU-10[g] + Cr + Am	NU-10[h] + Cr + Am	Am

[a]U1 = unidentified material; Cr = Cristobalite; Am = Amorphous

[b]No account taken of Al_2O_3

[c]A36, [d]A10, [e]B13, [f]A25, [g]A15, [h]B32.

Figure 3–2: XRPD patterns for products crystallised at 423 K from the composition 20 K_2O 2 Al_2O_3 60 SiO_2 3000 H_2O (B31) at t = 72 h (top) and t = 147 h (bottom)

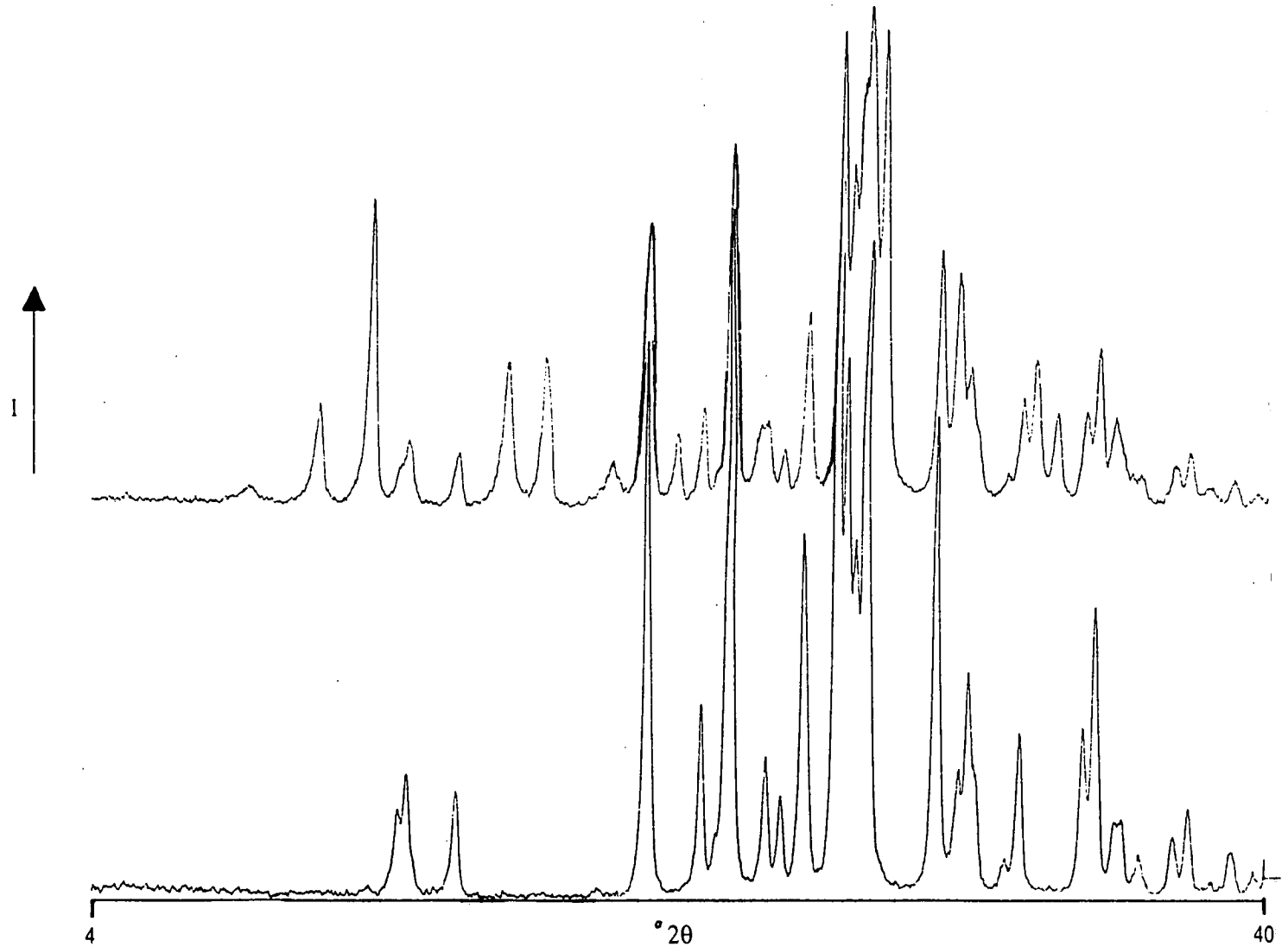

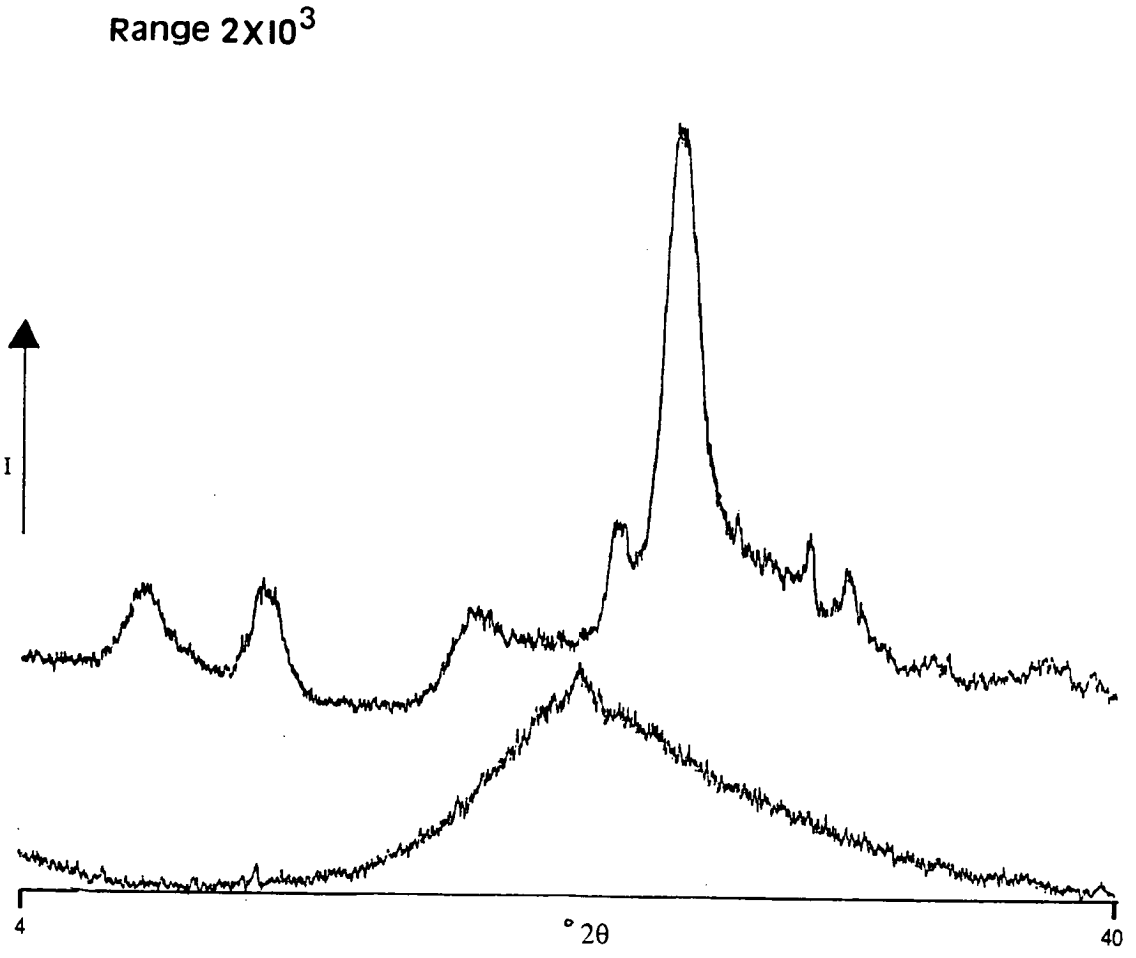

Figure 3–3: X-ray diffraction patterns of U1 (sample A11), as-synthesised (top) and after heating to 1173 K (bottom)

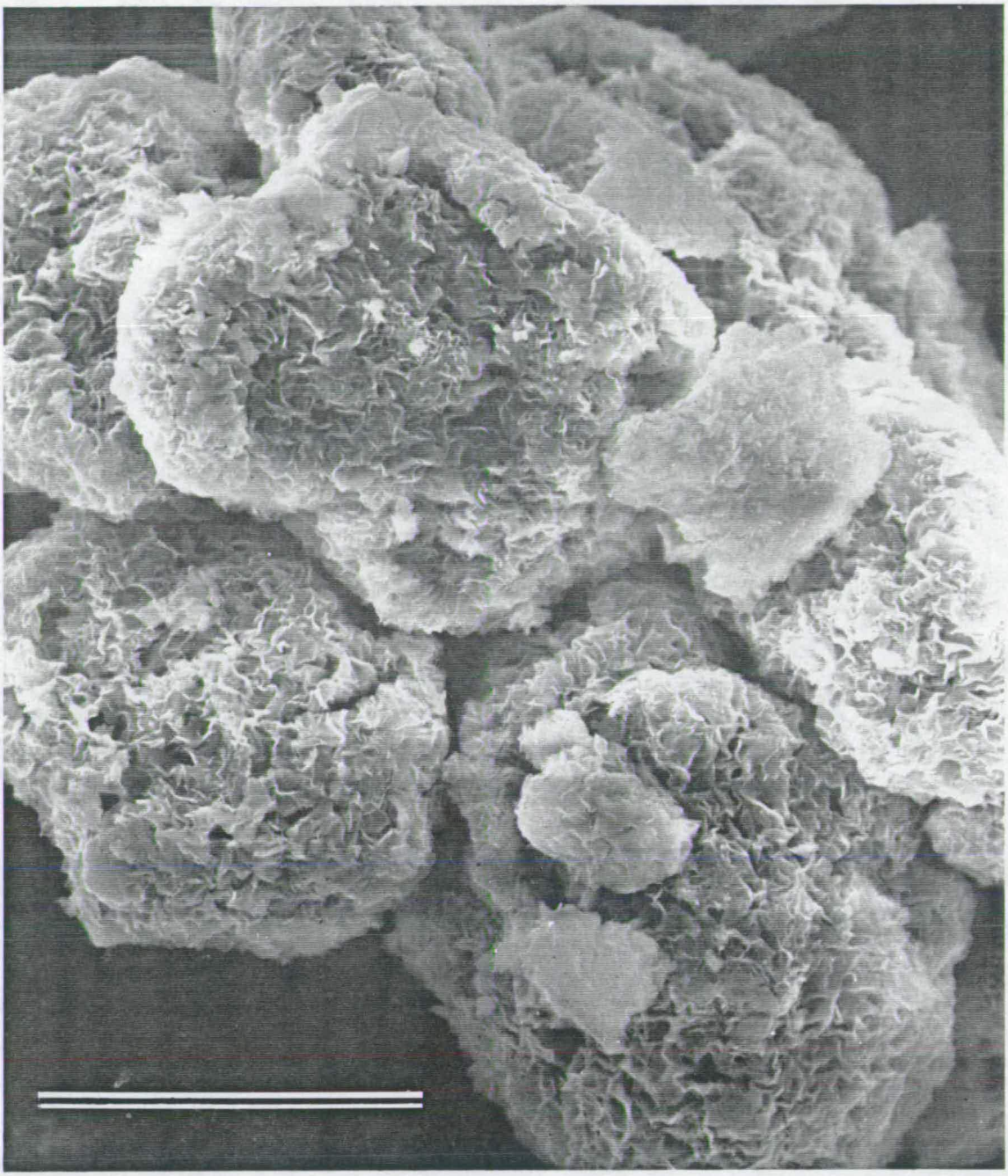

Figure 3–4: SEM photomicrograph of U1 (sample A11) showing the platey morphology commonly found with kenyaite (Bar = 15 μm)

Table 3–3: X-ray diffraction data for U1 (sample A11) and kenyaite

U1 (sample A11)		**Kenyaite**[a]	
d / pm[b]	**100I/I$_o$**[c]	**d / pm**	**100I/I$_o$**
-	-	1970	100
994	17	995	50
-	-	778	2
692	19	662	6
-	-	564	8
-	-	514	12
-	-	497	35
458	14	469	30
-	-	447	6
-	-	395	10
-	-	375	6
368	38	364	20
-	-	353	20
344	100	343	85
-	-	332	45
-	-	320	55
293	37	293	14
276	34	283	12
263	13	265	4
-	-	252	4
-	-	248	4
238	11	242	6
230	12	234	8

[a]Reference [215]

[b]Only d values within 30 pm are shown on the same line

[c]Relative intensity / % (*i.e.* relative to the most intense peak)

The only high-silica zeolites formed were K-NU-10 and K-ZSM-5. Unlike previous workers [209,210,211,212] no ferrierite or mordenite was detected; this may have been due to the lower temperature used in this study, together with the very low concentration of sodium ion impurities in the reaction mixtures. The K-NU-10 was formed at low base levels ($OH/SiO_2 < 0.14$) as reported in earlier work [165, 216] and was contaminated with cristobalite (samples A15 and B32), even when the crystallisation was repeated at a lower temperature (A28, 403 K). Examination of sample A15 by SEM showed the typical needle-like morphology (Figure 3–5) of NU-10. The fact that other workers [209,210,211,212] did not crystallise NU-10 in their potassium systems can be attributed to the higher temperatures used in their studies. X-ray diffraction data for sample A15 is given in Table 3–4. K-ZSM-5 was found to crystallise over a very narrow range of base levels ($OH/SiO_2 = 0.48$ - 0.49), somewhat higher than the optimum base levels (0.25 - 0.39) [217] for the crystallisation of Na-ZSM-5.

It is noteworthy that NU-10 and ZSM-5 form at similar SiO_2/Al_2O_3 ratios and whether one or the other forms depends primarily on the OH/SiO_2 ratio, *i.e.* the more open structure requires a higher base level, which gives a higher degree of aluminosilicate depolymerisation.

One problem encountered at high base levels was that reactions that gave K-ZSM-5 separated into solid and liquid phases early in the reaction (< 3 days) and the solid collected on the wall of the vessel and stirrer shaft at the liquid surface. This effect was most pronounced for the gel composition:

$$15\ K_2O\ 0.667\ Al_2O_3\ 60\ SiO_2\ 3000\ H_2O$$

(the *Scavenging Reaction* - see Chapter 4) which was found to behave in an apparently irreproducible fashion. The first time the crystallisation of this composition was attempted (A10), the product obtained was very unusual, comprising of free-flowing sphere-like particles (Figure 3–6).

This was a most unexpected finding made more exciting by the discovery that *spheres* contained small amounts of ZSM-5 ($\sim$ 17 %). Several attempts were

Figure 3–5: SEM photomicrograph of sample A15, showing crystals with needle-like morphology, commonly found with NU-10 together with traces of cristobalite (Bar = 3 μm)

Table 3–4: X-ray diffraction data for samples A15 and NU-10 [218]

Sample A15[a,b]		**(H, Na)NU-10**	
d / pm	**100I/I_o**[c]	**d / pm**	**100I/I_o**[d]
1098	76	1095	m - s
876	14	880	w - m
703	12	699	w - m
544	11	541	w
438	80	438	vs
368	100	369	vs
664	76	363	vs
347	35	348	m - s
334	13	336	w
252	33	253	m
244	14	244	w

[a]Crystallised from the composition: 5 K_2O 0.667 Al_2O_3 60 SiO_2 3000 H_2O

[b]Product also gave a major peak due to cristobalite at d = 411 pm

[c]Relative intensity / % (*i.e.* relative to the most intense peak)

[d]Key:

w = weak (I/I_o in the range 0 - 20)

m = medium (I/I_o in the range 21 - 40)

s = strong (I/I_o in the range 41 - 60)

vs = very strong ($I/I_o > 60$)

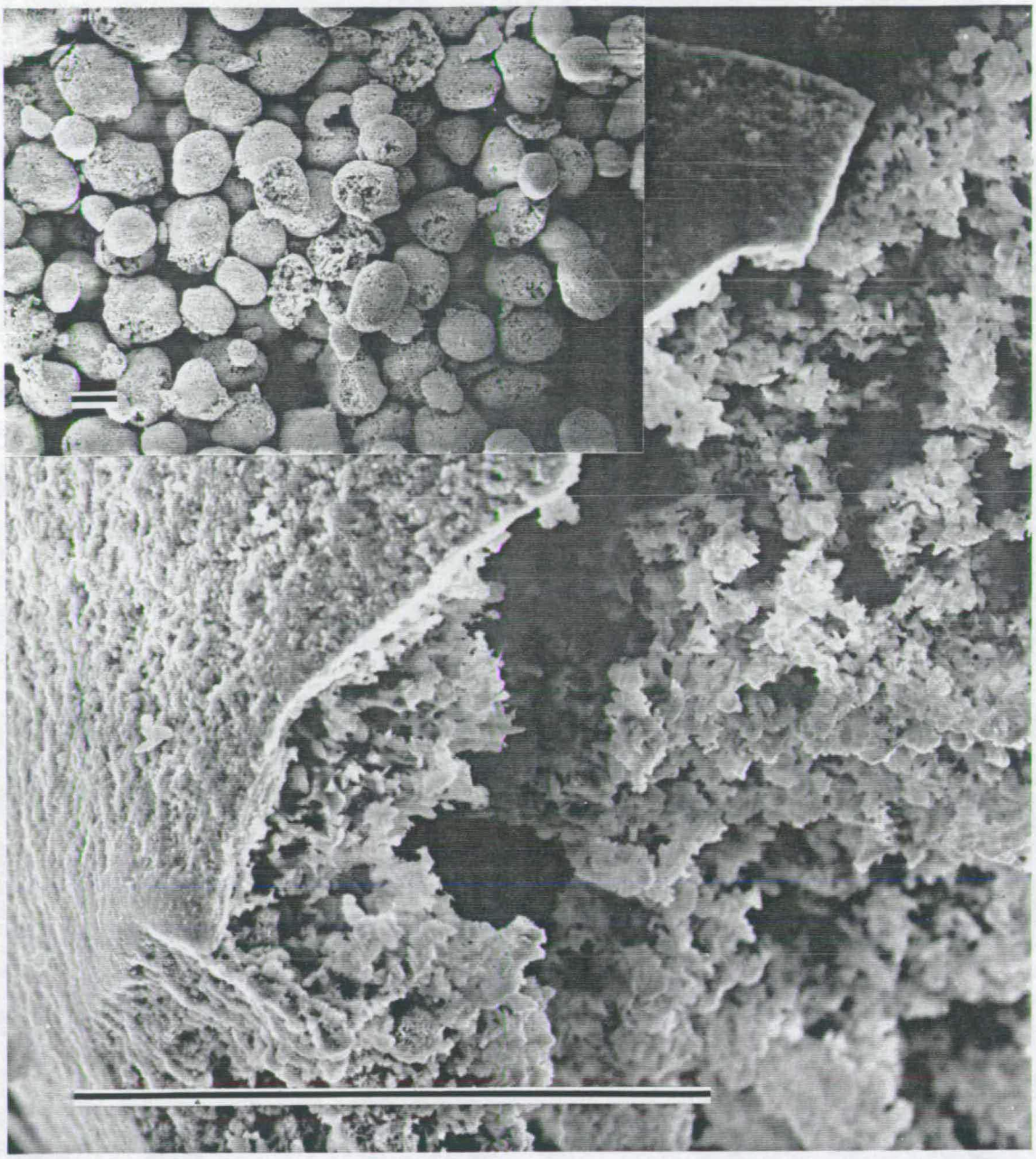

Figure 3–6: SEM photomicrographs of the unusual sphere-like particles obtained from the composition 15 K_2O 0.667 Al_2O_3 60 SiO_2 3000 H_2O (A10) (Bar = 50 μm)

made to repeat the synthesis (*eg.* reaction nos. B13, A25). However, neither spheres nor ZSM-5 was obtained, the solid and liquid phases simply separated, with the amorphous solid accumulating around the rim of the vessel and stirrer shaft as already described. It was subsequently discovered that this composition would crystallise ZSM-5 only in the presence of certain impurities. This finding prompted a more detailed investigation, which, because of its importance, will be discussed in the following chapter. The motivation for this investigation was the possibility that this composition could be used as a sensitive detector for traces of organic impurities and seed material.

The range of compositions that give K-ZSM-5 was restricted to OH/SiO_2 = 0.48 - 0.49 and a narrow range of Al/SiO_2 ratios ($0.011 < Al/SiO_2 < 0.017$), and even for these the 6-day product was contaminated with cristobalite and much amorphous material. At lower alumina levels the only crystalline phase obtained was the layered-silicate, kenyaite. The possibility that the reactions other than the *Scavenging Reaction* which crystallised ZSM-5 may have been seeded was investigated and will be described in the next chapter.

The amount of solid (amorphous + crystalline) recovered were somewhat lower than obtained in typical sodium systems and, not surprisingly, decreased as the base content of the reaction mixture was increased. Approximate yields based on the amount of silica and alumina used and the solid recovered were 50% (y = 5), 40% (y = 10), 30% (y = 15), and 20% (y = 20).

3.3.1 Effect of Gel Aging

The results of gel aging are shown in Table 3–5. No significant change in the crystallisation kinetics or the nature of the product obtained was observed for the gel composition:

$$10\ K_2O\ 1\ Al_2O_3\ 60\ SiO_2\ 3000\ H_2O,$$

aged for up to 3 weeks at 368 K. The product obtained was invariably the unknown phase U1 and kenyaite, contaminated with much amorphous material. Perhaps the

Table 3–5: Effect of gel aging at 368 K on the composition 10 K_2O 1 Al_2O_3 60 SiO_2 3000 H_2O

Run No	Time Aged / d	Run Time / h	Products
B17	0	166	Kenyaite + U1[a] + Amorphous
B18	7	163	Kenyaite + U1 + Amorphous
B19	14	163	Kenyaite + U1 + Amorphous
B20	21	163	Kenyaite + U1 + Amorphous

[a]Unknown phase (see Table 3–1)

most notable observation was the separation of the amorphous gel into solid and liquid phases during the aging process. This probably occurs in the same way as the stirred reactions mentioned above. Phase separation is not uncommon in alkali metal aluminosilicate reaction mixtures [219]. Indeed, it has been shown that, in sodium aluminosilicate systems at high base levels, the range of compositions over which solutions can be obtained free of any gel solid is considerably smaller than for quaternary ammonium aluminosilicate reaction mixtures [220]. Clearly the effect of aluminium on the solubility of silica [103] is also of considerable importance. Phase separation will be discussed in more detail in Chapter 4.

The composition 15 K_2O 0.5 Al_2O_3 60 SiO_2 3000 H_2O (A36) which was found to crystallise K-ZSM-5 (contaminated with amorphous material) was also aged at 368 K for several weeks. Again the gel phase separated on aging. However, crystallisation of this aged gel (A48) did not give ZSM-5. Instead, a mixture of kenyaite, tridymite, and quartz was obtained which was contaminated with much amorphous material. Clearly, aging this reaction mixture alters the character of

the gel sufficiently to suppress the crystallisation of K-ZSM-5 and promote the crystallisation of dense silicate phases. Thus the gel can no longer nucleate ZSM-5. Alternatively, if the crystallisation of K-ZSM-5 observed with the non-aged gel (A36) had been caused by undetected impurities, *eg.* seeds (see Chapter 4), then it may be that, following aging, the gel is unable to promote growth of ZSM-5 and in effect loses its ability to *detect* seed impurities. The effect of aging inorganic sodium gels was investigated for completeness. The results are summarised in the Appendix.

3.3.2 Effect of Sodium Cations

The results of reactions carried out with the composition:

$$(10\text{-}x)\ K_2O\ x\ (Na_2O)\ 1\ Al_2O_3\ 60SiO_2\ 3000H_2O$$

are given in Table 3–6. All compositions failed to crystallise anything other than kenyaite, U1, quartz or cristobalite.

The fact that ZSM-5 did not crystallise readily in the potassium system despite fairly large additions of sodium cations, suggests a number of possibilities:
i) The *success* of the sodium system depends not only on the base level and the SiO_2 / Al_2O_3 ratio of the gel, but also that a substantial amount of the base is provided by sodium. This implies that the sodium is required in a far greater excess than needed to merely occupy the ZSM-5 channel system.
ii) The structure directing ability of sodium is masked or inhibited by the presence of potassium cations.
iii) Competition between the cations for aluminosilicate species alters the distribution of these species in the reaction mixture, compared to the corresponding monocationic gels, thus inhibiting the nucleation of ZSM-5.
iv) Sodium cations do not nucleate ZSM-5 in the absence of an organic structure directing agent.
When sodium cations are included in the potassium reaction mixture there is a significant change in the appearance of the gel. Thus a change in gel chemistry

Table 3–6: Effect of sodium cations

Run	Molar Composition					Run	Products
No	Na_2O	K_2O	Al_2O_3	SiO_2	H_2O	Time / h	
A57	1	9	1	60	3000	72	Kenyaite + Quartz
						242	Quartz + Cristobalite
A62	3	7	1	60	3000	91	Kenyaite + Quartz
						237	Quartz + Cristobalite
A68	1	9	0.667	60	3000	141	Kenyaite + U1[a]
A69	3	7	0.667	60	3000	146	Kenyaite + U1

[a]Unknown phase (see Table 3–1)

would adequately account for the results in Table 3–6. However, while these results may not be unexpected, it does raise the question as to the ability of sodium cations to act as a structure directing agent for ZSM-5. This will be discussed further in Chapter 4.

3.4 Conclusions

The conditions used here to study the potassium system are those which by analogy with the sodium system are perhaps the most likely to give high-silica zeolites. It is clear from the results described above that in the absence of organic species the potassium system is considerably less favourable to the formation of high-silica zeolites than the corresponding sodium system. Even the addition of substantial amounts of sodium cations to certain gels failed to direct the crystallisation to ZSM-5. Quiescent aging of the reaction mixture was also found to be ineffective. Indeed, the composition:

$$15\ K_2O\ 0.5\ Al_2O_3\ 60\ SiO_2\ 3000\ H_2O,$$

(A36) which was found to crystallise K-ZSM-5, failed to crystallise ZSM-5 from the aged gel (A48).

Many crystallisations have been carried out with reaction mixtures that contain an organic structure directing agent as well as substantial amounts of sodium cations. Given that ZSM-5 crystallises readily from the inorganic sodium system, it is not surprising that ZSM-5 is the product most frequently obtained. Thus, it can be argued that, since the potassium system does not favour the formation of ZSM-5, this may be a better system in which to examine organic structure directing agents.

The very small range of compositions over which K-ZSM-5 can be crystallised is consistent with the results reported by Bellussi *et al.* [212], although the product was obtained at much higher base levels and was contaminated with much amorphous material.

The discovery that the composition:

$$15\ K_2O\ 0.667\ Al_2O_3\ 60\ SiO_2\ 3000\ H_2O,$$

(the *Scavenging Reaction*) would crystallise ZSM-5 only in the presence of seed or organic impurities suggests that the two compositions from which ZSM-5 was crystallised (B27 and A36) may also have been seeded. That these appeared to crystallise more readily than the *Scavenging Reaction* may simply be due to a difference in sensitivity to these impurities. Thus it is quite possible that the crystallisations reported by Bellussi *et al.* [212] may also have been caused by undetected impurities. It is also possible that similar effects may have gone undetected in the Nastro studies [209,210,211], where the formation of ZSM-5 may have been missed due to the high reaction temperatures used.

Chapter 4

The *Scavenging Reaction*

4.1 Introduction

It was mentioned in Chapter 3 that the composition:

$$15\ K_2O\ 0.667\ Al_2O_3\ 60\ SiO_2\ 3000\ H_2O,$$

was found to behave in an apparently irreproducible fashion. As can be seen from the phase diagram (Figure 3–1) this composition does not normally crystallise. However, the first time this reaction was carried out, the solid phase formed sphere-like particles which were found to contain a small amount of ZSM-5 (A10). When this run was repeated only hard amorphous lumps were obtained; this suggested that the crystallisation of ZSM-5 was possibly initiated by a trace of some impurity; probably organic or seed material in the the reaction vessel. Furthermore, it was thought that, in the case of contamination by organic impurities, it should be possible to remove (*scavenge*) these last traces by repeated attempts to crystallise the gel and thus obtain a completely organic-free reaction vessel; an important objective of this study.

An investigation to establish whether or not the *Scavenging Reaction* would only crystallise ZSM-5 and, therefore, be sensitive only to those organics that promote its crystallisation, allowed further ideas on the role of organics in the synthesis of high-silica zeolites, particularly ZSM-5 to be developed.

This chapter then, describes the detailed investigation carried out with the *Scavenging Reaction*, which resulted in the discovery of several novel applications.

Perhaps most significant, were results that allowed hypotheses to be made about the crystallisation of ZSM-5 from inorganic reaction mixtures, in particular, the ability of sodium cations to direct ZSM-5.

One of the problems encountered in the potassium system (Chapter 3) was the separation of the solid and liquid phases early in the reaction (< 3 days). This effect was most pronounced for the Scavenging Reaction. Thus, the chapter begins with an account of the attempts made to overcome the phase separation problem.

4.2 Experimental

4.2.1 Phase Separation

Several attempts were made to overcome the problem of phase separation:

1) Reaction A26

Potassium hydroxide was dissolved in ultrapure water ($\sim$ 17 g). Approximately half of this was added to the silica/water slurry and the other half used to dissolve the aluminium wire. The silica/water/hydroxide slurry was thoroughly mixed, placed in a 500 cm^3 stainless-steel autoclave and heated to 423 K, at which point the heater was set to trip. The mixture was allowed to cool naturally to room temperature before dismantling the autoclave and adding the alumina/hydroxide solution. The resulting gel was thoroughly mixed using a hand-held blender before re-assembling the autoclave and continuing the synthesis (423 K).

2) Reaction A35

The gel was prepared as described in Chapter 2 and placed in a water bath at 298 K for 7 days. The now virtually clear liquid was heated at atmospheric pressure to boiling point with occasional blending. This process was continued for about 1 hour until the liquid had become quite turbid (appearance similar to that of a thin wall paper paste). Hot ultrapure water was added to make up for the small weight loss. With the temperature of the mixture at 343 K, the autoclave was assembled and the reaction continued at 423 K.

3) Reaction B46

The gel was prepared as described in Chapter 2 and charged to a 500 cm^3 stainless-steel autoclave. The gel was heated to 338 K and stirred at 300 rpm. After 24 hours the autoclave was dismantled and the contents transferred to a polypropylene beaker where it was subjected to ultrasonic treatment for several minutes to break up the few gelatinous lumps that had formed. The autoclave was reassembled and heated at 363 K for 65 hours then dismantled once more. The contents were again placed in a clean polypropylene beaker and thoroughly blended for 5 minutes. The autoclave was reassembled and heated at 393 K for 24 hours followed by 25 hours at 403 K. Following this last heating step, the autoclave had to be dismantled again. However, this was because of a blockage in the dip-tube which could not be cleared with the high-pressure air line. The autoclave was reassembled and the reaction continued at the synthesis temperature of 423 K.

4.2.2 Procedure for Stirred Reactions

Gels were prepared as described in Chapter 2. Reactions were carried out at 423 K in 500 cm^3, 1000 cm^3 stainless-steel autoclaves (Baskerville and Lindsay Ltd.) and 125 cm^3 PTFE-lined Parr type 4748 bombs (Parr Instrument Company, Illinois, USA). A full description of these reaction vessels is given in Chapter 2. The amount of gel charged into these vessels was approximately 400, 700 and 50 g respectively.

4.2.3 Procedure for Static Reactions; Determination of *Detection Limits*

To test a large number of impurities in the *Scavenging Reaction* it was necessary to use a range of small reaction vessels. Although these did not allow the reaction to be agitated, preliminary tests showed that ZSM-5 would crystallise provided an impurity was present.

The gel (400 g) was prepared as described in Chapter 2. A calculated amount of impurity (either an organic compound or zeolite seed) was carefully weighed into a small glass sample bottle and then transferred to a 30 cm^3 PTFE-lined stainless-steel bomb. Any material remaining in the sample bottle was washed into the bomb with gel using a Pasteur pipette. The bomb was then charged with sufficient gel ($\sim$ 20 g) to give the desired concentration of impurity (mg kg^{-1}, based on the weight of impurity and gel) and placed in a pre-heated oven at 423 K for 6 days.

Preparation of gels with larger amounts of organic material

Crystallisation of the compositions:

$$15\ K_2O\ 20(Q)\ 0.667\ Al_2O_3\ 60\ SiO_2\ 3000\ H_2O$$

and

$$5\ K_2O\ 10(Q)\ 2\ Al_2O_3\ 60\ SiO_2\ 3000\ H_2O,$$

where Q = organic reagent, was investigated for a number of organic materials. Gels were prepared as follows:
Fumed silica was weighed into a polypropylene bottle (150 cm^3) and sufficient ultrapure water added to make a slurry, solution A. The bottle was sealed and vigorously shaken for a few seconds. Aluminium wire was added to another polypropylene bottle which contained a 50 % (wt/wt) solution of potassium hydroxide, solution B. Solution B was added to solution A as the contents vigorously shaken for 2 minutes. The organic component was carefully weighed into a plastic sample vial (10 cm^3) and dissolved in the minimum of ultrapure water. The contents of the vial were then added to the bottle containing the aluminosilicate gel, together with the remaining water to give the desired weight of gel (50 g). The reaction mixture was vigorously shaken for 5 minutes to ensure thorough mixing. The gels were also tumbled for a further 20 minutes before transfer to the 30 cm^3 PTFE-lined bombs. Reactions were carried out at 423 K without agitation for 6 days.

Effect of sodium impurities

Several crystallisations were carried out under the reaction conditions described above to test the effect of increasing sodium concentration in the *Scavenging Reaction.* Reaction mixtures were prepared as described in Chapter 2 with the exception that the aluminium wire was dissolved in a solution of a mixture of potassium and sodium hydroxides and no organic reagent was used.

4.3 Results and Discussion

4.3.1 Phase Separation

Attempts to prevent the phase separation of the composition:

$$15\ K_2O\ 0.667\ Al_2O_3\ 60\ SiO_2\ 3000\ H_2O$$

by altering the mixing/heating of the gel (A26, A35, and B46) were completely unsuccessful (Table 4–1). All reactions phase separated and no crystalline material was obtained.

The solution phase silicon and aluminium concentrations were determined by atomic absorption spectrophotometry[1] for a number of samples taken during another series of stirred reactions (Table 4–2). These results show that the aluminium concentration in the solution phase decreased dramatically within the first day of the reaction, from about 600 mg l^{-1} in the initial gel to < 5 mg l^{-1}, and thereafter decreased slowly until the solution phase was virtually aluminium-free (Figure 4–1).

[1]Courtesy of the Department's analytical group

Table 4–1: Effect of modifying the gel preparation and / or synthesis conditions of the *Scavenging Reaction*

Run No	Reaction Modification[a]	Run Time / h	Phase Separation	Products
A26	Aluminate added to silica / hydroxide, which had been heated to 423 K	162	Yes	Amorphous
A35	Gel aged at 298 K (7 d) then heated to about 373 K until turbid	233	Yes	Amorphous
B46	Stepwise heating and cooling with regular blending of the gel	257	Yes	Amorphous

[a] All reactions ultimately carried out at 423 K

Table 4–2: Change in solution phase silica and alumina concentrations during synthesis of the *Scavenging Reaction*

Run No	Run Time (h)	Conc$^{n.}$ / mg l^{-1}		Si/Al
		10^4Si	Al	
A25[a]	0	4.98	91.20	530
	29	3.34	3.35	9600
	54	2.66	4.03	6350
	73	4.46	3.02	14230
	96	3.18	2.86	10710
	120	5.28	2.95	17240
A163[b]	0	2.74	98.10	270
	28	2.82	2.20	12350
	48	2.74	1.82	14500
	120	2.44	1.51	15560
	139	2.58	0.95	26160
A172[c]	0	2.64	99.00	260
	1	4.52	7.97	5460
	21	3.34	2.14	15030
	45	3.16	2.33	13060
	65	4.80	2.41	19180
	87	4.38	1.10	38350
	109	3.72	0.50	71660
	143	2.84	0.50	54710

[a]Final product was amorphous

[b]Gel contained 25 mg kg^{-1} TPA-ZSM-5 seed; ZSM-5 *spheres* obtained

[c]Gel contained 25 mg kg^{-1} TPABr; ZSM-5 *spheres* obtained

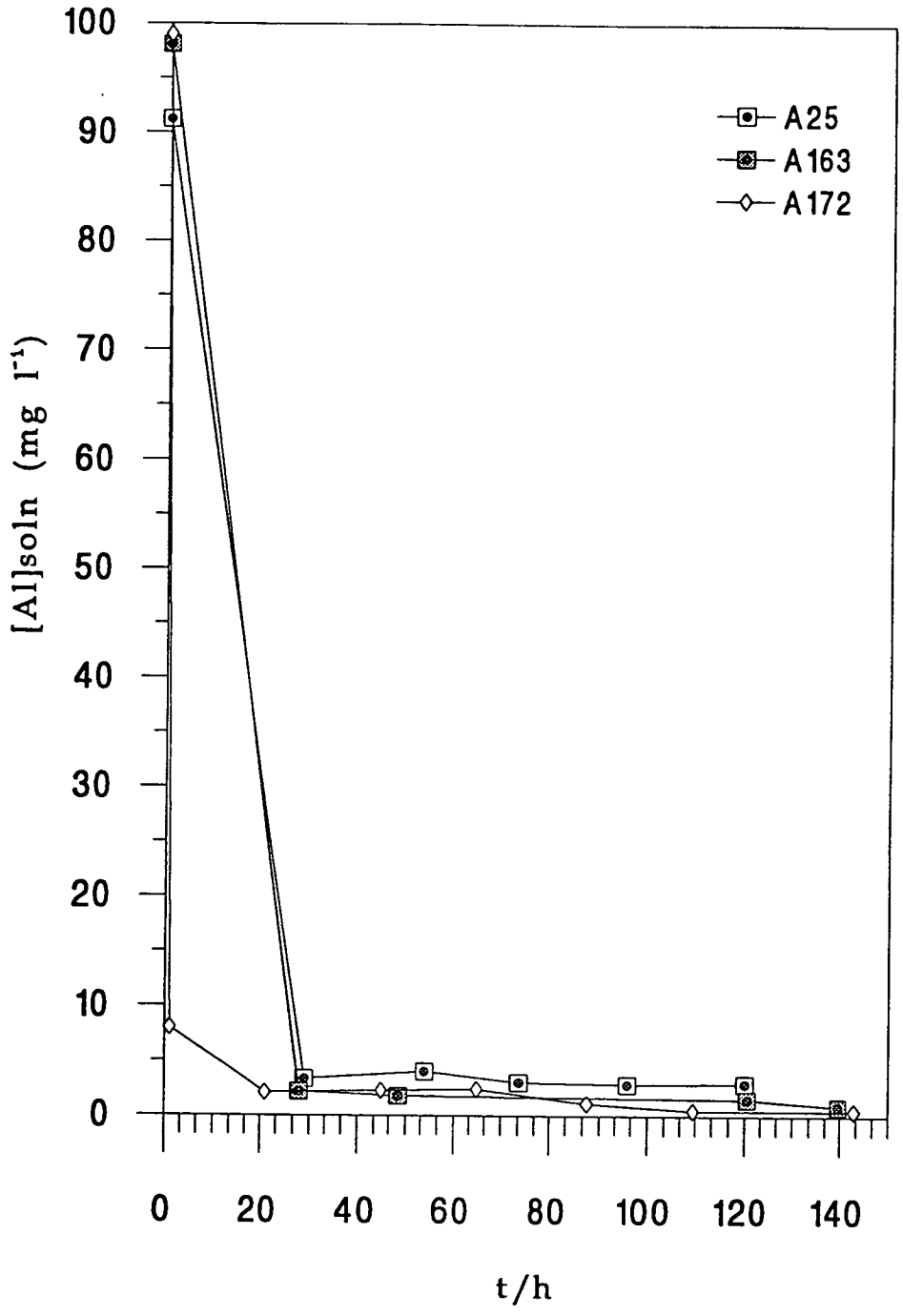

Figure 4–1: Change in the solution phase aluminium concentration with synthesis time

It should be recalled that a number of observations were made when working with this reaction mixture. The as-made gel:

(i) separated into a solid and liquid phase when heated to 423 K in stirred autoclaves

(ii) separated into a solid and liquid phase when heated at 368 K in non-agitated polypropylene bottles (aging experiments)

Furthermore it was found that the gel became virtually transparent on standing at room temperature (298 K). When this was heated to boiling point, a thin, translucent paste was formed.

A similar argument to that used to account for phase separation in the aging experiments (Chapter 3) can be used to account for that in the stirred reactions. On standing at room temperature, the unreacted gel dissolves, the extent of which will depend not only on the base level, but also the SiO_2/Al_2O_3 ratio in the reaction mixture. On heating, more gel dissolves, making it almost transparent. During this time, however, numerous polymerisation and depolymerisation processes take place, which results in a constant change in the solution phase chemistry. As more aluminosilicate oligomers are formed, there is a reduction in the solubility of the silica which ultimately leads to precipitation of virtually all the aluminosilicate species, leaving a solution phase composed almost entirely of silicate material (Table 4–2). It was also observed, with both static and stirred reactions, that the solid aluminosilicate phase had a tendency to exclude water. This suggests that it has a high degree of hydrophobic character, which would further suggest that the surface of the solid is composed predominantly of silica. It is also possible that much of this *hydrophobicity* is due to replacement of silanol protons with potassium cations. This restricts the ability of the gel to hydrogen-bond to the surrounding water. The relatively weak potassium hydration shell would favour strong interaction between the potassium cation and the aluminosilicate framework, *eg.*:

$$K^+ (H_2O)_n + AS^- (H_2O)_m \longrightarrow K\text{-}AS + (n + m)\, H_2O,$$

where AS = amorphous aluminosilicate phase.

This explanation would account for the aggregation of the solid phase on the stirrer

shaft and the wall of the reaction vessel at the liquid surface. The precipitation of the potassium aluminosilicate phase, thus starves the solution phase of nutrients may otherwise lead to the rapid crystallisation of a zeolitic phase. Indeed, it could well be that the tendency to phase separate makes crystallisation difficult in the potassium system.

That the corresponding aluminium-free reaction (B37) did not phase separate, clearly suggests that phase separation is linked to the aluminium content of the reaction mixture as well as the free-base level. These results, highlight the effect of aluminium on the solubility of silica.

4.3.2 Discovery of the *Scavenging Reaction*

It was thought that reaction A10 which gave ZSM-5 in the form of free-flowing *spheres* may have been contaminated with a trace of TPAOH, which nucleated ZSM-5. At the time this reaction was carried out, only one blender was available and this had recently been used to mix a gel that contained TPAOH. Although the blender was thoroughly cleaned, it was believed possible that it may have still contained a trace of TPA. To test this, an exact repeat of reaction A10 was carried out. The gel was mixed using a blender that had just been used to prepare a TPA-gel. Again the blender was thoroughly washed before preparing the organic-free gel. The repeat reaction (A45) proved to be quite successful in that a fine free-flowing material was obtained. The particles were much smaller than those obtained from A10, however, they contained substantially more ZSM-5. Differential thermal analysis (dta) of sample A45 showed a very small exotherm at approximately 673 K, which suggests the presence of organic material (Figure 4–2). As a result of this finding a new blender was bought for exclusive use in the preparation of potassium gels. It should be stressed that it is extremely unlikely that any of the other early potassium reaction mixtures were contaminated in this way, since only two gels were prepared that contained any organic component (C16 contained TPAOH and C23 contained TBAOH) during this period.

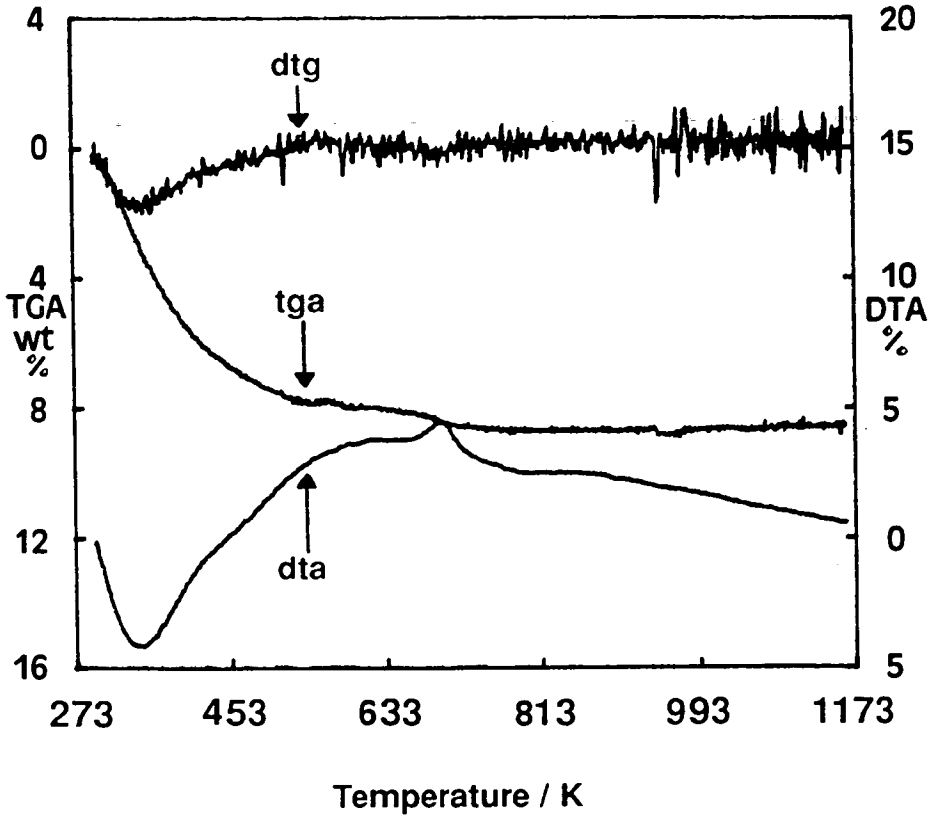

Figure 4–2: Thermal analysis profiles for sample A45 (t = 72 h), which suggest the presence of an organic species, probably TPA

These results led to the idea that the gel could perhaps be used as a *scavenger* of organic impurities, such that repeated crystallisations would reduce the organic impurity in the reaction vessel until it was effectively organic-free. As an added bonus, it was thought that the initial crystalline products would be in the form of *spheres* (it must be remembered that in the absence of organic impurities the system should not crystallise[2]).

To further test whether traces of organic material in the reaction vessel could indeed be scavenged by the gel and initiate the formation of ZSM-5, a series of reactions were carried out in autoclave C. This autoclave had been cleaned with potassium hydroxide (4 % wt/wt) and water (see Chapter 2), following a reaction which had involved the use of tetrapropylammonium hydroxide (TPAOH) to synthesise TPA-ZSM-5. Despite the cleaning procedure used, it was considered very likely that the vessel and/or ancillary parts were contaminated with traces of TPA. On scavenging the vessel with the gel composition:

$$15\ K_2O\ 0.667\ Al_2O_3\ 60\ SiO_2\ 3000\ H_2O$$

(C54, 423 K, 7 d, stirred (300 rpm)), a fine 'fluffy' powder was obtained, which on analysis by X-ray powder diffraction was shown to be predominantly ZSM-5 together with some cristobalite. Although it was thought that the crystallisation was initiated by traces of TPA, analysis of the product by TGA did not detect any organic material. Thus, the possibility of seeding could not be discounted.

Reactions C56 (4 d), C58 (6 d), C61 (7 d), C64 (8 d), and C65 (6 d) (Table 4–3) were then carried out in succession. These reactions were exactly the same as run C54 except for the reaction time. Before each run the autoclave was cleaned with 4 % (wt/wt) aristar potassium hydroxide heated to 373 K followed by ultrapure water heated to 453 K. This procedure was carried out twice before C56 and once before the other reactions.

---

[2]At this point, seeding was thought to be less important, given that the method of cleaning the autoclaves was considered adequate.

Table 4–3: Products obtained from the series of Scavenging Reactions carried out in autoclave C

Run No	Run Time / h	Products[a]	ZSM-5 / %[b]
C54[c]	162	ZSM-5 + Cr + Am	59
C56[c]	97	ZSM-5 + Am	58
C58[d]	136	ZSM-5 + Am	58
C61[d]	161	ZSM-5 + Cr + Am	56
C64[d]	185	ZSM-5 + Cr + Am	53
C65[d]	140	ZSM-5 + Am	62

[a]Key: Am = Amorphous; Cr = Cristobalite

[b]Relative to Na-ZSM-5 standard (100 % ZSM-5)

[c]Fine powder

[d]Sphere-like particles

Scavenging reaction C56, like C54, produced a fine 'fluffy' powder which was shown by XRPD to contain a substantial amount of ZSM-5. The subsequent reactions produced *spheres* of increasing size (Table 4–4). These too, were found to contain ZSM-5. The increase in the size of these *spheres* will be discussed later.

The results in Table 4–3 show that the maximum amount of ZSM-5 obtained after 6 days is approximately 60 %. On longer reaction times, the ZSM-5 content decreases as it transforms into the more dense cristobalite phase. Thus it would appear that the amount of ZSM-5 recovered is probably independent of the amount of seed at low loadings. Furthermore, whether the reaction is seeded by *free* crystals (*egs* C54 and C56) or those *trapped* in the sphere-like particles (C58-C65), also has little effect on the amount recovered.

It was thought that once the autoclave was free of any trace of TPA that the *Scavenging Reaction* would simply phase separate and fail to crystallise. However, even after six *Scavenging Reactions*, believed to be more than sufficient to remove

Table 4–4: Size distribution of *spheres* obtained from *Scavenging Reactions* carried out in autoclave C

Run No	Reaction Time	Description of Product	Size Distribution / %			
			420-300	300-250	250-180	< 180 μm
C54	162	Fine powder	-	-	< 1	> 99[a]
C56	97	Fine powder	-	-	< 1	> 99[a]
C58	136	Spheres	2.5	0.6	8.5	88.4
C61	161	Spheres	0.3	0.4	85.2	14.1
C64	185	Spheres	0.4	2.0	88.1	9.5
C65	140	Spheres	31.2	31.6	21.8	15.1

[a]Based on appearance only

all traces of TPA, fresh gel continued to give ZSM-5. This suggested that the later crystallisations were initiated by seed material alone.

To prove that seeding would lead to the formation of *spheres* which contained K-ZSM-5, the *Scavenging Reaction* was carried out in autoclave D. This autoclave had been used exclusively for organic-free Na-ZSM-5 syntheses for many months and was believed to be completely free of organic material. The autoclave was deliberately undercleaned and a small amount ZSM-5 could be seen on the stirrer shaft. It was thought that this would be sufficient to seed the reaction. As expected, *spheres* containing ZSM-5 were obtained (D67), confirming that this phenomenon was indeed the result of seeding (Table 4–5). Furthermore, this showed that the seed need not contain any occluded organic to be effective.

It was subsequently discovered that in the series of reactions C54 - C65 the dip-tube in autoclave C (as well as in the other autoclaves) could trap seed material in the 'well' where the external part of the dip-tube is connected to the autoclave (Figure 4–3). Consequently, after reaction C65, the dip-tube was disconnected and the 'well' thoroughly cleaned. The hydroxide/water wash was then carried

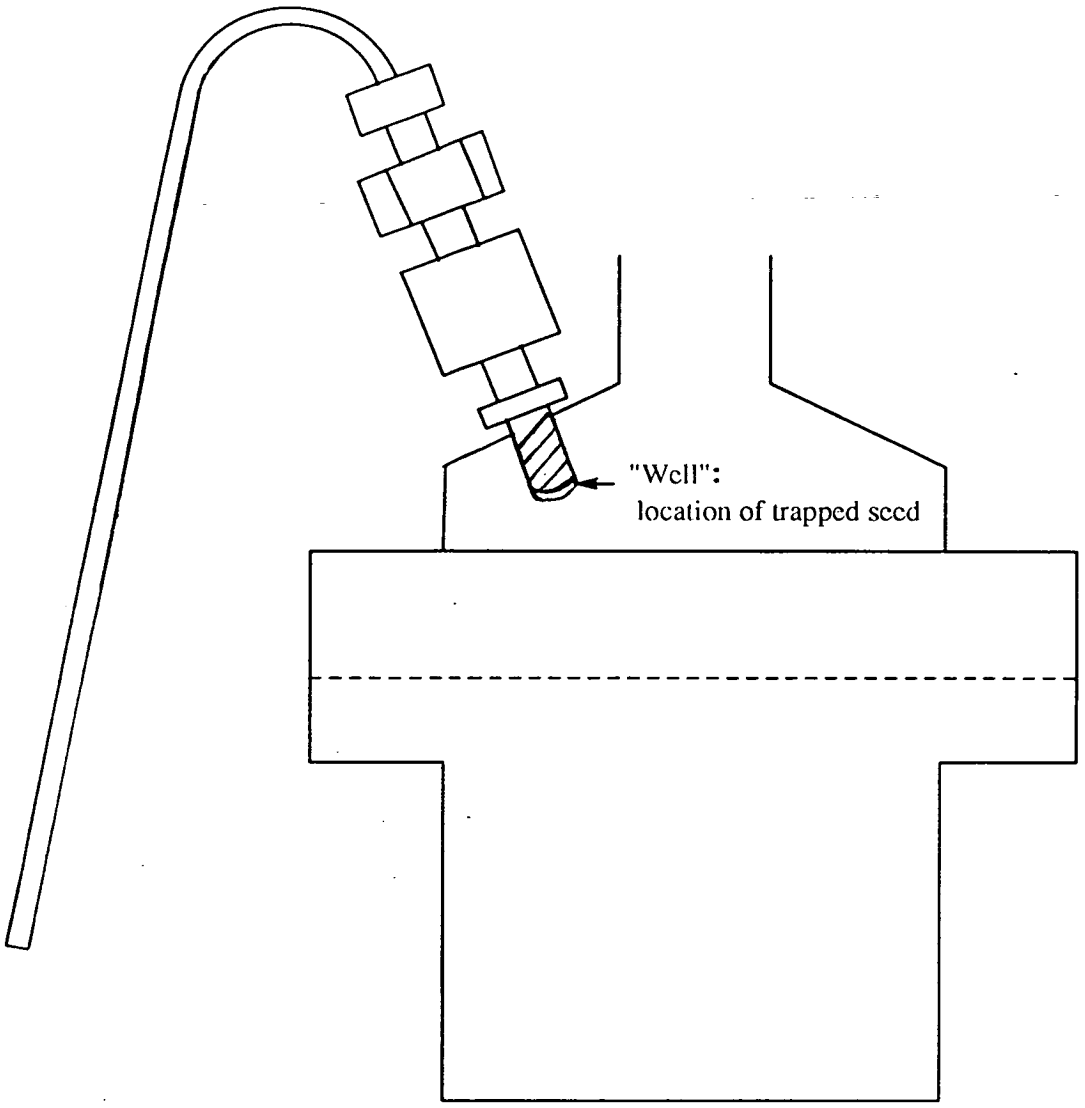

Figure 4–3: Schematic of the dip-tube showing the 'well' in which trapped seed material was found

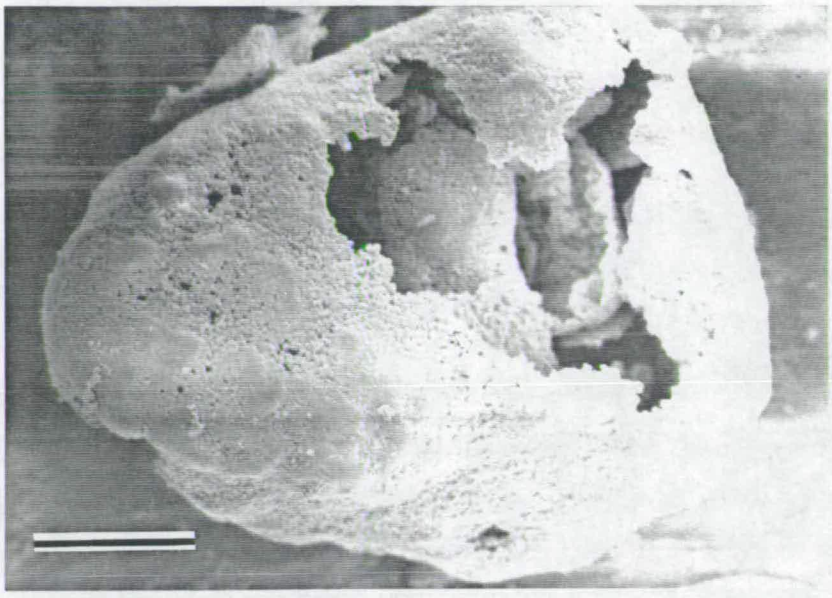

Figure 4–4: SEM photomicrograph showing the presence of a small *sphere* inside a larger one (Bar = 40 μm)

out three times with the result that on scavenging the autoclave again (C73, 6 d) the gel did not crystallise. It is thought that the increase in the size of the *spheres* on subsequent crystallisations (Table 4–4) was simply the result of seeding by progressively larger crystalline particles trapped in the dip-tube 'well' from preceding reactions. Thus it is possible that a *spheres* may act as a large seed for further crystallisation as suggested in the SEM photomicrograph in Figure 4–4.

The *Scavenging Reaction* was also carried out in autoclaves A and D. Again the products obtained were composed of free-flowing sphere-like particles which contained substantial amounts of ZSM-5 (Table 4–5). Unlike the reactions carried out in autoclave C, there was no obvious increase in the size of the *spheres* obtained with subsequent crystallisations and the size of the *spheres* was considerably smaller.

Autoclave B, on the other hand, did not give the usual sphere-like material on any occasion despite careful repetition of the runs described above. ZSM-5-containing *spheres* could not be obtained even from carefully controlled seeded reactions (Table 4–6). The products obtained from *Scavenging Reactions* that did crystallise ZSM-5 were rather lumpy, although careful examination by optical microscopy showed the presence of a small amount of broken *spheres*. It seems

Table 4–5: Products obtained from the *Scavenging Reaction* carried out in autoclaves A and D

Run No	**Run Time / h**	**Products**[a,b]	**ZSM-5 / %**
A81[c]	143.5	ZSM-5 + Am	56
A84	142.5	ZSM-5 + Am	51
A85	142	ZSM-5 + Am	54
A87	91	ZSM-5 + Am	55
A90	188	ZSM-5 + Cr + Am	52
	355	Q + Cr + Am	0
D80[d]	165	ZSM-5 + Cr + Am	50
D86	142	ZSM-5 + Am	46

[a]Very small sphere-like particles (< 120 μm); product perhaps best described as a coarse powder

[b]Key: Am = Amorphous; Cr = Cristobalite; Q = Quartz

[c]Followed a TPA-ZSM-5 reaction

[d]Followed an inorganic Na-ZSM-5 reaction

Table 4–6: Products obtained from seeded *Scavenging Reactions* carried out in autoclave B

Run No	Run Time / h	Seed Conc$^{n.}$ / mg kg^{-1}	Products	Texture of Product
B109	136	1[a]	Amorphous	Lumpy powder[b]
B115	140	14[a]	Amorphous	Lumpy powder[b]
B118	140	2[c]	Amorphous	Lumpy powder[b]
B141	62	12[d]	Amorphous	Lumpy powder[b]
B143	242	26[d]	ZSM-5[e] + Cristobalite + Amorphous	Very fine powder[f]

[a]Spheres containing approximately 17 % ZSM-5 (from reaction A10)

[b]Solid settles rapidly in mother liquor

[c]K-ZSM-5 (< 5 μm)

[d]TPA-ZSM-5 (< 0.1 μm)

[e]Approximately 55 %

[f]Comprised of sphere-like particles, < 20 μm

unlikely that the unusual behaviour of autoclave B could be attributed to a difference in heating/thermostatting or the nature of the vessel surface, since *spheres* that contained ZSM-5 were also obtained from two quite different experimental arrangements; a stirred 1 litre stainless-steel reaction vessel (E128) and a stirred 125 cm^3 PTFE-lined Parr bomb (P2) (Table 4–7). It remains unclear why autoclave B behaved in a different way to the others, although the presence of broken *spheres* may indicate some difference in agitation.

To find out if *spheres* containing ZSM-5 would only be obtained with the *Scavenging Reaction*, other compositions in the amorphous region of the phase diagram (Figure 3–1, Chapter 3) were tested in the presence of ZSM-5 seeds (Table 4–8). The results show that not only does ZSM-5 fail to crystallise from these seeded reactions, but also no sphere-like material is obtained.

Table 4–7: Products obtained from *Scavenging Reactions* carried out in the 1 litre stainless-steel autoclave (E) and the PTFE-lined Parr bomb (P)

Run No	Run Time / h	Products[a]	ZSM-5 / %
E128	137	ZSM-5 + Am	38
P2	137	ZSM-5 + Am	68

[a]Very small sphere-like particles; products perhaps best described as a coarse powder

Table 4–8: Effect of seeding other compositions in the amorphous region of the phase diagram with ZSM-5[a]

Run	Molar Compos[n,b]		Time	Seed Conc[n]	Products[c]	ZSM-5	Product
No	y K_2O	x Al_2O_3	/ h	/ mg kg^{-1}		/ %	Texture
A151[d]	15	0.667	42	Un[e]	ZSM-5+Am[f]	22	Spheres
A153	13	0.667	161	26	Cr + Am	33	LP[g]
A154	17	0.667	136	26	Am	Tr[h]	LP
A155	15	0.800	162	26	Cr + Am	Tr	LP
A166	15[i]	0.667	139	26	Am	53	Spheres

[a]TPA-ZSM-5 (< 0.1 μm)

[b]Based on the composition: y K_2O x Al_2O_3 60 SiO_2 3000 H_2O

[c]Key: Am = Amorphous; Cr = Cristobalite

[d]Reaction carried out at 453 K

[e]Un = Unknown (seed material already present in the reaction vessel)

[f]Trace of another phase, possibly ferrierite

[g]LP=Lumpy powder [h]Trace, may be the actual seeds

[i]Reagent grade KOH (contains approximately 0.5% sodium impurity)

The *Scavenging Reaction* was also carried out in non agitated systems in the presence of seeds (see Table 4–9, section 4.3.4). Although ZSM-5 was found to crystallise, no *spheres* were obtained.

Samples C65 and A95 were examined by SEM at ICI C&P Ltd., Wilton, (courtesy of Mr. R. Pendlebury), and are shown in Figures 4–5 and 4–6 respectively. The photomicrographs clearly show a dense amorphous-looking 'shell' containing a large number of ZSM-5 crystals with a wide range of sizes. Several micrographs also show the outer surface of the shell to be covered with ZSM-5 crystals.

4.3.3 Sphere Formation

There appears to be three essential conditions for the formation of the *spheres*,
(i) the reaction mixture must be stirred,
(ii) the gel composition must be that of the *Scavenging Reaction* mixture (or very close to it), and
(iii) there must be suitable seeds present.
In the absence of seeds the phase separation gives a lumpy, amorphous solid, whereas seeds, or organic impurities that lead to the formation of seeds, appear to assist in the initial separation of the particles of essentially amorphous gel. Indeed, they may act as centres for accretion of amorphous material. Alternatively [221], the amorphous gel may aid the agglomeration of seed crystals, where it acts like a glue. Stirring must also be essential for this process as gel particles do not form in its absence; no doubt vigorous stirring helps break up the amorphous gel solid. The initial particles are only roughly spherical, but as the reaction proceeds and the stirring is continued the particles become more spherical, probably as a consequence of abrasion (and possibly reaggregation). During this stage of the reaction further crystallisation takes place within the *spheres* and at their surface. The ready supply of nutrients at the surface of the particles gives the *spheres* a dense crystalline crust, whereas within the *spheres* the conversion of low density amorphous gel to the relatively dense zeolite crystals leads to an increase in the void space. Although these ZSM-5-containing *spheres* have similarities to prod-

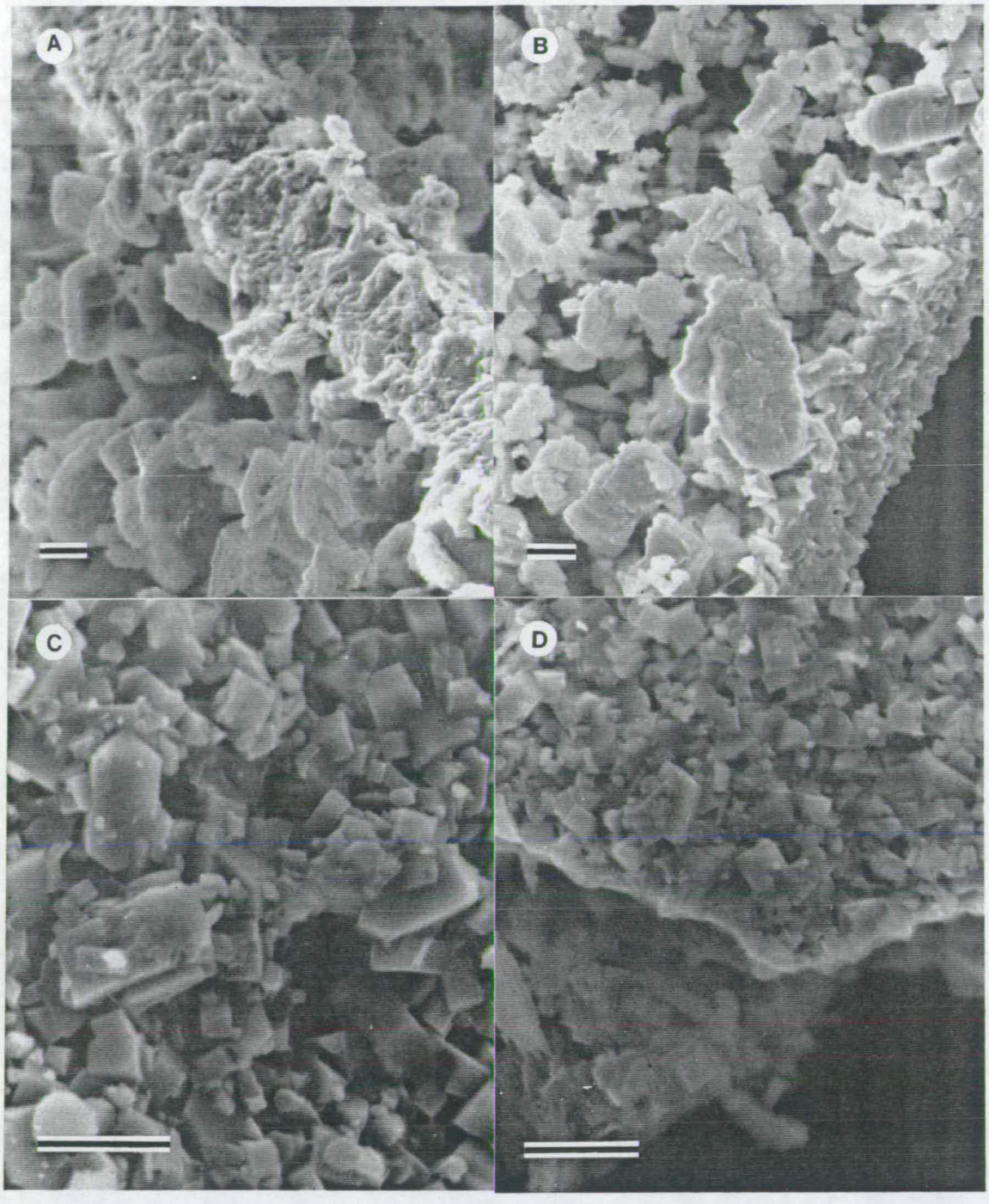

Figure 4–5: SEM photomicrographs of product C65; A and B show *shell* plus contents of particle, C and D show outer surface of *shell* (Bar = 1 μm)

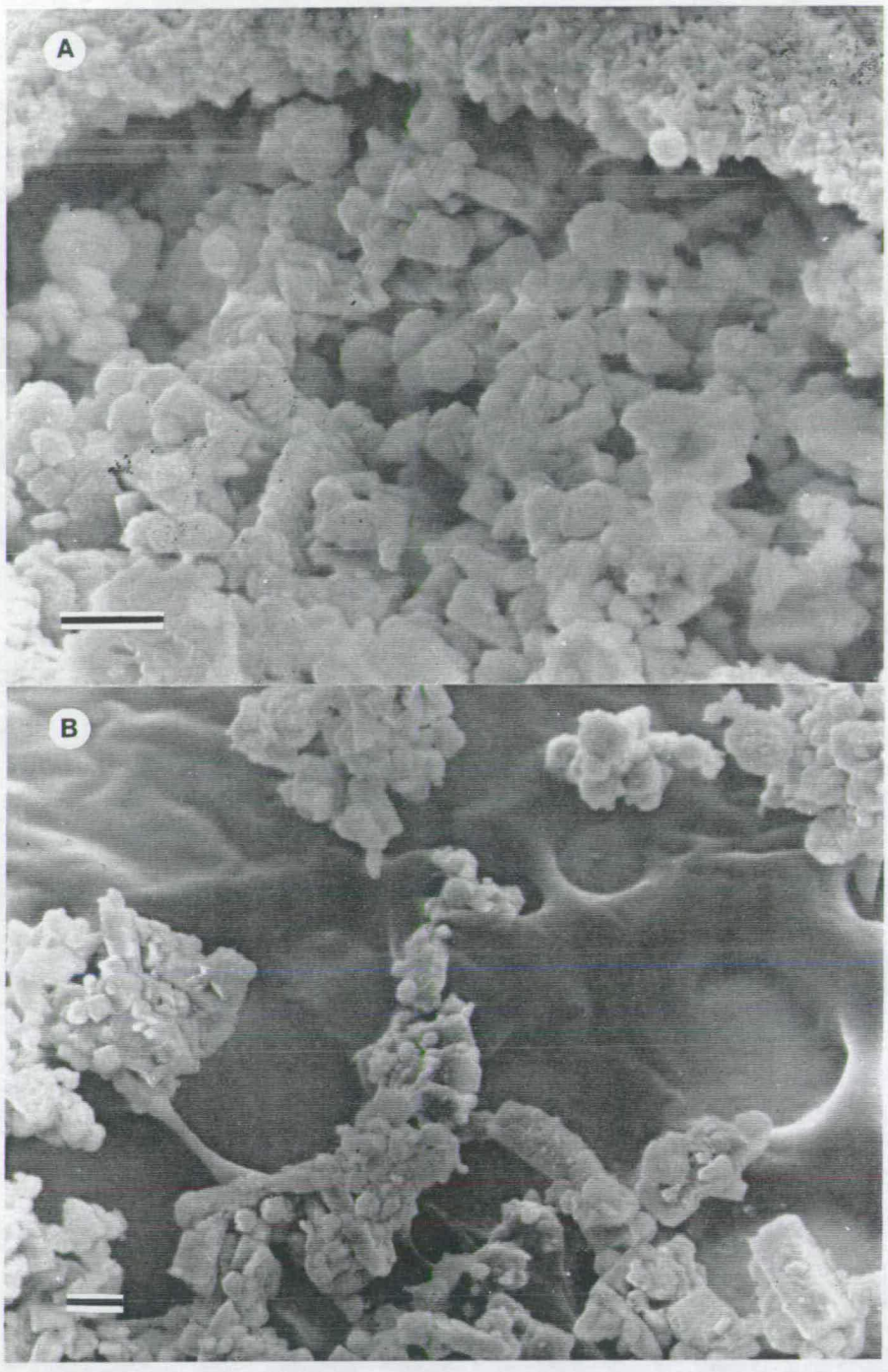

Figure 4–6: SEM photomicrographs of product A95; A shows the *shell* plus contents of particle, B shows aggregates of large and small crystals (Bar = 1 μm)

ucts obtained by pseudomorphic transformation [124,222,223,224] it is thought that crystallisation occurs via a gel particle intermediate [124] rather than a solid intermediate [223]. It is clear that since the crystalline phase is in intimate contact with the amorphous gel phase throughout the crystallisation, heterogeneous [225] nucleation at the gel surface must be the dominant nucleation mechanism.

The foregoing is only a general description of the way in which the *spheres* are thought to form, the exact details will depend on circumstances. For example, a low seed concentration might be expected to give relatively large *spheres* (Table 4–4), whereas a large number of very small seeds would be more likely to give a zeolite-rich powder. The latter case occurs in its extreme form when the presence of organic impurities initiates crystal growth at a variety of sites within the solid phase.

4.3.4 Use of the Scavenging Reaction to Detect Impurities

It was soon recognised from the results of experiments described above that the *Scavenging Reaction* was extremely sensitive to traces of organic impurity and seed material. Furthermore, it was apparent from the literature that a reliable method to establish the cleanliness of a reaction vessel was not available. This prompted a study to establish whether or not the *Scavenging Reaction* was sensitive to any type of organic or seed impurity.

To determine the sensitivity of the *Scavenging Reaction* to organic impurities and traces of seed material, a series of static crystallisations were carried out as described in Section 4.2.3. As-synthesised materials were used as seeds since this would be their usual form as impurities in reaction vessels. It should also be noted that any organic on the surface of the seed crystal is likely to play a part in the nucleation mechanism. Furthermore, it is thought that the organic material within the seed stabilises it toward dissolution.

Results of seeding experiments (Table 4–9) showed that the *Scavenging Reaction* is particularly sensitive to ZSM-5 and ZSM-11 seed crystals. Several zeolitic materials (NU-10, EU-1 and mordenite) were ineffective and the zeolites Beta and NU - 1 were only effective at relatively high loadings. It can be speculated that that the effect of NU-1 and Beta could be due to these materials being contaminated with small amounts of ZSM-5. It should be noted that NU-10 and mordenite contained no occluded organic material and so their stability in the alkaline reaction mixture may have been important.

Table 4–10 shows the effect of as-synthesised and calcined seed material in the *Scavenging Reaction.* Although there was very little difference in the amount of ZSM-5 obtained when the reaction mixture was seeded with as-synthesised and calcined ZSM-5 and as-synthesised ZSM-11, comparatively little crystallisation took place in the presence of calcined ZSM-11. This suggests that calcined ZSM - 11 seeds may be relatively unstable under the reaction conditions employed.

It is particularly significant that the *Scavenging Reaction* is especially sensitive to seeding by ZSM-5-type materials, and that even when seeding is initiated by

Table 4–9: Sensitivity of the *Scavenging Reaction* to seed impurities - determination of *detection limits*[a]

Impurity[b]	Impurity Conc$^{n.}$ / mg kg^{-1}			
	5	**25**	**100**	**250**
TPA-ZSM-5	maj[c]	-[d]	-	-
TBA-ZSM-11	maj	-	-	-
TEA-Beta	-	am	mt	min
TMA-NU-1	-	am	mt	min
K-NU-10	-	-	am	am
Hexa-EU-1	-	-	am	am
H-Mordenite	-	-	-	am
Na-Mordenite	-	-	-	am[e]

[a]Each value based on a minimum of two reactions

[b]TMA = Tetramethylammonium; TEA = Tetraethylammonium; TPA = Tetrapropylammonium; TBA = Tetrabutylammonium; Hexa = Hexamethonium

[c]Crystallinity (%): am = amorphous (0%); mt = minute trace (< 5%); t = trace (5 - 10%); min = minor (11 - 30%); med = medium (31 - 60%); maj = major (> 60%)

[d]- = not tested

[e]Based on one reaction

Table 4–10: Comparison of the amount of ZSM-5 obtained in the presence of as-synthesised and calcined seed material

Run No	Impurity	Conc$^{n.}$ of Impurity[a] / mg kg^{-1}	ZSM-5 / %
S147	TPA-ZSM-5	25	61
S148	H-ZSM-5	22	68
S149[b]	TBA-ZSM-11	25	57
S150[b]	H-ZSM-11	22	10

[a]Account taken of the weight difference between as-synthesised and calcined seed
[b]Trace of Kenyaite present

other crystalline materials, the product is always ZSM-5. This suggests that the *Scavenging Reaction* supports the growth of ZSM-5 but cannot nucleate it.

The effect of organic impurities is illustrated in Table 4–11. It should be noted that the impurity levels are in most cases much less than the amounts that would be used in a typical zeolite synthesis. All the quaternary ammonium compounds except TMABr gave some ZSM-5, even at the lowest loading (5 mg kg^{-1}).

It is noteworthy that the most effective quaternary ammonium salt was tetrahexylammonium bromide (THexABr) and that TPABr, which is recognised as the ideal *template* for ZSM-5, was not significantly more effective than TBABr, TPeABr and THepABr (Tables 4–12 and 4–13). This behaviour cannot be accounted for on a molar basis as for each mixture the molar content of TPABr is significantly higher than that of THexABr. Simple modelling shows that the THexA$^+$ cation fills the ZSM-5 void space about as well as the TPA$^+$ cation. The amount of void space filled by the larger cation at low concentrations will be more than that for the same amount of the smaller TPA cation. This, together with the higher hydrophobicity of the THexA$^+$ cation could well explain the observed behaviour. None of the other organic compounds tested gave detectable quantities

Table 4–11: Sensitivity of the *Scavenging Reaction* to organic impurities - determination of *detection limits*[a]

Impurity[b]	10^4z[c]	Impurity Conc$^{n.}$ / mg kg^{-1}				
		5	25	100	250	1000
n-Propylamine	10.00	-[d]	-	-	-	mt[e]
1,2-Ethylenediamine	9.84	-	-	-	-	am
Piperidine	6.94	-	-	-	-	am
Glycerol	6.42	-	-	am	am	am
1,6-Hexanediamine	5.09	-	-	mt	mt	t
1,6-Hexanediol	5.00	-	-	am	am	am
Pentaerythritol	4.34	-	-	am	am	am
Tri-n-propylamine	4.13	-	am	-	am	t
Triethylenetetramine	4.04	-	-	-	-	am
Triethanolamine	3.96	-	-	-	-	am
TMABr	3.84	-	am	am	-	am
TEABr	2.81	am	t	t	min	min
BzTMABr	2.57	-	-	-	-	am
TPABr	2.22	mt	t	t	min	med
BzTEABr	2.17	-	-	-	-	am
TBABr	1.83	am	t	t	min[f]	min
TPeABr	1.56	mt	t	t	min	med
THexABr	1.36	mt	t	t	med	maj
THepABr	1.21	mt	t	t	min	med

[a]Each value based on a minimum of two reactions

[b]Key: TMA = Tetramethylammonium; TEA = Tetraethylammonium; TPA = Tetrapropylammonium; TBA = Tetrabutylammonium; TPeA = Tetrapentylammonium; THexA = Tetrahexylammonium; THepA = Tetraheptylammonium; BzTMA = Benzyltrimethylammonium; BzTEA = Benzyltriethylammonium (all as bromide)

[c]For the composition: 15 K_2O z (Q) 0.667 Al_2O_3 60 SiO_2 3000 H_2O in which Q represents the organic impurity; the values of z correspond to an impurity level of 1 mg kg^{-1}

[d]- = not tested; [e]For key see note [c] in Table 4–9; [f]Probably a 5/11 intergrowth

Table 4–12: Comparison of the amount of ZSM-5 obtained from static *Scavenging Reactions*, spiked with increasing amounts of quaternary ammonium bromides (Q)

Q[a]	Relative Crystallinity[b,c]		
	100[d]	250	1000
TEABr	0.11	0.31	0.30
TPABr	-[e]	0.42	1.00
TBABr	0.18	0.29	-
TPeABr	0.22	0.48	-
THexABr	0.17	0.61	-
THepABr	0.19	0.26	0.56

[a]Key: TEABr = Tetraethylammonium bromide; TPABr = Tetrapropylammonium bromide; TBABr = Tetrabutylammonium bromide; TPeABr = Tetrapentylammonium bromide; THexABr = Tetrahexylammonium bromide; THepABr = Tetraheptylammonium bromide

[b]Relative to product obtained from gel with 1000 mg kg^{-1} TPABr

[c]XRPD analysis carried out by Mr. R. Pendlebury (ICI C & P Ltd., Wilton); the same weight of sample was examined each time

[d]Concentration of quaternary ammonium bromide in gel, mg kg^{-1}

[e]- = insufficient sample for XRPD

of ZSM-5, this is perhaps surprising as they are all sufficiently small to fit in the ZSM-5 channel system and several have been claimed to be effective in ZSM-5 synthesis in the sodium system [63]. This suggests that these materials act as void fillers rather than true structure directors.

A number of authors [18,28,63] have listed the wide range of organic compounds claimed to support the crystallisation of ZSM-5. Such lists can be rationalised if the compounds are divided into true structure directors and void fillers. The results in Table 4–11 clearly demonstrate that the *Scavenging Reaction* can be used to distinguish between true structure directors and void fillers. Several of

Table 4–13: Comparison of the amount of ZSM-5 obtained from stirred crystallisations of the composition 15 K_2O 0.2(Q) 0.667 Al_2O_3 60 SiO_2 3000 H_2O

Run No	Q[a]	Crystallinity / %				Relative Crystallinity[b,c]
		20 h[d]	24 h	27 h	44 h	
D194	TEABr	Am	Am	Am	100	0.78
D197	TPABr	85	84	87	100	0.91
D203[e]	TBABr	-	-	-	100	0.90
D192	TPeABr	90	90	97	100	0.97
D190	THexABr	92	94	100	100	1.00
D195	THepABr	87	87	98	100	0.83

[a]Key: see Table 4–12

[b]Relative to product obtained from reaction D190

[c]XRPD analysis carried out on the same day and with the same amount of sample

[d]Reaction time, h = hours

[e]Possibly a ZSM-5/11 intergrowth

these materials were tested at substantially higher concentrations where the overall reaction composition was:

$$15\ K_2O\ 20(Q)\ 0.667\ Al_2O_3\ 60\ SiO_2\ 3000\ H_2O,$$

where Q = organic.

The results in Table 4–14 show that even when tested at higher concentrations many of the void fillers do not give ZSM-5; the amines which might be considered as structure directors gave relatively small amounts of ZSM-5.

To test these materials for their ability to act as void fillers, reactions were carried out on gels which contained a fixed amount of ZSM-5 seed. Although the amount of ZSM-5 recovered was quite varied (Table 4–15), most products were found to contain occluded organic material when analysed by tga. However, it should be noted that the two compounds which were not found in the product ZSM-5, glycerol and pentaerythritol, are too large to readily enter the void space after crystallisation. This suggests that void fillers enter the channel system after crystallisation is complete and play no part in the crystal growth process. If so, their major contribution is their ability to stabilise the zeolite framework against dissolution and so prevent over-run.

It is clear from the results presented above that great care must be taken to exclude seed and organic materials from the reaction mixture. The usual way to examine new organic templates is to carry out crystallisation in the presence and absence of the organic in the reaction mixture. Thus any effect on the outcome of a crystallisation is attributed to the organic species. The effect of seed and/or other organic impurities, however, does not receive much attention. For example, it was shown in a study [110] which related the SiO_2/Al_2O_3 ratio of the reaction mixture to the type of product obtained, that ZSM-5 crystallised readily from the composition

$$10\ K_2O\ 10\ HXDM\ 1\ Al_2O_3\ 60\ SiO_2\ 3000\ H_2O.$$

In the absence of HXDM (1,6-hexanediamine) the only phases obtained are the unknown phase U1 and Kenyaite (reaction B17, Table 4–16). Thus HXDM may

Table 4–14: Static crystallisations of ZSM-5 from the composition 15 K_2O 20(Q) 0.667 Al_2O_3 60 SiO_2 3000 H_2O, where Q = organic, at 423 K for 6 d

Run No	**Q**[a]	**Relative Crystallinity**[b,c]
S222	TPABr	1.00
S230	1,4-Butanediamine	0.14
S227	Tri-n-propylamine	0.08
S231	1,6-Hexanediamine	0.06
S232	Triethylenetetramine	0.01
S228	n-Propylamine	0.04
S223	Piperidine	Am
S224	Piperazine	Am
S225	1,2-Ethylenediamine	Am
S226	Glycerol	Am
S229	1,6-Hexanediol	Am
S233	DABCO	Am

[a]Key: TPABr = tetrapropylammonium bromide;

DABCO = 1,4-Diazobicyclo[2,2,2]octane

[b]Expressed relative to that of reaction S222 (100% ZSM-5)

[c]XRPD analysis carried out on the same day and with the same amount of sample

Table 4–15: Relative amounts of ZSM-5 crystallised from the *Scavenging Reaction* at 423 K for 6 days, in the presence of organic impurities and 25 mg kg^{-1} ZSM-5[a] seed; test for void fillers

Run No	Impurity	Conc[n.] / mg kg^{-1}	Relative[b,c] Crystallinity	Wgt loss/% 623-873 K
S214	Blank	-	1.0	0.2
S209	Triethylenetetramine	1100	1.0	0.9
S210	1,6-Hexanediol	1000	1.0	2.0
S212	Piperidine	1200	1.0	1.8
S206	1,2-Ethylenediamine	1100	0.9	0.5
S211	DABCO[d]	1000	0.8	0.5
S207	Glycerol	1200	0.7	0.4
S208	Pentaerythritol	1000	0.7	0.1
S213	Morpholine	1050	0.7	0.5

[a]TPA-ZSM-5 (< 0.1 μm)

[b]Expressed relative to that of the blank reaction S214

[c]XRPD analysis carried out on the same day and with the same amount of sample

[d]DABCO = 1,4-Diazobicyclo[2,2,2]octane

Table 4–16: Effect of 100 mg kg^{-1} TPA-ZSM-5 seed on the crystallisation of 10 K_2O 1 Al_2O_3 60 SiO_2 3000 H_2O at 423 K (300 rpm)

Run No	Seeded	Product	ZSM-5 / %
B17	No	U1 + Ken + Am	0
D261	Yes	ZSM-5	73

be considered a good structure directing agent for ZSM-5. However, on repeating reaction B17 in the presence of a trace of TPA-ZSM-5 seed (100 mg kg^{-1}), a substantial amount of ZSM-5 was obtained (D261). Thus the role of HXDM as a true ZSM-5 structure director is questionable. More importantly, this result demonstrates the effect that a small amount of seed can have on a reaction. Thus if an organic material with unknown directing ability was being tested for the first time and similar results were obtained to those described above, then it it is likely that one would conclude, possibly incorrectly, that the organic had directed any ZSM-5 obtained, when in fact the presence of traces of impurities may have directed the crystallisation. It is believed that this may be the case for some of the materials listed by Lok *et al.* [63] as ZSM-5 structure directors. It should be added that in the presence of organic materials such as HXDM, the reaction mixture may be even more sensitive to seed or organic impurities. The findings of the present study highlight not only the need to carry out an organic-free crystallisation when investigating new organic templates, but also the need to investigate the influence of impurities, particularly seeds, on the outcome of these crystallisations. Only then can any effect on the outcome of a crystallisation be fully attributed to the organic species under investigation.

4.3.5 Effect of Gel Aging on Sensitivity to Impurities

Several reactions were carried with gels that had been aged at room temperature for up to 6 months. It should be recalled that such treatment renders the gel

Table 4–17: Effect of gel aging on the sensitivity of the *Scavenging Reaction*; tested with 250 mg kg^{-1} TPABr

Run No	Time Aged / d	Relative[a,b] Crystallinity
S93	0	1.0
S192	7	0.6
S193	32	0.7
S194	63	0.6
S195	85	0.6
S196	125	0.7
S197	169	0.7

[a]Expressed relative to that of the blank reaction S93

[b]XRPD analysis carried out on the same day and with the same amount of sample

virtually transparent. The results (Table 4–17) show that there was a initial decrease in the sensitivity of the gel toward the organic impurity. However, there was little difference in sensitivity between gels aged for several days and those aged for several months. The *Scavenging Reaction*, therefore, is more effective when carried out using freshly prepared gel. Although aged gel had been shown to be sensitive to seed impurity, a similar study was not undertaken for seed impurities.

4.3.6 Influence of Sodium Cations

At the outset of this work it was believed that sodium might act as a structure director for ZSM-5 formation and great care was taken to keep the sodium ion concentration as low as possible. However, when sodium concentrations as high as 2000 mg kg^{-1} (NaCl) were tested in the *Scavenging Reaction*, no ZSM-5 was formed (Table 4–18). This was a most unexpected finding and raises the question as to whether sodium actually does *template* ZSM-5. Indeed, this finding together

Table 4–18: Effect of sodium[a] impurities in the *Scavenging Reaction*

Run No	Na / mg kg^{-1}	Product
S220	790	Amorphous
S302	7600	Amorphous

[a] Added as NaCl

with the existence of a potassium composition which only gives ZSM-5 in the presence of minute traces of impurities, suggests that the corresponding sodium system might be even more sensitive to impurities and that it is these undetected impurities rather than the sodium ions themselves which direct the formation of *inorganic* ZSM-5.

Further reactions were carried out to examine the effect of increasing the sodium content (added as NaOH) of the *Scavenging Reaction.* The composition:

$$(15\text{-}x)\ K_2O\ x\ Na_2O\ 0.667\ Al_2O_3\ 60\ SiO_2\ 3000\ H_2O,$$

where x = 5, 7.5 and 10, was investigated. Not surprisingly perhaps, ZSM-5 was found to crystallise; in increasing amounts (Table 4–19). However, rather than contradicting the results described in Table 4–18, it can be argued that as the amount of Na_2O is increased in the reaction mixture, so the gel tends to behave more like the inorganic sodium gel. (It is worth noting that the viscosity of the gel increases with increasing Na_2O content so there is a significant change in the gel chemistry, which cannot be overlooked). Thus it is possible that an increase in the Na_2O content of the gel results in an increase in its sensitivity toward impurities.

The possibility that gels may have different sensitivities to impurities led to a re-examination of the compositions in the potassium system (B27 and A36) that gave K-ZSM-5 (Chapter 3, Table 3–1). There was now sufficient reason to believe that these crystallisations may have been caused by undetected impurities. When these reactions were carefully repeated (A75 and A78, Table 4–20 in 500 cm^3

Table 4–19: Products from the crystallisation of the composition (15-x) K_2O x Na_2O 0.667 Al_2O_3 60 SiO_2 3000 H_2O, where x = 5, 7.5 and 10

Run No	x Na_2O	Product	ZSM-5 / %
S234	5.0	ZSM-5 + Ken + Am	11
S236	7.5	ZSM-5 + Ken + Am	31
S235	10.0	ZSM-5 + Ken + Am	47
A260[a]	4.5	ZSM-5 + Am	15

[a]Stirred reaction carried out in a 500 cm^3 autoclave

stainless-steel autoclaves, which had been rigorously cleaned and scavenged, ZSM-5 was still obtained. However, it is possible that the gels (B27, A36, A75 and A78) that crystallised ZSM-5 are even more sensitive to impurities than the *Scavenging Reaction* and that it may be virtually impossible to get the stainless-steel autoclaves clean enough to prevent possible seeding effects. To obtain even cleaner conditions for these reactions, 125 cm^3 stirred PTFE-lined Parr bombs were used at 423 K. These bombs were cleaned and scavenged over a number of weeks and, following the final *Scavenging Reaction*, were cleaned with 4% (wt/wt) Aristar potassium hydroxide at 423 K for a week. The cleaning procedure was carried out without stirring (although the magnetic stirrer bar was inside the bomb) and the bombs inverted every day to ensure thorough cleaning. The reactions (P52 and P53) failed to crystallise ZSM-5 (Table 4–20). This, together with the observation that the crystallisation of K-ZSM-5 in the stainless-steel autoclaves, suggests that the alkali metal cations do not nucleate the product. The unidentified material U1 (Chapter 3) and kenyaite were the only crystalline phases obtained from reactions P52 and P53 and these were contaminated with much amorphous material. Although it is recognised that the actual experimental set up and gel preparation was not exactly the same as the original reactions (B27, A35, A75, and A78) it is believed that this was not a major factor in preventing the formation of K-ZSM-5. Hence, there is some evidence that organic impurities are essential for the nucleation of ZSM-5 in the potassium system, seeds promote growth.

Table 4–20: Products obtained from the crystallisation of the composition 15 K_2O x Al_2O_3 60 SiO_2 3000 H_2O, where x = 0.333 and 0.5

Run No	x Al_2O_3	Run Time / d	Reaction Vessel	Product[a] / %	ZSM-5
B27	0.333	162	500 cm^3 s-steel[b]	Ken + ZSM-5 + U1 + Am	26
A78	0.333	113	500 cm^3 s-steel	Ken + ZSM-5 + U1 + Am	12
P52	0.333	141	125 cm^3 Parr bomb[c]	Ken + U1 + Am	0
A36	0.5	140	500 cm^3 s-steel	ZSM-5 + Am	60
		171		ZSM-5 + Cr + Am	56
A75	0.5	140	500 cm^3 s-steel	ZSM-5 + Am	15
P53	0.5	141	125 cm^3 Parr bomb	Ken + U1 + Am	0

[a]Key: Am = Amorphous, Ken = Kenyaite, U1 = unknown phase (see Chapter 3)

[b]s-steel = stainless-steel, stirred 300 rpm

[c]PTFE-lined, stirred on a magnetic stirrer

4.3.7 NU-10 *Scavenging Reaction ?*

In a manner reminiscent of the *Scavenging Reaction* described above, the composition:

$$5\ K_2O\ 2\ Al_2O_3\ 60\ SiO_2\ 3000\ H_2O$$

did not crystallise even after 8 weeks at 423 K (Chapter 3). It was thought that this composition might also be sensitive to impurities in the same way as the *Scavenging Reaction.* Unlike the *Scavenging Reaction*, however, this composition did not phase separate and the yield of solid (amorphous) recovered was much higher (50 % *cf.* 30 %). Furthermore, the base level is similar to that from which NU-10 crystallised at lower Si/Al ratios. It was argued then, that this composition may be sensitive to materials that direct NU-10-type structures. Rather than carry out a detailed systematic study as with the Scavenging Reaction, it was decided to look at the effect of relatively high levels of impurities. Thus, crystallisations were carried out at 423 K in 30 cm^3 PTFE-lined bombs with the composition:

$$5\ K_2O\ 2\ Al_2O_3\ 60\ SiO_2\ 3000\ H_2O,$$

spiked with 1000 mg kg^{-1} organic impurity. As well as testing NU-10-type directing agents, a number of other organics were examined (Table 4–21). The results show that only the organics that readily direct ZSM-5 had any effect on this composition and the products obtained were, indeed ZSM-5, although the amount obtained was significantly less than with the *Scavenging Reaction.* 1,6-hexanediamine and tetraethylenepentamine, which are considered particularly suitable for the crystallisation of NU-10 [112,165,218,226] were ineffective. The fact that these amines failed to give NU-10 may be attributed to the high level of aluminium in the system [110]. However, it is more likely, that there was insufficient organic reagent in the reaction mixture. Thus, this composition is not be suitable as a detector of organic impurities that direct NU-10. This may also be due in part to the fact that the composition may not lie close enough to the phase

boundary that divides compositions that readily crystallise NU-10 from those that do not crystallise at all (Chapter 3, Figure 3–1). In other words, unlike the *Scavenging Reaction*, this composition does not lie on a compositional *knife edge*. It is interesting to note, however, that le Febre *et al.* [226] found it difficult to reproduce a number of the NU-10 crystallisations reported in the literature. They found that in many cases, the nature of the reaction vessel was important. On changing from a stainless-steel reaction vessel to one lined with PTFE, they were able to crystallise NU-10 readily. Given that such liners may be particularly prone to *memory* effects [189], it is quite possible that seed impurities may have affected the outcome of their crystallisations. Thus, it may be that the crystallisation of K-NU-10 in the present study, like K-ZSM-5, was caused by undetected impurities (either seed or organic). To test this, static crystallisations were carried out in 30 cm^3 PTFE-lined bombs which had been rigorously cleaned and tested with the *Scavenging Reaction*. None of the compositions crystallised, even after 17 d at 423 K (Table 4–22). Although only one composition was reacted in both the stirred and static systems (5 K_2O 1 Al_2O_3 60 SiO_2 3000 H_2O) and that it is recognised that these crystallisations are not strictly comparable, the results suggest that seeding cannot be ruled out.

Table 4–21: Products obtained after 6 d from the static crystallisation at 423 K of the composition 5 K_2O 2 Al_2O_3 60 SiO_2 3000 H_2O, spiked with 1000 mg kg^{-1} of organic (Q) impurity

Run No	Q	Product
S111	1,6-HXDM	Am
S113	TEPA[a]	Am
S108	TPABr	ZSM-5[b] + Am
S109	THexABr	ZSM-5[b] + Am
S110	$HexBr_2$	Am
S112	TMABr	Am
S114	DABCO	Am
S115	Piperidine	Am

[a]Tetraethylenepentamine

[b] < 10 %

Table 4–22: Products obtained after 17 d at 423 K from static crystallisation of the composition 5 K_2O x Al_2O_3 60 SiO_2 3000 H_2O

Run No	x Al_2O_3	Product
S156	1.00	Amorphous
S157	1.25	Amorphous
S158	1.50	Amorphous

4.4 Conclusions

The composition:

$$15\ K_2O\ 0.667\ Al_2O_3\ 60\ SiO_2\ 3000\ H_2O$$

was found to be sensitive to the presence of zeolite seed and organic material and provided these are suitable it will crystallise ZSM-5 under the specified reaction conditions. The nature of the seed is particularly important. Those of ZSM-5 and ZSM-11 are especially effective, possibly even at the 100 parts per billion level. However, seeding by other high-silica zeolites is generally ineffective even at much higher levels (1000 mg kg^{-1}). It should be noted that the detection limit (or sensitivity) of the gel is likely to vary according to the reaction conditions, for example agitation of the reaction mixture; choice of temperature; shape and volume of the reaction vessel, and the source of the reagents. For this reason, absolute values for the detection limits were not established.

The *Scavenging Reaction* may have several novel applications. It may be used to establish the cleanliness of a reaction vessel and in the case of contamination by certain organic impurities, remove these, leaving the reaction vessel completely organic-free. This application would be particularly important when working with *inorganic* systems. Since the *Scavenging Reaction* is sensitive only to organic materials that are able to direct ZSM-5, it can be used to distinguish between those that are true structure directors and and those that are void fillers, as well as giving a measure of their potency.

Many organic materials have been used as templates in the search for new high-silica zeolites and more often than not the product is ZSM-5. The *Scavenging Reaction* can be used to screen a potential organic template in order to establish whether or not it is likely to readily direct ZSM-5. Since very little organic template is required, such a test could save both time and money. It must be remembered that seeds and organic impurities must be completely absent if the results of the test are to be of any value.

In the presence of certain seed impurities, ZSM-5 crystallises in the form of sphere-like particles. It is unlikely that these particles would have any commercial application, primarily due to the low yield of material obtained. The attrition resistance is not known.

The existence of a composition in the potassium system that is extremely sensitive to seed and organic impurities together with the apparent inability of relatively high levels of sodium ions to direct the crystallisation to ZSM-5 suggests that the corresponding sodium system may be even more sensitive and it is these impurities rather than the sodium ions that direct the crystallisation to ZSM-5. Furthermore, although it cannot be proved beyond doubt, it may be that this also applies to the crystallisation of inorganic NU-10.

It is proposed that all work on the synthesis of zeolite molecular sieves should include an examination of the effect of traces of impurities on the outcome of the crystallisation for completeness.

Although the Bellussi group [212] carried out some reactions in new reaction vessels, there is still a distinct possibility that the ZSM-5 they obtained was seeded either by seed impurity, probably ZSM-5 which may be present as dust in the laboratory or by traces of organic impurity. Thus it is not sufficient to base the credibility of results on the use of new reaction vessels. There are many other ways of introducing impurities into a reaction mixture.

One can only speculate on the identity of the "non-reproducible phases" [209] reported by the Nastro group. It may well be that the irreproducibility of these reactions was a result of seeding.

Chapter 5

Alkali-Free Syntheses: Single Quaternary, Mixed Quaternary, and Quaternary/Amine Systems

5.1 Introduction

5.1.1 Single Quaternary Systems

The crystallisation of high-silica zeolites in the absence of alkali and alkaline earth metal cations has already been discussed in Chapter 1 (section 1.4.6). In the present work, the results of alkali metal-free syntheses will be presented in two chapters, this chapter will deal with crystallisations from single quaternary, mixed quaternary and quaternary/amine systems and the following chapter (Chapter 6) will examine the quaternary/diol system. The motivation for the latter study will be discussed in the appropriate chapter.

This chapter begins with an investigation into the crystallisation of high-silica zeolites from alkali metal-free, single quaternary reaction mixtures based on the following composition:

$$10\ Q_2O\ 1\ Al_2O_3\ 60\ SiO_2\ 3000\ H_2O,$$

where Q = tetramethylammonium (TMA), tetraethylammonium (TEA), tetrapropylammonium (TPA) or tetrabutylammonium (TBA). The aim of this study was to establish whether high-silica zeolites could be crystallised from systems in which

the quaternary ammonium hydroxide serves as the structure director, charge balancing cation and mineraliser. Although it has been reported [153,154] that TPA-ZSM-5 can be obtained from such systems, there are no reports in the open literature of analogous studies in which the quaternary is TMAOH, TEAOH or TBAOH. Indeed the only reports of crystallisations involving TMA alone are those which describe the synthesis of TMA-gismondine and TMA-sodalite [227, 228]. Several research groups [229,230,231,232] claim that alkali metal cations are essential in order to obtain zeolite Beta from reaction mixtures that contain TEA as the structure directing agent. The crystallisation of Beta from alkali metal-free fluoride systems has been reported [233]. However, the product could only be obtained from seeded (Beta) reaction mixtures. While TBAOH has been used to synthesise silicalite II from similar alkali metal-free reaction mixtures [81], there are no reports in the open literature on the synthesis of the aluminium-containing analogue, TBA-ZSM-11, from gels containing TBAOH alone. Furthermore, it is not known whether or not TBA-ZSM-11 can be crystallised free of any 5/11 intergrowth from such systems. It should be noted, however, that the presence of potassium ions is claimed [76] to favour the formation of ZSM-11 as a pure phase. The effects of changing the SiO_2/Al_2O_3 in the starting gel was also examined for a number of these compositions.

Two other quaternary ammonium hydroxides were examined in less detail, namely nonamethonium hydroxide ($Nona(OH)_2$) and benzyltrimethylammonium hydroxide (BzTMAOH). It has been reported [234] that nonamethonium cations can direct crystallisations to give ZSM-5 under certain conditions. However, these crystallisations were usually carried out in the presence of high concentrations of sodium ions and it was thought possible that any structure directing effect of the organic may have been masked by the sodium ions. BzTMA has not been widely used in high-silica zeolite crystallisations. The only high-silica zeolites that have been made from gels containing this organic reagent are Theta-3 [235], ZSM-12 [236], and ZSM-58 [237], and the reaction mixtures always contained substantial amounts of alkali metal cations, which again may have influenced the outcome of these crystallisations.

There are no reports in the open literature of alkali-free crystallisations of reaction mixtures that contain BzTMAOH. It may well be that in the absence of alkali metal cations this quaternary might direct towards a different phase.

The products obtained from static crystallisations of alkali-free reaction mixtures are also reported for a number of potentially interesting quaternary ammonium hydroxides.

TPAOH has been widely used in the synthesis of ZSM-5. However, TPAOH can contain substantial amounts of alkali metal cations, particularly potassium, depending on the grade [161]. Several reactions were, therefore, carried out with TPAOH of different quality, to investigate the effect of alkali metal impurities on the crystallisation of TPA-ZSM-5. The results of this work led to a more detailed examination of the effects of several small cations on the crystallisation kinetics. The results of this study will be discussed in Chapter 7.

5.1.2 Mixed Quaternary and Quaternary/Amine Systems

Studies on the crystallisation of high-silica zeolites from alkali metal-free mixed quaternary ammonium hydroxide and quaternary ammonium hydroxide/amine systems are not well documented. The most notable report is found in the patent literature [160]. There are, however, several studies of crystallisations from aluminium-free reaction mixtures that contain more than one organic component [106,115,158], where materials such as silicalite [106,115,158], ZSM-48 [158], EU-19 [106] and the clathrasil ZSM-39 [106] have been crystallised. Therefore, the effect of TMA cations on the product obtained, crystallisation kinetics, crystal size, etc., was investigated for a number of mixed quaternary reaction mixtures. Furthermore, TMA has been used in the synthesis of a large number of crystallographically distinct frameworks [63] and it was thought possible that under certain conditions, a reaction mixture that contained TMA plus another quaternary ammonium cation or an amine might give an unexpected product. The results of these crystallisations are discussed together with reactions in which TMA^+ is replaced with $BzTMA^+$, a more bulky cation.

Table 5–1: Sodium and potassium content[a] of quaternary ammonium hydroxides

Quaternary	Supplier	Grade	Conc$^{n.}$ mg l^{-1}	
			Na	K
TMAOH $5H_2O$	Aldrich	99 %	< 1	< 1
TEAOH	SACHEM	HPLC	< 1	< 1
TPAOH	Fluka	Pract	300	5750
TPAOH	Fluka	Purum	250	570
TPAOH	SACHEM	Special	38	2
TBAOH	Fluka	Pract	240	8500
TBAOH $30H_2O$	Fluka	Purum	1	< 1
TBAOH	SACHEM	HPLC	< 1	2
BzTMAOH	Fluka	Pract	600	6300

[a]Determined by flame photometry

5.2 Experimental

5.2.1 Materials

The reagents used in this work and the synthesis conditions are described in Chapter 2. The alkali metal content of several quaternary ammonium hydroxides widely used in this work are further given in Table 5–1. All quaternary ammonium hydroxides were standardised as already described.

5.2.2 Gel Preparation

Reactions were carried out with mixtures of composition:

$$10\ Q_2O\ y\ Al_2O_3\ 60\ SiO_2\ 3000\ H_2O,$$

where Q = quaternary ammonium cation and $0 < y < 2$. The method of gel preparation was described in Chapter 2. For static crystallisations in *TOM* reaction vessels, the gel preparation was as follows:
The quaternary ammonium hydroxide was weighed into a small polypropylene bottle and aluminium wire added (if required). Fumed silica was carefully weighed into a plastic Sterilin tube (capacity 20 cm^3) and the hydroxide/alumina added, quickly followed by the rest of the water so as to give a total weight of gel of 10 g. The Sterilin tube was capped and vigorously shaken for 5 minutes to ensure thorough mixing. The contents of the tube were further mixed for 30 minutes using an automatic tumbler. The gel ($\sim$ 1 g) was transferred to the teflon-lined TOM using a Pasteur pipette and placed in a pre-heated oven set at the desired temperature for different times.

5.2.3 Analysis of Products

Procedures for analysing samples were as described in Chapter 2. TEM analysis was carried out on several samples obtained from single quaternary reactions by ICI C & P Ltd., Wilton.

Products obtained from mixed quaternary systems, where it was thought that more than one organic species could be occluded in the framework, were examined by ^{13}C MASNMR with cross polarisation at UMIST by Ms. B. Gore. CHN analyses were also carried out on these products at Edinburgh by members of the Analytical Group.

5.2.4 Sorption Studies

Surface area and micropore volume were determined at Wilton using sorption techniques, with n-heptane as the sorbate. Sorptive properties of samples obtained early on in this research were carried out under the supervision of Dr. S. Maberly and Mr. I. Milne. Later samples were examined by Mr. I. Milne.

5.2.5 Catalytic Examination

The TPA-ZSM-5 material crystallised in the absence of alkali metal cations was calcined at 773 K (12 h) and 1073 K (2 h) for catalytic evaluation. This was carried out in the catalysis laboratory at ICI C & P Ltd., Wilton under the supervision of Dr. I. Lake. The test reaction used was the disproportionation of ethylbenzene which gives diethylbenzene (DEB) and benzene as products:

Disproportionation

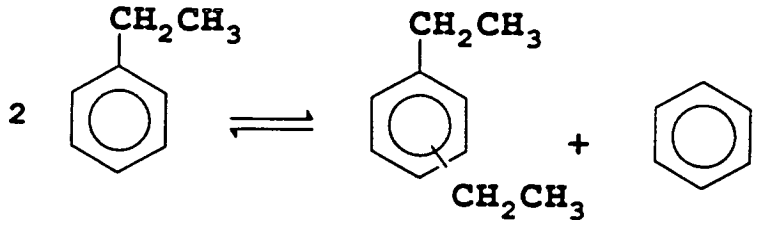

Alkylation/dealkylation reactions can also take place:

Dealkylation

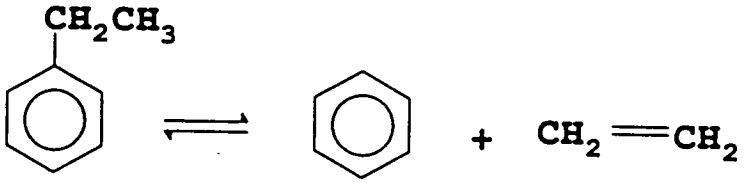

Alkylation

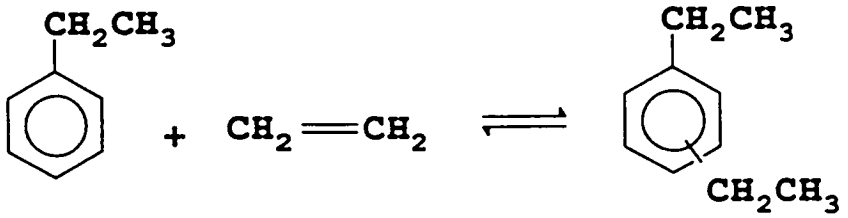

The ratio of benzene/total DEB gives an indication of the reactions taking place. If, for example, this ratio is > 1 then disproportionation and dealkylation are the dominant reactions. If the ratio is < 1 then disproportionation and alkylation are dominant. It is only when the ratio is equal to one that disproportionation occurs in the absence of alkylation and dealkylation.

It was argued that since the crystallisation was carried out in the absence of any other charge balancing cation, the framework aluminium would have to be located at, or very close to, the channel intersections, where the negative framework charge can be balanced by the TPA^+ cations. Thus, on calcination, the acid sites associated with the framework aluminium would have a larger effective volume. This then, could give rise to unusual catalytic behaviour, with a possible change in the product distribution. Furthermore, the presence of tiny crystals might give enhanced catalyst performance by virtue of reduced diffusional restraints within the zeolite framework.

5.3 Results and Discussion

5.3.1 Single Quaternary Reactions

Table 5–2 gives the products obtained from the composition:

$$10\ Q_2O\ 1\ Al_2O_3\ 60\ SiO_2\ 3000\ H_2O,$$

where Q = TMA, TEA, TPA, or TBA, crystallised at 423 K (403 K for TEA) with stirring (300 rpm).

Tables 5–3 and 5–4 give product compositions based on weight percent and moles of oxide. As expected the alkali metal content of the products was extremely low.

Table 5–2: Products obtained from the composition 10 Q_2O 1 Al_2O_3 60 SiO_2 3000 H_2O

Run No	Q[a]	Cryst[n.] Time / d		Product
		t_{nuc}	$t_{100\%}$	
D91	TMA[b]	20	25	NU-1
B89[c]	TEA	-[d]	28	Beta
C76	TPA	-[e]	32	ZSM-5
C178	TPA	28	33	ZSM-5
B49	TBA	15	21	ZSM-11

[a]Supplied by SACHEM

[b]Supplied by Aldrich

[c]Crystallised at 403 K

[d]t = 10 d amorphous, t = 18 d 44% Beta

[e]t = 19 d amorphous, t = 25 d 85% ZSM-5

Table 5–3: Percentage composition of products

Run No	Composition % [a]				Si/Al	Wgt. loss at 1173 K / % [b]
	Na	K	Al	Si		
D91	nd[c]	nd	1.75	36.6	20.1	16.6
B89	nd	nd	1.82	37.0	19.5	21.1
C76	0.019	0.003	1.35	36.9	26.3	13.8
B49	nd	0.009	1.58	36.4	22.1[d]	18.9

[a]Determined by ICP and flame AES

[b]Determined by tga

[c]Non detected, detection limit for Na and K = 0.003%

[d]Below the theoretical minimum ratio of 31.0 (assuming ~ 3.0 TBA^+/unit cell, see text)

Table 5–4: Molar oxide composition of products and unit cell content for TPA-ZSM-5 and TBA-ZSM-11

Run	Composition[a]		Unit Cell Content			
No	Al_2O_3	SiO_2	SiO_2	Al_2O_3	Q[b,c]	H_2O[c]
C76	1	52.6	92.5	1.75	3.6	5.4
B49	1	44.2	91.8	2.1[d]	3.5[e]	16.0

[a] Alkali metal content negligible

[b] Occluded organic cation

[c] Determined by tga

[d] Should be $\sim$ 1.5 (see text and Table 5–3)

[e] Slightly higher than the theoretical maximum value of $\sim$ 3.0 [238]

XRPD data for each product are compared with those in the literature in Tables 5–5, 5–6, 5–7, and 5–8 and the XRPD patterns are shown in Figures 5–1, 5–2, 5–3, and 5–4. Thermal analysis profiles are shown in Figures 5–5, 5–6, 5–7, and 5–8. SEM photomicrographs of the products are shown in Figure 5–9.

TMA-NU-1

The composition:

$$10\ (TMA)_2O\ 1\ Al_2O_3\ 60\ SiO_2\ 3000\ H_2O\ (D91),$$

crystallised the high-silica zeolite NU-1 in 25 days at 423 K (300 rpm). The SEM photomicrograph (Figure 5–9) showed no unusual features. The product consisted of ellipsoidal crystals, ranging from about 0.5 - 3 μm. Thermal analysis (Figure 5–5 of the product showed three distinct weight losses above 633 K corresponding to the oxidative decomposition of the occluded organic material. The three exotherms give some indication as to the location and fit of the TMA in the framework. The first exotherm may be attributed to removal of non-occluded organic, perhaps from the surface of the crystals and probably in the form of TMAOH. This would suggest

Table 5–5: XRPD data for sample D91 (TMA-NU-1)

D91		NU-1[a]	
d[b] / pm	100 I/I$_o$	d / pm	100 I/I$_o$
1152	1.4	1133	2.5
896	8.1	880	8.0
832	20	822	41
661	14	694	2.5
652	12	649	32
625	29	617	55
563	4	561	11
539	7	534	10
447	41	441	46
432	49	428	49
410	49	-	-
405	100	401	100
401	61	395	38
397	55	-	-
391	62	-	-
384	31	383	62
371	18	-	-
356	35	351	35
344	8	342	24
331	19	-	-
327	24	324	11
312	20	308	11
298	15	298	11
294	13	294	5

[a] As-synthesised NU-1 (Reference [239], Table 3)

[b] Additional peaks thought not to be an impurity phase (based on SEM analysis)

Table 5–6: XRPD data for sample B89 (TEA-Beta)

B89		**Beta**[a]	
d / pm	**100 I/I_o**	**d / pm**	**100 I/I_o**
1144	11	1150	s[b]
749	1	744	w
667	1	686	mw
414	16	417	m
395	100	398	vs
351	7	354	w
333	15	333	mw
302	16	303	m
292	6	290	m
268	5	269	w
207	13	208	w

[a]As-synthesised Beta (Reference [73], Table 2)

[b]Key: w = weak; m = medium; s = strong; vs = very strong

Table 5–7: XRPD data for sample C76 (TPA-ZSM-5)

C76		TPA-ZSM-5[a]	
d / pm	**100 I/I_o**	**d / pm**	**100 I/I_o**
1116	11	1113	63
1001	9	1001	29
974	4	971	24
745	4	744	3
636	5	635	16
461	5	460	8
436	8	435	5
426	9	426	3
401	7	400	6
385	100	384	100
383	75	382	79
376	32	375	31
372	41	371	48
365	29	364	40
344	12	343	14
335	10	335	1
331	9	330	10
306	12	304	12
299	15	298	8
298	13	297	9
295	8	294	7
261	7	261	7
249	8	249	2
240	7	241	3
201	19	200	7
200	21	199	9

[a]Reference [191] p. 442S

Table 5–8: XRPD data for sample B49 (TBA-ZSM-11)

B49		**ZSM-11**[a]	
d / pm	**100 I/I_o**	**d / pm**	**100 I/I_o**
1153	8	1120	27
1010	8	1007	23
439	8	437	9
387	100	386	100
374	48	373	39
348	6	349	6
337	8	335	5
308	6	307	6
301	12	300	10
298	10	-	-
201	23	201	21

[a]Reference [75]

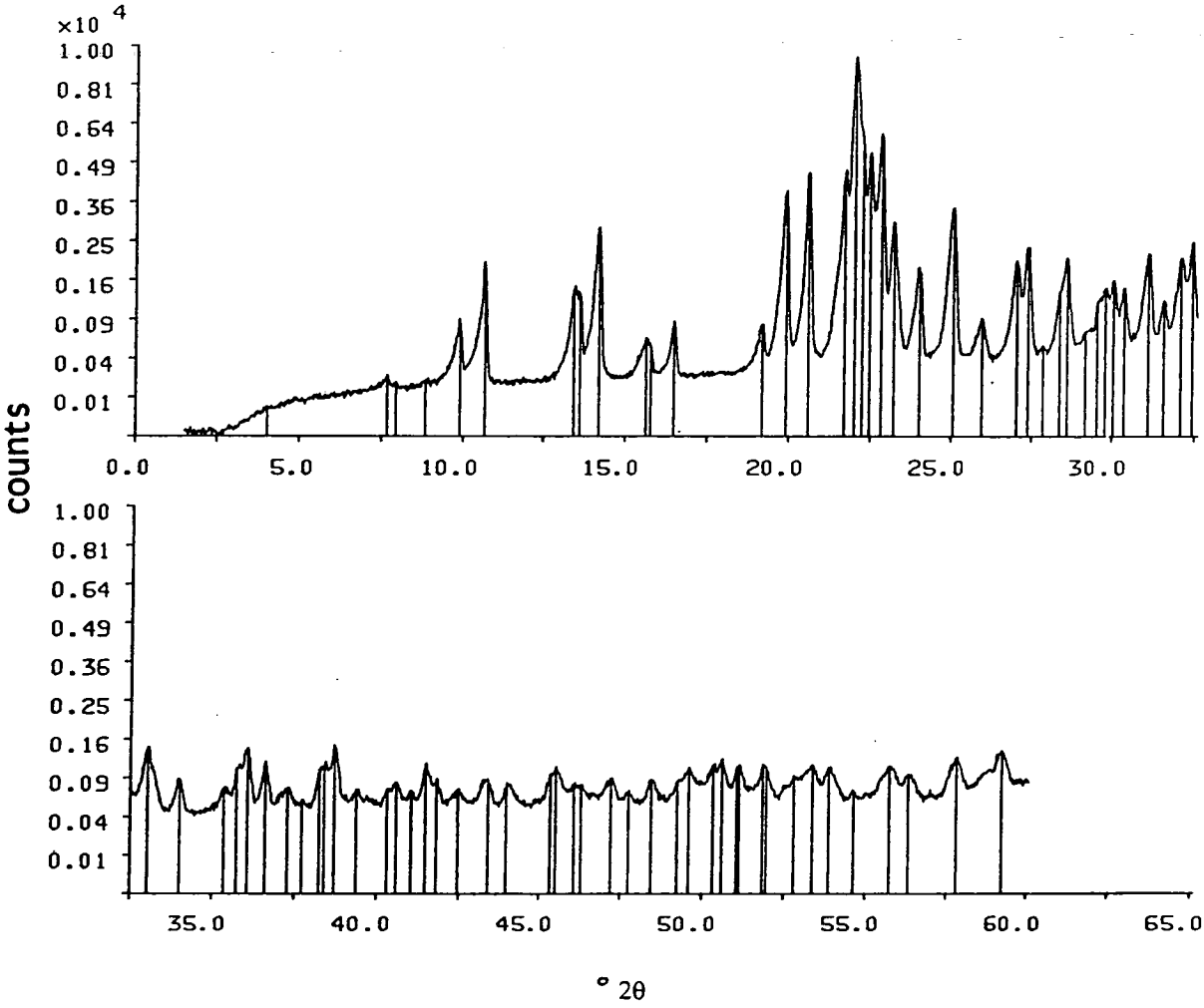

Figure 5–1: XRPD pattern of TMA-NU-1 (D91)

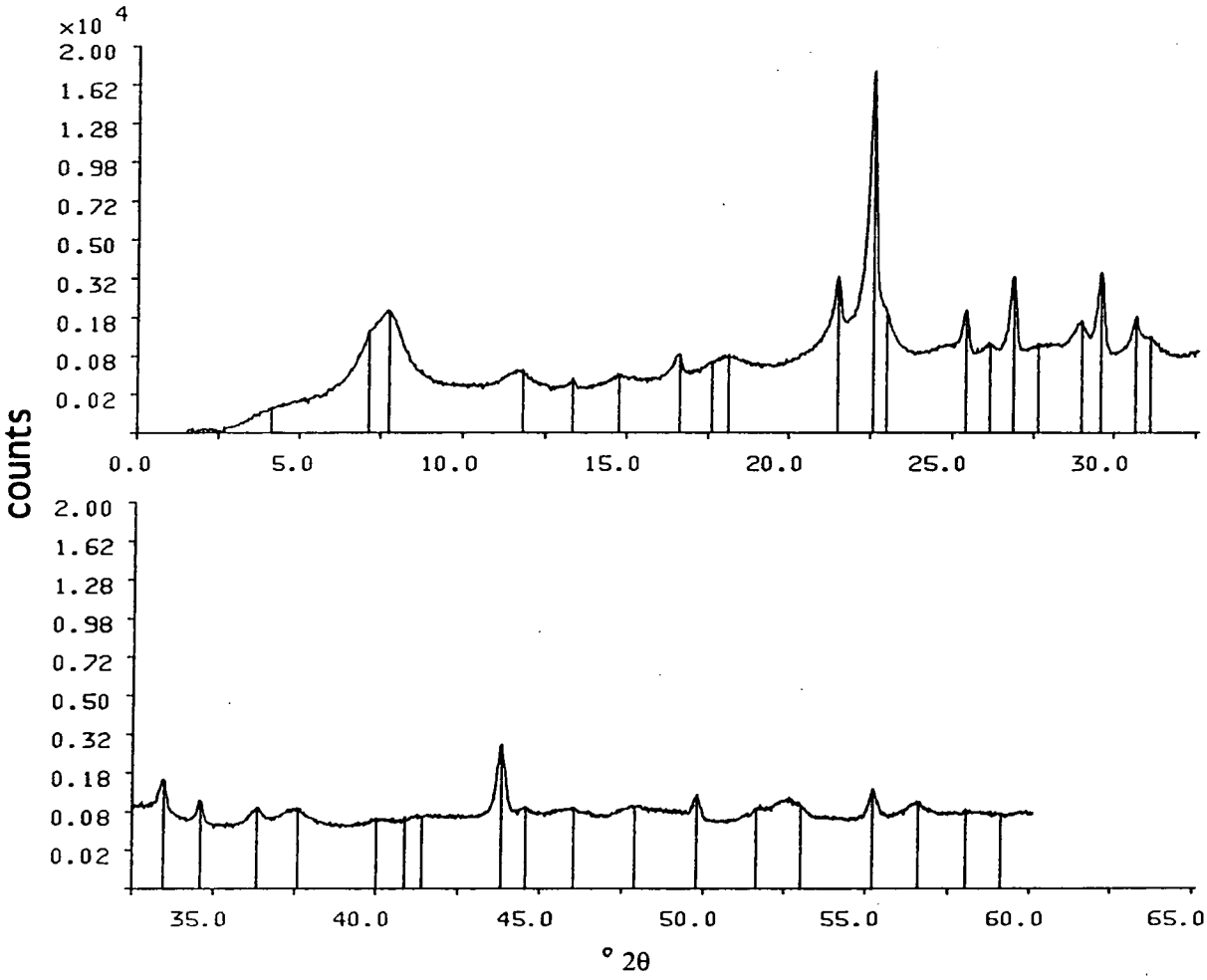

Figure 5–2: XRPD pattern of TEA-Beta (B89)

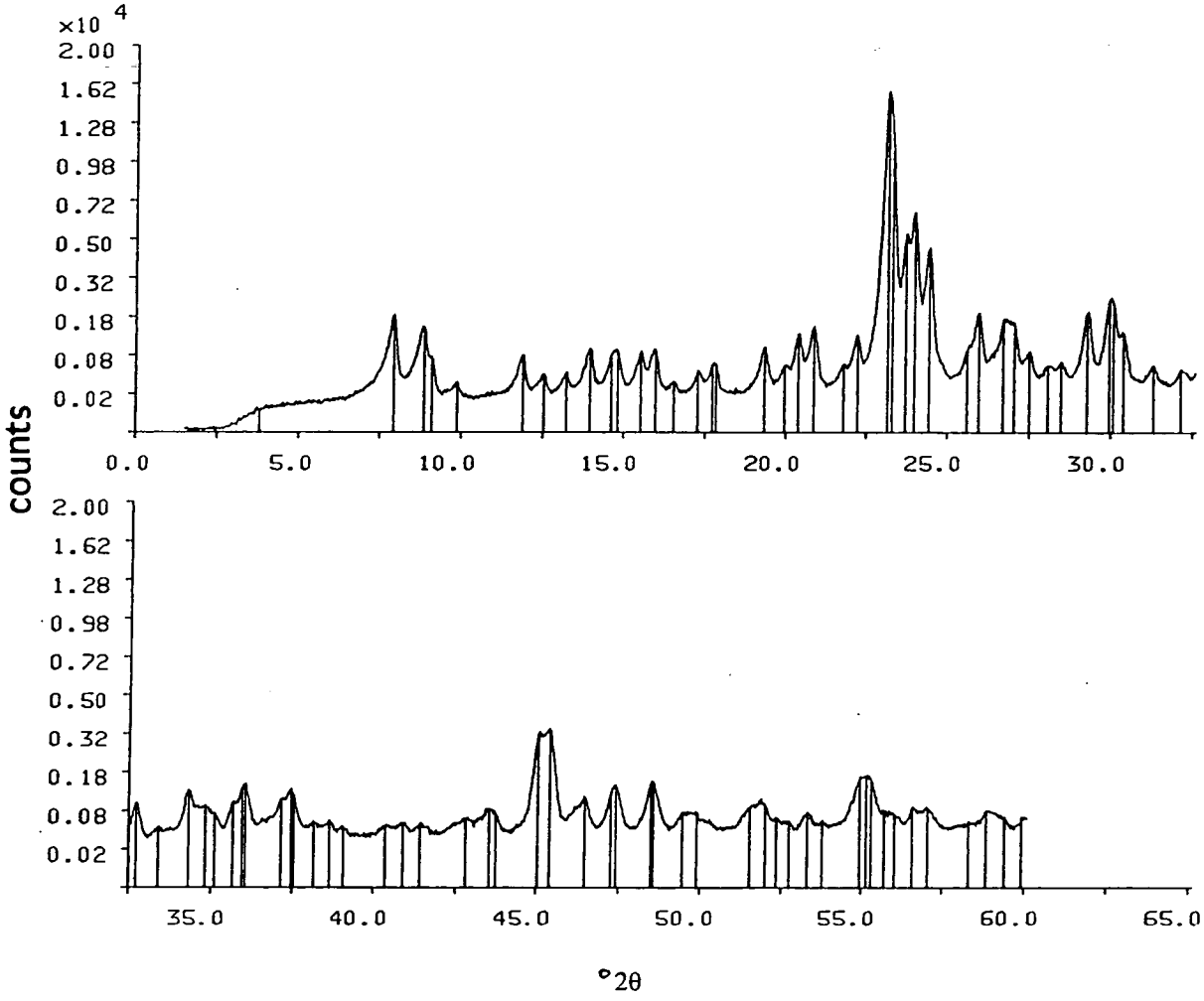

Figure 5–3: XRPD pattern of TPA-ZSM-5 (C76)

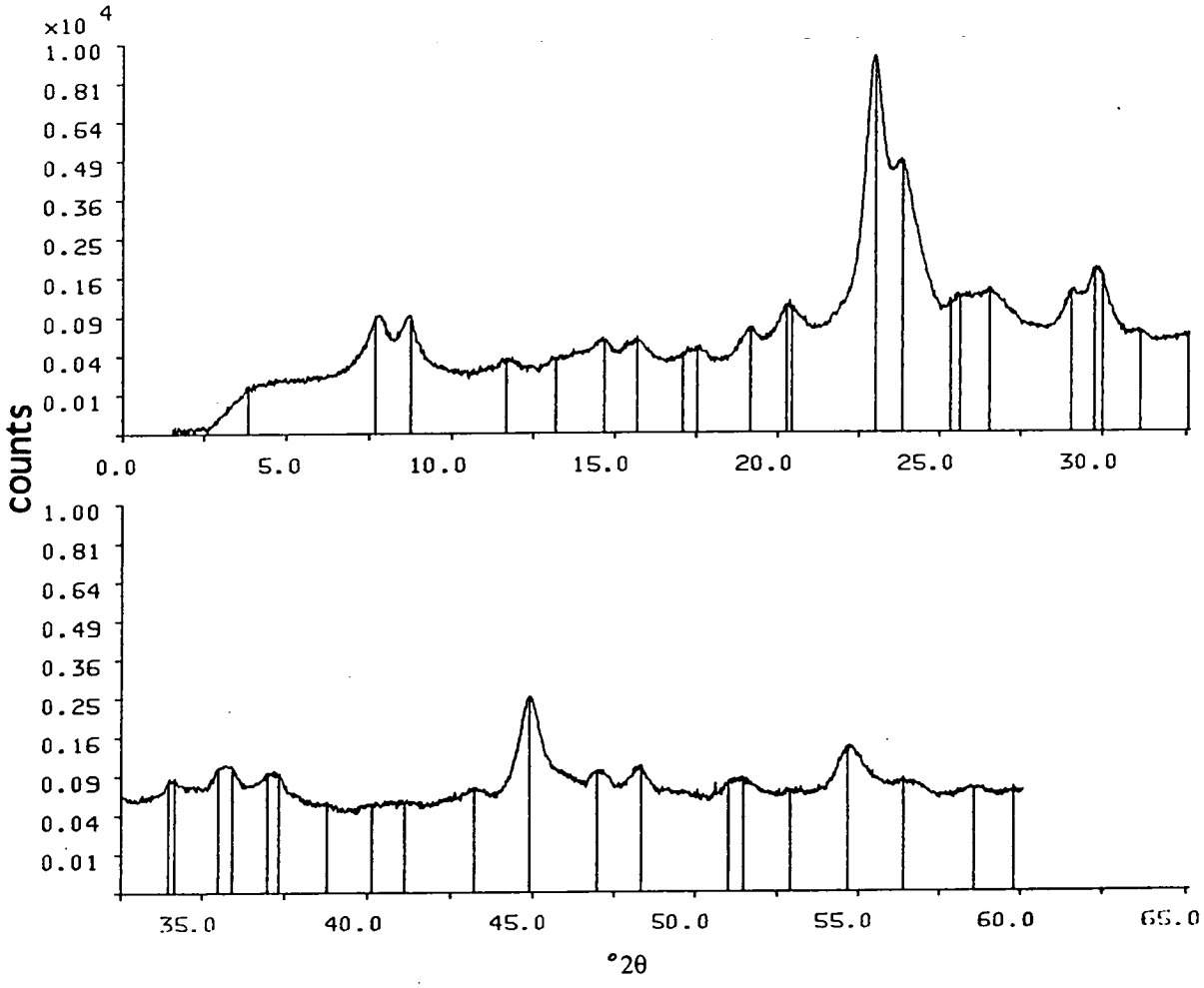

Figure 5–4: XRPD pattern of TBA-ZSM-11 (B49)

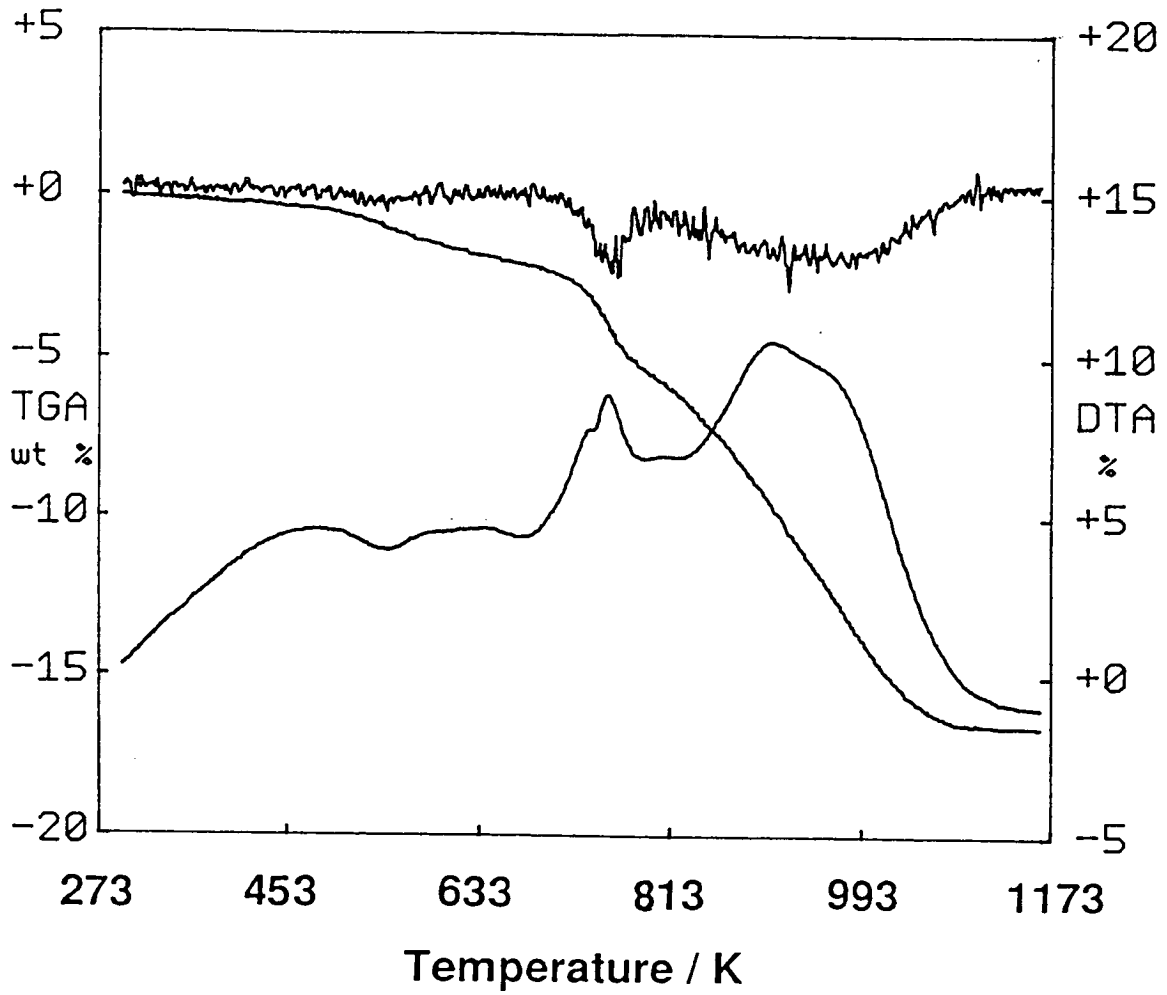

Figure 5–5: tga, dtg and dta profiles for TMA-NU-1 (D91)

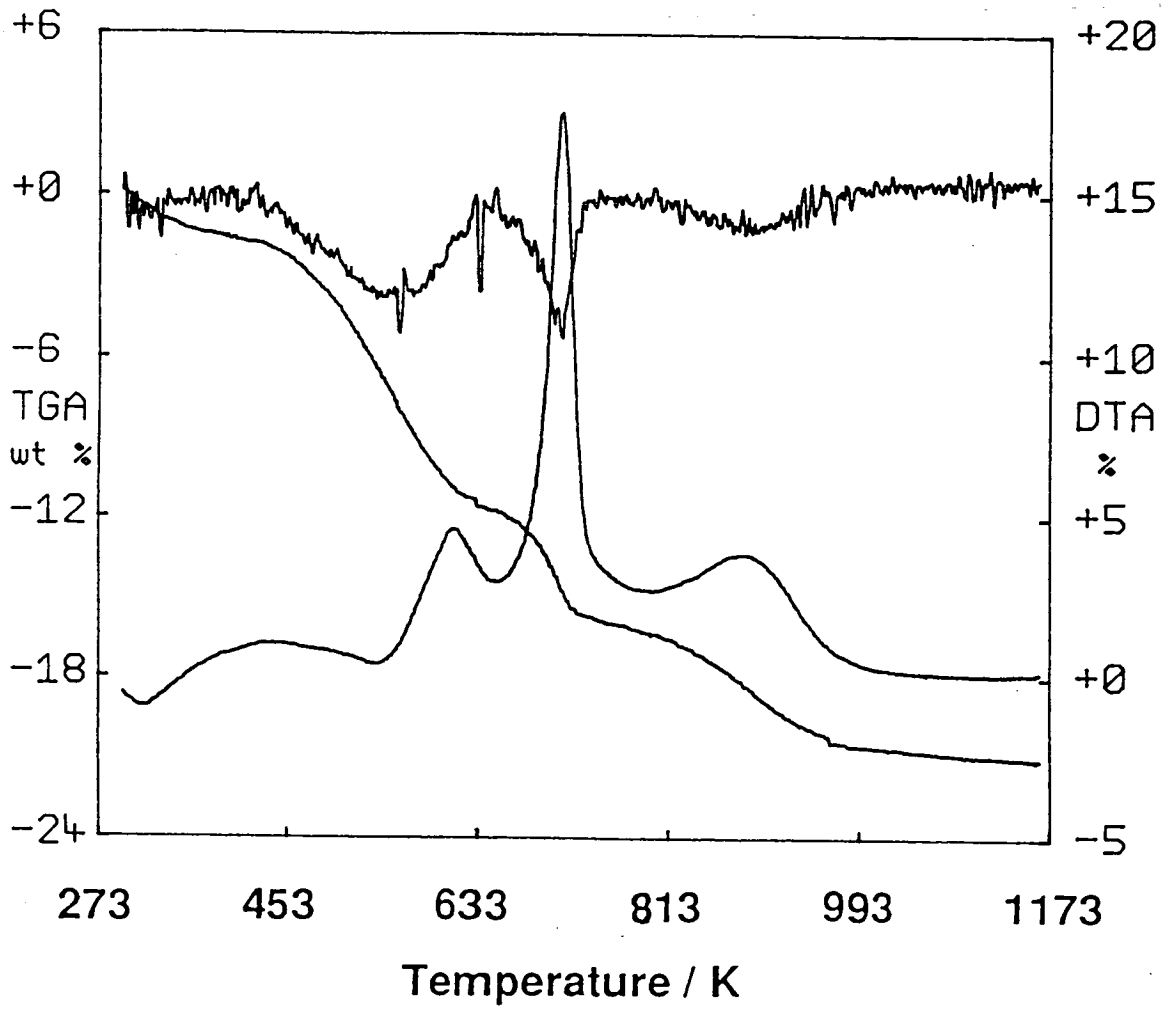

Figure 5–6: tga, dtg and dta profiles for TEA-Beta (B89)

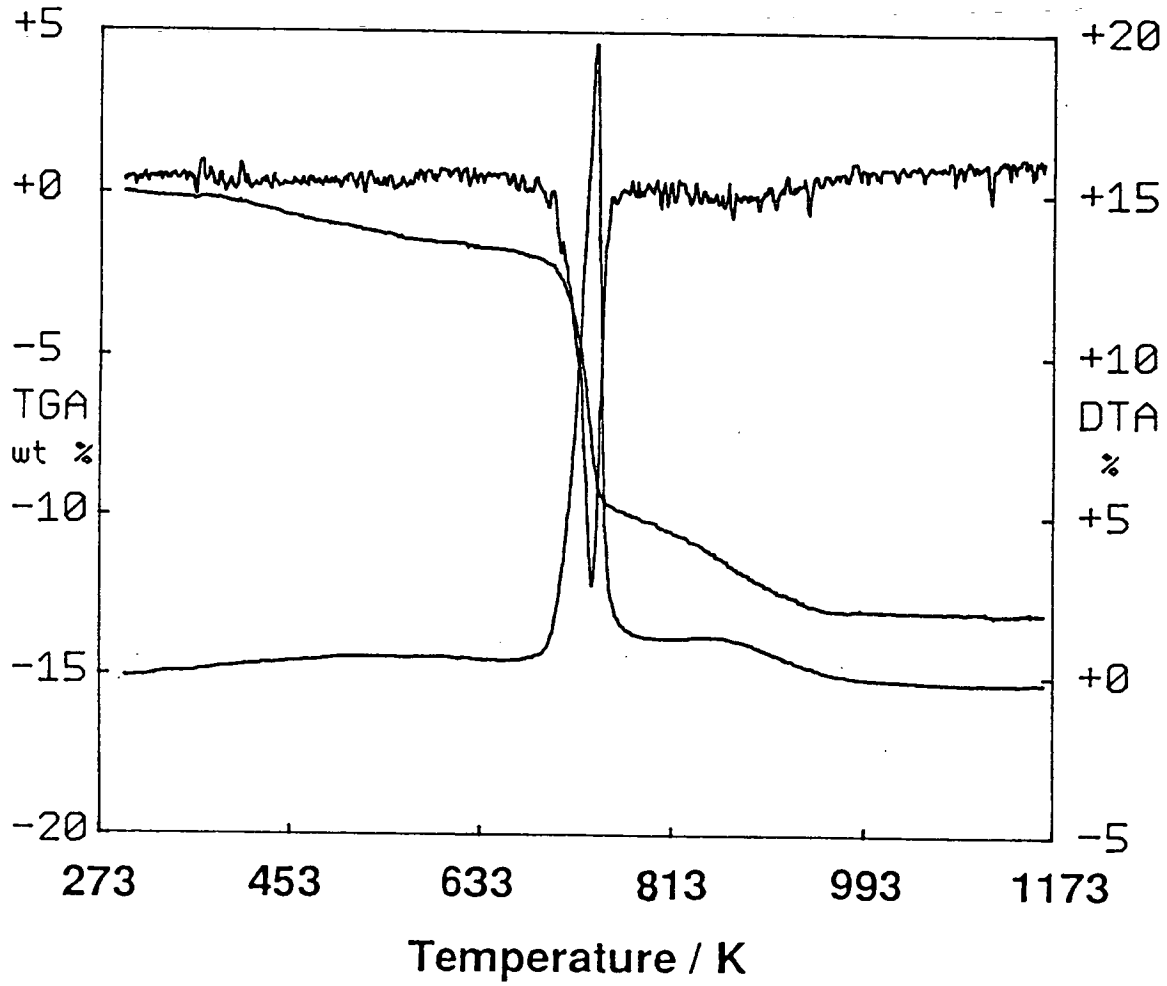

Figure 5–7: tga, dtg and dta profiles for TPA-ZSM-5 (C76)

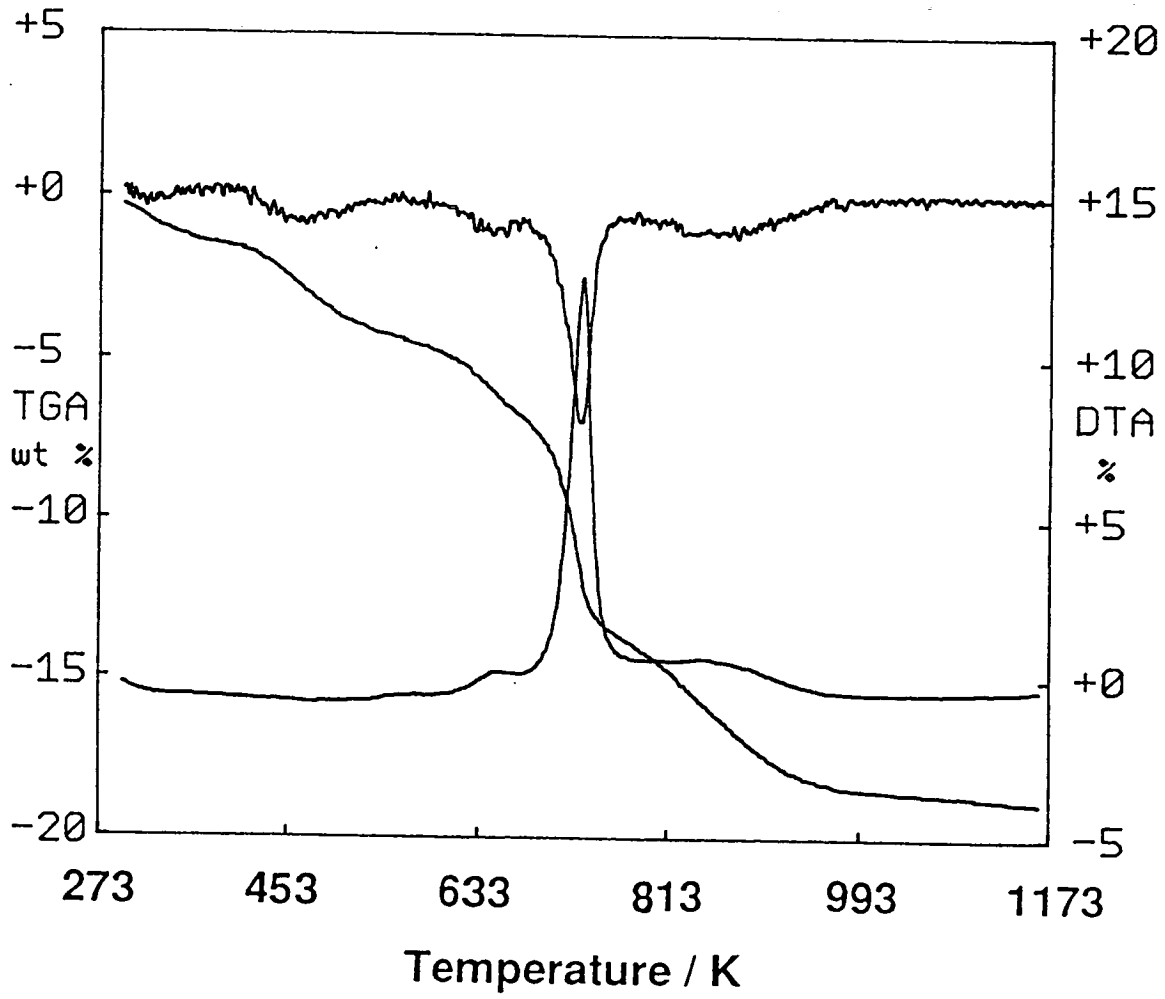

Figure 5–8: tga, dtg and dta profiles for TBA-ZSM-11 (B49)

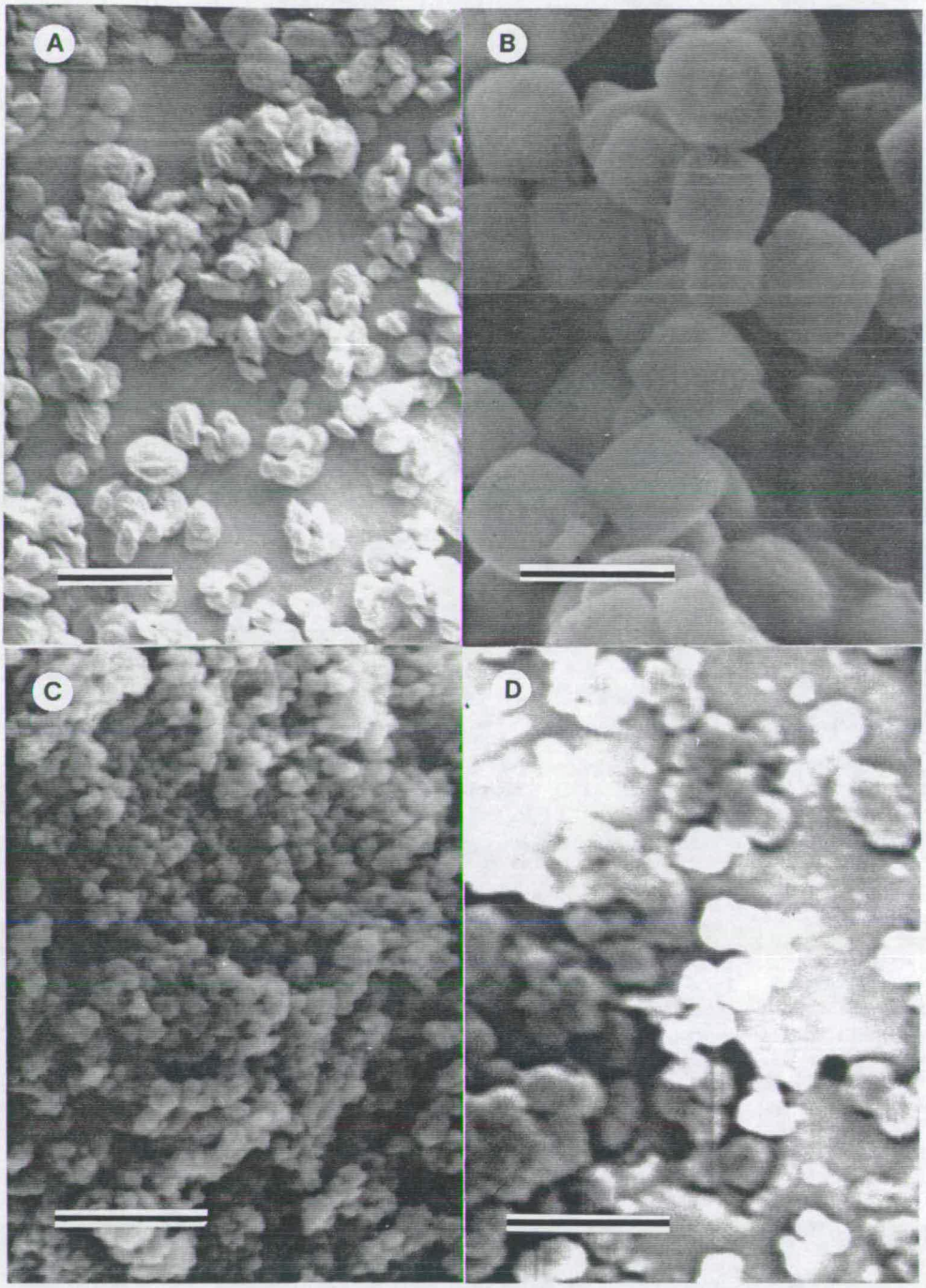

Figure 5–9: SEM photomicrographs of A) TMA-NU-1 (D91, Bar = 5μm), B) TEA-Beta (B89), C) TPA-ZSM-5 (C76), and D) TBA-ZSM-11 (B49) (Bar = 1 μm)

that the product was not adequately washed. The second and third exotherms are probably due to occluded organic material. The first may be due to TMA^+ associated with silanol groups or present within the framework as the hydroxide. The exotherm between 900 and 960 K can be attributed to charge balancing TMA^+ cations which interact strongly with the framework aluminium. Indeed, XRPD of the organic-free residue showed that it had lost much of its crystallinity. Even when sample D91 was calcined at 550 K (19 h) then 1073 K (2 h), it was found by X-ray diffraction to have lost much of its crystallinity. This suggests that NU-1 is not thermally stable at the relatively high temperatures required to completely remove the occluded organic material. It may well be that the thermal energy generated on combustion of the organic, coupled with the strong interaction between the organic and the framework causes the framework to collapse.

Although NU-1 is reported to have been synthesised from reaction mixtures of very low sodium content (Example 13 in ref. [239]), its synthesis in the complete absence of alkali metal cations has not been reported.[1] This is particularly interesting as the only zeolites that have been made from reaction mixtures that contain TMA alone are gismondine and TMA-sodalite [227,228], neither of which are classed as high-silica zeolites. It is also interesting that NU-1 can be obtained quite readily and reproducibly from alkali-free reaction mixtures in which TMA is the sole source of cations. It is not possible to comment on the precise role of TMA in these crystallisations since the structure of NU-1 is not known. However, it would seem that TMA readily directs NU-1 although, like most zeolite crystallisations, this will depend on other factors such as the SiO_2/Al_2O_3 and OH/SiO_2 ratios in the reaction mixture, as well as reaction temperature. That relatively large crystals were obtained suggests that alkali metal cations are not essential for growth.

---

[1]Although the NU-1 patent covers the alkali-free synthesis, it gives no examples

TEA-Beta

In contrast to published work [229,230,231,232] zeolite Beta was found to crystallise in the complete absence of alkali metal cations from the composition:

$$10\ (TEA)_2O\ 1\ Al_2O_3\ 60\ SiO_2\ 3000\ H_2O\ (B89)$$

after 28 d at 403 K (stirred at 300 rpm). This finding raises the question as to the role of alkali metal cations[2] in the synthesis of zeolite Beta. Camblor and Perez-Pariente [229] suggest that alkali metal cations regulate the aluminium concentration in the liquid phase during the synthesis and found that the alkali metal content of the solid phase varies as crystallisation proceeds. They also found that these cations neutralise only a small amount of the framework charge and that they occupy positions in the framework which cannot be accessed by the larger TEA^+ cations. They conclude that alkali metal cations are essential in the nucleation of zeolite Beta and that it cannot be crystallised in their absence.

In the absence of alkali metal cations, the time taken to the onset of crystallisation of TEA-Beta (B89) was very long, approximately 18 d. Furthermore, the growth rate was also found to be slow. Since the crystallisation of Beta in the presence of alkali metal cations [229,230,231,232] is much faster, it is clear that these cations must promote nucleation.

Examination of the alkali-free TEA-Beta sample (B89) by SEM (Figure 5–9) showed that the crystals were quite large (up to 1.0 μm) and with typical cubic morphology. The size of these crystals is not entirely surprising considering the slow rate of nucleation. Furthermore, they are comparable in size to those obtained from reaction mixtures that contained substantial amounts of alkali metal cations [229,230,231]. Clearly then, growth is much less dependent on their being alkali metal cations in the reaction mixture. Sample B89 was also found to have a rather

---

[2]It is generally accepted that in the synthesis of zeolites alkali metal cations can influence crystallisation kinetics, crystal size and morphology

wide crystal size distribution (Figure 5–10), which is very similar to that reported by Camblor and Perez-Pariente (Ref. [229], Figure 6 (e)) for crystallisations with TEA in the presence of potassium cations. This suggests that potassium does not significantly affect either the crystal size or size distribution. That an effect was observed in the presence of sodium and potassium cations [229] is most likely due to the presence of sodium in the reaction mixture.

It is possible that the role of alkali metal cations in the synthesis of Beta is *catalytic*, simply speeding up the nucleation and growth processes, while not being important in balancing the negative framework charge. This may account for only 7% of the framework charge being neutralised by alkali metal cations [229].

The tga and dta profiles for sample B89 (Figure 5–6) were very similar to those reported in the literature [231] for Beta crystallised in the presence of alkali metal cations. Four weight loss events can be seen in Figure 5–6. The first, below 453 K is due to dehydration, which is an endothermic process. This is followed by three distinct exotherms which correspond to decomposition of the occluded organic material. The weight loss between 543 K and 633 K is probably due to TEAOH species which do not interact strongly with the zeolite framework. The two weight loss events between 633 K and 1043 K are ascribed to the loss of TEA^+ cations, which interact more strongly with the framework, hence the higher decomposition temperature. That this occurs in two steps suggests that the TEA^+ cations are located in more than one environment.

One of the most sought after goals in zeolite synthesis is to crystallise each of the polymorphs that make up zeolite Beta.[3] Simulated X-ray diffraction patterns [240] of each polymorph show that the extent of the Beta intergrowth can be determined by the degree of splitting of the broad peak at $2\theta = 7.5°$. Although the XRPD pattern for alkali metal-free Beta crystallised in this study (B89) shows some sign of splitting at this angle (Figure 5–2), no preference was shown for

---

[3]Zeolite Beta is thought to be a 50-50 mixture of tetragonal and monoclinic polymorphs

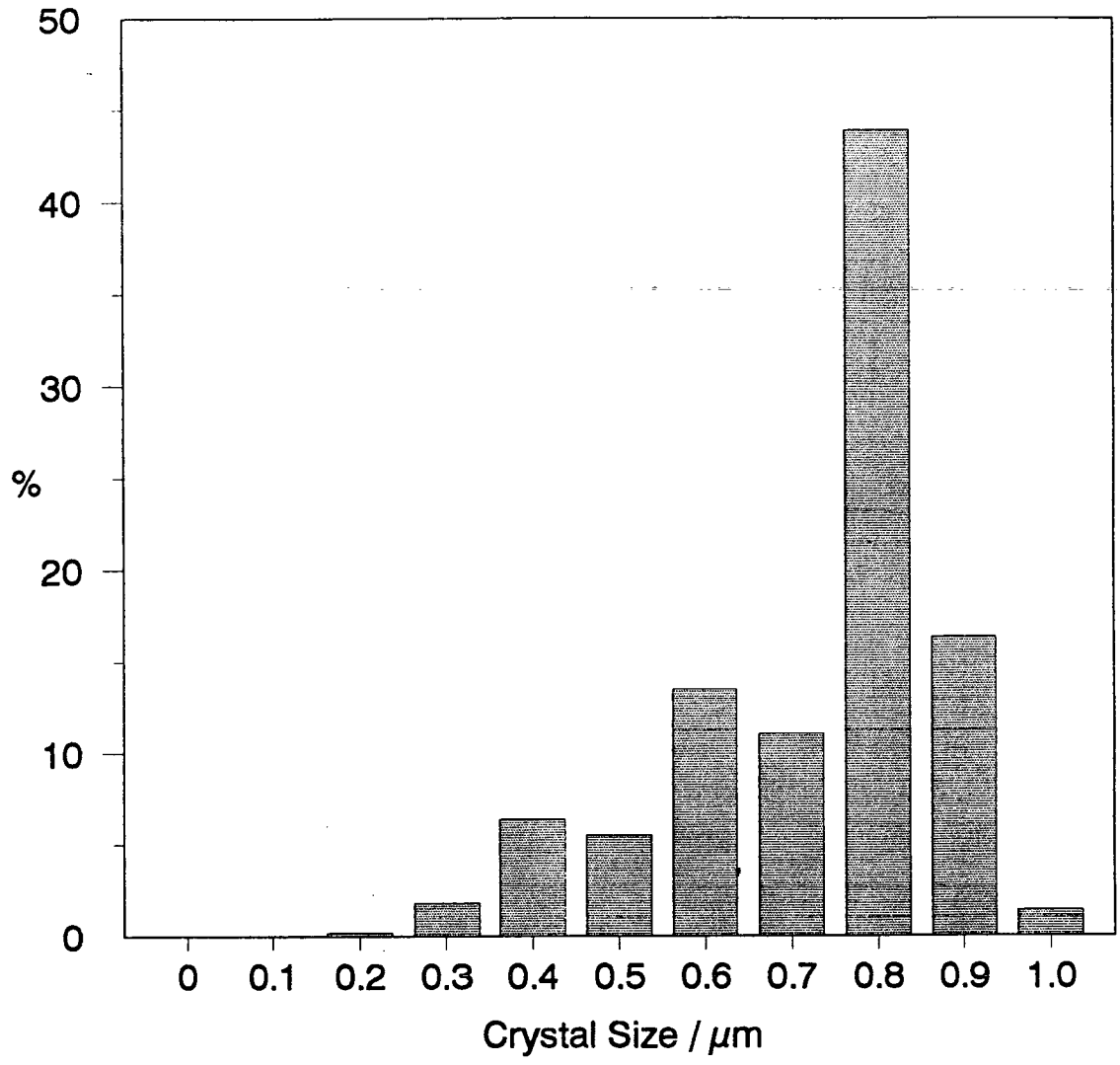

Figure 5–10: Crystal size distribution of zeolite Beta crystallised from the composition 10 $(TEA)_2O$ 1 Al_2O_3 60 SiO_2 3000 H_2O (B89)

either of the polymorphs. That a 50/50 intergrowth was obtained in the absence of alkali metal cations, suggests that neither sodium nor potassium influence the relative amounts of these polymorphs in the crystalline product. Despite this, it is thought that research into the synthesis of either polymorph may be best carried out under alkali-free conditions, which would allow nucleation to take place slowly, thus possibly reducing the chance of crystallising the intergrowth. It may also be that chiral organic directing agents may be required.

TPA-ZSM-5

The composition:

$$10\ (TPA)_2O\ 1\ Al_2O_3\ 60\ SiO_2\ 3000\ H_2O\ (C76, C178)$$

crystallised ZSM-5 after more than 30 days at 423 K (300 rpm). During the synthesis, the pressure in the autoclave was found to increase from 5 to 7 bar which suggested that the TPAOH had degraded[4] to some extent. Furthermore, a strong smell of amine was also noted on dismantling the autoclave. The following results were obtained for CHN analysis of sample C178:

$$C = 9.36\%,\ N = 2.03\%,\ \text{and}\ H = 0.78\%$$

From this, the C/N and H/C ratios were calculated as 14.0 and 2.6 respectively. This suggests that although there was a certain amount of organic degradation, the material occluded in the product is essentially TPAOH and/or TPA^+. It is difficult to establish precisely the extent of template degradation and the effect this may have had on the crystallisation kinetics.

SEM analysis of sample C76 (Figure 5–9) showed it to be composed of aggregates of tiny crystallites ($< 0.2\ \mu m$) which were very difficult to resolve and which

[4]It has been shown [189] that degradation of the quaternary can be extensive in the early part of the reaction

showed considerable peak broadening in powder X-ray diffraction (Figure 5–3). Further examination of the sample by TEM (Figure 5–11) showed the sample to be composed of cubic crystals about 200 nm across. This is consistent with the findings made by Ghamami and Sand [154] who obtained sub-micron ZSM-5 crystals from their alkali-free reactions. Clearly, the TPAOH is able to generate so many nuclei that the reaction mixture becomes depleted of nutrients that would otherwise be available for crystal growth. Although there was a small amount of sodium ion impurity in the reaction mixture ($\sim$ 12 mg l^{-1}) it is thought unlikely that this would have initiated the formation of ZSM-5 nuclei. Indeed, even in the complete absence of alkali metal cations (C258, Chapter 7), TPA-ZSM-5 could still be obtained. Unlike the Beta case described above, however, growth depends very much on the presence of alkali metal cations in the reaction mixture. The influence of alkali metal cations on the crystallisation kinetics of TPA-ZSM-5 will be discussed later in this chapter and in more detail in Chapter 7.

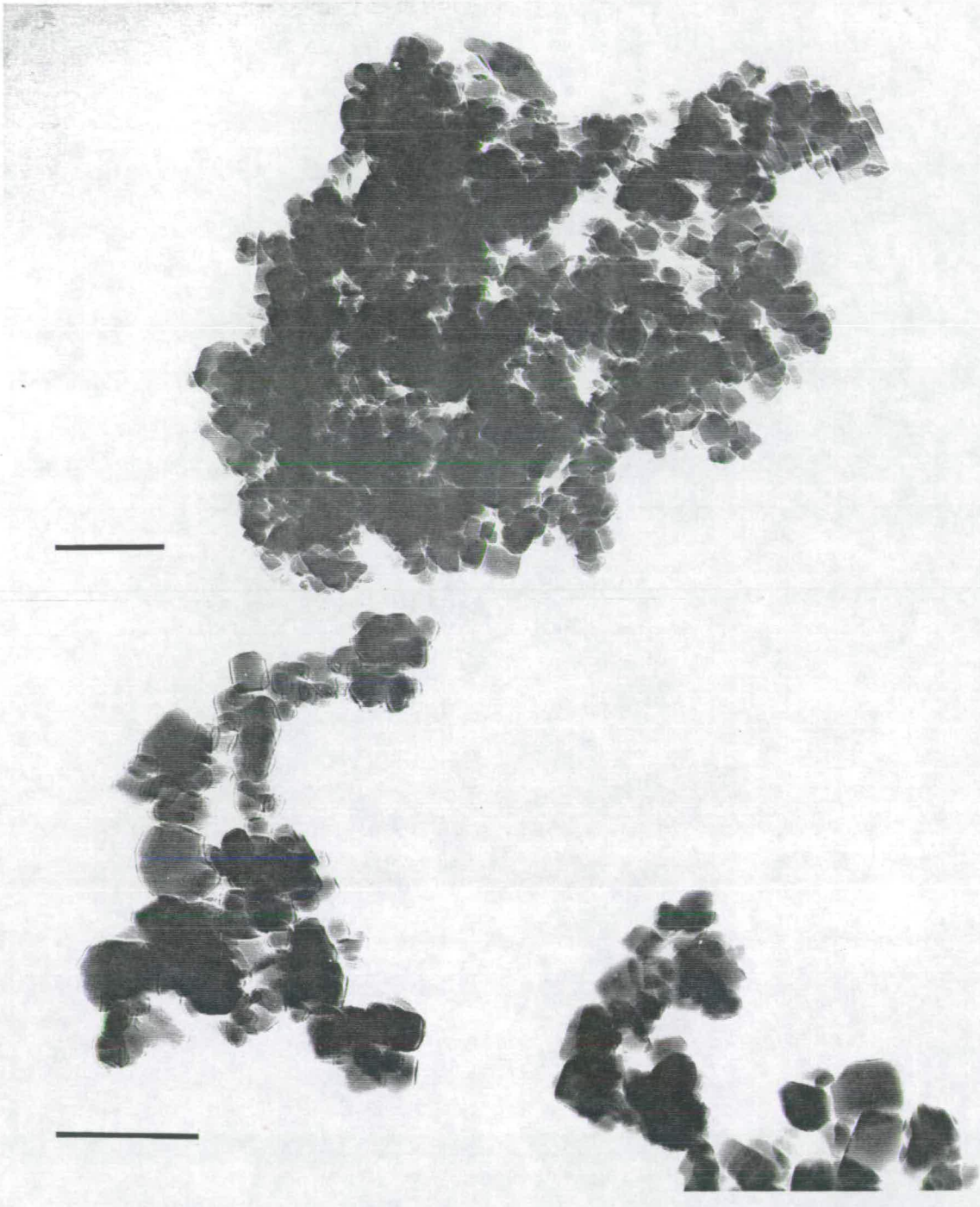

Figure 5–11: Transmission electron photomicrographs of sample C76 (Bar = 1 μm)

TBA-ZSM-11

The composition:

$$10\ (TBA)_2O\ 1\ Al_2O_3\ 60\ SiO_2\ 3000\ H_2O\ (B49)$$

crystallised ZSM-11 after 21 days at 423 K (300 rpm). This is considerably faster than the corresponding TPA reaction (C76) which took over 30 days to crystallise. The difference may be attributed to the degree of pore filling and the ability of the organic to effectively neutralise the framework charge. Since the TPA cation is smaller than the TBA cation and the ZSM-5 framework can accommodate 4.0 TPA cations per unit cell, compared to about 3.0 TBA cations per unit cell in ZSM-11 [238], one would expect TPA-ZSM-5 to accommodate more aluminium in its framework and thus have a lower SiO_2/Al_2O_3 ratio than the TBA-ZSM-11 product. However, as can be seen in Table 5–4, the SiO_2/Al_2O_3 ratio for TPA-ZSM- 5 was 52.6 compared with 44.2 for TBA-ZSM-11. Thus, based on these results TPA-ZSM-5 should crystallise faster than TBA-ZSM-11, since the incorporation of aluminium into the framework can be considered a disruptive process. Careful examination of the unit cell composition of sample B49, however, shows that there is apparently too much aluminium in the framework for the TBA^+ cations to balance the framework charge. The most likely explanation for this is discrepancy is an error in the chemical analysis. It is therefore difficult to attribute the difference in the crystallisation rate on a difference in the SiO_2/Al_2O_3 ratio of the product. It may well be, then that the difference is due to the extent of quaternary ammonium hydroxide degradation under the reaction conditions. Furthermore, there may be a bias in the composition used to study these crystallisations towards the formation of ZSM-11.

Effect of changing the SiO_2/Al_2O_3 in the reaction mixture

Table 5–9 shows the effect of varying the SiO_2/Al_2O_3 ratio in the composition:

$$10\ Q_2O\ y\ Al_2O_3\ 60\ SiO_2\ 3000\ H_2O,$$

where Q = TEA, TPA, or TBA and $0 \leq y \leq 1.5$. As expected, the crystallisation rate increased as the SiO_2/Al_2O_3 ratio in the reaction mixture increased, for both ZSM-5 and ZSM-11. This behaviour is probably due to a decrease in the amount of free OH^- in the system as the amount of aluminium is increased, since more $Al(OH)_4^-$ species are formed which reduces the free base level in the system. Thus the rate of depolymerisation of the amorphous silica is reduced.

TPA readily directs ZSM-5 over a wide range of SiO_2/Al_2O_3 ratios, however, even this cation is ineffective in aluminous reaction mixtures. The theoretical maximum Al/Si ratio of the ZSM-5 framework is 1/11 [177]. Since it seems likely that most preparations of TPA-ZSM-5 starting with TPAOH are contaminated with alkali metal cations, it was decided to determine the outcome of this preparation under ultrapure conditions in the presence of relatively large amounts of aluminium. As has already been mentioned, the maximum number of TPA^+ cations per unit cell of 96 T-atoms is 4. Thus the maximum Al/Si ratio that TPA could sustain is 1/23, corresponding to $(TPA)_4\ (AlO_2)_4\ (SiO_2)_{92}$. The idea was to try to reach or force the system to go beyond this Al/Si limit using Special grade TPAOH.[5] It was thought that forcing the system beyond this limit might crystallise a different product.

The results (Table 5–9) show that TPA-ZSM-5 did not crystallise readily from reaction mixtures with a SiO_2/Al_2O_3 ratio of 40/1 (A222). Indeed this crystallisation took over 50 days at 423 K. It should be noted that the SiO_2/Al_2O_3 ratio of this reaction mixture is below that which would give a product with a SiO_2/Al_2O_3 ratio of at least 46/1 (*i.e.* Al/Si = 1/23). This means that even if all the silica were used up in the crystallisation, some aluminium would have to remain in solution which is very unlikely. Thus the fact that A222 crystallised is surprising. The SiO_2/Al_2O_3 ratio for A222 was 44.1 (Table 5–10) which is very close to the theoretical minimum and certainly within experimental error. However, the XRPD pattern not only contained broad peaks but also suggested the presence of amorphous material. Thus it is possible that the reaction mixture may have

---

[5]Contains 38 mg l^{-1} Na, 2 mg l^{-1} K

disproportionated. From thermal and chemical analyses the unit cell composition for sample A222 was calculated as:

$$(TPA)_{4.0}\ (AlO_2)_{4.2}\ (SiO_2)_{91.8}\ (H_2O)_{7.0}$$

Careful analysis of sample A222 by TEM would establish its phase purity and providing there is no amorphous material present, further analysis should be carried out to determine whether or not the aluminium atoms are located at the channel intersections.

The crystallisation rate for zeolite Beta was found to decrease as the SiO_2/Al_2O_3 ratio increased (Table 5–9). For the reaction mixture with a SiO_2/Al_2O_3 ratio of 90 (B94), the product was found to contain only about 28% Beta after 50 days. This result suggests that it is extremely difficult, if at all possible, to crystallise aluminium-free Beta from aqueous, alkaline silicate gels and is in agreement with other workers [231,232].

Effect of alkali metal impurities in the reaction mixture

Two systems were investigated using reagents of different purity (Table 5–1): the TPA-ZSM-5 system and the TBA-ZSM-11 system. In both systems, the effect of impurities on the crystallisation kinetics and crystal size was very marked. The results are shown in Table 5–11 and SEM photomicrographs for the ZSM-5 materials are shown in Figure 5–12. As expected, larger crystals were obtained from reaction mixtures that contained relatively high levels of alkali metal impurities which suggests that these cations are more important for crystal growth (as already mentioned earlier).

Not surprisingly, the Si/Al ratio in the product decreased with an increase in the alkali metal content of the reaction mixture. This reflects the ease with which aluminium is incorporated into the framework when cations other than TPA cations are present in the reaction mixture.

A plot of ln[Na+K] versus the time taken to crystallise TPA-ZSM-5 (Figure 5–13) shows that below Na + K concentrations of approximately 400 mg kg^{-1},

Table 5–9: Products obtained from the composition 10 Q_2O y Al_2O_3 60 SiO_2 3000 H_2O, where Q = TEA, TPA, or TBA and $0 \leq y \leq 1.5$

Run No	Q[a]	y Al_2O_3	Cryst[n.] Time / d		Product
			t_{nuc}	$t_{100\%}$	
B94	TEA	0.667	25	-[b]	Beta + Amorphous
B89		1	-[c]	28	Beta
D265	TPA	0	< 1	1	Silicalite
C76		1	-[d]	32	ZSM-5
C178		1	28	33	ZSM-5
A222		1.5	-[e]	64	ZSM-5
A196	TBA	0	1	2	Silicalite II
A216		0.25	10	12	ZSM-11
B49		1	15	21	ZSM-11

[a]Supplied by SACHEM

[b]t = 50 d 28% Beta

[c]t = 10 d amorphous, t = 18 d 44% Beta

[d]t = 19 d amorphous, t = 25 d 85% ZSM-5

[e]t = 35 d amorphous, t = 43 d 60% ZSM-5

Table 5–10: Percentage composition of products obtained from the composition 10 Q_2O y Al_2O_3 60 SiO_2 3000 H_2O, where Q = TPA, or TBA and $0 \leq y \leq 1.5$

Run	Composition[a] / %				Si/Al
No	Na	K	Al	Si	
C76	0.019	0.003	1.35	36.9	26.3
A222[b]	nd[c]	nd	1.60	36.8	22.1
A196[d]	0.004	nd	nd	34.7	> 600
A216	nd	nd	0.31	35.1	109.8
B49	nd	0.009	1.58	36.4	22.1[e]

[a]Determined be ICP and flame AES

[b]Determined by XRF

[c]None detected

[d]Fe = 52 mg kg^{-1}

[e]See Table 5–3 and text

Table 5–11: Effect of Na and K impurities on the crystallisation of the composition 10 Q_2O 1 Al_2O_3 60 SiO_2 3000 H_2O, where Q = TPA or TBA

Run[a] No	Quaternary	Cryst$^{n.}$ Time / d		Product	Si/Al
		t_{nuc}	$t_{100\%}$		
C16[b]	TPAOH[c]	< 1	< 1	ZSM-5	20.8
C47	TPAOH[d]	-[e]	-	ZSM-5	25.1
C76	TPAOH[f]	-[g]	32	ZSM-5	26.3
C178	TPAOH[f]	28	33	ZSM-5	-
D264[b]	TBAOH[c]	2	3	ZSM-11	-
C23[b]	TBAOH[d]	13	18	ZSM-11	-
B49[b]	TBAOH[h]	15	21	ZSM-11	-

[a]Product filtered through 0.2 μm filter, or centrifuged

[b]Product filtered through Whatman No. 1 filter paper

[c]Fluka pract grade

[d]Fluka purum grade

[e]t = 25 d amorphous, t = 32 d 100% ZSM-5

[f]SACHEM Special grade

[g]t = 19 d amorphous, t = 25 d 85% ZSM-5

[h]SACHEM HPLC grade

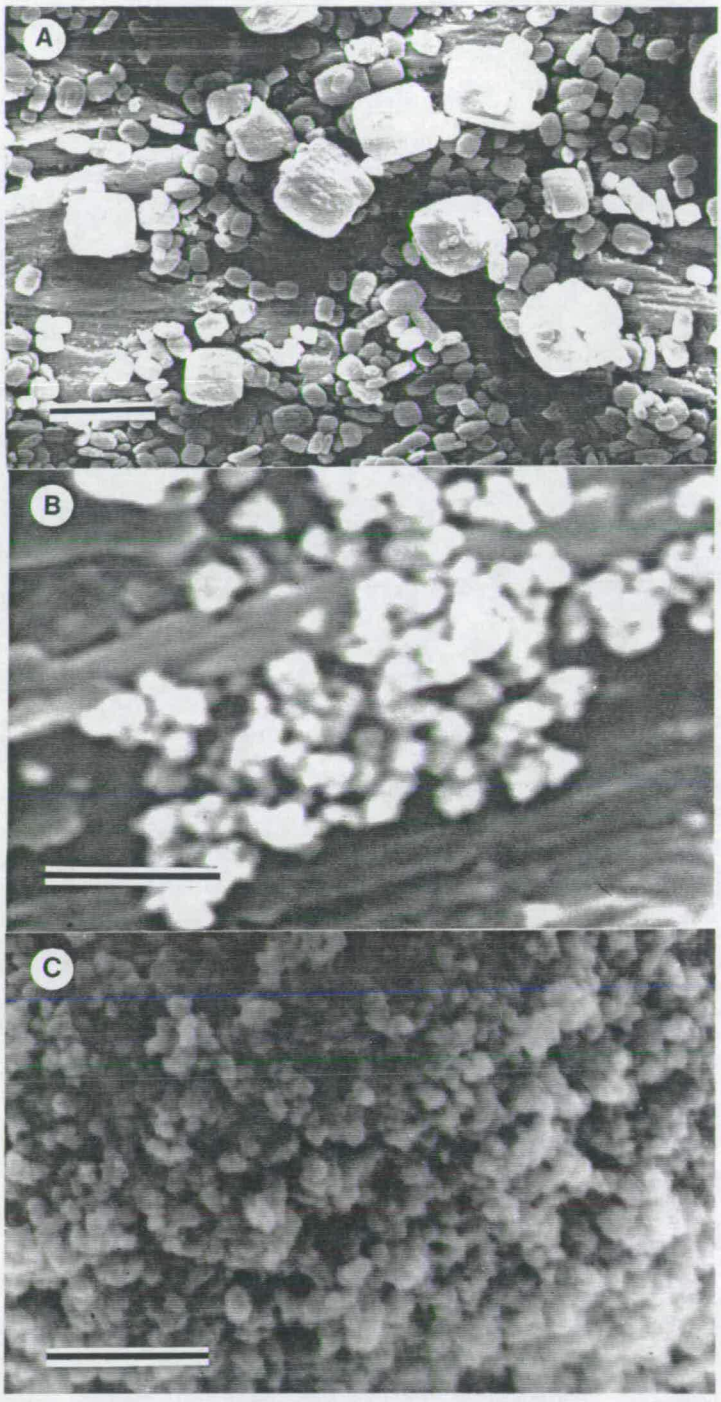

Figure 5–12: Scanning electron photomicrographs of TPA-ZSM-5; A) C16, B) C47, and C) C76 (Bar = 5, 1, and 1 μm respectively)

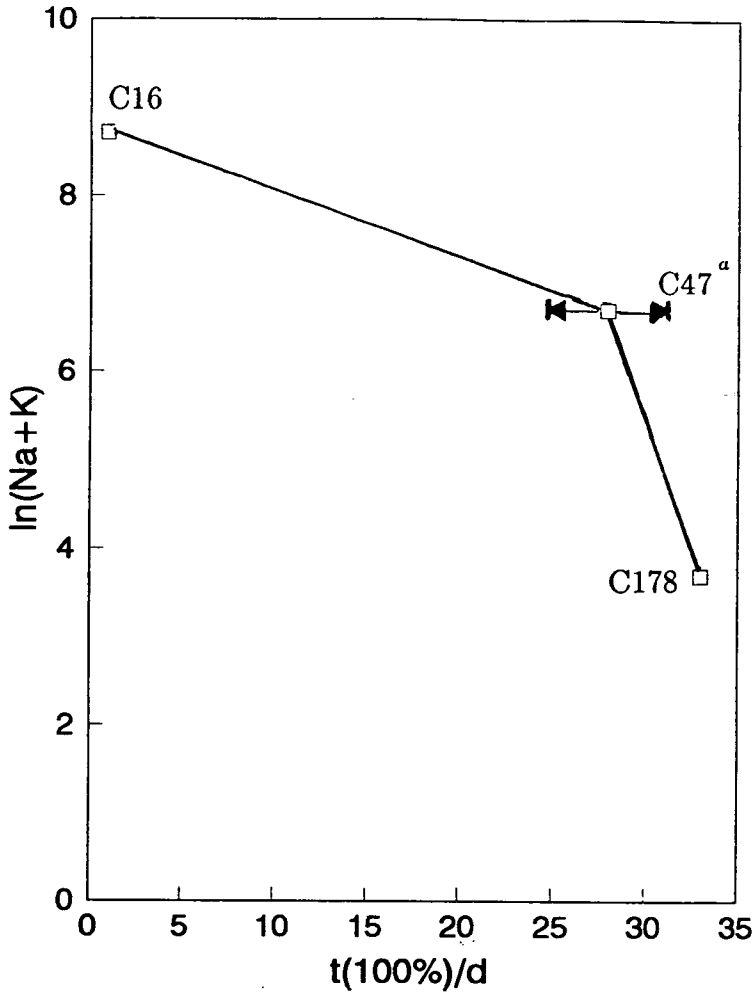

[a]t = 25 d amorphous, t = 32 d 100% ZSM-5

Figure 5–13: Plot of ln[Na + K] versus crystallisation time / d for TPA-ZSM-5 crystallised in the presence of TPAOH of different quality

there is little effect on the time taken to crystallise ZSM-5. This suggests that:
i) Even in the presence of low concentrations of alkali metal cations there are insufficient to promote the crystallisation of ZSM-5. The competition for aluminosilicate species will be very much in favour of TPA^+ cations and few growth species will be provided by the alkali metal cations.
ii) There may be two crystallisation mechanisms in operation, one in which the alkali metal cation plays a significant role (predominantly in crystal growth) at levels above about 400 mg kg^{-1} and the other, below this level, in which it appears to have very little effect. This is by far the most interesting possibility.

A detailed investigation was therefore carried out into the effect of low levels of alkali metal cations on the crystallisation kinetics in the TPA-ZSM-5 system. The aim of this work was to establish whether or not two crystallisation mechanisms operated in this system (which essentially depend on the level of alkali metal impurity) and thus allow further speculation as to the role played by these cations in the synthesis of TPA-ZSM-5. This work is described in Chapter 7.

Careful examination of the XRPD data for the products obtained from the composition:

$$10\ (TBA)_2O\ 1\ Al_2O_3\ 60\ SiO_2\ 3000\ H_2O,$$

C23, B49, and D264 showed no significant differences from data reported in the literature for ZSM-11, which suggests that the products are all pure ZSM-11 phases, with no apparent intergrowth. As expected, the diffraction patterns contained fewer diffraction lines than that given by ZSM-5 due to the higher symmetry of ZSM-11. The most significant differences in the XRPD patterns of ZSM-11 and ZSM-5 are:

i) the absence of peaks at 9.06° and 24.4° 2θ, and

ii) splitting of the peak at 45° 2θ.

None of the products (C23, B49, D264) gave diffraction peaks at 9.06° or 24.4° 2θ despite large amounts of alkali metal cation impurities (D264). Although the diffraction patterns of products C23 and B49 contained broad peaks (due to the presence of small crystals) it is thought unlikely that the 9.06° 2θ peak was masked by the relatively intense peak at 8.8° 2θ. This is reinforced by the absence of the 9.06° 2θ peak from the diffraction pattern of product D264 which contained narrow, well defined peaks. Close inspection of the peak at 45° 2θ showed no splitting in any of the diffraction patterns, which further suggests that the products C23, B49 and D264 are intergrowth-free ZSM-11 phases. Clearly the presence of sodium impurities does not appear to shift the crystallisation towards ZSM-5. This is probably because the amount of potassium in these reactions was substantially larger and possibly masked any effect by the sodium cations. Indeed, it has been reported that potassium promotes the formation of intergrowth-free ZSM-11 [76].

It must be stressed that these results are by no means conclusive and indeed the use of X-ray powder diffraction data to study ZSM-5/11 intergrowths is very difficult and imprecise. For example, Jablonski *et al.* [76] used the peak at 45° 2θ for mechanical mixtures of the two zeolites in order to quantify the extent of ZSM-5/11 intergrowths in products they crystallised. Even for mixtures that contained up to 50% ZSM-5, it was difficult to detect any splitting of this peak.

Despite the relatively small size of the crystals obtained from the alkali-free crystallisations (C23, B49), it would be of interest to establish as far as possible whether these products are indeed pure ZSM-11. This would best be achieved with the use of electron diffraction with lattice imaging [241].

It should be noted that in all of the TBA-ZSM-11 reactions carried out in the present study, traces of magadiite were found in samples taken before crystallisation. However, no magadiite could be detected by XRPD once crystallisation of the ZSM-11 had started. It is difficult to account for this observation, particularly in the alkali-free reactions, but it may be that just a few parts per million of alkali metal cations are required to generate a little magadiite. It is noteworthy that magadiite was a common phase encountered by Jablonski *et al.* [76] in their crystallisations, although they used significantly larger amounts of alkali metal cations.

5.3.2 Surface Area of C76

The micropore volume and surface area of sample C76 (TPA-ZSM-5) were determined as described in Chapter 2. The adsoption/desorption isotherm of n-heptane at 298 K (Figure 5–14) showed good reversibility up to $p/p^o = 0.7$. From extrapolation of the alpha plot the micropore volume and external surface area were calculated as 0.15 $cm^3\ g^{-1}$ and 130 $m^2\ g^{-1}$ respectively. The surface area is typical of materials composed of very small crystals and the micropore volume is what would normally be expected of ZSM-5. Thus the product showed no unusual features in this respect.

Figure 5–14: Adsoption/desorption isotherm of n-heptane at 298 K over ZSM-5 (sample C76)

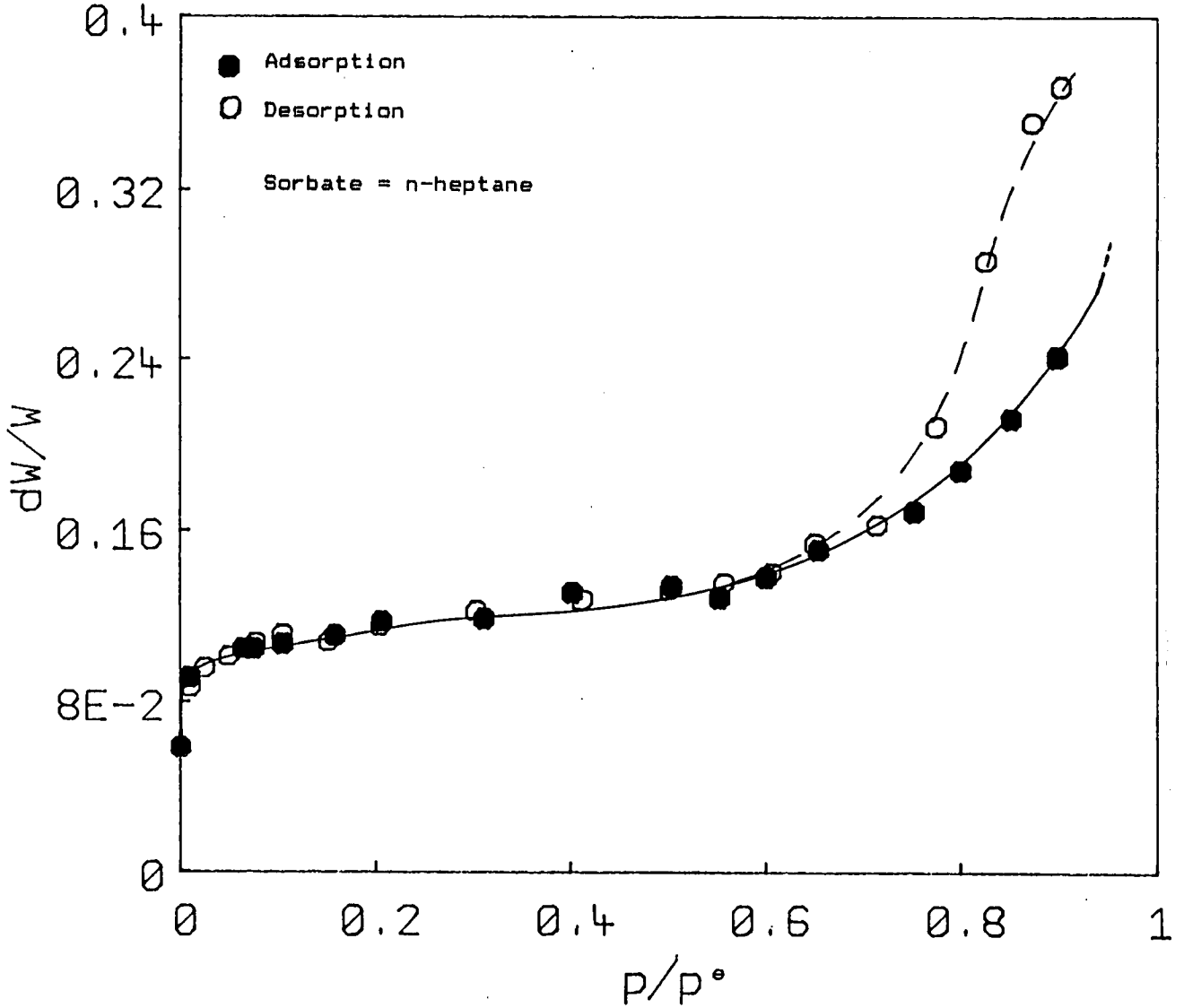

5.3.3 Catalytic Evaluation of C76

Figure 5–15 shows the conversion (%) versus time (h) for sample C76. The steps in these plots are simply changes in the feed rate. The important points to note are the actual percent conversion for a given feed rate and the stability of the catalyst (shown by the gradient). Figure 5–16 shows the plot of activity (corrected at 673K) versus time (h). The activity essentially gives a measure of the rate of conversion. The results shown in both plots show the ZSM-5 product synthesised in this work to be more stable than typical ZSM-5 catalysts, however, it showed low selectivity for the para-DEB isomer due to the small size of the crystals. Reasonable selectivity was only obtained at very high feed rates.

It is difficult to establish from these results, however, the effect that the aluminium distribution had on the behaviour of the catalyst. This was probably due to the very small size of the crystals. It may well be that such a study would be best carried out with larger crystals.

5.3.4 Other Single Quaternary Reactions

The products obtained from stirred reaction mixtures that contained nonamethonium hydroxide ($Nona(OH)_2$)[6] or benzyltrimethylammonium hydroxide (BzTMAOH)[7] are shown in Table 5–12. Nonamethonium hydroxide crystallised silicalite (D251, 2 d) and ZSM-5 (A248, 14 d) in the absence and presence of aluminium respectively. The ZSM-5 product was found to be contaminated with amorphous material. Although a phase other than the MFI type was not obtained under alkali-free conditions, it is believed that further studies under these conditions may well lead to the formation of another zeolite phase. The product obtained from the composition:

$$10\ (BzTMA)_2O\ 1\ Al_2O_3\ 60\ SiO_2\ 3000\ H_2O \text{ (D160, 61 d)}$$

---

[6]Prepared by ion exchange of the bromide with silver oxide

[7]Pract grade

Figure 5–15: Plot of conversion (%) (ethylbenzene to diethylbenzene) versus time (h) for ZSM-5 (sample C76)

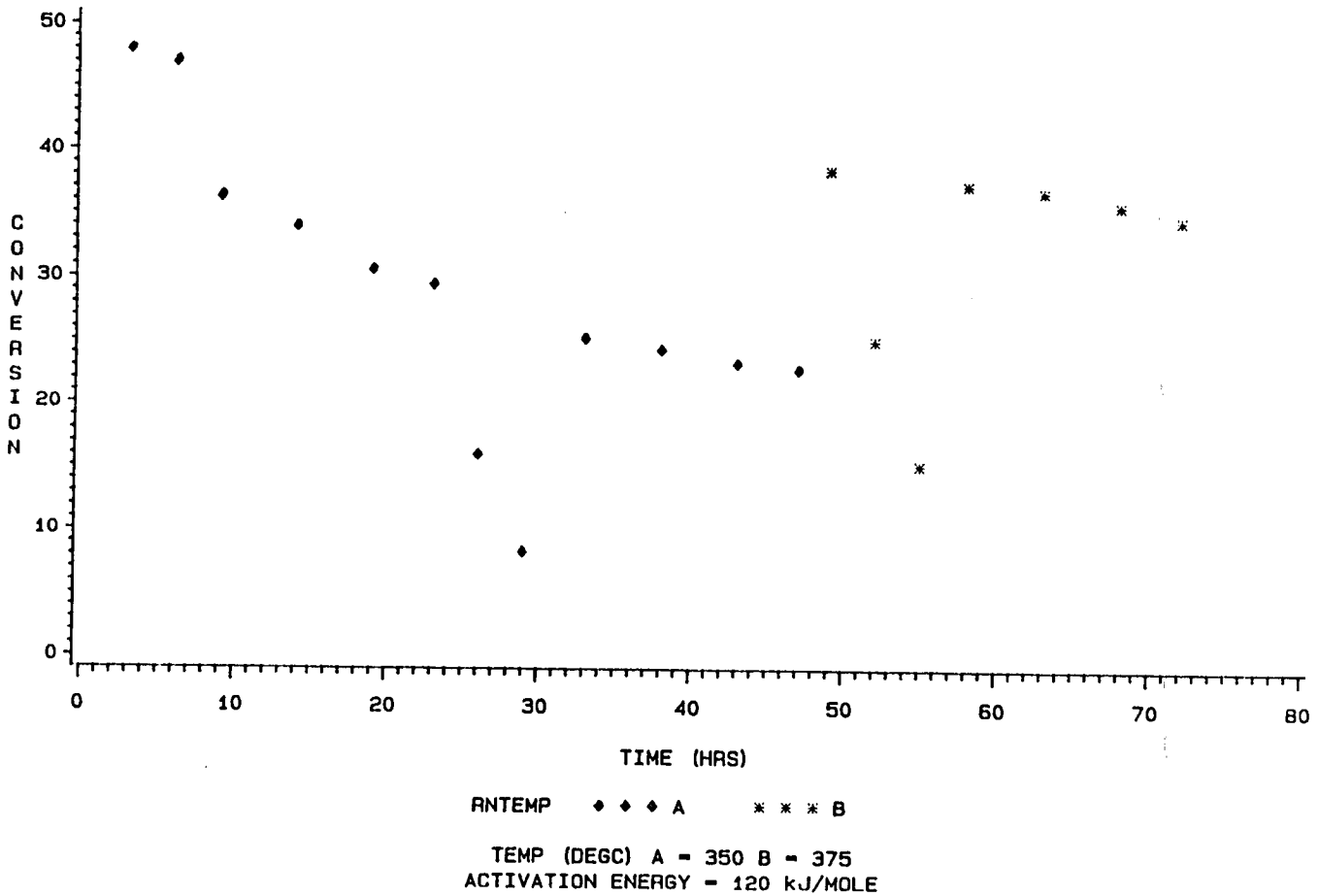

Figure 5–16: Plot of activity (at 673 K) versus time (h) for ZSM-5 (sample C76)

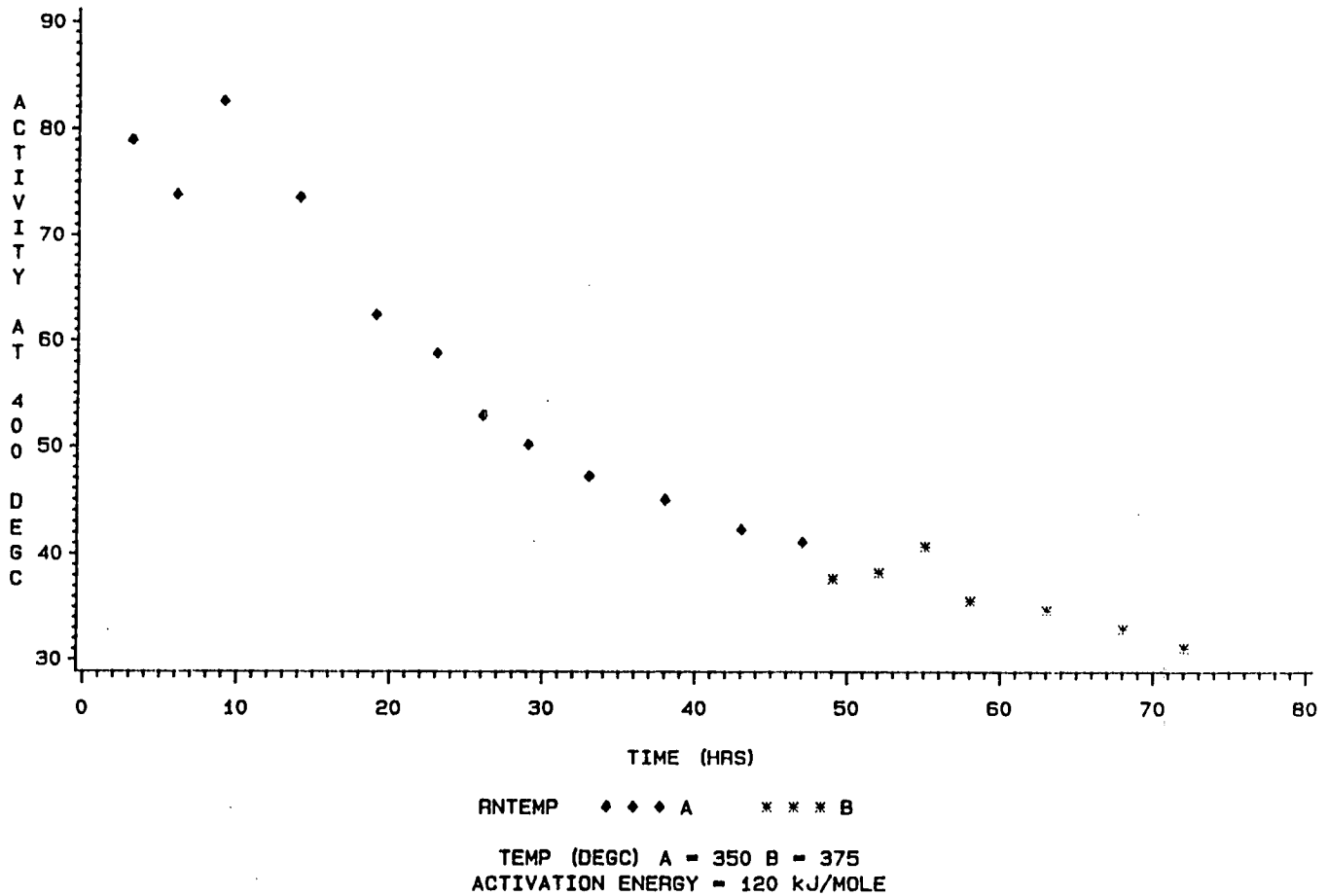

Table 5–12: Products obtained from the composition 10 Q_2O y Al_2O_3 60 SiO_2 3000 H_2O, where Q = $Nona(OH)_2$ or BzTMAOH and $0 < y < 1$

Run No	Q	y	Run Temp / K	Run Time / d	Product
D160	BzTMAOH	1	423	61	ZSM-39 + ZSM-48
A248	$Nona(OH)_2$	1	453	14	ZSM-5 + Amorphous
D251	$Nona(OH)_2$	0	453	1.5	Silicalite

contained ZSM-39 plus a small amount of ZSM-48. However, simple modelling shows that the BzTMA cation is too large to fit into the ZSM-39 cavities. It is likely, therefore, that the product was nucleated by organic species derived from the degradation of BzTMAOH. The presence of large amounts of alkali metal cation impurities may also account for the crystallisation of ZSM-39. BzTMAOH shows some promise in that it does not readily direct any molecular sieve under the conditions used in this study. More importantly, it does not give ZSM-5. It is possible that the presence of substantial amounts of alkali metal cation impurities in the reaction mixtures may have masked any weak structure directing ability of this organic. Furthermore, it is possible that the compositions studied were not appropriate for the formation of zeolitic phases in the presence of BzTMAOH. Thus, a more systematic study of BzTMAOH under carefully controlled alkali-free conditions should be undertaken. Such a study could well lead to the discovery of potentially interesting phases.

Table 5–13 shows the products obtained from static crystallisations of the composition:

10 Q_2O y Al_2O_3 60 SiO_2 3000 H_2O,

where Q = quaternary ammonium hydroxide[8] and $0 < y < 1$, carried out in *TOM* reaction vessels at 423 and 453 K.

The crystalline phases obtained from these static reactions were EU-2 (T2, T19, T20), EU-4 (T3, T4, T13-T15), ZSM-5/silicalite (T5-T8, T17, T18) and Beta (T9). None of the results were particularly surprising. The quaternaries with long alkyl groups favoured the formation of ZSM-5-type materials. Beta was obtained from the reaction mixture that contained dibenzyldimethylammonium cations, however, no crystalline phase was obtained from the corresponding aluminium-free reactions (T11, T12). EU-4 was obtained in the presence of propyltrimethylammonium cations from aluminium and aluminium-free reaction mixtures, which is consistent with the work reported by Casci *et al.* [242]. That diethylpyrrolidinium promotes the crystallisation of EU-4 may not be entirely unexpected since it is claimed that EU-4 is related to the ZSM-23 family of zeolites [242] and pyrrolidine is reported to direct the formation of ZSM-23 [243].

With the exception of the reactions involving cetyltrimethylammonium hydroxide, which was found to be heavily contaminated with alkali metal cations, the results support earlier findings that alkali metal cations may not be required in the synthesis of a large number, if not all, high-silica zeolites.

XRPD data and patterns for sample T3 and a reference sample of EU-4 are shown in Table 5–14 and Figure 5–17 respectively. Thermogravimetric analysis showed a weight loss of approximately 4% and examination of the residue suggested that all the organic had not been removed. This is in accordance with Casci [143], who found that the removal of the occluded organic species became more difficult as the SiO_2/Al_2O_3 ratio of EU-4 increased.

---

[8]Prepared by ion exchange of the bromide with Ag_2O

Table 5–13: Products obtained from the composition 10 Q_2O y Al_2O_3 60 SiO_2 3000 H_2O, where Q = quaternary ammonium cation and $0 < y < 1$

Run No	Q[a]	y	Run Temp / K	Run Time / d	Product[b]
T1	DEP	1	453	14	Quartz, tr
T2	DEP	1	423	47	EU-2, maj
T3	DEP	0	453	14	EU-4, maj
T4	DEP	0	423	47	EU-4, maj
T5	MPP	1	453	14	ZSM-5, min
T6	MPP	1	423	47	ZSM-5, min
T7	MPP	0	453	14	ZSM-5[c], maj
T8	MPP	0	423	47	ZSM-5[c], maj
T9	DBzDMA	1	453	14	Beta, min
T10	DBzDMA	1	423	47	Amorphous
T11	DBzDMA	0	453	14	Amorphous
T12	DBzDMA	0	423	47	Amorphous
T13	PTMA	1	453	14	EU-4, min
T14	PTMA	1	423	47	EU-4, min
T15	PTMA	0	453	14	EU-4, maj + EU-2, tr + Cristob, tr
T16	PTMA	0	423	47	EU-4, min
T17	CeTMA	1	453	14	ZSM-5, min
T18	CeTMA	1	423	47	ZSM-5, min
T19	CeTMA	0	453	14	EU-2, maj
T20	CeTMA	0	423	47	EU-2, maj

[a]Key: DEP = Diethylpyrrolidinium; MPP = Methyl-n-pentylpiperidinium; DBzDMA = Dibenzyldimethylammonium; PTMA = Propyltrimethylammonium; CeTMA = Cetyltrimethylammonium

[b]Key: tr = trace; min = minor; maj = major

[c]Probably silicalite

Table 5–14: XRPD data for the product obtained from the composition 10 $(DEP)_2O$ 60 SiO_2 3000 H_2O (T3), crystallised without agitation at 453K

T3		EU-4[a]	
d / pm	100 I/I_o	d / pm	100 I/I_o
1078	8	1110	vs[b]
903	20	920	w-vs
738	6	762	m
676	3	687	m
615	1	629	m
591	2	598	w-m
455	64	463	vs
443	27	447	w-s
428	100	429	vs
393	34	398	vs
372	22	380	w
369	19	368	s
353	21	358	w-s
340	8	342	m
330	33	332	s
324	35	327	s-vs
320	14	323	m
310	7	311	w

[a]Reference [143]; data for the as-synthesised material

[b]Key: w = weak; m = medium; s = strong; vs = very strong

Figure 5–17: XRPD patterns of T3 (top) and EU-4 (bottom)

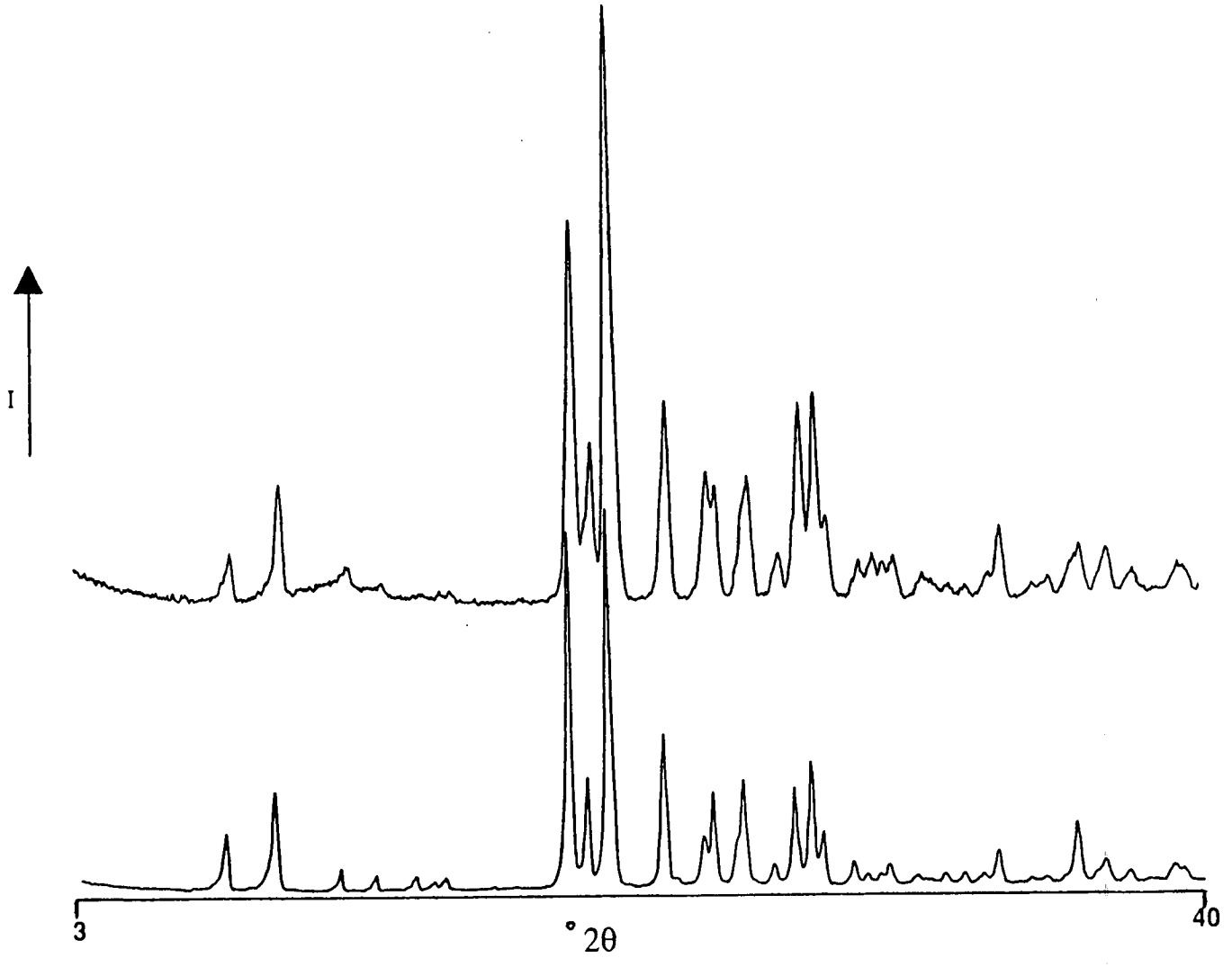

5.3.5 Mixed Quaternary Reactions

Reactions containing TMA

The products obtained from the composition:

$$9\ Q_2O\ 1\ (TMA)_2O\ 1\ Al_2O_3\ 60\ SiO_2\ 3000\ H_2O,$$

where Q = TEA, TPA, and TBA, crystallised at 423 K with stirring (300 rpm) are shown in Table 5–15.

All compositions gave products that would have crystallised in the absence of TMA. However, the presence of TMA in the reaction mixture did affect the crystallisation kinetics, although to different extents. The most notable result in Table 5–15 was the increase in the rate of crystallisation of ZSM-5 from the composition:

$$10\ Q_2O\ 1\ Al_2O_3\ 60\ SiO_2\ 3000\ H_2O,$$

where Q = 9 $(TPA)_2O$ + 1 $(TMA)_2O$ (D77, A129). The product was obtained in less than 4 days and was easily filtered through Whatman No. 1 filter paper. This is a remarkable result when one considers that the corresponding TMA-free composition:

$$10\ (TPA)_2O\ 1\ Al_2O_3\ 60\ SiO_2\ 3000\ H_2O\ (C76, C178),$$

crystallised sub-micron TPA-ZSM-5 in over 30 days at the same reaction temperature. Clearly then, in the alkali-free system, the TMA cation not only has a dramatic effect on the crystallisation kinetics but it also encourages the growth of larger crystals. Although the dramatic effect on crystallisation kinetics is not widely reported in either the open or patent literature, the effect of TMA on crystal size is widely reported in the presence [244,245,246,247] and absence [160] of alkali metal cations.

In a similar study by Rossin and Davis [248], where reactions were carried out in the presence of low and high concentrations of sodium cations, TMA was found

Table 5–15: Products obtained from the composition (10-x) Q_2O x $(TMA)_2O$ 1 Al_2O_3 60 SiO_2 3000 H_2O (423 K, 300 rpm)

Run No	Q[a]	x	Cryst[n]. Time / d		Product	Yield[b] / %
			t_{nuc}	$t_{100\%}$		
D107[c,d]	TEA	1	-	-	Amorphous	-
B89[c]	TEA	0	-[e]	28	Beta	59
A129	TPA	1	1.5	3.5	ZSM-5	66
C76	TPA	0	-[f]	32	ZSM-5	54
A105	TBA	1	14	17	ZSM-11	52
B49	TBA	0	15	21	ZSM-11	57

[a]Supplied by SACHEM

[b]Based on SiO_2 + Al_2O_3

[c]Reaction carried out at 403 K

[d]Approximately 25% of autoclave contents lost during reaction, t = 25 d amorphous

[e]t = 10 d amorphous, t = 18 d 44% Beta

[f]t = 19 d amorphous, t = 25 d 85% ZSM-5

to have little effect on the crystallisation kinetics in their systems. It is possible that even the presence of low amounts of sodium ions would have masked any effect that the TMA cation may have had on the crystallisation kinetics.

It is particularly surprising that, given the structural similarity of ZSM-11 and ZSM-5, the presence of TMA in the corresponding TBA reaction, *i.e.*

$$9\ (TBA)_2O\ 1\ (TMA)_2O\ 1\ Al_2O_3\ 60\ SiO_2\ 3000\ H_2O\ (A105),$$

did not significantly affect the crystallisation kinetics of TBA-ZSM-11. This composition was found to crystallise ZSM-11 in 17 days, only 4 days faster than the corresponding TMA-free reaction (B49). The difference between the crystallisation rates for A129 and A105, may simply be due to the degree of pore filling. Thus, it is likely that more void space will be occupied by TMA and TPA cations in ZSM-5 than TMA + TBA cations in ZSM-11. However, it should be noted that neither CHN nor ^{13}C MASNMR analyses were carried out on these samples so it is difficult to establish whether or not TMA was actually incorporated into the ZSM-11 framework.

As can be seen from Table 5–16, the composition range over which the TMA cation was effective in the TPA system is quite narrow. Although there was a marked change in the crystallisation kinetics, the most significant effect of varying the TPA/TMA ratio in the reaction mixture, while keeping the OH/SiO_2 and SiO_2/Al_2O_3 ratios constant, was the change in the nature and yield of the product obtained. As the proportion of TPA in the reaction mixture was decreased (with a corresponding increase in TMA), not surprisingly the product obtained shifted from pure TPA-ZSM-5 to pure TMA-NU-1, with mixtures of the two crystalline phases obtained with intermediate ratios. With the exception of the compositions:

$$9\ (TPA)_2O\ 1\ (TMA)_2O\ 1\ Al_2O_3\ 60\ SiO_2\ 3000\ H_2O\ (A129)$$

and

$$8.5\ (TPA)_2O\ 1.5\ (TMA)_2O\ 1\ Al_2O_3\ 60\ SiO_2\ 3000\ H_2O\ (A126),$$

Table 5–16: Crystallisation of the composition (10-x) $(TPA)_2O$ x $(TMA)_2O$ 1 Al_2O_3 60 SiO_2 3000 H_2O (423 K, 300 rpm)

Run No	x	Cryst$^{n.}$ Time / d		Product	Yield[a] / %	Si/Al
		t_{nuc}	$t_{100\%}$			
C76	0	-[b]	32	ZSM-5	54	26.3
C106	0.5	12	15	ZSM-5	51	-
A129	1	1.5	3.5	ZSM-5	66	23.0
A126	1.5	4	7	ZSM-5 + Amorphous	37[c]	16.1[d]
D96	9.5	< 4	9	ZSM-5 + NU-1	54[e]	-
D91	10	20	25	NU-1	48	-

[a]Based on SiO_2 + Al_2O_3

[b]t = 19 d amorphous, t = 25 d 85% ZSM-5

[c]Total solid recovered contained about 78% of fully crystallised ZSM-5

[d]Sample may have contained some amorphous material

[e]Total solid recovered, ZSM-5 major phase

the amount of solid material recovered was reasonably constant, approximately 50% (based on SiO_2 + Al_2O_3). The amount of solid recovered from reaction A129 was considerably higher (66%) which suggests this composition is close to that which would give the maximum amount of ZSM-5. In contrast, a small reduction in the TPA/TMA ratio from 9/1 (A129) to 8.5/1 (A126) dramatically reduced the yield. Furthermore, the product was also found to be contaminated with much amorphous material (A126).

SEM photomicrographs of the products obtained from reaction mixtures in which the ratio of TPA/TMA was 10/0 (C76), 9/1 (A129) and 8.5/1.5 (A126) are shown in Figure 5–18. The increase in crystal size with decreasing TPA/TMA ratio is clear but what is striking is the unusual morphology of A126. These *marrowbone* shape crystals were found to be contaminated with amorphous material as well as

a second, possibly crystalline phase (probably quartz). This product also showed unusual behaviour on thermal analysis. After drying for 4 hours at 393 K, the product was equilibrated over a saturated solution of sodium chloride before tga. An enormous weight loss ($\sim$ 45%) was recorded below 473 K which suggested that the product contained a substantial amount of water. The analysis was repeated on a sample that had been dried for 2 days at 393 K. This time, however, the weight loss due to water was much smaller ($\sim$ 4%). The discrepancy in these results is difficult to account for but could be linked to the unusual morphology of the crystals (*eg.* the outer *sheath* of the *marrowbone* might restrict the ready removal of water).

It is not known whether this unusual morphology offers any catalytic advantages over conventional ZSM-5 materials. Sorption studies were carried out to determine the surface area and micropore volume of sample A126. The results of these studies will be discussed later. The chemical composition of the *sheath* and *core* was not determined.

The precise role of the TMA cation in the mixed quaternary systems described above is open to debate. It is thought that, in the TPA-ZSM-5 system, it might play a role similar to that of the sodium cation in view of their similar size[9]. In the absence of TMA, the alkali-free TPA system clearly struggles to make ZSM-5 (C76). This is undoubtedly due to the presence of large amounts of aluminium in the reaction mixture. As has already been mentioned, since TPA^+ cations are the only ones available to balance the framework charge, the aluminium must be located at or very close to the channel intersections, on the basis that TPA^+ cations occupy the channel intersections. Thus the incorporation of aluminium into the framework is very precise and much less random than in systems where other, usually smaller, charge balancing cations are present. Clearly then, the presence of a small amount of TMA^+ cations enables a more random distribution of aluminium in the product. Thus there role is similar to that of alkali metal

---

[9]Ionic radius = 720 pm, 730 pm, and 690 pm for Na (hydrated), TMA (hydrated) and TMA (anhydrous) respectively [62]

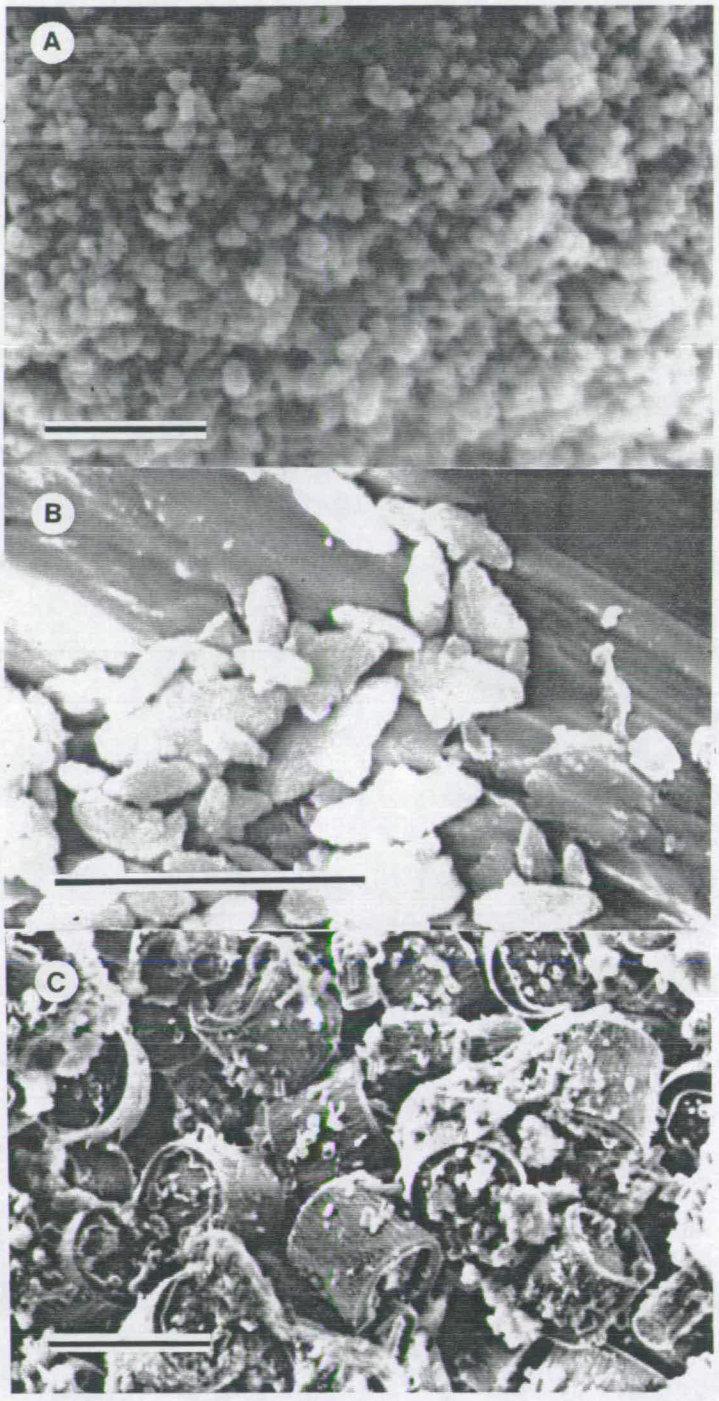

Figure 5–18: SEM photomicrographs of A) C76, B) A129, and C) A126 (Bar = 1, 5, and 10 μm respectively)

cations. Unlike sodium and potassium, however, TMA^+ cations may replace some of the occluded TPA^+ cations. Thus TMA is thought to hold an intermediate position between sodium and potassium cations and TPA cations in promoting the crystallisation of ZSM-5. It should be recalled from Chapter 4, however, that it is believed that TMA cannot nucleate ZSM-5. Evidence for the occlusion of TMA^+ together with TPA^+ comes from ^{13}C MASNMR analysis (Table 5–17). Furthermore, CHN analysis (Table 5–18) strongly suggests that TMA cations may actually replace some of the occluded TPA cations and it is possible that some will occupy the channel intersections.

It is estimated from the C/N data that the framework can accommodate over 50% of the occluded organic material as TMA (A126). The increase in the crystallisation kinetics may also, therefore, be attributed to the ease with which the ZSM-5 channel system is filled with both TMA and TPA cations as opposed to TPA cations alone. Indeed, this may also account for the slight increase in the rate of TBA-ZSM-11 crystallisation, although as was mentioned earlier, it is not clear whether TMA is occluded in the ZSM-11 framework. That TMAOH was unable to improve the crystallisation kinetics of Beta may be attributed to similarities between TMA^+ and TEA^+ cations for aluminosilicate species. Furthermore, it is likely that both the gel chemistry and the structure of the resultant crystalline phase are important in determining whether synergistic or competitive effects are dominant.

The results in Table 5–16 also show that, as the TMA content of the reaction mixture increases from 0 to 1.5, the Si/Al ratio of the product decreases, *i.e.* the product becomes more aluminous. This again implies that TMA is readily occluded in the framework to neutralise the negative charge. What is interesting is that the structure appears willing to sacrifice some of the stabilisation energy gained from complete pore filling by TPA cations in order to accommodate more framework aluminium. It can be seen from Table 5–18 that, although the total weight of occluded organic in the product decreases as the ratio TPA/TMA decreases, the total number of moles of organic remains almost constant. This implies that there is a reduction in the amount of void space occupied by organic

Table 5–17: ^{13}C MASNMR data for the products crystallised in the presence of TMA, TMA + TPA, and TPA

Run No	TPA/TMA	Chemical Shift (δ) / ppm				
B228	0/10	-	57.4	-	-	-
C158	10/0	61.6	-	15.8	11.0	10.3
A129	9/1	62.8	56.3	16.4	11.2	10.1
A126	8.5/1.5	62.9	56.7	16.4	11.2	10.2

material. This may account for the decrease in crystallisation kinetics and yield of ZSM-5 when the ratio TPA/TMA in the reaction mixture is decreased. In the case of sample A126, it would appear that there is only 1 TPA cation per unit cell (*i.e.* 1 per four channel intersections, Table 5–19). This may account for the very poor product yield and unusual morphology. This probably represents the minimum number of TPA cations per unit cell that the system is prepared to tolerate in the presence of relatively large amounts of TMA^+ cations. Beyond this, the system will disproportionate and crystallise both ZSM-5 and NU-1.

That TPA-ZSM-5 crystallises in the absence of TMA cations (C76, C178) clearly demonstrates that these cations are not required for nucleation. However, TMA cations certainly promote crystal growth.

The effect of the SiO_2/Al_2O_3 ratio of the reaction mixture on the crystallisation rate was examined for the compositions:

$$9\ (TPA)_2O\ 1\ (TMA)_2O\ y\ Al_2O_3\ 60\ SiO_2\ 3000\ H_2O$$

and

$$8.5\ (TPA)_2O\ 1.5\ (TMA)_2O\ y\ Al_2O_3\ 60\ SiO_2\ 3000\ H_2O,$$

where $0 < y < 2$.

In all the compositions studied only ZSM-5 or silicalite was obtained (Tables 5–20 and 5–21).

Table 5–18: Change in the amount of occluded organic with TPA/TMA ratio in the reaction mixture

Run No	TPA/TMA	C/N	Organic weight loss / %			TPA^+/TMA^+	Moles of Organic[b]
			TMA^+ [a]	TPA^+ [a]	Total		
C76	10/0	14.0	-	10.20	10.2	-	0.05
C106	9.5/0.5	10.8	1.53	8.67	10.20	5.7	0.05
A129	9/1	10.0	2.35	7.05	9.4	3.0	0.07
A126	8.5/1.5	7.8	3.15	2.85	6.0	0.9	0.06

[a]Calculated from C/N data as follows:

$$y = 12x + 4(1 - x)$$

Rearranging and simplifying:

$$x = \frac{y - 4}{8}$$

where x = fraction of TPA^+ and y = C/N ratio.

Then for a total organic weight loss, w, the weight loss due to TPA^+, z is:

$$z = w\left\{\frac{y - 4}{8}\right\}$$

[b]Based on relative amounts of TMA and TPA

Table 5–19: Unit cell composition

Run	Unit Cell Composition				
No	SiO_2	Al_2O_3	TMA^+	TPA^+	H_2O
C76	92.5	1.75	-	3.6	5.4
A129	92.0	2.0	2.1	2.6	4.5
A126[a]	90.4	2.8	2.6	0.9	13.3

[a]The large difference between the number of Al atoms and TMA + TPA may be due to the fact that the sample contained some amorphous phase, which may be Al-rich

As with the single quaternary system, an increase in the SiO_2/Al_2O_3 ratio in the reaction mixture resulted in an increase in the crystallisation rate. Not surprisingly, the C/N ratio decreased as the SiO_2/Al_2O_3 ratio in the reaction mixture decreased, since more TMA is required to balance the framework charge and so more is occluded in the framework at the expense of TPA cations. Furthermore, products crystallised from reaction mixtures that contained a higher proportion of TMA, *i.e.* TPA/TMA = 8.5/1.5 (A126, A212) compared with TPA/TMA = 9/1 (A129, A126), were more aluminous.

It can be seen from a comparison of the results in Tables 5–20 and 5–21 that for a slight decrease in the TPA/TMA ratio, for a given SiO_2/Al_2O_3 ratio in the reaction mixture, the growth rate is not significantly affected. However, the time taken to the onset of crystallisation varied markedly. Reaction mixtures with SiO_2/Al_2O_3 ratios > 60 crystallised faster with a TPA/TMA ratio of 9/1 (A202, A129) compared to those with a ratio of 8.5/1.5 (A204, A126). On reducing the SiO_2/Al_2O_3 ratio below 60, there was a change-over in these trends. Thus, as the SiO_2/Al_2O_3 ratio in the reaction mixture decreased, those with a TPA/TMA ratio of 8.5/1.5 crystallised faster than those with a ratio of 9/1 (*eg.* A212 compared with A206). This can be attributed to the *availability* of the TMA cation for neutralisation of the framework. Both systems clearly have a lower SiO_2/Al_2O_3

Table 5–20: Effect of SiO_2/Al_2O_3 ratio on the crystallisation of ZSM-5 from the composition 9 $(TPA)_2O$ 1 $(TMA)_2O$ y Al_2O_3 60 SiO_2 3000 H_2O

Run No	y	Cryst$^{n.}$ Time / d		Yield[a]	Si/Al_{prod}	C/N
		t_{nuc}	$t_{100\%}$			
A202	0	5 h[b]	13 h	52	> 600[c]	10.4
A129	1.0	1.5	3.5	66	23.0	10.0
A206	1.5	18	22	65	18.3	8.0
D137[d]	2.0	-	-	-	-	-

[a]Based on $SiO_2 + Al_2O_3$

[b]Hours

[c]Aluminium not detected (detection limit = 0.05%)

[d]t = 60 d amorphous

threshold from which ZSM-5 can crystallise. Below a SiO_2/Al_2O_3 ratio of 30, neither system crystallised and it is likely that even a further increase in the TMA content of the reaction mixture would not promote the crystallisation of ZSM-5, without the co-crystallisation of another phase (probably NU-1).

For both systems where y = 0 (A202, A204) and y = 1.5 (A206, A212), the amount of crystalline material recovered was fairly similar. However, when y = 1 (A129, A126) the yields were substantially different, as has already been mentioned. It should be noted however that the XRPD pattern for sample A212 was very poor, consisting of very broad ill-defined peaks. It is quite possible, then, that this sample may have contained amorphous material which was not readily seen in the XRPD pattern. Clearly, unlike the 9 TPA/1 TMA system, the product yield from the 8.5/1.5 system is particularly sensitive to the SiO_2/Al_2O_3 ratio in the reaction mixture.

It is likely that the effect of TMA on the crystallisation kinetics of TPA-ZSM-5 would have gone undetected if alkali-free reagents had not been used. This is supported by the fact that the composition:

Table 5–21: Effect of SiO_2/Al_2O_3 ratio on the crystallisation of ZSM-5 from the composition 8.5 $(TPA)_2O$ 1.5 $(TMA)_2O$ y Al_2O_3 60 SiO_2 3000 H_2O

Run No	y	Cryst$^{n.}$ Time / d		Yield[a]	Si/Al$_{prod}$	C/N
		t_{nuc}	$t_{100\%}$			
A204	0	11 h[b]	19 h	57	>600[c]	10.4
A126	1.0	4	7	37[d]	16.1	7.8
A212[e]	1.5	4	9	60	16.5	8.7
A253[f]	2.0	-	-	-	-	-

[a]Based on $SiO_2 + Al_2O_3$

[b]Hours

[c]Aluminium not detected (detection limit = 0.05%)

[d]Total solid recovered contained about 78% of fully crystallised ZSM-5

[e]May contain amorphous material (see text)

[f]t = 33 d amorphous

Table 5–22: Crystallisation of the composition 8.5 $(TPA)_2O$ 1.5 $(TMA)_2O$ 1 Al_2O_3 60 SiO_2 3000 H_2O using Pract grade and Special grade TPAOH

Run No	TPAOH	Cryst$^{n.}$ Time / d			Yield[a]	Si/Al	C/N
		t_{nuc}	$t_{100\%}$	t_{growth}			
D211	Pract	0.3	7	6.7	61	24.7	9.4
A126	Special	4	7	3	37[b]	16.1	9.4

[a]Total solid recovered contained about 78% of fully crystallised ZSM-5

10 $(TPA)_2O$ 1 Al_2O_3 60 SiO_2 3000 H_2O (C16),

crystallised TPA-ZSM-5 in less than 1 day when Pract grade TPAOH (approximately 6 g l^{-1} K^+) was used. Crystallisation of the composition:

8.5 $(TPA)_2O$ 1.5 $(TMA)_2O$ 1 Al_2O_3 60 SiO_2 3000 H_2O (A126),

was repeated using Pract grade TPAOH to establish whether or not the unusual *marrowbone* morphology would be retained in the presence of alkali metal cation impurities. The product obtained from this reaction (D211) crystallised in roughly the same time as that from the corresponding alkali-free reaction (A126) (Table 5–22). However, the time taken to the onset of crystallisation was much shorter, which suggests that alkali metal cations are more effective than TMA cations in promoting nucleation. What is rather surprising, is the difference in the growth rates. In contrast to what would normally be expected, crystal growth appeared to be inhibited by the presence of both alkali metal cations and TMA cations. However, this may be rationalised if competition between the alkali metal cations and TMA cations is considered. These cations will compete, together with TPA cations, for aluminosilicate species. This, coupled with the possibility that in the presence of alkali metal cations TMA cations become ineffective for ZSM-5 growth and instead favours the crystallisation of another phase, may account for the difference observed in the growth rates. That no other phase is observed is

probably due to the very fast crystallisation kinetics for ZSM-5. The fact that the alkali-free reaction mixture (A126) disproportionates, may also be an important factor since the *effective* composition from which the ZSM-5 crystallises will be very different from the overall starting composition. Indeed it may well be that reactions D211 and A126 are not strictly comparable.

The results of CHN analyses show that less TMA is occluded in the ZSM-5 framework when alkali metal cations are present which demonstrates a preference for the smaller alkali metal cations to balance the framework charge. Thermogravimetric analysis also showed a larger weight loss for the alkali-free product (A126). However, the product obtained in the presence of alkali metal cations (D211) has a higher Si/Al ratio than the corresponding alkali-free product (A126). Although this is difficult to account for adequately, it may be that because the TMA cation can replace some of the TPA cations in the ZSM-5 framework, many more TMA cations can be accommodated. Alkali metal cations, on the other hand, do not replace the TPA cation and so the number of sodium cations per unit cell is more restricted. Alternatively, sample A126 may have contained a small amount of amorphous material rich in aluminium.

Unlike the corresponding alkali-free reaction (A126), no amorphous material was obtained from the reaction that contained alkali metal impurities (D211). Furthermore, the yield of TMA/TPA-ZSM-5 obtained was increased significantly. On analysis by XRPD, the product showed preferred orientation effects which suggested that the crystal morphology had changed from the *marrowbone* morphology to one with a large length/aspect ratio. Indeed, examination of the product (D211) by SEM (Figure 5–19) showed that the *marrowbone* morphology had not been retained when alkali metal impurities were present in the reaction mixture. The photomicrograph shows large rectangular crystals covered with a large number of very small crystals, which suggests that during the crystallisation a second nucleation event occurred at the surface of the larger crystals. Unfortunately, due to charging effects, the quality of the micrograph is rather poor. A number of others were taken, however, these too were poor in quality.

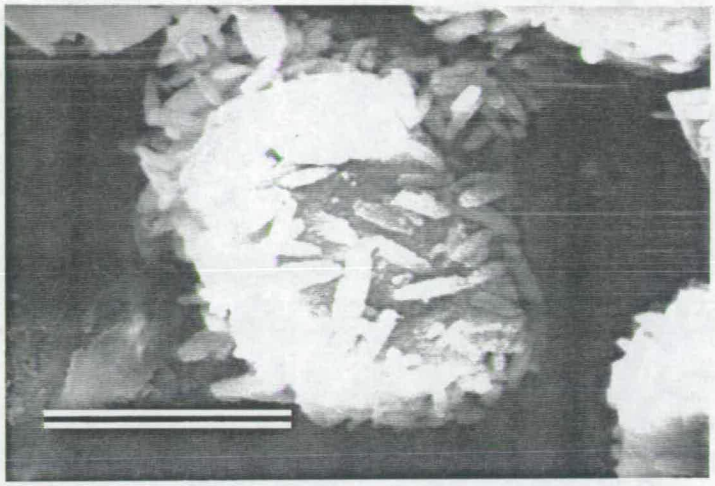

Figure 5–19: SEM photomicrograph of sample D211 (Bar = 5 μm)

The surface area and micropore volume were determined for samples crystallised from the composition:

$$8.5\ (TPA)_2O\ 1.5\ (TMA)_2O\ y\ Al_2O_3\ 60\ SiO_2\ 3000\ H_2O$$

where y = 0 (A204), 1 (A126), and 1.5 (A212). These were compared to sample D211 described above. The results (Table 5–23) show that both the surface area and micropore volume are much reduced for the *marrowbone* product (A126). This suggests that it will probably make a poor catalyst or sorbent. The values for A204 (aluminium-free) and D211 (Si/Al = 24.7) were very similar. It has already been mentioned that the XRPD pattern for A212 contained very broad peaks which suggested the presence of tiny crystals. This is borne out by the surface area measurement which was substantially higher than that for any of the other samples.

Table 5–23: Surface area and micropore volume values for samples crystallised from the composition 8.5 $(TPA)_2O$ 1.5 $(TMA)_2O$ y Al_2O_3 60 SiO_2 3000 H_2O

Run No	y	BET Area / $m^2\ g^{-1}$	Micropore Vol / $cm^3\ g^{-1}$
A204	0	379	0.147
A126[a]	1	302	0.089
D211[b]	1	365	0.137
A212	1.5	497	0.129

[a] *Marrowbone* morphology

[b] Crystallised using Pract grade TPAOH

Other mixed quaternary and quaternary/amine systems

The crystallisation of other high-silica zeolites from alkali-free reaction mixtures was investigated using TMAOH[10] as the base and relatively inexpensive quaternary halides or amines as the organic structure directing agent. Table 5–24 shows the products obtained from the composition:

$$10\ (TMA)_2O\ 10\ R\ y\ Al_2O_3\ 60\ SiO_2\ 3000\ H_2O,$$

where R = hexamethonium bromide ($HexBr_2$), nonamethonium bromide ($NonaBr_2$), or 1,6-hexanediamine (HXDM) and $0 < y < 2$, crystallised in stirred autoclaves at 423 K and 453 K. The products obtained were generally those that would have crystallised in the absence of TMA (*i.e.* with NaOH as the base).

Perhaps the most interesting results were those obtained with $HexBr_2$ (D179) and $NonaBr_2$ (B225) which gave EU-1 (10 d, 453 K) and ZSM-5/NU-1 (9-11 d, 453 K) respectively. Although the preparation of EU-1 in the absence of alkali metal cations has been reported in the open literature [156], it is believed that

---

[10] It was believed that this would have the least structure directing ability

Table 5–24: Products obtained from the composition 10 $(TMA)_2O$ 10 Q y Al_2O_3 60 SiO_2 3000 H_2O, where R = organic and $0 < y < 2$, crystallised at 423 K (300 rpm)

Run No	Q[a]	y	Cryst[n.] Time / d		Product	Yield[b]	C/N
			t_{nuc}	$t_{100\%}$			
C136	$HexBr_2$	1	25	31	EU-1	52	5.4
D179[c]	$HexBr_2$	1	< 10	< 10	EU-1	72	-
B225	$NonaBr_2$[c]	1	6-7	9	ZSM-5	67[d]	4.9
			8	11	+ NU-1		
D237	HXDM	0	-	16	ZSM-48	54	-
D231	HXDM	2	4	6	NU-1	66	4.0

[a]Key: $HexBr_2$ = Hexamethonium bromide, $NonaBr_2$ = nonamethonium bromide, and HXDM = 1,6-Hexanediamine

[b]Based on SiO_2 + Al_2O_3

[c]Reaction carried out at 453 K

[d]Total yield (ZSM-5 + NU-1)

Table 5–25: ^{13}C MASNMR data for EU-1 crystallised in the presence of TMAOH or BzTMAOH

Run No	Chemical Shift (δ) / ppm				
B228[a]	-	57.4	-	-	-
GC7[b]	67.6	-	54.3	-	23.5
C136[c]	67.8	-	54.4	53.5	24.9
D226[d]	67.0	-	54.4	-	23.3

[a]NU-1 crystallised in the presence of TMAOH

[b]EU-1 reference sample, crystallised in the presence of $HexBr_2$

[c]EU-1 crystallised in the presence of TMAOH + $HexBr_2$

[d]EU-1 crystallised in the presence of BzTMAOH + $HexBr_2$

this is the first time such a crystallisation has been carried out in the presence of TMAOH. The amount of EU-1 obtained was over 70% (based on SiO_2 + Al_2O_3), which compares favourably to the corresponding reaction in which TMAOH is replaced by NaOH [143]. Both ^{13}C MASNMR (Table 5–25) and CHN analyses (Table 5–24) suggest that TMA may not be occluded in the EU-1 framework.

It has already been mentioned that reaction mixtures that contain $NonaBr_2$ can give ZSM-5. However, the presence of NU-1 in the product (B225) suggests that not only is $NonaBr_2$ a weak structure director, it is not a particularly good ZSM-5 structure directing agent. The crystallisation of ZSM-48 (D237) and NU-1 (D231) shows that HXDM has limited structure directing ability.

Benzyltrimethylammonium (BzTMA) has already been shown to crystallise ZSM-39 (D160) but only after 60 days. Thus it has limited structure directing ability under the reaction conditions employed in this study. This made it an appropriate choice to replace the TMAOH in the reactions just described. The idea was that the presence of another bulky organic might lead to the crystallisation of a new phase.

Table 5–26: Products obtained from the composition 10 $(BzTMA)_2O$ 10 Q y Al_2O_3 60 SiO_2 3000 H_2O, where Q = organic, crystallised at 453 K (300 rpm)

Run No	Q	y	Cryst$^{n.}$ Time / d		Product	Yield[a]	C/N
			t_{nuc}	$t_{100\%}$			
D227	$HexBr_2$	0	1	2	EU-2	75	6.5
D226	$HexBr_2$	1	3	5	EU-1	83	6.0
D239[b]	HXDM	1	-	-	ZSM-48 + Am	-	-

[a]Based on SiO_2 + Al_2O_3

[b]Reaction carried out at 423 K

The products obtained from stirred (300 rpm) crystallisations at 423 K and 453 K of the composition:

$$10\ (BzTMA)_2O\ 10\ Q\ y\ Al_2O_3\ 60\ SiO_2\ 3000\ H_2O,$$

where Q = hexamethonium bromide ($HexBr_2$) or 1,6-hexanediamine (HXDM) and y = 0 or 1, are shown in Table 5–26.

As with the TMA system, no new phase was obtained. However, what is striking is the improvement in the yield of EU-1 from 72% (D179) to 83% (D226). However, this may be attributed to the presence of large amounts of alkali metal cation impurities in the BzTMAOH solution (Pract grade) used. The C/N ratio suggests that no $BzTMA^+$ is occluded in the framework. This was confirmed by ^{13}C MASNMR (Table 5–25). Thus it would appear that BzTMAOH acts only as the source of hydroxide ions, perhaps in the same way as neopentyltrimethylammonium species used in the synthesis of LOSOD [176].

5.4 Conclusions

The overwhelming finding of this work is that all the common high-silica zeolites can be synthesised from monocationic, alkali-free reaction mixtures and it is likely that many more, if not all, high-silica zeolites can be made under such conditions.

The crystallisation of zeolite Beta under alkali metal-free conditions has not been previously reported. Furthermore, since it is possible that the natural analogue of Beta exists, namely Tschernichite [249], this may be another rare example[11] of a natural zeolite having been crystallised as a high-silica material in the absence of alkali metal cations.

It would appear that alkali metal cations are not required for the crystallisation of high-silica zeolites, although they may influence crystallisation kinetics. Possibly with the exception of Beta, alkali metal cations are more important in crystal growth. The role of alkali metal cations will be discussed further in Chapter 7.

The products obtained from systems in which some of the structure directing quaternary is replaced by TMA cations are the same as those obtained in the absence of TMA. Not only does the presence of TMA affect the crystallisation kinetics, particularly in TPA/TMA-ZSM-5 systems, it can also modify crystal morphology and yield. The combination of TMAOH with quaternary halides offers another alkali-free route to many high-silica zeolites.

Further work on alkali metal-free systems that include $Nona(OH)_2$ or BzTMAOH stand a good chance of crystallising something more interesting.

---

[11] Alkali-free ferrierite may be the only other

Chapter 6

Alkali Metal-Free Syntheses: Quaternary/Diol System

6.1 Introduction

In the previous chapter, it was shown that TMAOH could be used as the mineraliser in alkali metal-free reaction mixtures that contained an additional quaternary ammonium salt, without influencing the nature of the product obtained. This illustrates the relatively weak competitive nature of TMA cations in reaction mixtures that contain more than one quaternary ammonium compound. This, together with the fact that TMA can be used to crystallise a wide variety of products (usually in conjunction with alkali metal cations) [63], suggests that the TMA cation may be considered a weak structure director. TMAOH was therefore selected for the study of weak or non-specific structure directing agents. It was reasoned that the effects of these organics in many of the reactions reported in the literature may have been masked by the presence of impurities, particularly alkali metal cations (Chapter 4). Diols were selected for this study on the basis that they are considered weak structure directors, have a wide range of shapes (Figure 6–1), have good solubility under the reaction conditions used, and are not particularly hazardous. Specifically, the diols investigated were 2,3-dimethyl-2,3-butanediol (2,3-DMBD), 2,4-dimethyl-2,4-pentanediol (2,4-DMPD), 2,5-dimethyl-2,5-hexanediol (2,5-DMHD) and 1,6-hexanediol (1,6-HXDL).

A number of other quaternary/diol reactions were also carried out. Success with the Beta synthesis led to an investigation of its synthesis from TEA/diol

reaction mixtures at low temperature. Both stirred and static reactions were carried out.

6.2 Experimental

Gel preparation and synthesis conditions were as described in Chapter 2. Diols were dissolved in hot water (except 2,4-DMPD which is a liquid), then added to the aluminosilicate gel before adding the remaining water. Reactions were carried out at 423 K in stirred 500 cm^3 autoclaves and at 368 K in 10 cm^3 polypropylene bottles (without agitation) and in 1 litre stainless-steel vessels (stirred at 160 rpm). Samples were processed as described in Chapter 2.

6.3 Results and Discussion

6.3.1 TMA/Diol System

The composition:

$$10\ (TMA)_2O\ 20\ Diol\ 1\ Al_2O_3\ 60\ SiO_2\ 3000\ H_2O,$$

where Diol = 2,3-DMBD, 2,4-DMPD, 2,5-DMHD and 1,6-HXDL, crystallised TMA-NU-1 at 423 K (300 rpm) irrespective of the nature of the diol (Table 6–1). Even reaction mixtures that contained large amounts of diol (Table 6–2) failed to crystallise anything other than TMA-NU-1.

These results suggest that the diols examined in this study have limited, if any, structure directing ability. This remark probably extends to all diols and possibly alcohols since the interactions between neutral organic molecules with charged aluminosilicate species are much weaker than those that involve charged organic (or inorganic) cations. The crystallisation of TMA-NU-1 from reaction

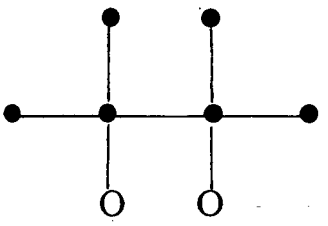

2,3-dimethyl-2,3-butanediol (2,3-DMBD)

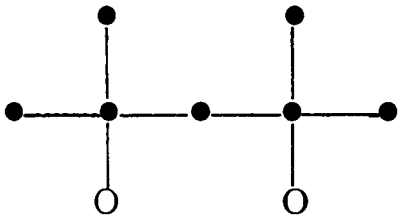

2,4-dimethyl-2,4-pentanediol (2,4-DMPD)

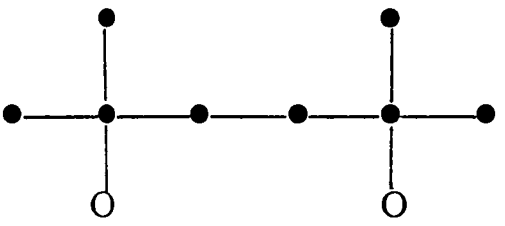

2,5-dimethyl-2,5-hexanediol (2,5-DMHD)

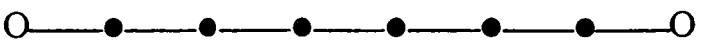

1,6-hexanediol (1,6-HXDL)

● = C
O = OH

Figure 6–1: Schematic of the diols used in this investigation

Table 6–1: Crystallisation of TMA-NU-1 from the composition 10 $(TMA)_2O$ 20 Diol 1 Al_2O_3 60 SiO_2 3000 H_2O at 423 K (300 rpm)

Run No	Diol[a]	Cryst$^{n.}$ Time / d		C/N[b]	Yield[c] / %	Si/Al
		t_{nuc}	$t_{100\%}$			
D91	None	21	25	-	53	20.1
A99	1,6-HXDL	27	35	3.0	48	23.1[d]
C100	2,3-DMBD	23	32	3.2	45	22.4[d]
B233	2,4-DMPD	19	28	2.8	53	-
D101	2,5-DMHD	< 7	< 7	3.6	58	21.3[d]
D266	2,5-DMHD	3	6	-	-	-
B228[e]	2,5-DMHD	5	7.5	-	-	-

[a]Key: 1,6-HXDL = 1,6-Hexanediol; 2,3-DMBD = 2,3-Dimethyl-2,3-butanediol; 2,4-DMPD = 2,4-Dimethylpentanediol; 2,5-DMHD = 2,5-Dimethylhexanediol

[b]C / N for TMA^+ = 4.0

[c]Based on SiO_2 + Al_2O_3

[d]Determined by XRF

[e]Composition 10 $(TMA)_2O$ 20 (2,5-DMHD) 2 Al_2O_3 60 SiO_2 3000 H_2O

Table 6–2: Effect of increasing 2,5-DMHD content on the crystallisation of TMA-NU-1

Run No	x[a]	Cryst[n.] Time / d		Product	Yield[c] / %
		t_{nuc}	$t_{100\%}$		
D91	0	21	25	NU-1	53
D132	10	11	15	NU-1	53
D266	20	3	6	NU-1	58
C104	50	8	12	NU-1	62
A120[c]	200	9	13	NU-1	61

[a]Based on the composition 10 $(TMA)_2O$ x (2,5-DMHD) 1 Al_2O_3 60 SiO_2 3000 H_2O

[b]Based on SiO_2 + Al_2O_3

[c]On cooling, the diol crystallised in the mother liquor

mixtures that contained high levels of diol, suggests that it may be possible to obtain TMA-NU-1 from non-aqueous reaction mixtures.

Two major effects can be noted from Table 6–1:

a) 2,5-DMHD significantly reduced the overall crystallisation time and improved the yield of TMA-NU-1 (D101, D266), and

b) all the other diols increased the overall crystallisation time (by as much as 10 days for 1,6-HXDL (A99)) and reduced the product yield.

The extent to which diols affect the crystallisation of alkali metal-free TMA-NU-1 is illustrated in plots of crystallisation (%) (determined by XRPD) versus reaction time (Figure 6–2).

It is clear from the results in Tables 6–1 and 6–2 that nucleation of TMA-NU-1 was promoted by the presence of 2,5-DMHD in the reaction mixture. However, there appeared to be little effect on the rate of crystal growth, even with large amounts of the diol (Table 6–2). This is consistent with the observation that the smallest crystals were obtained from reaction mixtures that contained this diol. In

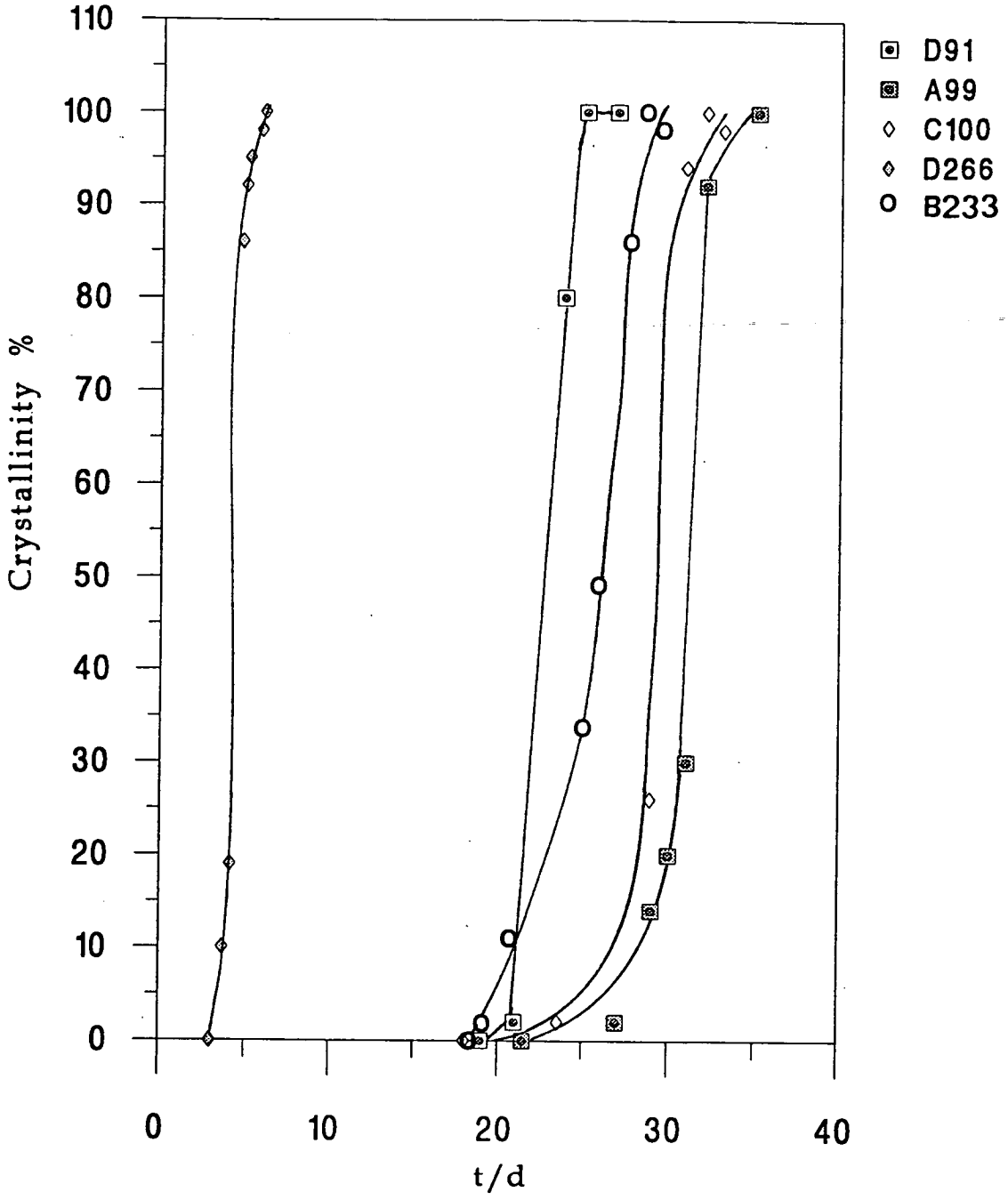

Figure 6–2: Crystallisation (%) versus reaction time (d) for the composition 10 $(TMA)_2O$ 20 Diol 1 Al_2O_3 60 SiO_2 3000 H_2O, crystallised at 423 K (300 rpm)

contrast, the other diols had a less marked effect on nucleation. Only 2,4-DMPD improved it, but only marginally, while the others increased the time to nucleation. Furthermore, these diols were found to inhibit the growth rate (Table 6–1).

At higher aluminium concentrations (B228), the crystallisation kinetics for TMA-NU-1 crystallised in the presence of 2,5-DMHD were not significantly affected. This suggests that the effect of 2,5-DMHD is not dependent of the aluminium content of the reaction mixture.

SEM photomicrographs are shown in Figures 6–3, 6–4, 6–5, 6–6, and 6–7. All samples contained a mixture of small ellipsoidal and larger, rounded crystals of variable quality. Crystal size distribution (CSD) plots, based on a minimum of 400 crystals counted in three SEM fields (Figures 6–8, 6–9, 6–10, 6–11, and 6–12), show that the CSD varied widely depending on the nature of the diol. This was very narrow for sample D101 but considerably wider for the others. Furthermore, the CSD for this sample showed no signs of a bimodal distribution, unlike the others, including the sample crystallised from the diol-free reaction (D91). This suggests that in the reaction involving 2,5-DMHD, there was only one nucleation event (*i.e.* no subsequent nucleation). Although the average size of the crystals for sample C100 (2,3-DMHD) differed markedly from sample D91 (diol-free), there were similarities in the size distribution profiles. This may reflect the fact that 2,3-DMBD did not significantly affect the nucleation kinetics.

With the exception of the sample obtained from the 2,5-DMHD reaction mixture (D101), all the diols increased the average crystal size compared to that of the diol-free sample (D91) (Table 6–3). Particularly large crystals were obtained in the presence of 2,4-DMPD. These observations are generally in accordance with results reported for the crystallisation of aluminous zeolites from reaction mixtures that contained an alkanolamine [250,251,252]. The average crystal size of sample D101, however, was less than half that of the corresponding sample obtained from the diol-free reaction (D91). A similar effect on crystal size has been reported in the patent literature [253], where submicron crystals of ZSM-22 and ZSM-23 were obtained from reaction mixtures that contained, in addition to the organic structure directing agent, an alcohol or diol having 1-6 carbon atoms. However,

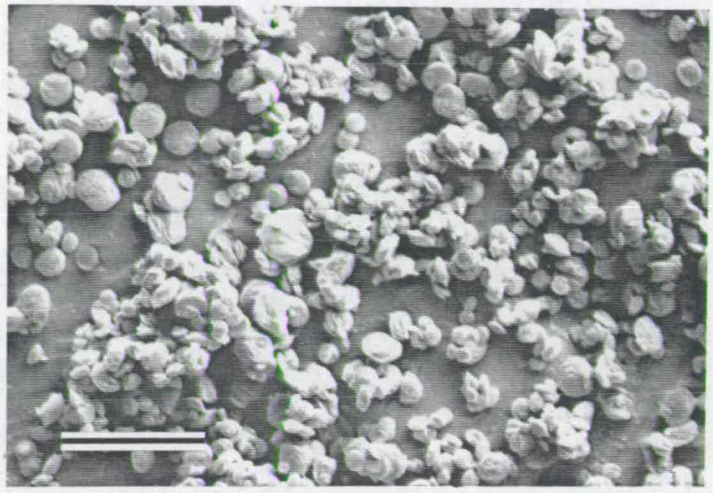

Figure 6–3: SEM photomicrograph of D91 (diol-free)

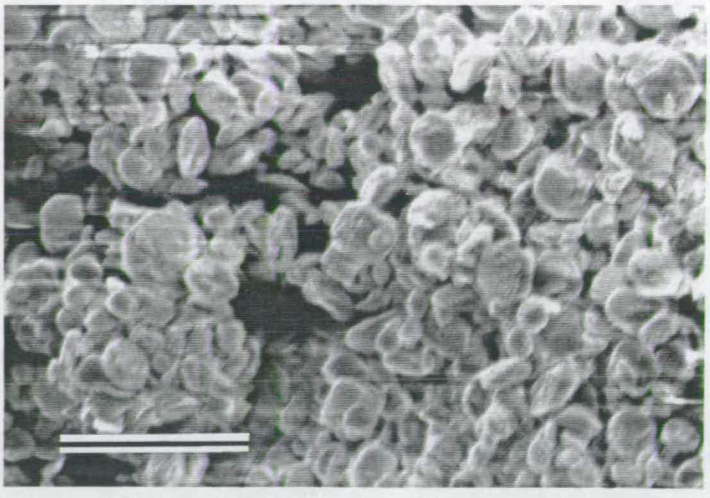

Figure 6–4: SEM photomicrograph of A99 (1,6-HXDL)

(Bar = 10 μm)

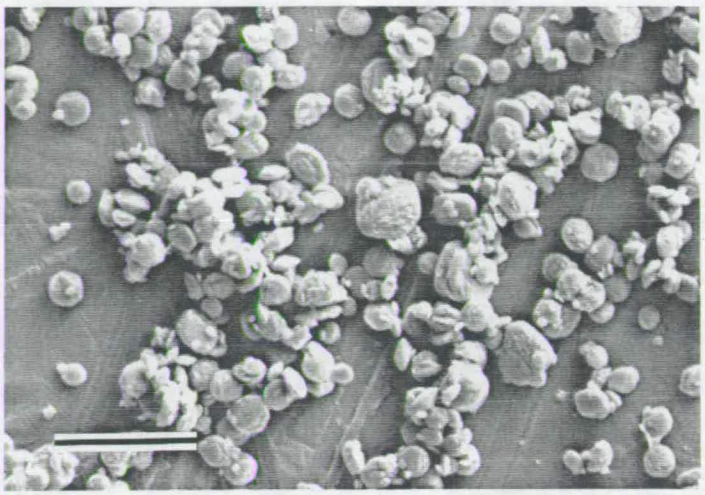

Figure 6–5: SEM photomicrograph of C100 (2,3-DMBD)

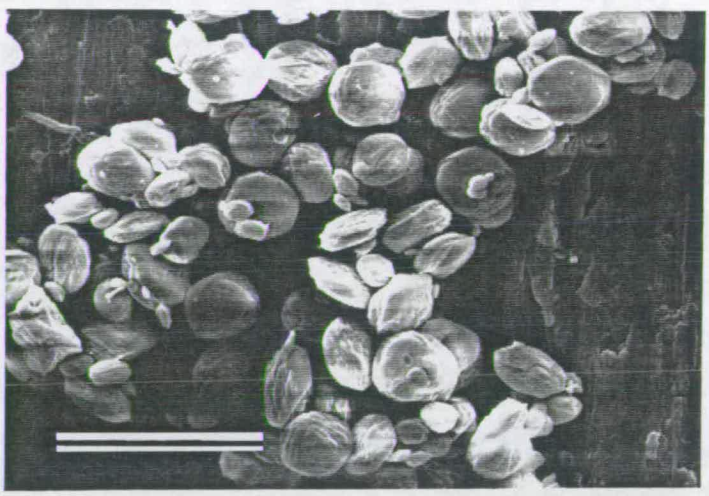

Figure 6–6: SEM photomicrograph of B233 (2,4-DMPD)

(Bar = 10 μm)

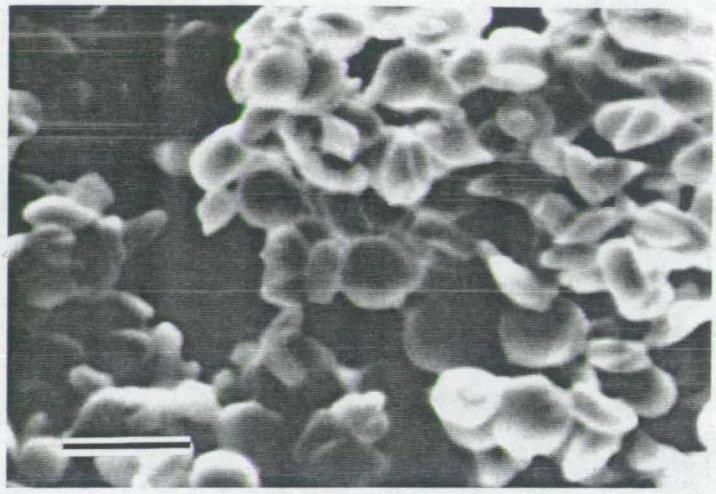

Figure 6–7: SEM photomicrograph of D101 (2,5-DMHD)

(Bar = 1 μm)

there is no mention of any change in the crystallisation rate or, indeed, speculation as to the role of the alcohols/diols in these crystallisations.

Since 2,5-DMHD improved the crystallisation rate considerably, it was decided to carry out further studies with this diol. The results in Table 6–2 show that there was an optimum diol concentration at which the effect on the crystallisation kinetics was most pronounced. This is further illustrated in Figure 6–13. It is noteworthy that for 2,5-DMHD, the addition of more than 50 moles (C104) to the reaction mixture resulted in relatively little change in either the nucleation or crystallisation kinetics compared with those of lower diol content. However, even at these high loadings, the crystallisation rate was faster than the diol-free reaction (D91). If interaction of the diol with silicate/aluminosilicate species in either the solution or solid phase is an important mechanism in promoting the nucleation of TMA-NU-1, then the limiting factor may well be the amount of these species available in the system. Thus, as the amount of diol is increased, there may be an increase in the number of diol-silicate/aluminosilicate interactions. There will come a point, however, when these species become *saturated* and any further addition of diol will be ineffective. Alternatively, at high diol concentrations, crystallisations are effectively being carried out from a *less-aqueous* reaction mix-

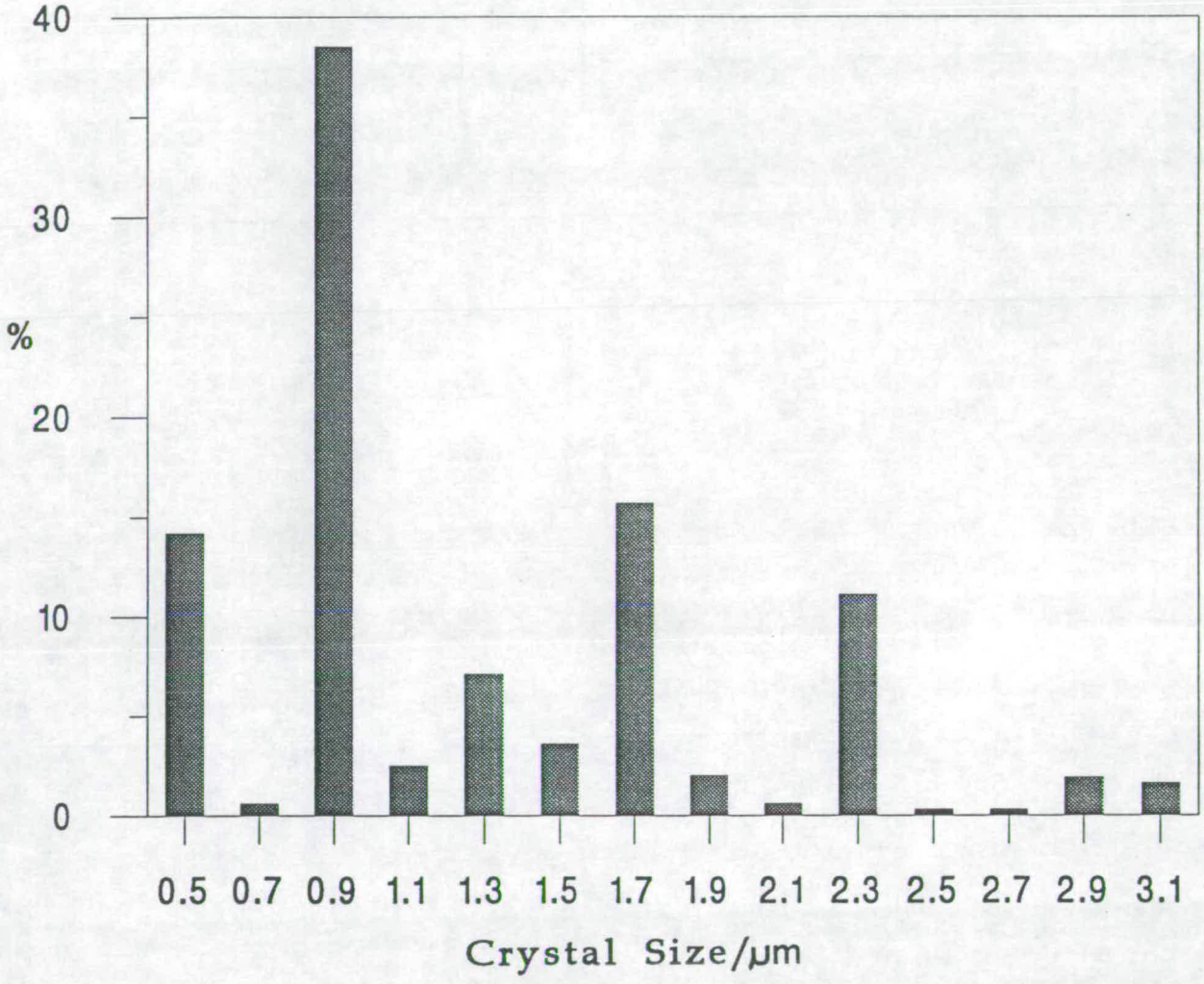

Figure 6–8: Crystal size distribution for D91 (diol-free)

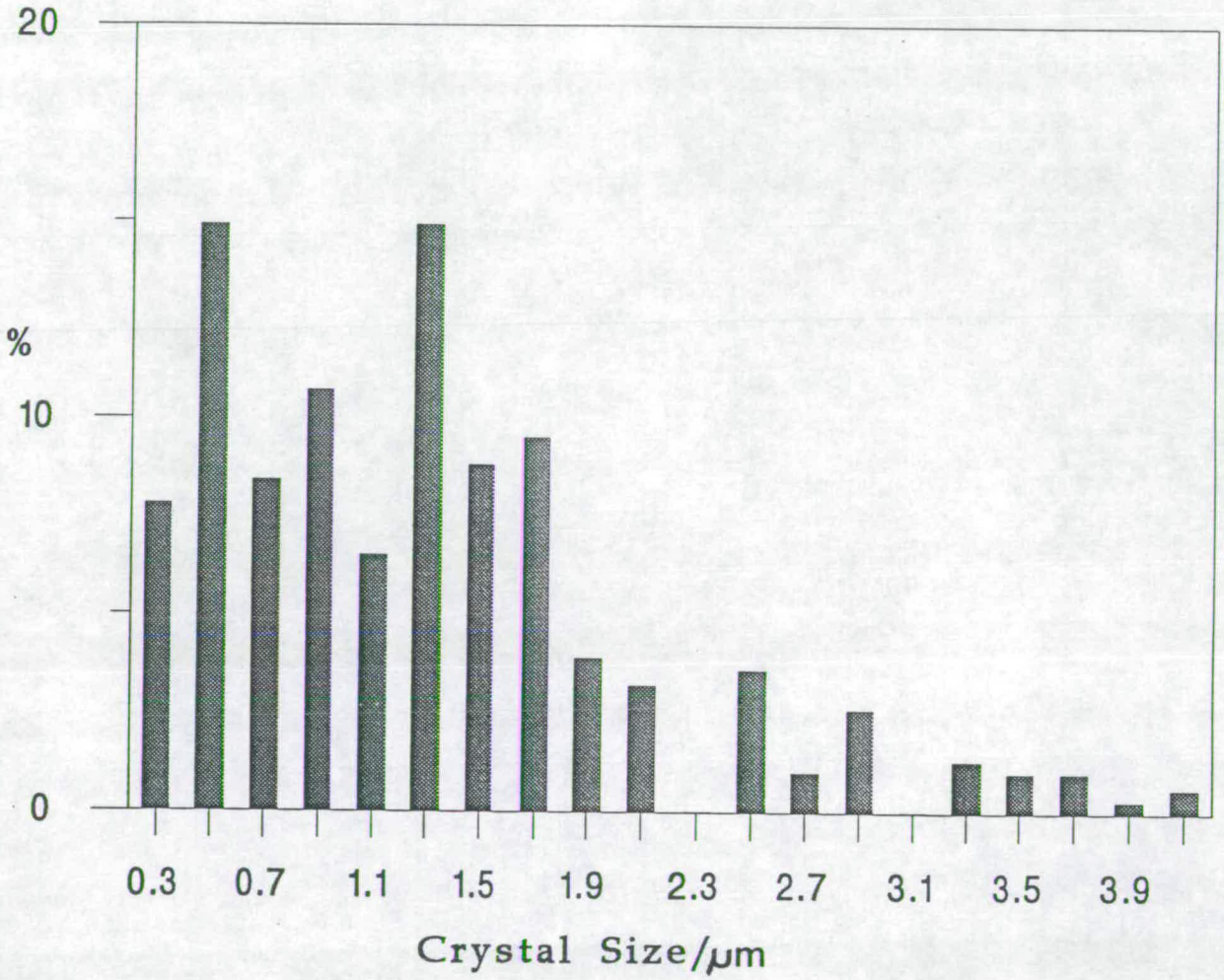

Figure 6–9: Crystal size distribution for A99 (1,6-HXDL)

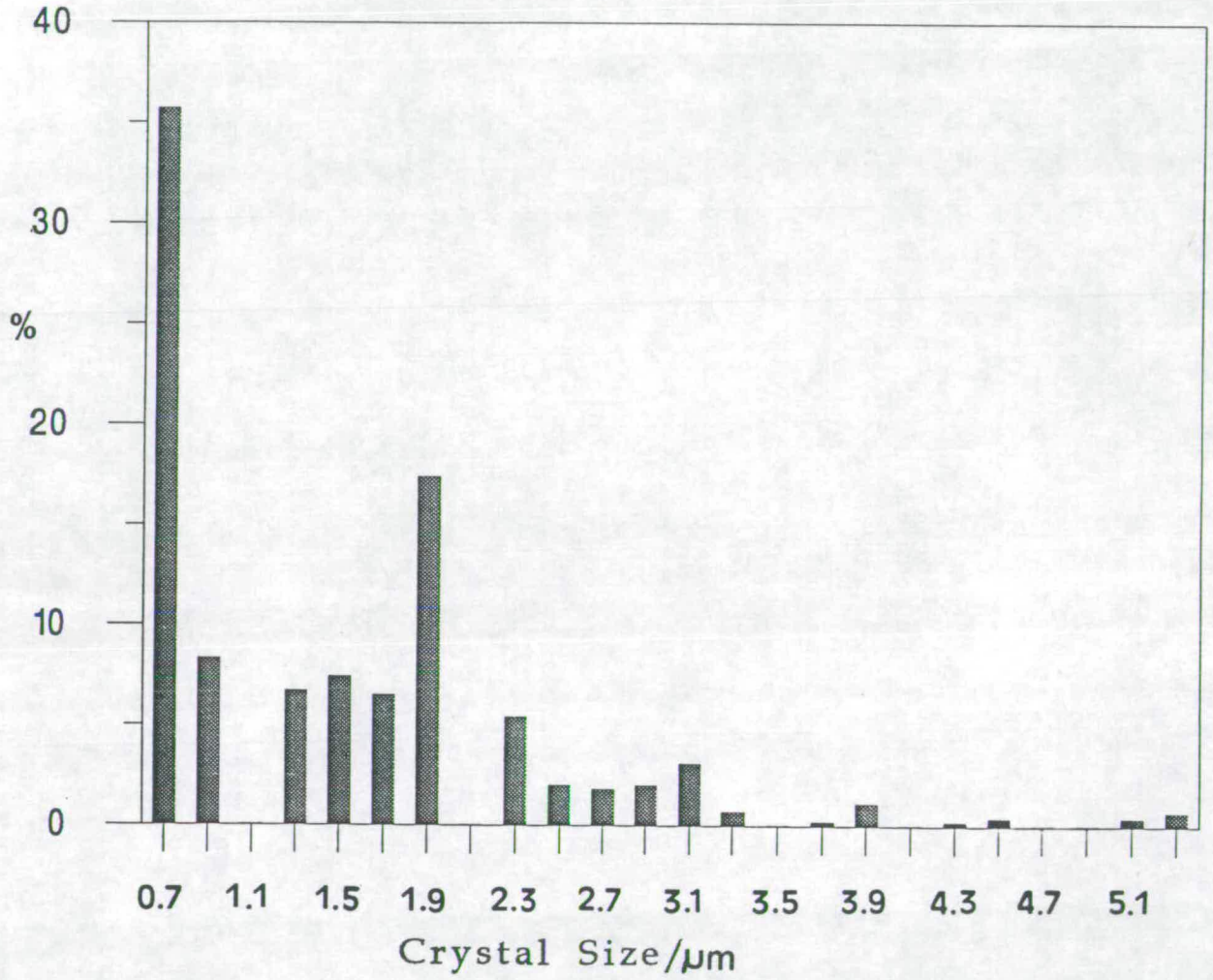

Figure 6–10: Crystal size distribution for C100 (2,3-DMBD)

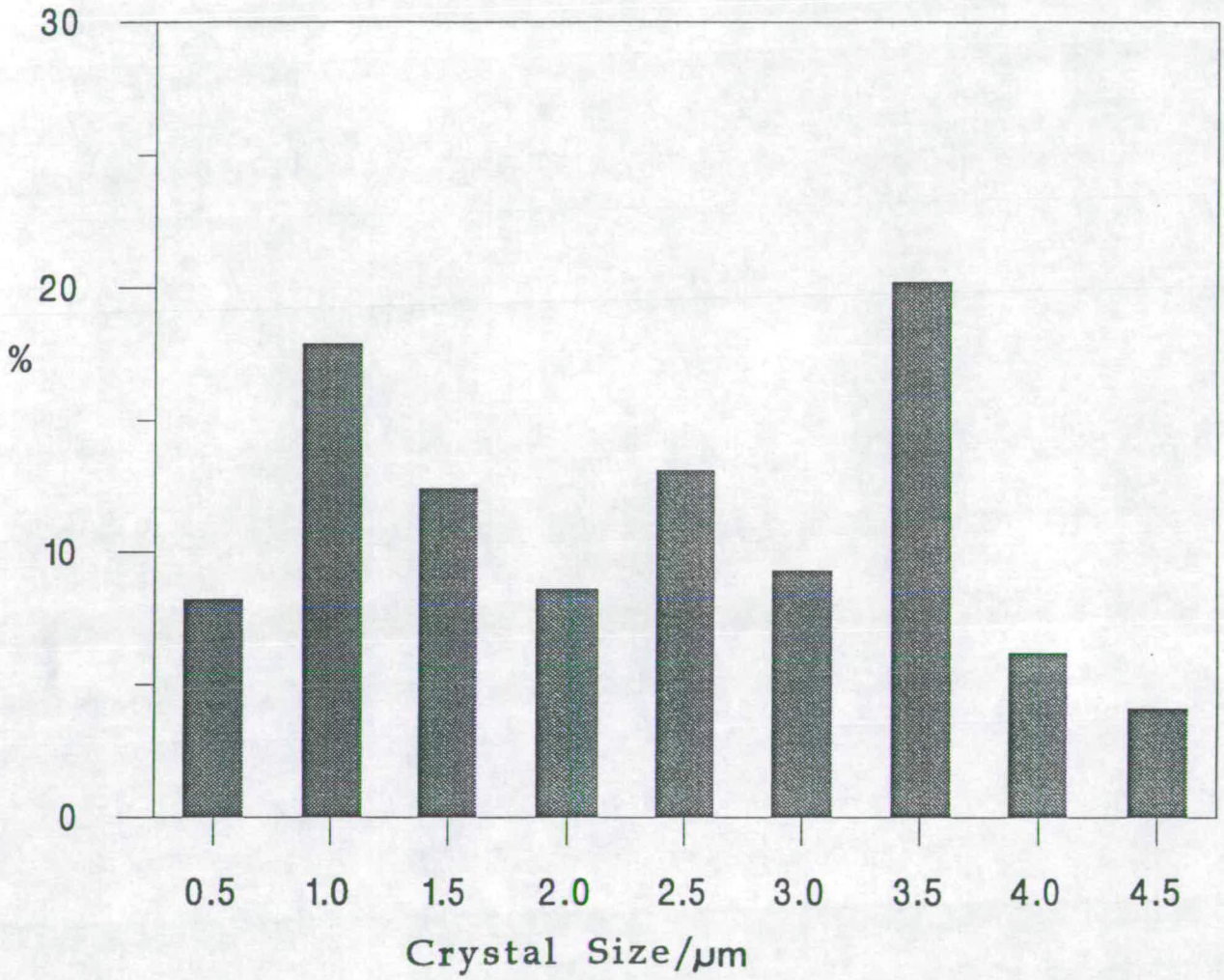

Figure 6–11: Crystal size distribution for B233 (2,4-DMPD)

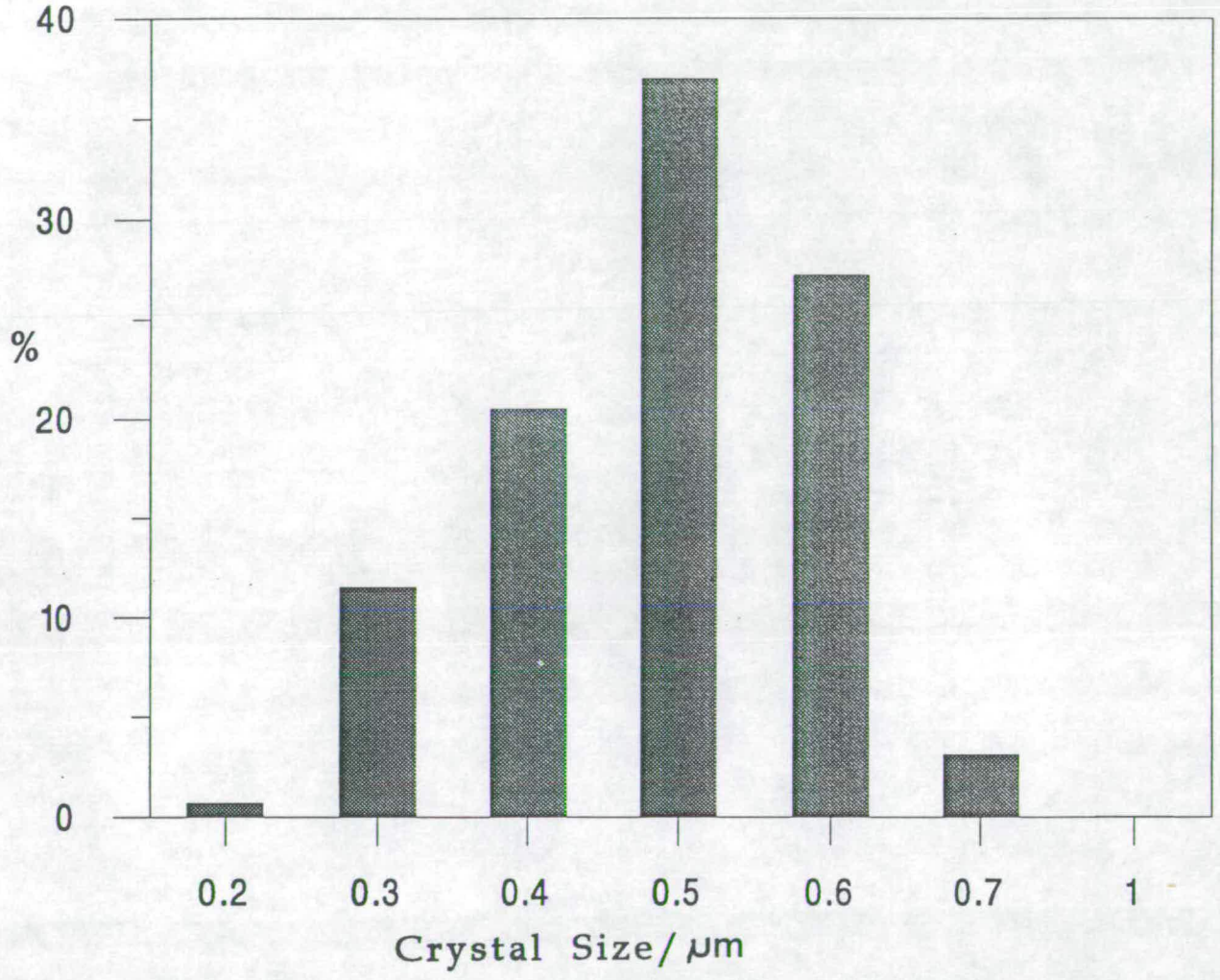

Figure 6–12: Crystal size distribution for D101 (2,5-DMHD)

Table 6–3: Average crystal size for TMA-NU-1 samples obtained from diol- and diol-free reaction mixtures

Run No	Diol[a]	Average Crystal Size / μm
D91	None	1.24
A99	1,6-HXDL[b]	1.30
C100	2,3-DMBD	1.50
B233	2,4-DMPD	2.48
D101	2,5-DMHD	0.49

[a]Based on the composition:
10 $(TMA)_2O$ 20 (Diol) 1 Al_2O_3 60 SiO_2 3000 H_2O
[b]Key: see Table 6–1

ture. In other words, the gel chemistry is shifted from an aqueous to an organic solvent-based system.

CSD plots for products obtained from compositions with increasing 2,5-DMHD content (Figure 6–14) show that as the amount of diol was increased, the distribution became more bimodal and the average crystal size increased (Table 6–4, Figure 6–15). At particularly high diol concentrations (A120, 200 (2,5-DMHD)) both the crystal size distribution and average crystal size were similar to those of the diol-free sample (D91). This may be close to the maximum amount of 2,5-DMHD in the reaction mixture from which the largest crystals can be obtained from these systems, *i.e.* a further increase in diol content would not increase the average crystal size. Furthermore, it was found that for sample A120, the diol crystallised in the mother liquor as it cooled.

The XRPD patterns for TMA-NU-1 crystallised in the presence of diols were typical of that for the product obtained from the diol-free reaction and showed no unusual features. No significant peak broadening was observed, even with the sample that contained particularly small crystals (D101).

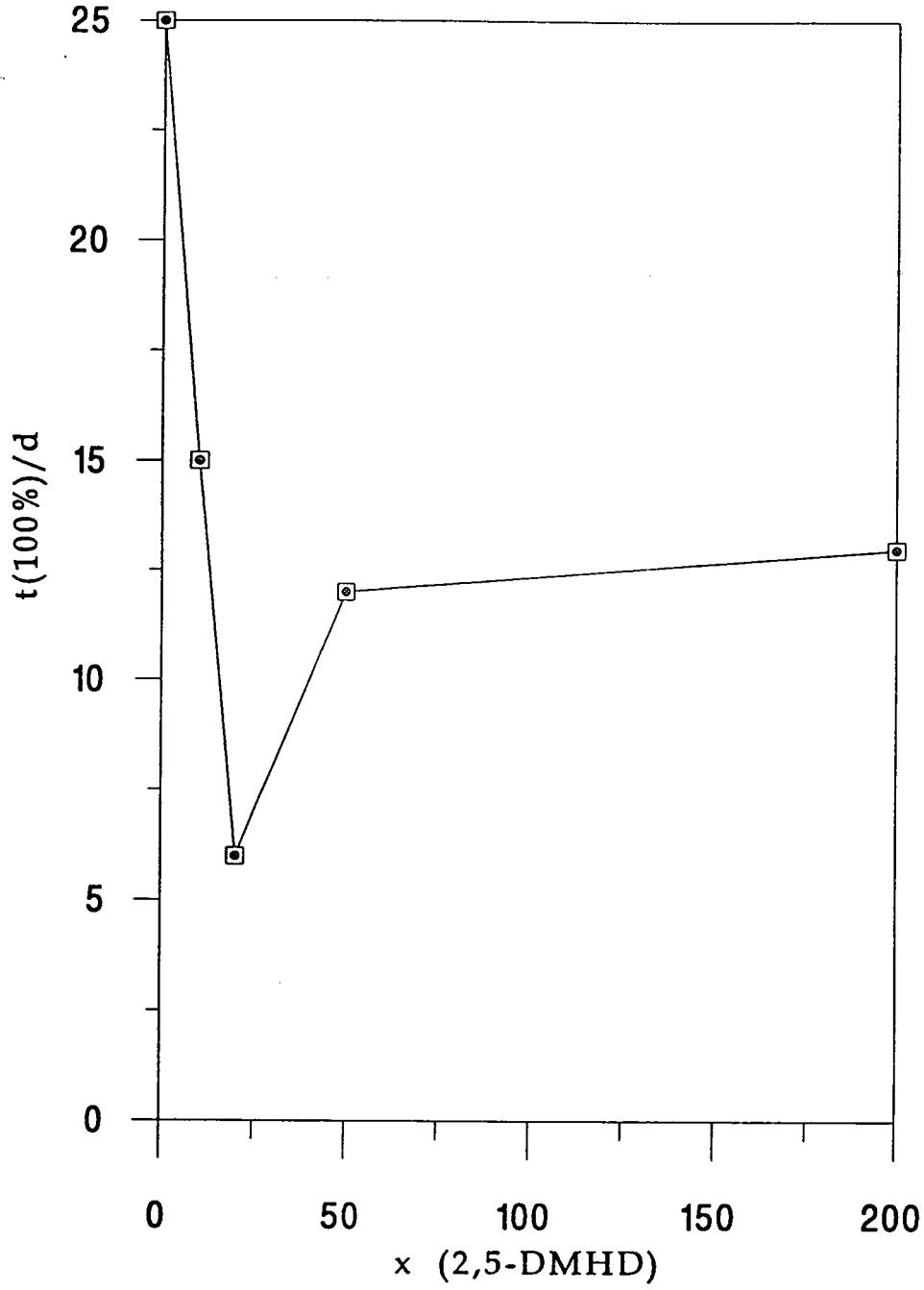

Figure 6–13: Effect of 2,5-DMHD content in the reaction mixture on the crystallisation of NU-1

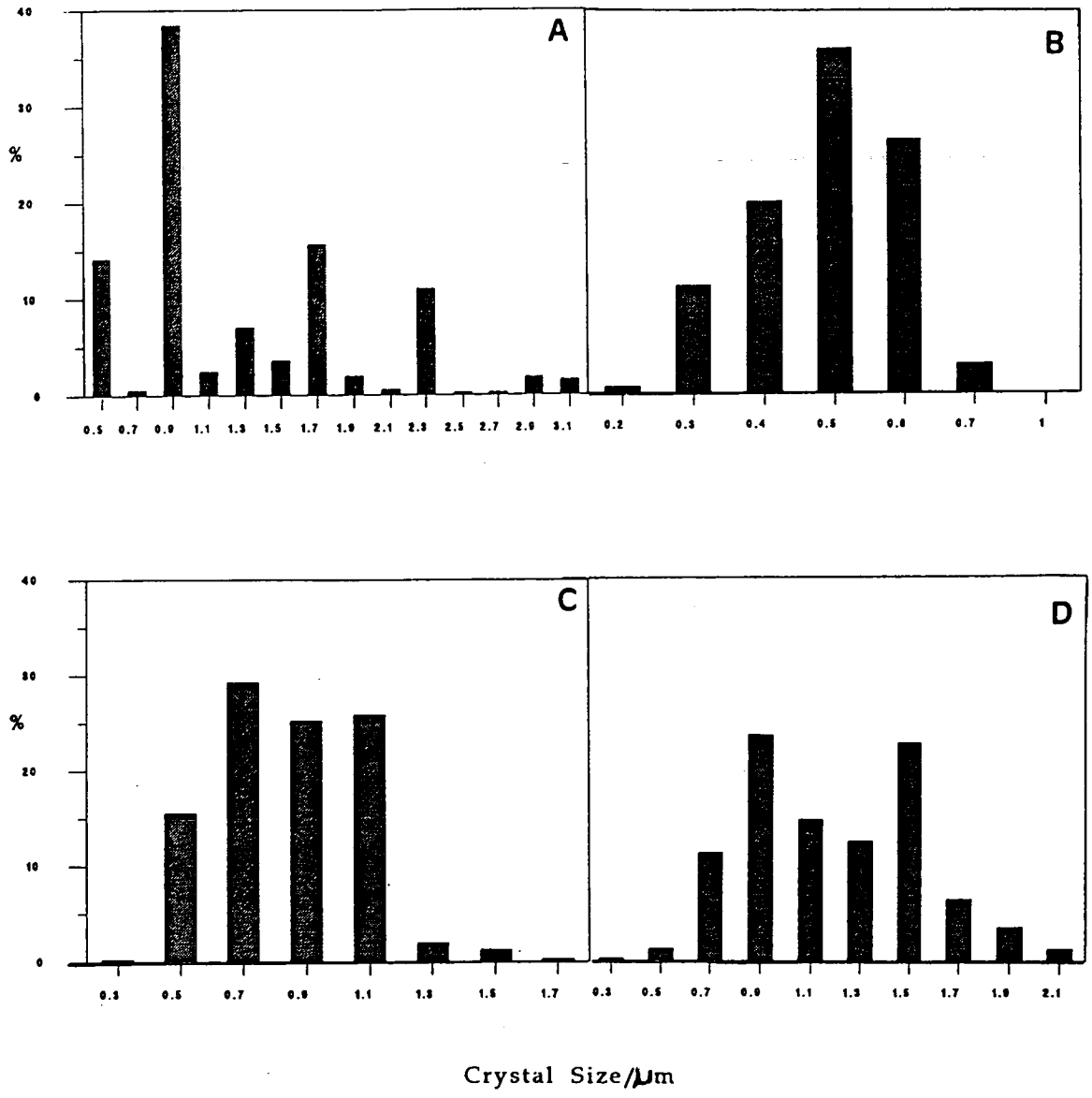

Figure 6–14: Crystal size distribution of TMA-NU-1 crystallised from the composition 10 $(TMA)_2O$ x (2,5-DMHD) 1 Al_2O_3 60 SiO_2 3000 H_2O, where A) x = 0, B) x = 20, C) x = 50, and D) x = 200

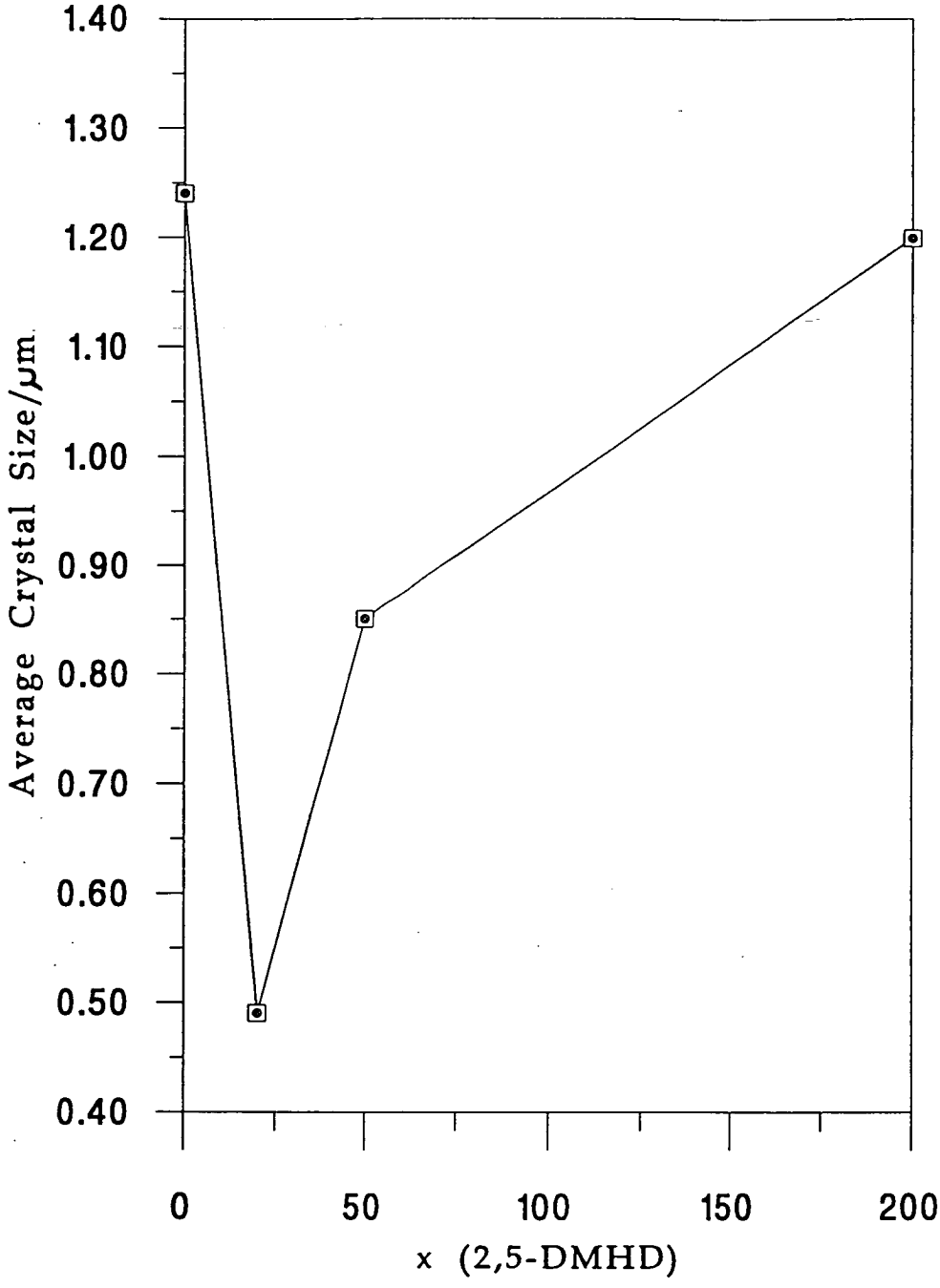

Figure 6–15: Effect of 2,5-DMHD concentration on the average crystal size for TMA-NU-1

Table 6–4: Effect of diol concentration on the average crystal size for TMA-NU-1

Run No	x[a]	Average Crystal Size / μm
D91	0	1.24
D101	20	0.49
C104	50	0.85
A120	200	1.20

[a]Based on the composition 10 $(TMA)_2O$ x (2,5-DMHD) 1 Al_2O_3 60 SiO_2 3000 H_2O

[b]Key: see Table 6–1

Careful examination of thermal analysis profiles showed that the presence of diol could not be readily detected. In general, the shape of the profiles were similar to that of the diol-free reaction. However, the shape of the dta profile for sample D101 (2,5-DMHD) was quite different, in that the exotherm above 670 K was much more well defined (Figure 6–16). This is probably due to the fact that the crystals were much smaller than those of other samples, which would allow the removal of the occluded TMA species to take place more easily. Although it was difficult to establish the presence of diol in any of the samples from the tga profiles, careful examination of the thermal analysis data (Table 6–5) showed that, not only was the total weight loss of each sample virtually identical to that of the diol-free sample (D91), but the weight losses above and below 670 K were also very similar; that is, the occluded material was lost in a very similar manner. The results show an average total weight loss of about 16.7% of which approximately 2.3% was due to water loss (< 670 K) and 14.4% was due to removal of TMA (> 670 K). These results strongly suggest that the diols were not occluded in TMA-NU-1. This was confirmed by CHN analysis (Table 6–1). Furthermore, ^{13}C MASNMR spectra showed only one major peak at about 57.4 ppm, which is the signal due to TMA. The spectrum for sample D101 contained a very small peak at about 82 ppm. However, it is thought that this peak was not due to the presence of diol. This

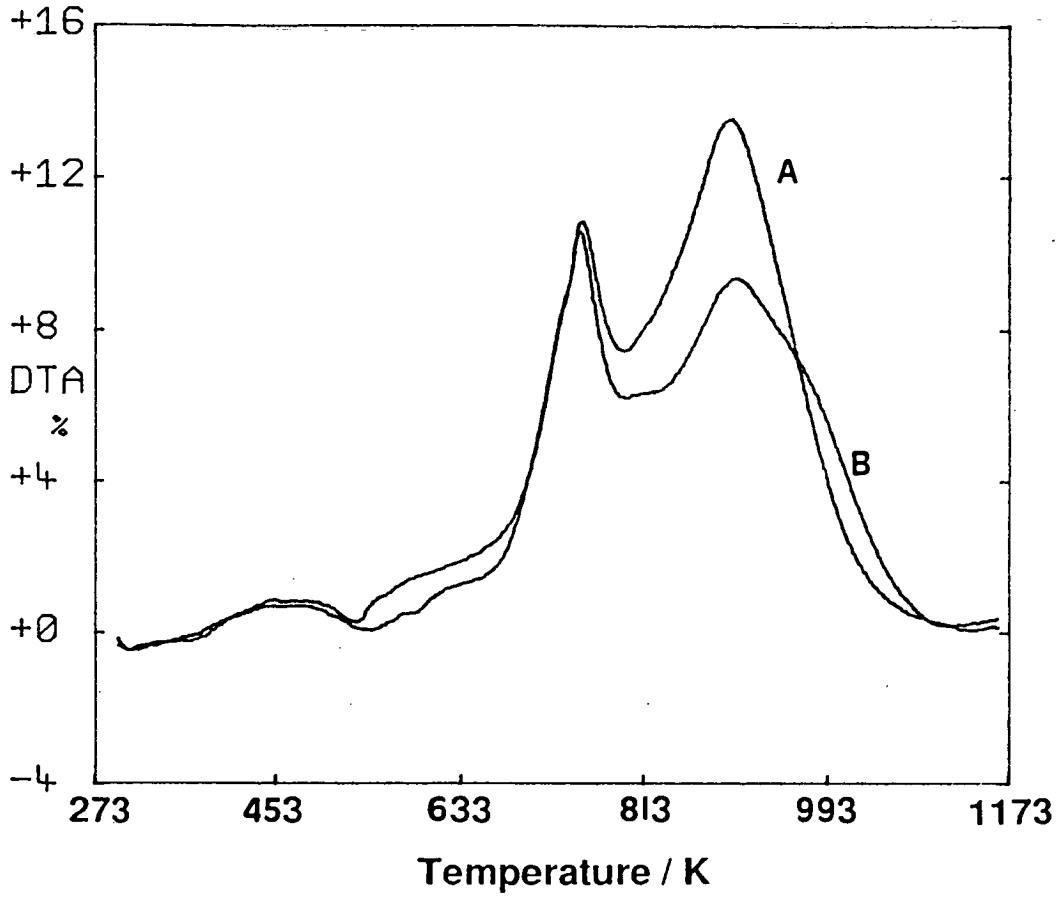

Figure 6–16: dta profiles for A) D101 and B) D91 (diol-free)

Table 6–5: Thermal analysis data for TMA-NU-1 obtained in the presence and absence of diol

Run No	Diol[a]	Weight loss / %[b]		
		< 623 K	623-1173 K	Total
D91	None	1.7	14.9	16.6
A99	1,6-HXDL[c]	1.8	14.7	16.5
C100	2,3-DMBD	2.1	14.6	16.7
B233	2,4-DMPD	1.8	14.9	16.7
D101	2,5-DMHD	2.0	14.9	16.9
B228[d]	2,5-DMHD	3.5	13.6	17.1

[a]Based on the composition 10 $(TMA)_2O$ 20 (Diol) 1 Al_2O_3 60 SiO_2 3000 H_2O

[b]Determined by tga

[c]Key: see Table 6–1

[d]2 Al_2O_3

is based on the fact that in the corresponding spectrum for a Beta sample, which was also found to crystallise much faster in the presence of 2,5-DMHD (A111, see later), no peak was observed at this chemical shift.

Although none of the diols were detected in any of the final crystalline products, it was thought that they might be present in samples taken before the onset of crystallisation, *i.e.* associated with the amorphous solid phase. Furthermore, it was thought that such a study might help to establish the role of the diol in these crystallisations. However, the thermal analysis profiles, and in particular the dta profiles of these intermediate samples, did not show anything that would allow any hypotheses to be made and it is difficult to establish the extent, if any, of the interaction between the amorphous silica and the diol. Furthermore, it is highly likely that the diol may have been removed from the amorphous solid when the samples were washed.

Table 6–6: Change in pH during the crystallisation of TMA-NU-1 from diol- and diol-free reaction mixtures

Run	pH		
No	Initial	Final	Increase
D91	12.28	12.49	0.21
A99	12.12	12.41	0.27
C100	12.47	12.79	0.32
B233	12.68	12.86	0.18
D101	12.23	12.50	0.27
D266	12.80	13.12	0.32

The pH values of the initial gel and the mother liquor of the sample deemed to be 100% TMA-NU-1 are shown for each reaction in Table 6–6. Generally, the change in pH on crystallisation was much the same for each reaction, irrespective of whether a diol was present or not. Furthermore, the initial pH values were similar, which suggests that there is no change in the basicity of the system when diols are included in the reaction mixture. Thus it is may be assumed that the presence of diols does not significantly increase the solubility of silica. If it did, then the crystallisation rate may be expected to have increased irrespective of the nature of the diol. This is consistent with work reported on the crystallisation of Na-ZSM-5 in the presence of 1,6-HXDL [178].

A plot of the time taken to crystallise NU-1 versus the number of carbon atoms in the structurally related diols (*i.e.* 2,3-DMBD, 2,4-DMPD and 2,5-DMHD) (Figure 6–17) shows that the crystallisation rate increases with carbon number. This together with the effect on the average crystal size discussed earlier, may be related to the *hydrophobicity* of the diol. The difference in crystallisation rates found with reaction mixtures that contained empirically equivalent, but structurally different diols, *i.e.* A99 (1,6-HXDL, $C_6H_{14}O_2$) and C100 (2,3-DMBD, $C_6H_{14}O_2$) (Table 6–1), further suggests that the geometry of the diol may be important in promot-

ing crystallisation. This is consistent with the possibility that interaction of the diol with silicate/aluminosilicate species may be important in the stabilisation of nuclei which subsequently leads to rapid nucleation.

6.3.2 Other Quaternary/Diol Systems

The products obtained from the composition:

$$10\ Q_2O\ 20\ (2,5\text{-DMHD})\ 1\ Al_2O_3\ 60\ SiO_2\ 3000\ H_2O,$$

where Q = TEA, TPA, and TBA, are given in Table 6–7.

The results show that 2,5-DMHD had little effect on the crystallisation rate of TPA-ZSM-5 (D123) and TBA-ZSM-11 (A181). However, the overall crystallisation time for zeolite Beta (A111) was reduced significantly (by 17 d).[1]

As with the TMA-NU-1 system, no diol was found to be occluded in the Beta framework (or any of the other frameworks), (Table 6–7, Figure 6–18). This was confirmed by ^{13}C MASNMR; the spectrum contained two major peaks at 52.3 and 6.5 ppm due to TEA^+. An increase in the amount of 2,5-DMHD in the reaction mixture also reduced the time taken to crystallise Beta (Table 6–8). The results of chemical analyses (Table 6–8) suggest that as the amount of diol was increased in the reaction mixture, the Si/Al ratio of the product increased. However, at the highest diol concentration (A111), there appears to be an abrupt decrease in this ratio, to that of the product obtained from the diol-free reaction (B89). If this is a genuine trend, then the effect may be due to a change in gel chemistry coupled with the reluctance of the Beta system to readily crystallise a siliceous product. However, there is insufficient data on which to draw any firm conclusions and it is likely that the spread of these values is within experimental error. The results in Table 6–9 show that there was very little difference in the change in pH on crystallisation for any of the reactions.

---

[1]This may make the synthesis of alkali-free Beta a more commercially viable option.

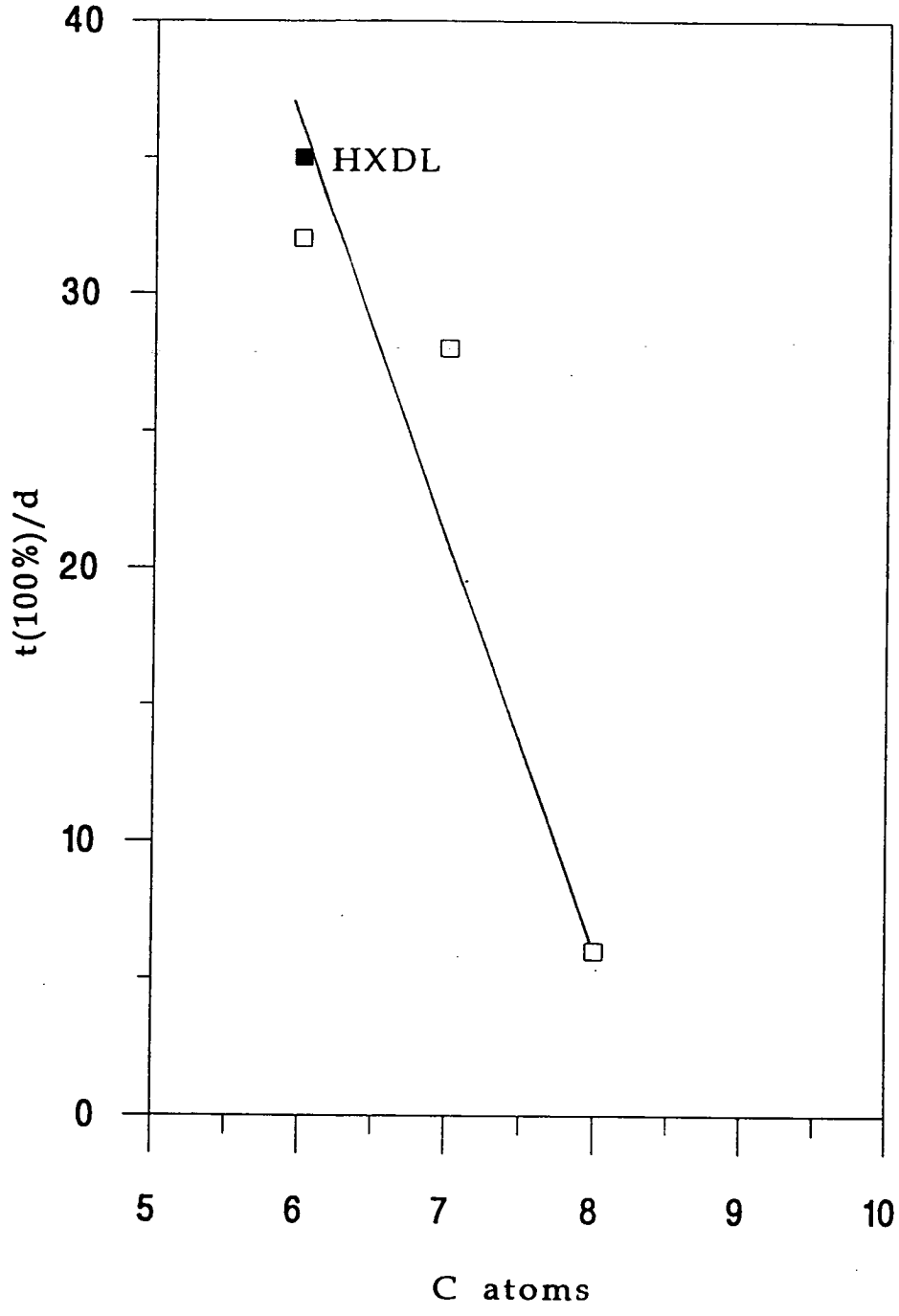

Figure 6–17: Plot of the number of carbon atoms in the diol versus crystallisation time for TMA-NU-1

Table 6–7: Products obtained from the reaction composition: 10 Q_2O x (2,5-DMHD) 1 Al_2O_3 60 SiO_2 3000 H_2O, where Q = TEA, TPA, and TBA

Run No	Q[a]	x	Cryst[n.] Time / d		Product	C/N
			t_{nuc}	$t_{100\%}$		
A111[b]	TEA	20	6-7[c]	11	Beta	7.4[d]
B89[b]	TEA	0	-[e]	28	Beta	-
D123	TPA	20	25-26	31	ZSM-5	-
C178	TPA	0	28	32	ZSM-5	-
A181	TBA	20	> 19[f]	-	Magadiite[g] + Amorphous	-
B49	TBA	0	15	21	ZSM-11	-

[a]Key: TEA = Tetraethylammonium; TPA = Tetrapropylammonium; TBA = Tetrabutylammonium

[b]Reaction carried out at 403 K

[c]t = 5 d amorphous; t = 8 d 47 % Beta

[d]C/N for TEA^+ = 8.0

[e]t = 10 d amorphous; t = 18 d 44 % Beta

[f]Reaction terminated after 19 d

[g]Trace

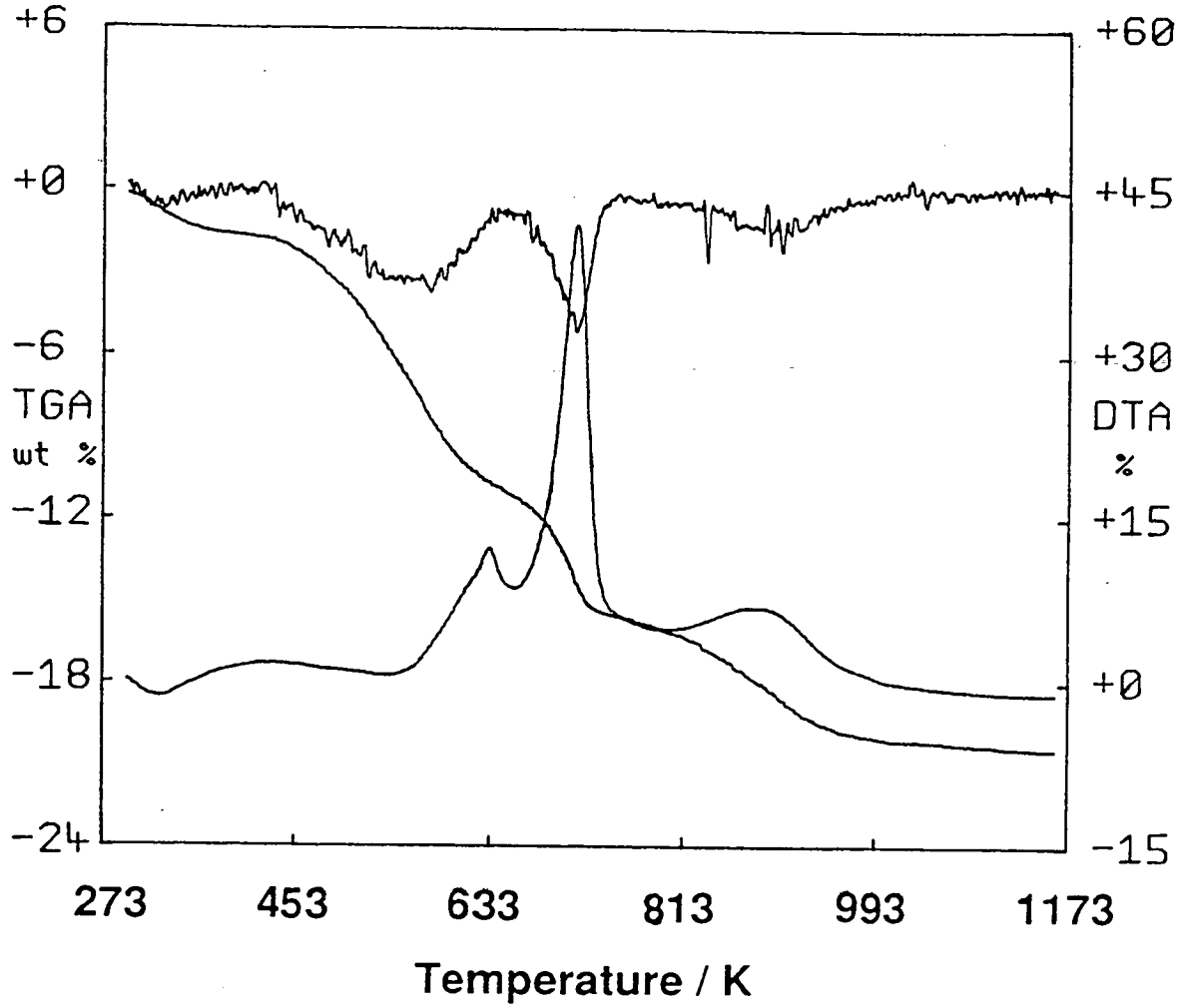

Figure 6–18: Thermal analysis profiles for sample A111

In contrast to the TMA-NU-1 system, however, the presence of 2,5-DMHD also affected the crystal growth rate, as shown by the change in slope of the crystallisation curve with the diol content of the reaction mixture (Figure 6–19). This may be due in part to a difference in the solubility of the diol at the reaction temperatures used in these systems (*i.e.* TMA-NU-1, 423 K and 403 K, TEA-Beta). A change in solubility will naturally affect the gel chemistry.

Comparison of the dta profiles (Figure 6–20) and data (Table 6–10) of the products obtained in the presence (A111) and absence (B89) of 2,5-DMHD shows that in the former, the exotherm usually seen at 607 K was increased to 633 K. This exotherm is probably associated with the degradation of TEAOH species.

Table 6–8: Effect of increasing 2,5-DMHD content on the crystallisation of TEA-Beta

Run No	x[a]	t_{nuc} / d	$t_{100\%}$ / d	Si / Al	Yield[b] / %
B89	0	-[c]	28	19.5	57
B200	5	10	19	22.0	53
B209	10	10	19	24.1	54
A111	20	6-7[d]	11	20.3	67

[a]Based on the composition 10 $(TEA)_2O$ x (2,5-DMHD) 1 Al_2O_3 60 SiO_2 3000 H_2O

[b]Based on SiO_2 + Al_2O_3

[c]t = 10 d amorphous; t = 18 d 44 % Beta

[d]t = 5 d amorphous; t = 8 d 47 % Beta

Table 6–9: Effect of 2,5-DMHD on the change in pH during the crystallisation of TEA-Beta

Run No	x[a]	pH		
		Initial	Final	Increase
B89	0	11.78	11.98	0.20
B200	5	12.63	12.80	0.17
B209	10	12.71	12.82	0.11
A111	20	11.97	12.11	0.14

[a]Based on the composition 10 $(TEA)_2O$ x (2,5-DMHD) 1 Al_2O_3 60 SiO_2 3000 H_2O

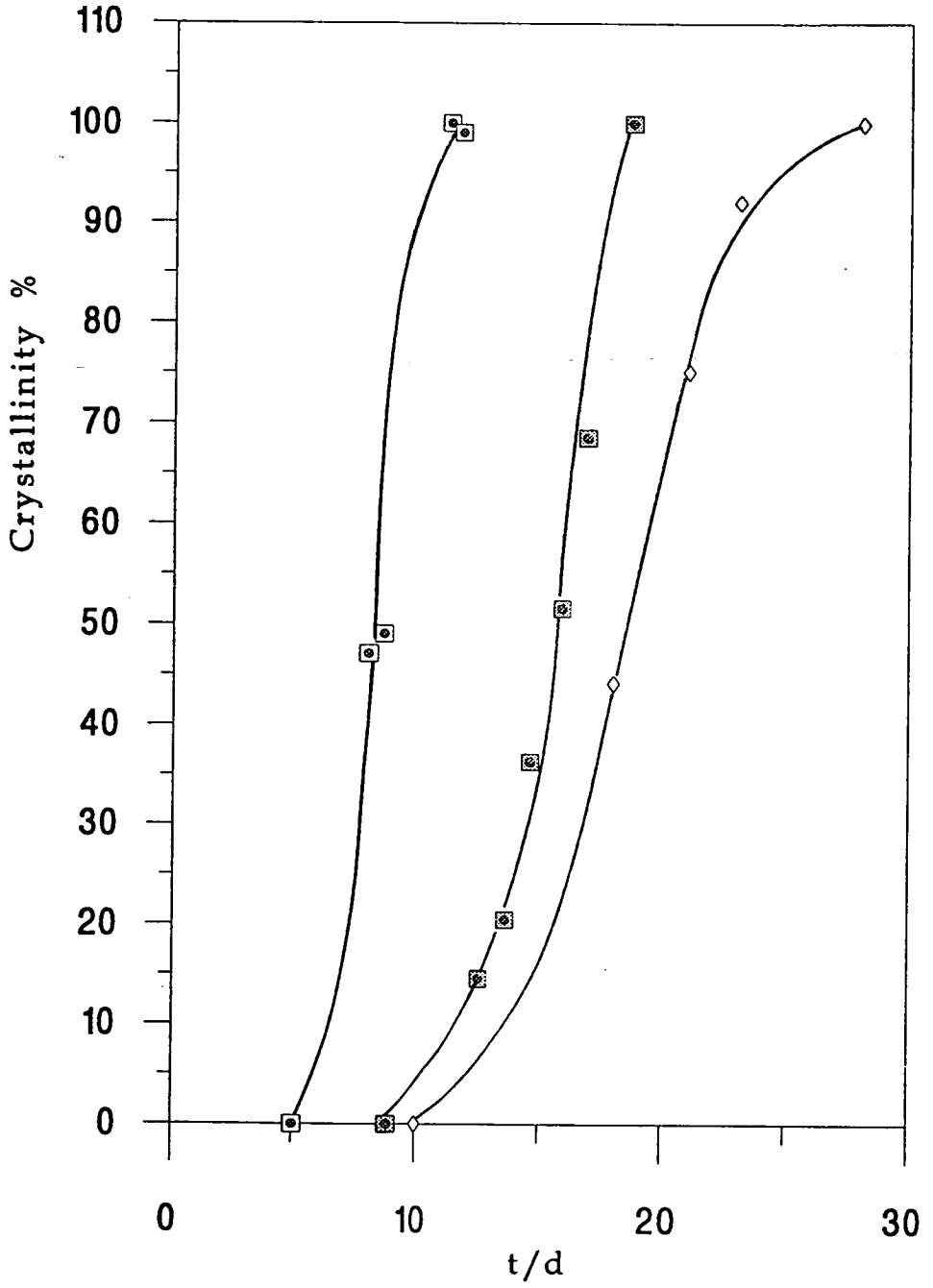

Figure 6–19: Crystallisation curves for the composition 10 $(TEA)_2O$ x (2,5-DMHD) 1 Al_2O_3 60 SiO_2 3000 H_2O (403 K, 300 rpm), where x = 0 (◇), 10 (▣), and 20 (▣)

Table 6–10: Thermal analysis data for samples B89 and A111

Run	Decomposition temperature[a] / K			Weight loss / %		
No	1st Exo[b]	2nd Exo	3rd Exo	< 543 K	> 543 K	Total
B89[b]	607	710	885	6.5	14.3	20.8
A111	633	710	885	6.0	14.4	20.4

[a]Temperature at the exotherm maximum

[b]Exo=Exotherm

[c]Diol-free reaction

The relatively large shift in this decomposition temperature cannot, however, be attributed to a change in crystal size, since examination of the product by SEM showed that the crystals were similar in size to those obtained from the diol-free reaction. It may be argued that a change in the Si/Al distribution within the crystal could account for the shift in the TEAOH decomposition temperature. Thus, an aluminium rich surface may increase framework-TEAOH interactions, although how the diol would influence the aluminium distribution is not clear.

6.3.3 Low Temperature Beta Syntheses

Table 6–11 shows the reaction compositions and products obtained from static reactions carried out at 368 K. Although the crystallisations were very slow, the effect of introducing a diol into the reaction mixture can still be seen. The crystallisation rate for reactions that contained a diol were fairly similar and all were slightly faster than the corresponding diol-free reaction. This suggests that under these reaction conditions, the nature of the diol is not important. Although this is in contrast to the trend found in the TMA-NU-1 system (Table 6–1), it should be remembered that completely different synthesis conditions were used in these reactions. It is likely that under comparable conditions (*i.e.* stirred, higher temperature), the nature of the diol could influence the crystallisation kinetics. The apparent ineffectiveness of 2,5-DMHD in these low temperature static crystallisa-

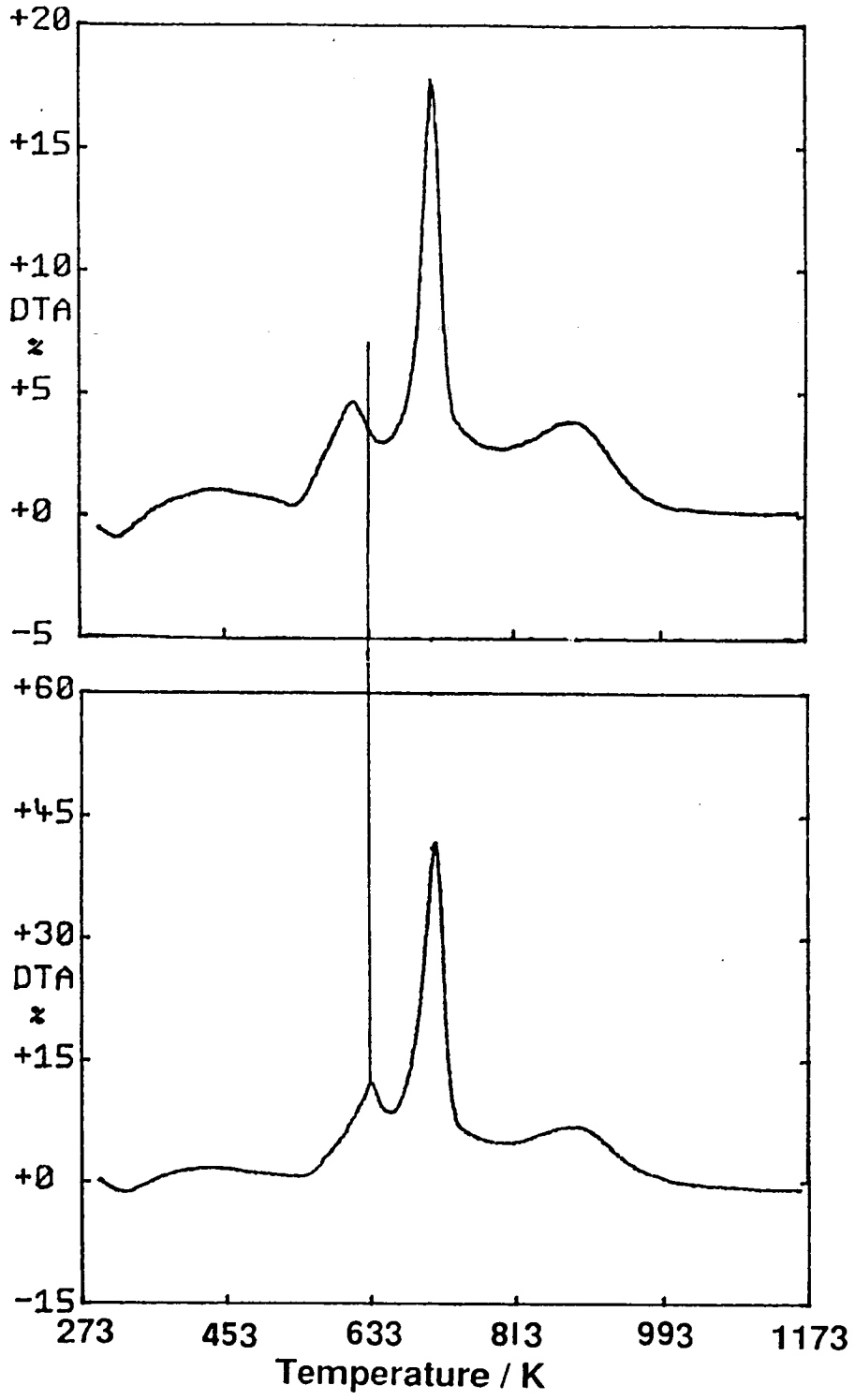

Figure 6–20: dta profiles for B89 (diol-free) (top) and A111 (2,5-DMHD) (bottom)

Table 6–11: Effect of diols on the crystallisation of Beta from the composition 10 $(TEA)_2O$ 10 (Diol) 1 Al_2O_3 60 SiO_2 3000 H_2O at 368 K without agitation

Run No	Diol[a]	Beta / %[b]		
		61 d	101 d	122 d
S39	None	9	-	34
S6	2,3-DMBD	5	24	26
S4	2,5-DMHD	6	28	30
S7	1,6-HXDL	5	27	34

[a]Key: see Table 6–1

[b]Based on A111 (100 % Beta)

tions was probably due to the fact that they were carried out at a temperature very close to the melting point of this diol (363 K), where the solubility would be low.

As with the stirred system at 403 K, the rate of crystallisation of Beta varied with the amount of 2,5-DMHD in the reaction mixture (Table 6–12). The optimum composition found in the static system at 368 K was:

10 $(TEA)_2O$ 5 (2,5-DMHD) 1 Al_2O_3 60 SiO_2 3000 H_2O (S5).

It is likely that low concentrations of diol are more effective in these low temperature crystallisations because of the difficulties in mobilising the diol.

The results of low temperature, stirred (160 rpm) reactions (Table 6–13) show that Beta did not crystallise readily from reaction mixtures that contained both TEAOH and 2,5-DMHD, even in the presence of seed material (Beta). Although this appears disconcerting, it should be remembered that the synthesis was carried out close to the melting point of the diol.[2] Bearing in mind that in the corresponding crystallisation at 403 K (A111, stirred at 300 rpm), Beta crystallised in only

[2]Melting point = 363 K

Table 6–12: Effect of 2,5-DMHD content in the reaction mixture on the crystallisation of TEA-Beta at 368 K

Run No	x[a]	Beta / %[b]		
		61 d	101 d	122 d
S39	0	9	-	34
S5	5	12	30	46
S4	10	6	28	30
S3	20	9	28	34

[a]Based on the composition 10 $(TEA)_2O$ x (2,5-DMHD) 1 Al_2O_3 60 SiO_2 3000 H_2O

[b]Based on A111 (100 % Beta)

11 days, it is reasonable to predict that the crystallisation of alkali metal-free Beta at temperatures close to 373 K within a reasonable time period may be achieved.

6.3.4 Role of Diols in Alkali-Free Systems

The role of the diols in these reactions is difficult to rationalise. The increase in crystal size found in the TMA-NU-1 system in the presence of 1,6-HXDL, 2,3-DMBD, and 2,4-DMPD suggests that there may be interactions between the diol and silicate/aluminosilicate species in either the solution of gel phase as was mentioned earlier. In a study on the crystallisation of the aluminous zeolite A, large crystals were obtained in the presence of triethanolamine [252,254,255]. It was shown that triethanolamine could chelate aluminate species in solution and thus reduce the solubility of these species and so the reactivity of the system. However, such a chelation mechanism can be ruled out on the basis that 2,5-DMHD *increased* the crystallisation rate of both TMA-NU-1 and TEA-Beta. The increase in the crystallisation rate of Beta could certainly not involve the formation of aluminate-diol complexes, since it can only crystallise in the presence of relatively large amounts of aluminium.

Table 6–13: Amount of Beta crystallised from stirred reactions (160 rpm) at 368 K from the composition:10 $(TEA)_2O$ 5 (2,5-DMHD) 1 Al_2O_3 60 SiO_2 3000 H_2O

Run No	Run Time / d	Beta / %[a]
95A13	30	nd[b]
95B14[c]	30	nd
95D17[d]	39	9

[a]Based on A111 (100 % Beta)

[b]nd = non detected (based on XRPD)

[c]Based on the composition:10 $(TEA)_2O$ 10 TEABr 5 (2,5-DMHD) 1 Al_2O_3 60 SiO_2 3000 H_2O

[d]Contained 5 % Beta seed (A111)

It is notable that 2,5-DMHD is only effective in systems that do not favour the formation of all-silica molecular sieves, *i.e.* only the crystallisation rates of Beta and NU-1 were significantly increased and neither of these can be obtained from aluminium-free reaction mixtures, unlike ZSM-5 and ZSM-11, the crystallisation rates of which were unaffected by the presence of diol. It is clear from these observations that the diol may interact with species that are involved in the nucleation process. Thus, as was mentioned in Chapter 5, it has been suggested [111] that in the synthesis of ZSM-5, aluminium-free nuclei form (*i.e.* silicalite precursors) initially and that aluminium is only incorporated during the growth process. It can be envisaged then that the diol does not interact strongly with, and stabilise these silicate precursors. On the other hand, since the crystallisation of Beta and NU-1 requires aluminium in the reaction mixture, nuclei must contain aluminium. Thus the diol may interact favourably with, and stabilise these aluminosilicate precursors. The interaction of aluminosilicate species and the diol may indeed involve chelation. Clearly such interactions would depend on the geometry, *hydrophobicity*, and solubility of the diol. Furthermore, these interactions may in fact modify the solubility of the aluminosilicate species themselves, which would account for the increase in the crystallisation rate. In addition, the diol

may modify the silicate/aluminosilicate distribution in the system. For example, a system that favours nucleation may change to one that favours crystal growth, depending on whether or not a diol is present in the reaction mixture. That the diols are not occluded in the crystalline product suggests that they do not have a void filling role.

Clearly, more work is required in this area to establish the precise role of diols in the crystallisation of high-silica zeolites. It is suggested that such work should involve ^{27}Al, ^{29}Si, and ^{13}C MASNMR analysis of aluminate, silicate, and TMA^+ species respectively in the presence and absence of diol.

6.3.5 Effect of Alkali Metal Cations on Diol/Quaternary Reactions

The effect of alkali metal cations on the crystallisation rate of TMA-NU-1 in the presence and absence of 2,5-DMHD is shown in Table 6–14. As expected, in the absence of diol (A245), the time taken to crystallise TMA-NU-1 was reduced significantly compared to that of the corresponding alkali-free reaction (D91). Furthermore, the yield was also improved significantly, probably due to the more efficient use of nutrients in the reaction mixture. Comparison of reactions D101 and A243 show that, in the presence of 2,5-DMHD and potassium cations, the time taken to crystallise TMA-NU-1 was increased. Furthermore, there was also a slight decrease in the product yield. The effect on the crystallisation rate was a most unexpected result but may be rationalised on the basis of differences in gel chemistry. Thus, in the absence of the diol, potassium cations readily interact with aluminosilicate species and are able to promote the nucleation and growth of TMA-NU-1. The increase in the crystallisation time observed when both 2,5-DMHD and potassium cations were present (A243) may be attributed to the effect of increasing the *hydrophobicity* of the system, which could inhibit the interaction between potassium ions and aluminosilicate species or suppress any synergism between K^+ and TMA^+ cations in solution.

Table 6–14: Effect of alkali metal cations on the crystallisation of TMA-NU-1

Run No	TMAOH Grade	x[a]	Cryst[n.] Time / d		Yield[b] / %
			t_{nuc}	$t_{100\%}$	
D91	> 99%[c]	0	21	25	53
D101	> 99%	20	3	6	58
D266	> 99%	20	3	6	-
A245	Pract[d]	0	9	11	70
A243	Pract	20	9	14	54

[a]Based on the composition 10 $(TMA)_2O$ x (2,5-DMHD) 1 Al_2O_3 60 SiO_2 3000 H_2O

[b]Based on SiO_2 + Al_2O_3

[c]Supplied by Aldrich

[d]Supplied by Fluka

Thermal analysis (Table 6–15) showed similar weight losses due to dehydration and organic decomposition for samples D91 (K^+-free + diol-free), D101 (K^+-free + diol), and A245 (K^+ + diol-free). A smaller organic weight loss was found for sample A243 (K^+ + diol). The results suggest that the presence of a diol modifies the relative amount of K^+ and TMA^+ cations occluded in the product. *i.e.* in the presence of both potassium cations and diol, less TMA is occluded in the framework. This may imply an interaction between the diol and TMA species.

Table 6–16 shows the change in pH on crystallisation of TMA-NU-1 from reaction mixtures that contained diol and alkali metal cations. The largest pH change was found with reactions that contained alkali metal cations, irrespective of whether any diol was present, which illustrates the effectiveness of potassium over 2,5-DMHD in modifying silica solubility. The crystallisation rate of Beta from reaction mixtures that contained 2,5-DMHD (Table 6–17) was also reduced in the presence of alkali metal cations, in this case sodium cations.

Table 6–15: Thermal analysis data for TMA-NU-1 samples crystallised from gels that contained alkali metal impurities, with and without 2,5-DMHD

Run No	x[a]	Decomposition Temp[b] / K			Wgt loss / %		
		1st Exo[c]	2nd Exo	3rd Exo	< 673 K	673-1173 K	Total
D91[d]	0	751	906	952	2.1	14.4	16.6
D101[d]	20	751	895	-	2.2	14.7	16.9
A245[e]	0	762	917	963	2.2	14.7	16.9
A243[e]	-[f]	20	916	967	1.8	13.9	15.7

[a]Based on the composition 10 $(TMA)_2O$ x (2,5-DMHD) 1 Al_2O_3 60 SiO_2 3000 H_2O

[b]Temperature at the exotherm maximum

[c]Exo = exotherm

[d]Alkali-free reaction mixture

[e]Contained substantial alkali metal impurities

[f]Three small peaks at 733, 761, and 803 K

Table 6–16: Effect of alkali metal impurities on the change in pH during the crystallisation of TMA-NU-1 from diol and diol-free gels

Run No	x [a]	pH		
		Initial	Final	Increase
D91[b]	0	12.28	12.49	0.21
D101[b]	20	12.23	12.50	0.27
A245[c]	0	12.34	12.92	0.58
A243[c]	20	12.56	13.19	0.63

[a]Based on the composition 10 $(TMA)_2O$ x (2,5-DMHD) 1 Al_2O_3 60 SiO_2 3000 H_2O

[b]Alkali-free reaction mixture

[c]Contained substantial alkali metal impurities

Table 6–17: Effect of alkali metal cations on the crystallisation of TEA-Beta in the presence of 2,5-DMHD

Run No	x NaBr[a]	t_{nuc} / d	$t_{100\%}$ / d	Beta / %
A111	0	7	11	100
B219	5	24	-	mt[b] + Am

[a]Based on the composition 10 $(TEA)_2O$ 20 (2,5-DMHD) x NaBr 1 Al_2O_3 60 SiO_2 3000 H_2O

[b]mt = minute trace (< 5 %)

6.4 Conclusions

The crystallisation rates for the high-silica zeolites NU-1 and Beta were improved significantly by the addition of 2,5-DMHD to the alkali-free reaction mixtures. The presence of relatively large amounts of alkali metal cations (in particular potassium) together with the diol, however, resulted in longer crystallisation times. It is possible that the ability of potassium cations to interact with aluminosilicate species in solution is disrupted by the presence of 2,5-DMHD in the reaction mixture. This may extend to modifying the water structure of the hydrated cation and may account for the poor growth rates observed in systems that contained both diol and alkali metal cations.

The diols were found to modify crystal size distribution and average crystal size, although they had little, if any, affect on crystal morphology. The precise role of the diols in these crystallisations is not known, though it is thought that *hydrophobicity*, geometry, and solubility are important criteria for their ability to interact with, and stabilise aluminosilicate species during nucleation. The use of inexpensive *synthesis modifiers* such as diols requires further investigation, not least to establish their role in these crystallisations. It is likely that the crystallisation of other high-silica zeolites can be improved by the addition of diols or

similar synthesis modifiers, although this might be restricted to those that cannot be crystallised in the absence of aluminium.

The ability to crystallise Beta relatively quickly from alkali metal-free reaction mixtures that contained 2,5-DMHD, coupled with the fact that the diol is extremely cheap, may make its synthesis more commercially viable. Furthermore, the use of this diol may allow a reduction in the amount of TEA used in the reaction mixture. The effect of 2,4-DMPD in alkali-free Beta crystallisations would be especially worth investigating to establish whether large crystals can be obtained, as was found in the corresponding TMA-NU-1 system.

Chapter 7

Effect of Alkali Metal Cations on the Crystallisation of ZSM-5

7.1 Introduction

The crystallisation of ZSM-5 from organic-free and alkali-free reaction mixtures was described in Chapters 3 and 5 respectively and the ability of sodium cations, and indeed potassium cations, to act as structure-directing agents for ZSM-5 was questioned in Chapter 4. The work described in this chapter follows on from the study of TPA-ZSM-5 crystallisations from reaction mixtures that contained alkali metal impurities. The results in Chapter 5, (section 5.3.1) suggested that below a certain impurity level, the effect of alkali metal cations on the crystallisation time was not significant. This suggested that there may be more than one crystallisation mechanism in operation which depended primarily on the alkali metal content of the reaction mixture.

A number of crystallisations are reported in which different levels of sodium and potassium impurities were added to the reaction mixture. In view of the effect of TMA cations on the crystallisation of alkali metal-free TPA-ZSM-5 (Chapter 5), reactions were also carried out with different levels of TMA impurities.

It must be stressed at this point that due to the length of time taken to carry out many of these crystallisations and the difficulty in precisely locating the time at which crystallisation started, detailed kinetic studies were not possible.

7.2 Experimental

Reaction mixtures and synthesis conditions were as described in Chapter 2. The bromide (Na, K or TMA) was dissolved in a small amount of ultrapure water and added to the reaction mixture before adding the remaining water required to bring the weight of gel to 400g. In order to minimise possible *autoclave effects*, crystallisations were carried out in one autoclave (autoclave C) only.

7.2.1 Analysis of Products

The solid phase was examined by thermal analysis, XRPD, and TEM (by ICI C&P Ltd., Wilton). As well as measuring the sample pH, the alkali metal content of the solution phase was determined as described in Chapter 2.

7.3 Results and Discussion

Tables 7–1, 7–2, and 7–3, give the results of crystallisations of the composition:

$$10\ (TPA)_2O\ 1\ Al_2O_3\ 60\ SiO_2\ 3000\ H_2O,$$

in the presence of Na, K, and TMA impurities, respectively. It was very difficult to establish the nucleation times very accurately, however, the crystallisation times are accurate to +/- 1 day.

As expected, the time taken to crystallise TPA-ZSM-5 decreased with an increase in the impurity level of the reaction mixture. Furthermore, there was also an increase in crystal size, based on the degree of difficulty in separating the solid and liquid phases. In general, the growth rate in the presence of TMA cations was much better than for either of the alkali metal cations. This is not totally surprising as it should be recalled from Chapter 5 that TMA cations were found

to dramatically accelerate the crystallisation of alkali-free TPA-ZSM-5. Furthermore, since they may replace TPA^+ cations at the channel intersections, it was concluded that they may hold an intermediate position between sodium and TPA^+ cations in terms of their ability to promote the crystallisation of ZSM-5.

The effect of varying the amount of Na, K and TMA impurities in the reaction mixture on the crystallisation time is shown in Figure 7–1. The correlation was similar to that reported in Chapter 5 (section 5.3.1) for the crystallisation of TPA-ZSM-5 from reaction mixtures that contained TPAOH of different alkali metal content. The curves show that the crystallisation time was affected to different extents which depended on the concentration of the impurity. At very high concentrations (> 2 (M_2O), where M = Na, K or TMA) there was very little effect on the time taken to crystallise TPA-ZSM-5. Indeed it is likely that an increase from 2 to 10 moles would not improve the crystallisation time by more than a day. Similarly, at very low levels (< 0.5 (M_2O)) a change in the impurity concentration had relatively little effect on the crystallisation time. Between these two extremes (0.5 - 2 (M_2O)), the crystallisation time was very sensitive to the impurity content of the reaction mixture. Not only do these results suggest a possible change in crystallisation mechanism with alkali or TMA cation content of the reaction mixture, they also strongly suggest that TPA-ZSM-5 will crystallise in the complete absence of alkali metal cations. Indeed, run no. C257, which contained no detectable alkali metal impurity, crystallised TPA-ZSM-5.

Table 7–4 shows the difference in crystallisation times for a given amount of Na_2O, K_2O, and $(TMA)_2O$. At levels < 0.5, there was little difference in the crystallisation times, which suggests that at these levels, the nature of the cation impurity is not important. However, above this level, each cation improved the crystallisation rate to different extents. This probably reflects the difference in competition between each of these cations with TPA^+ cations for aluminosilicate species as well as the difference in the distribution of these species. At a level of 1.0, TMA cations appeared to be the most effective and potassium was the better of the two alkali metals examined. That TMA is more effective in promoting the crystallisation of ZSM-5 at these levels, may be related to the fact that, in

Table 7–1: Effect of Na impurities (added as NaBr[a]) on the crystallisation of TPA-ZSM-5, at 423 K, 300 rpm

Run	Na in gel[b]		x Na_2O[c]	Cryst[n.] Time / d		Si/Al
No	mg kg^{-1}	10^3 mol l^{-1}		t_{nuc}	$t_{100\%}$	
C257	0[d]	0	0	30	33	-
C76	12[e]	1.3	0.02	-[f]	32	-
C178	12[e]	1.3	0.02	30	33	26.4
C148	78	2.9	0.09	-[g]	31	-
C158	367	15.4	0.48	25	27	26.4
C110[h]	755	32.3	1.00	-[i]	16	-
C144	1936	83.7	2.58	1.5	2	23.1

[a]Contained 149 mg kg^{-1} KBr

[b]Includes contribution from SACHEM TPAOH

[c]Based on the composition 10 $(TPA)_2O$ x Na_2O 1 Al_2O_3 60 SiO_2 3000 H_2O

[d]TPAOH prepared from TPABr + Ag_2O

[e]Impurity from SACHEM TPAOH [f]t = 19 d amorphous, t = 25 d 85 % ZSM-5

[g]t = 23 d amorphous, t = 29 d 96 % ZSM-5

[h]10 $(TPA)_2O$ 2 NaBr 1 Al_2O_3 60 SiO_2 3000 H_2O, contained slightly less TPAOH than the other reactions

[i]t = 10 d amorphous, t = 14 d 90 % ZSM-5

Table 7–2: Effect of K impurities (added as KBr[a]) on the crystallisation of TPA-ZSM-5, at 423 K, 300 rpm

Run	K in gel[b]		x K_2O[c]	Cryst$^{n.}$ Time / d	
No	mg kg^{-1}	10^3 mol l^{-1}		t_{nuc}	$t_{100\%}$
C257	0[d]	0	0	30	33
C232	113	2.9	0.09	26	30
C234	287	7.3	0.23	28	31
C240	603	15.4	0.48	24	27
C249	1257	32.1	0.99	5-6[e]	7
C247	3272	83.7	2.58	0.5	1

[a]Contained 136 mg kg^{-1} NaBr

[b]Negligible contribution from SACHEM TPAOH

[c]Based on the composition 10 $(TPA)_2O$ x K_2O 1 Al_2O_3 60 SiO_2 3000 H_2O

[d]TPAOH prepared from TPABr + Ag_2O

[e]t = 4 d amorphous, t = 6.8 d 100 % ZSM-5

Table 7–3: Effect of TMA impurities (added as TMABr) on the crystallisation of TPA-ZSM-5, at 423 K, 300 rpm

Run	TMA in gel		x $(TMA)_2O^a$	Cryst$^{n.}$ Time / d	
No	mg kg^{-1}	10^3 mol l^{-1}		t_{nuc}	$t_{100\%}$
C250	213	2.9	0.09	33	35
C191	544	7.3	0.23	29	30
C207[b]	1168	15.7	0.49	24[c]	30
C221	1587	21.4	0.66	-	8[d]
C215	1842	24.8	0.77	6	7
C186	2405	32.4	1.00	2	3

[a]Based on the composition 10 $(TPA)_2O$ x $(TMA)_2O$ 1 Al_2O_3 60 SiO_2 3000 H_2O

[b]Comparison with run no. C106 (9.5 $(TPA)_2O$ 0.5 $(TMA)_2O$ 1 Al_2O_3 60 SiO_2 3000 H_2O, Chapter 5) suggests this to be a rogue result

[c]t = 22 d amorphous, t = 24 d 85 % ZSM-5, t = 28 d 93 % ZSM-5

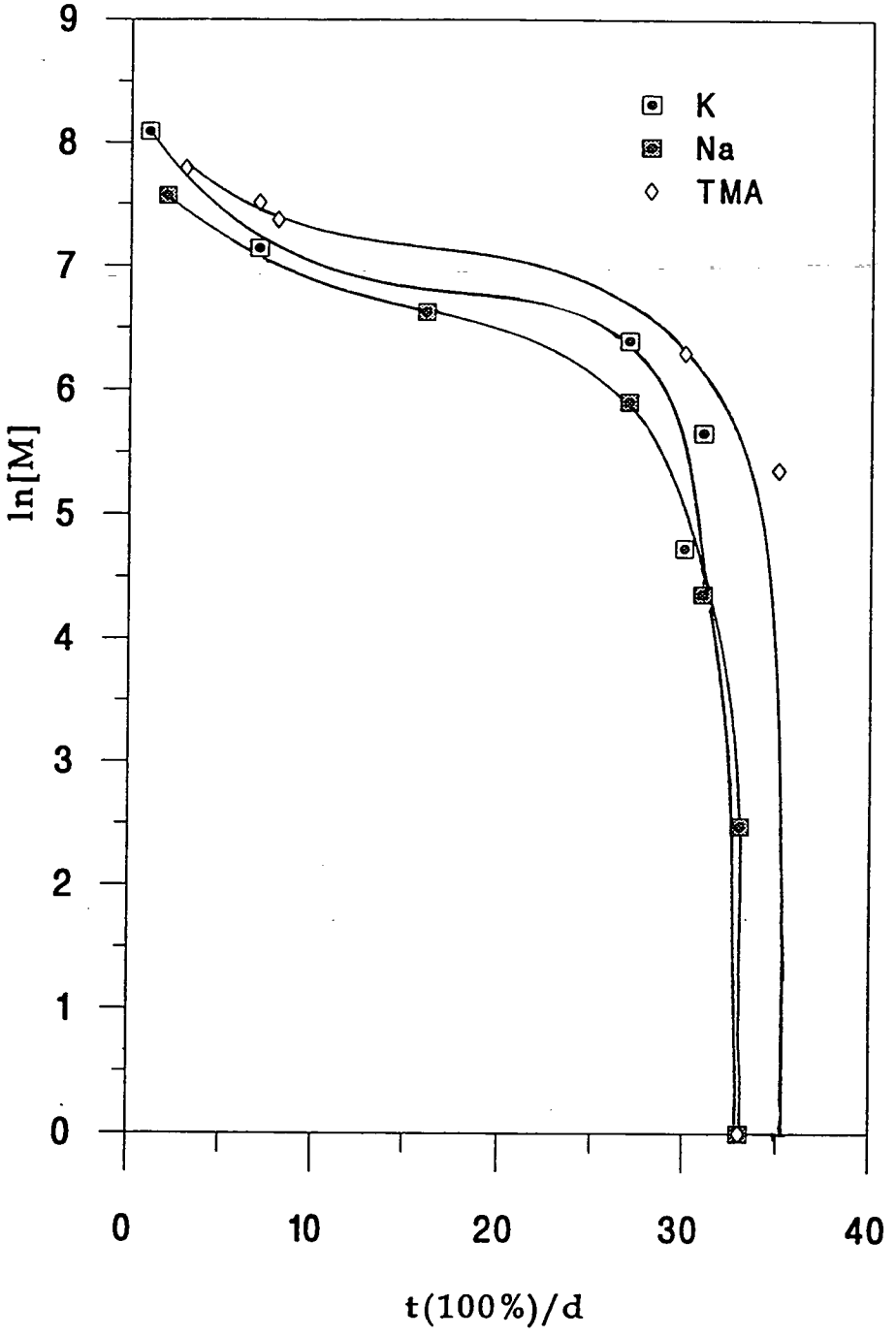

Figure 7–1: Effect of Na, K, and TMA on the crystallisation of TPA-ZSM-5

Table 7–4: Comparison of crystallisation times for TPA-ZSM-5 in the presence of increasing amounts of Na_2O, K_2O, and $(TMA)_2O$

	Crystallisation Time / d				
x / mol	0.09	0.23	0.48	1.00	2.58
Na_2O	31	-	27	16[a]	2
K_2O	30	31	27	7	1
$(TMA)_2O$	35	30	-	3	-

[a]Reaction C110 (see Table 7–1)

addition to balancing some of the framework charge, it can stabilise the framework to some extent by virtue of its hydrophobic methyl groups. TMA was not tested at higher concentrations since it had already been shown (Chapter 5) that the co-crystallisation of NU-1 would be favoured.

The results of detailed examination of the thermal analysis[1] data are shown in Tables 7–5 and 7–6. The total amount of organic material occluded in the product was found to decrease as the amount of alkali metal increased. At the same time, the proportion of the organic in the form TPA^+ remained constant at about 94%. This, together with the decrease in the amount of TPA^+ cations may be accounted for by an increase in competition between alkali metal cations and TPA^+ cations for silicate and aluminosilicate species, at impurity levels above 0.5 M_2O. Thus, significantly more of the framework charge will be balanced by alkali metal cations above this level.

The organic weight loss for amorphous samples, collected before the onset of crystallisation, was determined for the sodium samples only. This weight loss was significantly less than that of their crystalline counterparts. Furthermore,

---

[1]Thermal analysis was not carried out for TMA/TPA samples, since it would be difficult to establish the extent to which TMA was occluded at particularly low levels

Table 7–5: Detailed thermal analysis data for TPA-ZSM-5 crystallised in the presence of sodium

Run No	Wgt loss (%) Over Temp Range (K)				$\frac{TPA^+}{TPA^+ + TPAOH}$
	< 623	623-683	683-873	873-1173	
	H_2O	TPAOH	TPA^+	Si-OH[a]	
C178	1.6	0.6	10.2	1.6	0.94
C148	2.0	0.5	10.0	1.4	0.95
C158	1.8	0.8	9.9	1.3	0.93
C110	2.1	0.6	9.6	2.0	0.94
C144	2.3	0.7	9.7	1.3	0.93

[a]Loss of silanol OH [256]

the amount of occluded organic material was found to decrease when the sodium content of the reaction mixture was increased (Table 7–7), although the proportion of organic as TPA^+ increased slightly. This reflects the ability of sodium cations to interact more effectively with the 'aluminium rich' amorphous gel phase.

A plot of organic weight loss between 623 and 683 K against the amount of crystalline material present (Figure 7–2), suggested the presence of X-ray amorphous crystallites [131] in samples taken before crystallisation could be detected by XRPD. This plot is similar to that obtained by Derouane *et al.* [131] for crystallisations from their *synthesis method B*, where they claim that their crystallisations occurred via a solid gel phase transformation mechanism [166]. It is unlikely, however, that these crystallisations would proceed in the absence of a solution phase, thus this mechanism may be better described as a solution mediated solid phase transformation. Alternatively, it may be described as a *solid hydrogel-dominated* mechanism, where nucleation takes place in the bulk of the gel phase. The fact that the products obtained in the present study, from low alkali metal reaction mixtures, were in the form of aggregates of tiny crystals (Chapter 5, Figure 5–11), further suggests that such a mechanism operates in these reactions.

Table 7–6: Detailed thermal analysis data for TPA-ZSM-5 crystallised in the presence of potassium

Run No	Wgt Loss (%) Over Temp Range / K				$\frac{TPA^+}{TPA^+ + TPAOH}$
	< 623	623-683	683-873	873-1173	
	H_2O	TPAOH	TPA^+	Si-OH[a]	
C232	1.8	0.4	9.9	1.4	0.96
C234	2.5	0.5	9.8	1.7	0.95
C240	2.7	0.6	9.4	1.7	0.94
C249	2.4	0.4	9.3	1.7	0.96
C247	1.9	1.0	8.8	0.8	0.90

[a]Loss of silanol OH [256]

Table 7–7: Effect of increasing sodium content on the relative amounts of TPAOH and TPA^+ occluded in the amorphous precursor

Run No	Na_{total} 10^3 mol l^{-1}	Wgt loss (%) Over Temp Range (K)			$\frac{TPA^+}{TPA^+ + TPAOH}$
		< 623	623-683	683-873	
		H_2O	TPAOH	TPA^+	
C178	1.3	8.7	3.4	4.3	0.56
C148	2.9	9.2	2.0	5.1	0.72
C158	15.4	8.7	2.4	3.8	0.61
C110	32.3	7.0	1.6	3.3	0.67
C144	83.7	7.1	0.9	2.0	0.69

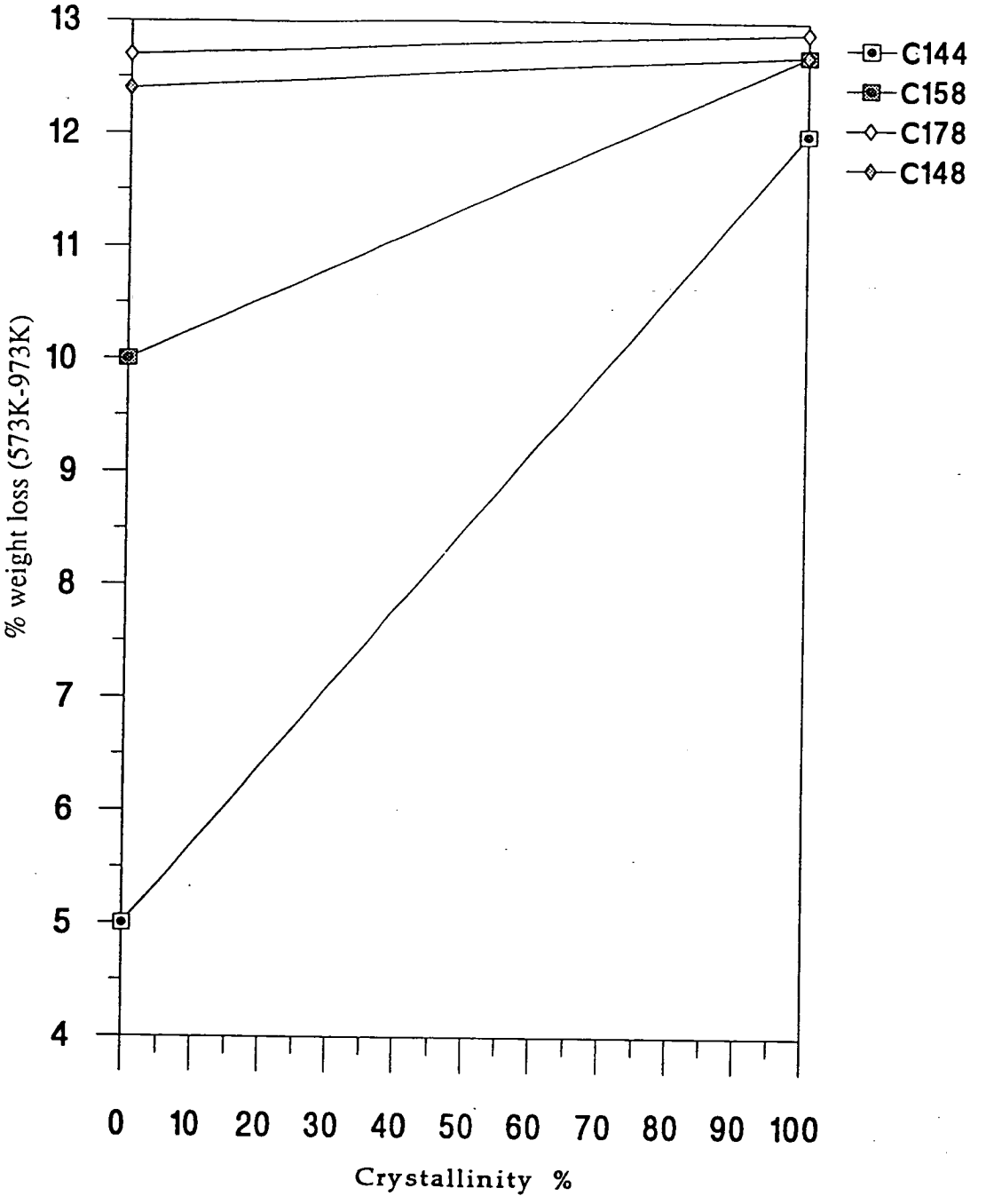

Figure 7–2: Correlation between organic weight loss (%) and X-ray crystallinity (%) for TPA-ZSM-5 crystallised in the presence of sodium

Table 7–8: Change in solution pH and sodium concentration

Run	pH			K / mg l^{-1}		
No	Initial[a]	Final[b]	Increase	Initial[a]	Final[b]	Increase
C76	11.64	12.56	0.92	3	4	1
C178	11.92	12.97	1.05	5	13[c]	-
C148	12.25	12.97	0.72	26	64	38
C158	12.28	12.97	0.69	122	285	163
C110	12.24	12.93	0.69	218	610	392
C144	11.53	12.36	0.83	1150	1538	388

[a]Calculated as the mean of several samples collected before the onset on crystallisation

[b]Value for sample deemed 100% ZSM-5

[c]Higher than theoretical amount, therefore possible contamination

At the onset of crystallisation, as well as the normal increase in pH, there was a large increase in the solution phase alkali metal content (Tables 7–8 (sodium) and 7–9 (potassium)). Not surprisingly, as the amount of alkali in the reaction mixture was increased, greater differences were found for the alkali contents before and after crystallisation.

The distribution of sodium and potassium cations between the solid and liquid phases of amorphous samples taken before the onset of crystallisation and the final crystalline product are given in Tables 7–10 and 7–11 respectively, where they are compared to values for the unreacted gel. The proportion of alkali metal cations in the unreacted gel solid was found to decrease as the total alkali content of the reaction mixture (C76-C144 and C232-247) increased, irrespective of the nature of the alkali, although the solid gel contained almost 2-3 times more potassium than sodium for a given loading in the respective reaction mixtures. Thus, the solution phase is more depleted of cations than in the corresponding sodium system. That the solution phase is more depleted in potassium cations may not be totally unexpected, given the behaviour of these cations in aluminosilicate reac-

Table 7–9: Change in solution pH and potassium concentration

Run	pH			K / mg l^{-1}		
No	Initial[a]	Final[b]	Increase	Initial[a]	Final[b]	Increase
C232	12.01	12.71	0.68	4	28	24
C234	12.12	12.84	0.72	10	130	120
C240	12.38	13.21	0.83	36	358	322
C249	12.52	13.51	0.99	248	798	550
C247	-	13.33	-	-	1976	-

[a]Calculated as the mean of several samples collected before the onset on crystallisation

[b]Value for sample deemed 100% ZSM-5

tion mixtures where they have a tendency to promote phase separation (Chapters 3 and 4). The difference in the alkali metal distribution between the solid gel and solution phases for both sodium and potassium cations may account for the difference in their ability to promote the crystallisation of high-silica zeolites. Indeed, this argument could account for the difference in sensitivity of inorganic sodium and potassium reaction mixtures toward seed or organic impurities (Chapter 4), where the cation content of the solution phase may be one of the most important factors.

A similar but less obvious trend was found with samples taken during the reaction, before the onset of crystallisation. The amorphous solids from the potassium reactions contained significantly more potassium cations than those which contained sodium in the corresponding sodium reactions. Indeed, at levels < 0.5 K_2O, virtually all the potassium was found in the amorphous solid phase. In general, the rise in the potassium content of the amorphous solid during the synthesis was similar to that found with sodium on a molar basis and was found to be essentially independent of the initial alkali metal content of the reaction mixture, above

Table 7–10: Sodium distribution between solid and liquid phases during synthesis

Run No	Na_{total} 10^3 mol l^{-1}	Sodium Distribution / %					
		Gel[a]		Amor. Sample[b]		Crys. Sample[c]	
		L[d]	S	L	S	L	S
C76	1.3	42	58	25	75	33	67
C148	2.9	64	36	33	67	82	18
C158	15.4	90	10	33	67	78	22
C110	32.3	82	18	29	71	81	19
C144	83.7	92	8	59	41	79	21

[a]Unreacted

[b]Calculated as the mean of several amorphous samples collected before the onset on crystallisation

[c]Value for sample deemed 100% ZSM-5

[d]Key: L = liquid phase, S = solid phase

0.5 (M_2O). Below this value, the increase was much lower and probably reflects limited competition for silicate and aluminosilicate species.

As mentioned earlier, at the onset of crystallisation there was a large increase in the solution phase alkali metal content for both sodium and potassium. Clearly, a large proportion of the alkali metal is tied up with the solid aluminosilicate gel in the early stages of the reaction. On crystallisation, many of these cations are displaced as T-O-T bonds are formed. For levels between 0.5 and 1.0 mol, this was essentially independent of the nature of the alkali metal. However, at particularly low levels, the increase in the potassium concentration of the solution phase was less marked which suggests that more potassium was retained in the crystalline phase than sodium in the corresponding reactions.

Figure 7–3 shows that measurement of the solution phase alkali metal content can be used to monitor the progress of a reaction in the same way as pH and XRPD measurements. Indeed, similar profiles were obtained for all reactions carried

Table 7–11: Potassium distribution between solid and liquid phases during synthesis

Run No	K_{total} 10^3 mol l^{-1}	Potassium Distribution / %					
		Gel[a]		Amor. Sample[b]		Crys. Sample[c]	
		L[d]	S	L	S	L	S
C232	2.9	34	66	4	96	25	75
C234	7.3	64	36	3	97	45	54
C240	15.4	64	36	6	94	59	41
C249	32.1	70	30	20	80	63	37
C247	83.7	79	21	-	-	60	40

[a]Unreacted

[b]Calculated as the mean of several amorphous samples collected before the onset on crystallisation

[c]Value for sample deemed 100% ZSM-5

[d]Key: L = liquid phase, S = solid phase

out in this investigation. It should also be mentioned that in the 'alkali-free'[2] TMA/TPA reactions, a similar change in the solution phase sodium content was observed on crystallisation. This suggests that these impurities were involved in the crystallisation to some extent and their effect, therefore, cannot be neglected. It is thought, however, that any effect would be trivial compared to that of the TMA^+ cations. Since the TMA^+ content of the solution phase was not determined, it is difficult to establish the relative contributions of TMA and sodium in these crystallisations.

There is insufficient evidence to draw any firm conclusions on the relevance of the magnitude of the increase in the solution phase alkali metal content, *eg.*whether this is related to silica solubility or product stability [116].

In general, the proportion of the alkali metal found in the final mother liquor (and thus the crystalline solid phase) was independent of the concentration of the alkali in the reaction mixture. However, there was a marked dependence on the nature of the alkali metal cation. The proportion of sodium cations in the crystalline product was about 20% compared to about 40% for potassium. This implies that potassium cations may compete more favourably than sodium cations with TPA^+ for silicate and aluminosilicate species, or alternatively, potassium cations may be more selective towards the formation of ZSM-5 as has been claimed in work by Erdem and Sand [107].

The change in alkali metal content of the solution and solid phases during synthesis is shown schematically in Figures 7–4 and 7–5. Although these are grossly over simplified, they give a good visual impression of the change in the distribution of alkali metal cations between the solid and solution phases during synthesis. One may speculate from Figure 7–4 that these illustrate a change in crystallisation mechanism, in that at high sodium concentrations, the sodium profiles for the solid and liquid phases do not intersect. Thus, plots of alkali metal content of the solid and solution phases as a function of crystallisation time

---

[2]TPAOH contained 38 mg l^{-1} Na

Figure 7–3: Comparison of the change in the solution phase alkali metal content with pH and XRPD measurements during crystallisation

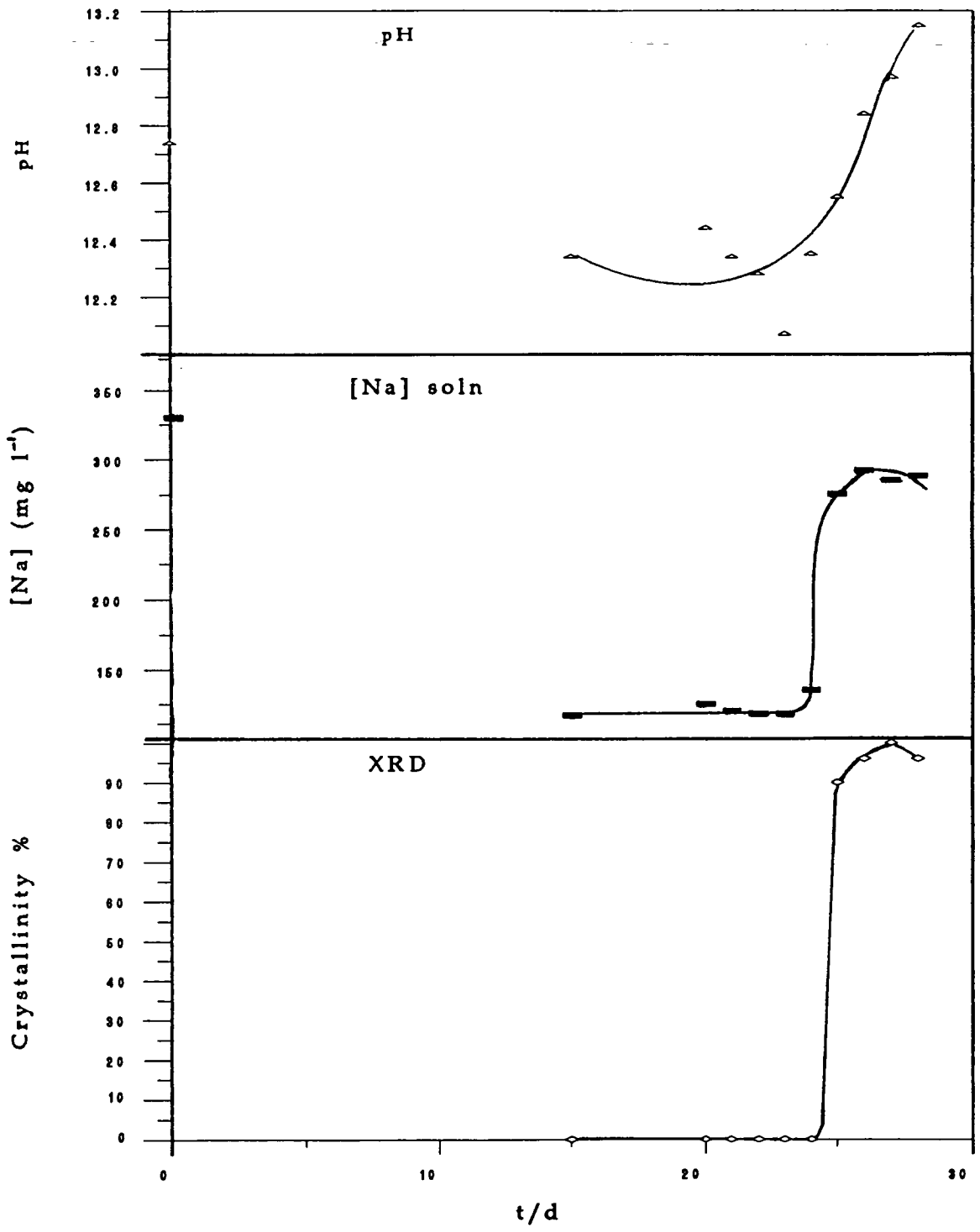

which do not intersect could be interpreted as illustrating crystallisation via one particular crystallisation mechanism, *eg.* a solution phase mechanism. Those that do intersect could illustrate crystallisation via a different mechanism, *eg.* a gel dominated mechanism. Again, this is pure speculation, and without more experimental data and analysis, it is difficult to establish whether or not a change in the alkali metal content (or indeed TMA content) of the reaction mixture is indeed related to the crystallisation mechanism.

Figures 7–6 and 7–7 show how the alkali metal content of the unreacted gel, amorphous and crystalline solids varies as a function of the alkali metal content of the reaction mixture. These plots show a point of inflection at about 0.5 (M_2O), which may possibly be close to a threshold value, above which the crystallisation occurs predominantly in the solution phase (solution dominated mechanism) and below which it occurs predominantly in the solid gel phase (gel dominated mechanism).

It is obviously not possible to comment on the distribution of TMA cations between the solid and liquid phase during reaction primarily because of lack of experimental results.

Much of the above cannot be adequately substantiated for lack of experimental data. It may simply be that the change in the crystallisation time with alkali metal (or TMA) content shown if Figure 7–1 can be explained in terms of competition between cations for silicate and aluminosilicate species as well as perhaps synergistic effects. Thus at relatively high concentrations of alkali (or TMA), where the crystallisation takes less than 3 days, there are sufficient cations to compete favourably with TPA cations and form appropriate growth species. Although nucleation is clearly promoted by these cations, it is believed that they do not themselves nucleate the product. It is apparent that these small cations favour growth. At intermediate alkali concentrations, where the effect on the crystallisation time is significant, competition between cations swings in favour of TPA^+. Thus nucleation competes favourably with crystal growth with the result that smaller crystals are obtained. Finally at the lowest alkali concentrations, where

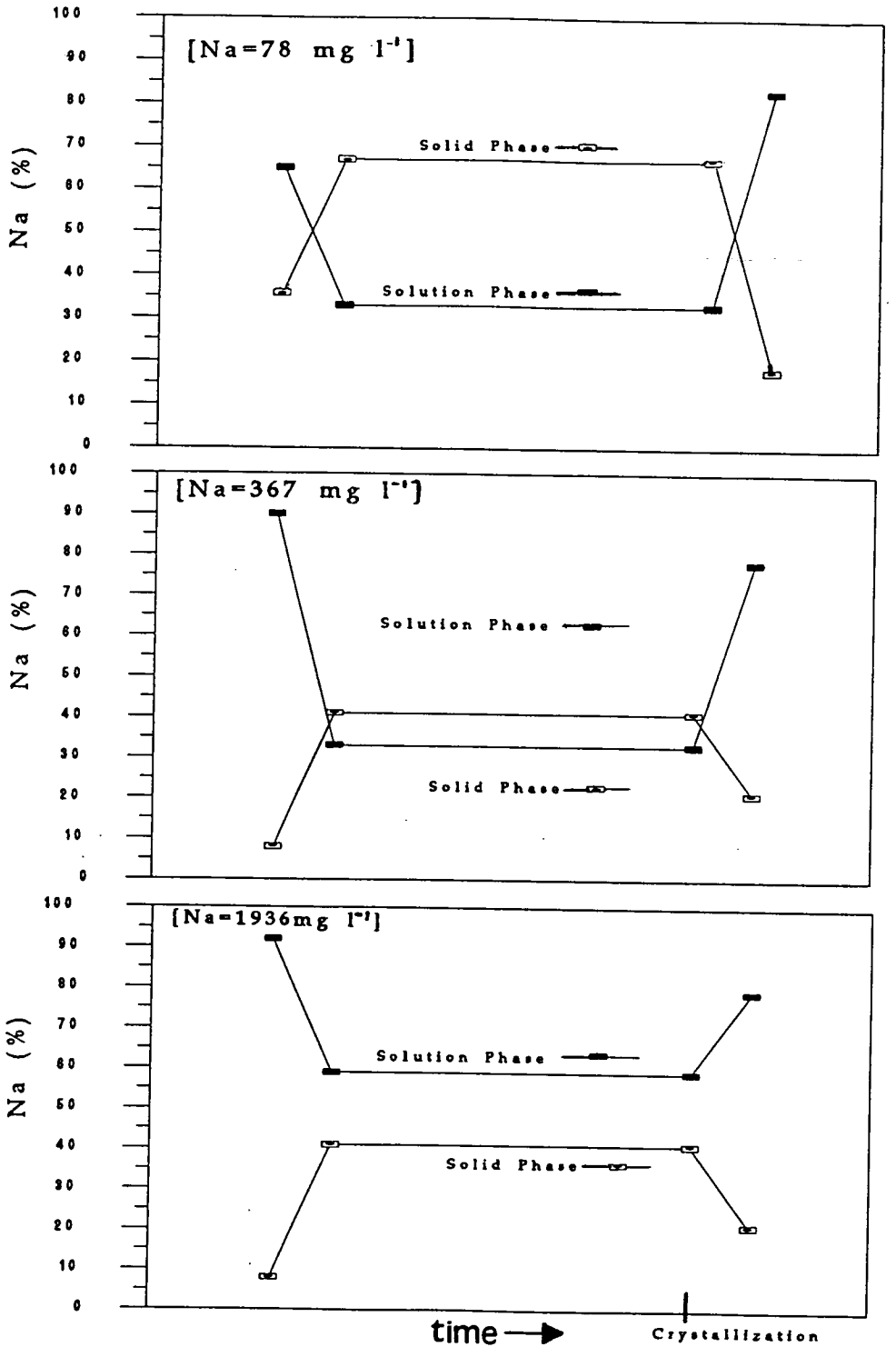

Figure 7–4: Schematic representation of the change in sodium concentration in both the solid and liquid phases during reaction

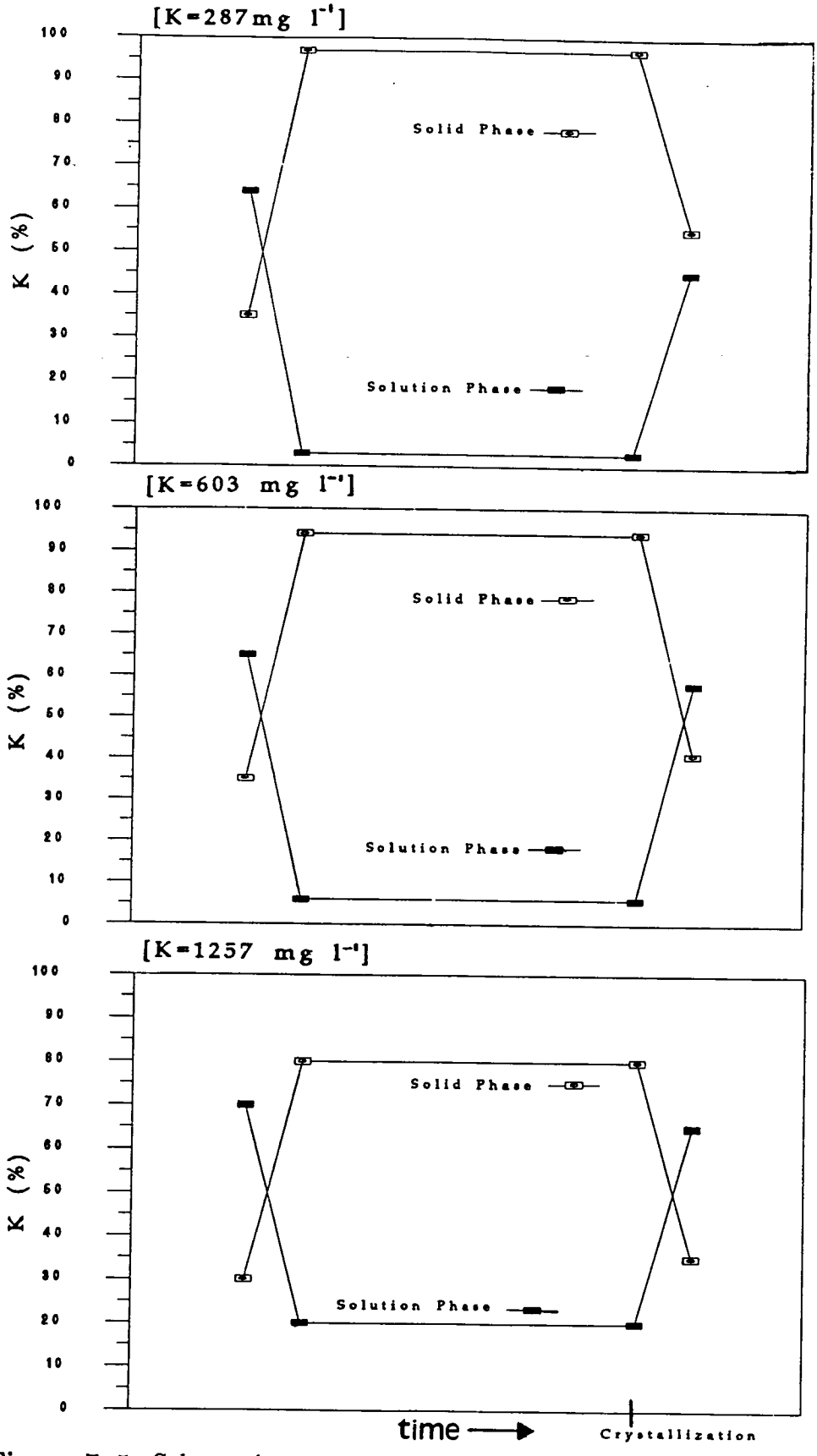

Figure 7–5: Schematic representation of the change in potasssium concentration in both the solid and liquid phases during reaction

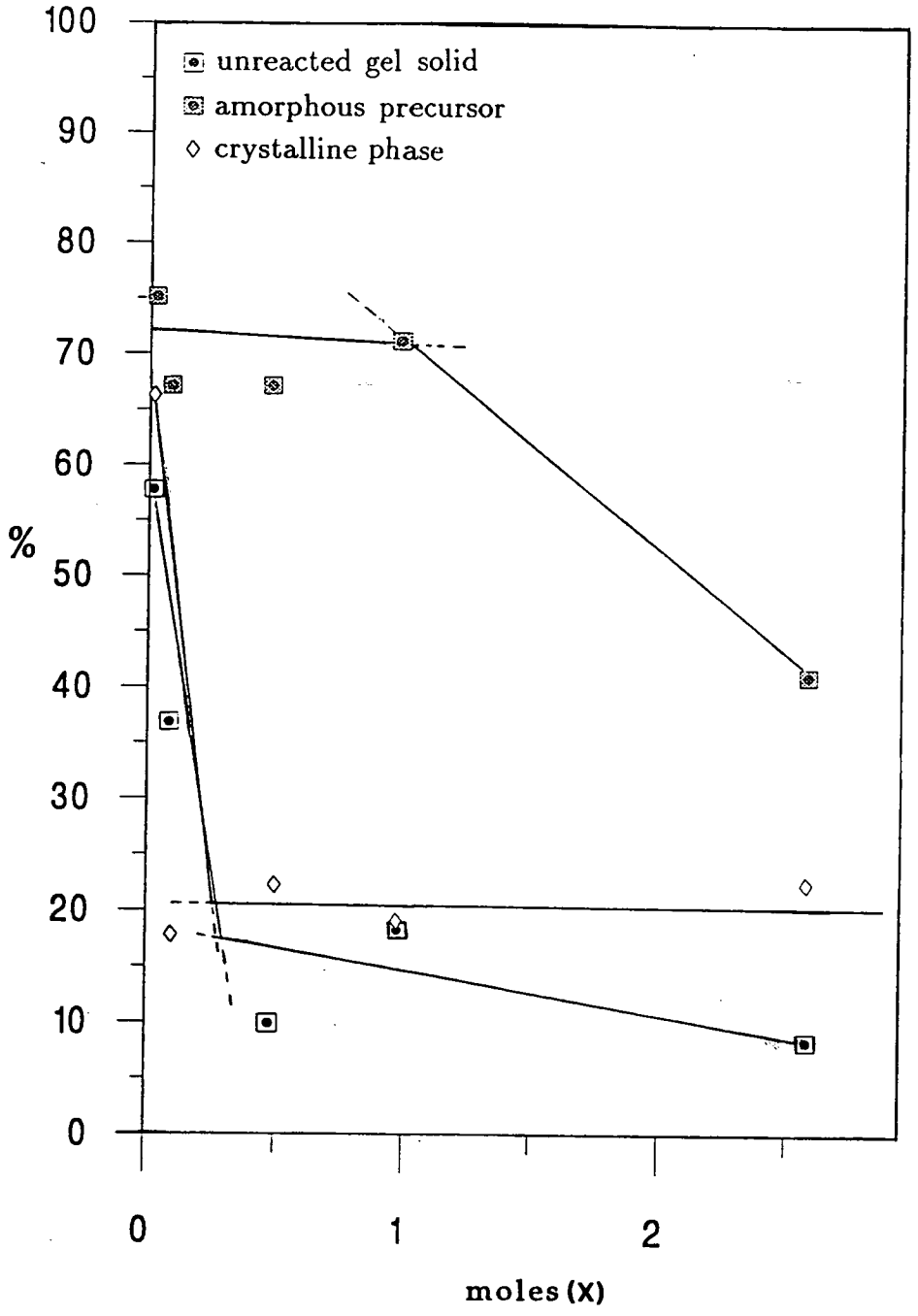

Figure 7–6: Change in the sodium content of unreacted gel solid, amorphous precursor, and crystalline solids with increasing sodium content of the reaction mixture

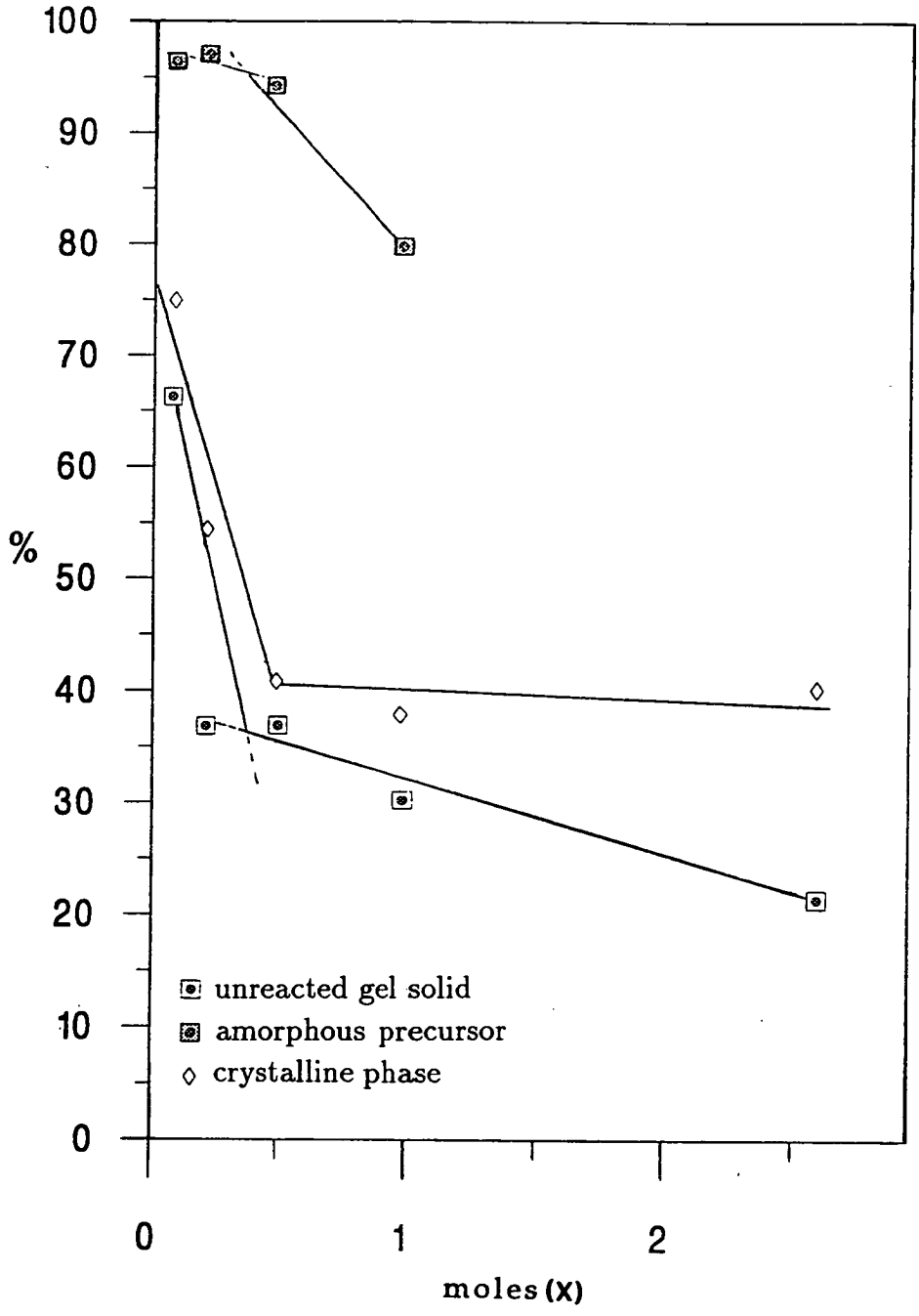

Figure 7–7: Change in the potassium content of unreacted gel solid, amorphous precursor, and crystalline solids with increasing potassium content of the reaction mixture

the effect on the crystallisation time is minimal, nucleation dominates and since there are very few growth species available, extremely small crystals are obtained.

Although much of the above cannot be proved beyond doubt, there is sufficient evidence to suggest that the measurement of the alkali metal content in either the solution or, preferably, solid phase may give important information with regard to the crystallisation mechanism and to the possible roles of these cations. It is interesting to note that Derouane *et al.* [131] reported that for a solid phase transformation mechanism, both the Si/Al and Al/Na ratios remained constant until nearly 100% crystallinity, at which point they both increased. This suggests that, in their studies, the sodium content of the gel phase decreased rapidly on crystallisation, as in the present work. Thus, based on their results for a solution phase mechanism, the sodium content of the solution phase should decrease steadily during the course of the crystallisation. Thus it may well be possible to establish the crystallisation mechanism by simply measuring the solution phase alkali metal content. This is certainly an area that requires further investigation.

7.4 Conclusions

On the basis of thermal analysis and measurements of the alkali metal cation distribution in the reaction mixture, it is believed that the crystallisation of TPA-ZSM-5 from the composition:

$$10\ (TPA)_2O\ x\ M_2O\ 1\ Al_2O_3\ 60\ SiO_2\ 3000\ H_2O,$$

where $x < 0.5$, crystallises at 423 K (300 rpm) predominantly via a gel dominated crystallisation mechanism. Above this threshold, it is thought that this mechanism may shift in favour of a solution phase mechanism. A change in the crystallisation mechanism with alkali metal content of the reaction mixture may account for the effects of very high and low levels of cation impurities on the crystallisation kinetics. While this is certainly an attractive hypothesis, the effects may simply be attributed to a difference in competition between these cations and TPA cations for silicate and aluminosilicate species in the reaction mixture.

The role of alkali metal cations in these crystallisations is thought to be primarily in crystal growth, although they may promote nucleation by helping to stabilise nuclei.

Analysis of the solution phase for alkali metal content provides yet another method with which to follow the progress of a reaction and detect the onset of crystallisation. However, it is thought that this method may not be readily applicable to crystallisations from inorganic reaction mixtures, or others in which the alkali metal content is very high, since the change in the solution phase content on crystallisation may not be readily detected. Although analysis by flame photometry can be rather laborious, it is believed that the use of Ion-Selective Electrodes would make measurements quick and easy, as with pH measurements. Unlike pH measurements, however, information may be gained on the crystallisation mechanism.

Chapter 8

Overall Conclusions and Further Work

8.1 General Comments

The results of the present work show that much can be gained by carrying out syntheses with reagents of high purity and in systems where great care is taken to exclude impurities.This has led to a number of important findings, both theoretical and practical. In the former, much has been gained to further help understand the role of templates and void fillers in the crystallisation of high-silica zeolites. Furthermore, this work has brought into question the role of sodium cations as a structure-directing agent in the synthesis of Na-ZSM-5. The discovery that inorganic reaction mixtures can be extremely sensitive to seed or organic impurities is of practical importance. Thus when carrying out high-silica zeolite crystallisations with a new organic *template*, then not only should a 'blank' reaction be carried out in the absence of the organic (as is usual), but also the 'blank' reaction should be tested with traces of seed impurity. Only then can any structure directing effect be truly attributed to the organic species. This has been adequately demonstrated in the present work for a number of materials thought to be ZSM-5 structure directors. While this certainly applies to the crystallisation of ZSM-5 there is no reason to suggest that this should not extend to other systems, perhaps even to zeotypes.

That crystallisations in the absence of alkali metal cations take a very long time has undoubtedly led to misleading reports, the most notable of which are those that claim that Beta cannot be crystallised in the absence of alkali metal cations [229,230,231,232]. The important lesson to learn here is that "As long

as the synthesis remains amorphous, it's still in with a chance of crystallising something" [257].

8.2 Organic-Free Syntheses

Investigation of the potassium system showed that high-silica zeolites did not crystallise readily. Indeed only two such phases were obtained, K-NU-10 and K - ZSM - 5, and it was proved that this latter phase could only be obtained from reaction mixtures that contained seed or organic impurities. It is possible that this may also apply to NU-10, although there is insufficient evidence to establish this.

The *Scavenging Reaction*:

$$15\ K_2O\ 0.667\ Al_2O_3\ 60\ SiO_2\ 3000\ H_2O$$

was found to be a most interesting and remarkable composition. It was found to be extremely sensitive to traces of seed material and certain organic impurities. An interesting *side effect* was that in the presence of seed material, sphere-like particles were obtained. It is believed that these were initiated by seeds which are thought to act as centers for accretion of amorphous material. Crystallisation then occurred both inside and outside the particle. The shape of the particle owes much to the phase separation phenomenon as well as collisions in the solution.

It would be interesting to examine this composition in the presence of surfactants, which would reduce phase separation. While this would undoubtedly affect the formation of *spheres*, it may also inhibit the ability of the gel to detect impurities. Unfortunately there was insufficient time to explore any possible applications of these *spheres*.

Several novel applications have been proposed for the *Scavenging Reaction*. The most useful of these is based on its ability to detect minute traces of impurities. Thus, it can be used to check the cleanliness of reaction vessels and so establish the

effectiveness of the cleaning method. This is particularly important if the effects of seeding is to be avoided in subsequent crystallisations. Furthermore, repeated use of this reaction can scavenge organic impurities, thus leaving the reaction vessel completely organic-free. This may be of practical importance where it may be used in commercial reactors when manufacturers wish to switch from one product (*eg.* ZSM-5) to another. This may also be useful in novel zeolite synthesis where the influence of impurities may be extremely important.

While the above highlights some of the practical applications of the *Scavenging Reaction* there are far reaching implications for the study of templates and their role in high-silica zeolite crystallisations. Perhaps the most important finding was the ability of the reaction to distinguish between true ZSM-5 structure directors and void fillers. Thus, the reaction was used to rule out a number of organic materials previously thought to be ZSM-5 structure directors [63]. The results of this work suggests that organic materials that promote the crystallisation of ZSM-5 would be better classified as either structure directors or void fillers.

Probably the most contravertial claim of the present work is that sodium does not appear to nucleate ZSM-5. There is sufficient evidence on which to base this, not least of which was the inability of the *Scavenging Reaction* to crystallise ZSM-5 in the presence of relatively high levels of sodium (added as NaCl) impurity. Only at very high levels of Na_2O (constant base level) was ZSM-5 obtained and this was contaminated with much amorphous material. It can be argued that aside from significantly modifying the gel chemistry, the presence of sodium also increases the sensitivity of the *Scavenging Reaction* to impurities, since the composition essentially moves towards that of the inorganic sodium one. Furthermore, the existence of a composition in the potassium system that is sensitive to organic and seed impurities also suggests that it is these impurities and not sodium cations that nucleate ZSM-5 in the corresponding inorganic sodium system. The important difference between the potassium and sodium systems then, is their sensitivity to these impurities. While it believed that sodium and potassium do not nucleate ZSM-5, there is little doubt that they influence the nucleation kinetics. However, there primary role is in crystal growth.

Further work is required with the *Scavenging Reaction* to test the many organic compounds claimed to direct ZSM-5. Work should also be carried out to establish whether or not inorganic compositions analogous to the *Scavenging Reaction* exist for other zeolites or indeed zeotypes.

The results of crystallisations carried out in the inorganic sodium system (Appendix), while less spectacular, were nonetheless very interesting. Possibly the most significant finding was that aging the reaction mixture increased the time taken to crystallise Na-ZSM-5 (aging was also found to inhibit the crystallisation of K-ZSM-5). Although this may be rationalised on the basis of a change in gel chemistry, it is possible that aging affects the ability of the reaction mixture to *detect* impurities. Thus while the overall stoichiometry or the reaction mixture remains unaltered, the solution and solid phase compositions will be very different from those in the corresponding non-aged reaction mixture. This may affect the *sensitivity* of the composition to organic or seed impurities and thus, it will take much longer for the gel to reorganise and supply the growth units necessary to facilitate crystallisation.

Since alkali metal cations, particularly sodium, do not appear to nucleate ZSM-5, which is generally recognised as an easy phase to crystallise in the absence of an organic template, it is thought unlikely that other high-silica zeolites will be readily obtained from inorganic aluminosilicate reaction mixtures. This does not rule out, however, the possibility of synthesising other high-silica zeolites from systems which contain appropriate impurities and can thus still be considered inorganic reaction mixtures. It is suggested then, that more effort should be directed at attempting to grow high-silica zeolites, rather than nucleating them, from seeded inorganic reaction mixtures.

8.3 Alkali-free syntheses

A number of high-silica zeolites were crystallised from alkali-free reaction mixtures that contained only the quaternary ammonium hydroxide, which served both as the structure director and mineraliser. The most notable of these was the crystallisation of Beta, of which there are no reports in the open literature. It was concluded that although alkali metal cations promote nucleation they are not required to initiate it. Their primary role, therefore, is in crystal growth, as mentioned in the previous section. Thus it came as no surprise that products obtained from alkali-free reactions contained extremely small crystals, very often < 0.5 μm. The growth of Beta, however, did not appear to be significantly affected by the absence of alkali metal cations in the reaction mixture. Based on these results it seems likely that one should be able to crystallise all high-silica zeolites from similar alkali-free reaction mixtures.

The crystallisation of TPA-ZSM-5 took over 30 days in the absence of alkali metal cations (C257). However, when some of the TPAOH was replaced with TMAOH the effect on crystallisation rate was remarkable, reducing it to less than 3 days (A129). Concomitant with this was an increase in the crystal size. Further experimentation showed that there was an optimum amount of TMA at which the effect was most pronounced. With particularly high levels of TMA, NU-1 co-crystallised. One particular composition (A126), however, crystallised ZSM-5 with a most unusual morphology, which resembled *marrowbone* dog treats. It is not known whether this morphology offers any sorptive or catalytic advantages over conventional materials.

The inclusion of TMA in other alkali-free reaction mixtures that contained a second quaternary ammonium compound did not affect the crystallisation kinetics significantly, which was particularly surprising for the TBA-ZSM-11 system, given its structural similarity to TPA-ZSM-5. Clearly then, the use of TMA to accelerate crystallisation of high-silica zeolites appears to be quite restricted, unlike inorganic cations such as sodium.

That no new materials were crystallised from combinations of TMAOH with other quaternaries was hardly surprising since TMA is likely to be a weak structure-directing species. However, its use as a mineraliser provides a flexible route to the synthesis of a number of alkali-free, high-silica zeolites from reaction mixtures that contain, for example, a quaternary halide as the structure director. Furthermore, it is relatively cheap and readily available. Although similar systems have been reported for the crystallisation of ZSM-5 using pyrrolidine or ammonium hydroxide as the mineraliser, the use of TMA is more likely to lead to the formation of a new phase, given that it is a non-specific directing species and has been used to synthesise a number of zeolites and, more importantly, does not favour the formation of ZSM-5 in the absence of TPA. Thus the use of the composition:

$$x\ (TMA)_2O\ y\ (Q)\ z\ Al_2O_3\ 60\ SiO_2\ 3000\ H_2O,$$

where either TMA or Q is in the form of the hydroxide, to examine other quaternary ammonium *templates* under alkali-free conditions would be worthy of a more rigorous investigation.

Crystallisation of reaction mixtures that contained TMAOH and a diol did not give a new phase, which suggests that the diols have limited, if any, structure-directing ability. However, the use of 2,5-dimethyl-2,5-hexanediol (2,5-DMHD) to improve the crystallisation kinetics of Beta and NU-1 was an important discovery. The inclusion of this *synthesis modifier* in the alkali-free Beta reaction mixture dramatically reduced the overall crystallisation time. As with the TMA reactions described above, however, the diol did not improve the crystallisation rate of all the zeolites examined, the crystallisation of TMA-NU-1 was the only other affected. Of the diols examined, only 2,5-DMHD was found to improve the crystallisation rate of Beta and NU-1, although they all modified the crystal size distribution and average crystal size to different extents. Crystal morphology, however, appeared to be unaltered. The results generally suggest that nucleation was affected more than growth. It is thought that a number of factors influence the effectiveness of a given diol. These include *hydrophobicity*, geometry, and solubility, all of which may affect their ability to interact with other species in solution.

In the presence of alkali metal impurities, the crystallisation of Beta and NU-1 was inhibited when the diol was also present in the reaction mixture. This appears to be an unusual result but may be due to a modification in the interaction between the alkali metal cations and aluminosilicate species in solution or solid gel phase.

Further work is required to establish the precise role of diols in these crystallisations. This should include ^{27}Al, ^{29}Si, and ^{13}C MASNMR studies to determine the nature and extent of the interactions between the diol and the various species in solution. It would also be worthwhile carrying out crystallisations of other high-silica zeolites in the presence of diols, particularly 2,5-DMHD, to establish whether or not the diol is only effective for zeolites that cannot crystallise from all-silica systems.

Investigation of the crystallisation of TPA-ZSM-5 in the presence of controlled amounts of alkali and TMA impurities showed that at very high and low concentrations, the crystallisation kinetics were not affected significantly. At intermediate concentrations, however, there was an essentially linear relationship between the level of impurity and the crystallisation time. The variation in the crystallisation time with alkali (or TMA) content may be attributed to an increase in competition for silicate and aluminosilicate species, although a change in the crystallisation mechanism cannot be ruled out. The sudden increase in the solution phase alkali metal content suggests that many alkali metal cations are initially associated with the solid gel phase and are then released into the solution phase when T-O-T bonds are formed on crystallisation. Although it cannot be confirmed, it is thought that the concentration of alkali metal cations in the reaction mixture may influence the crystallisation mechanism. Thus, crystallisation from reaction mixtures that contain substantial amounts of alkali metal cations are thought to proceed via a solution phase mechanism while those that contain little or no alkali metal proceed via a *gel dominated-* or solution mediated, solid phase transformation mechanism. Furthermore, analysis of the solution phase alkali metal content suggests that it may be possible to use such measurements to establish the crystallisation mechanism, although much more work is needed in this area.

While the above highlights the theoretical implications of this work, measure-

ment of the solution phase alkali metal content has an important practical application. As with pH measurements, the change in alkali metal content of the solution phase on crystallisation provides yet another method with which to follow the progress of a reaction. Although the use of flame photometry is not as convenient as pH measurements, Specific Ion Electrodes would allow measurements to be made quickly and accurately. The clear advantage of such measurements over pH measurements may come from information gained that might allow determination of the crystallisation mechanism, although as stated above, this area requires further development.

APPENDIX

Organic-Free Syntheses; Sodium System

Introduction

Several crystallisations were carried out in the inorganic sodium system to allow comparison with results obtained from the corresponding potassium system. In particular, the effect of gel aging on the crystallisation of Na-ZSM-5 was examined in an attempt to further develope the claim that seeding or traces of organic impurities may be responsible for the crystallisation of Na-ZSM-5 and not the sodium cations themselves.

Experimental

Materials

Aristar NaOH, CAB-O-SIL M-5, aluminium wire and ultrapure water.

Gel preparation and synthesis conditions

Gels were prepared in the same way as the organic-free potassium reaction mixtures. The batch composition studied, expressed as ratios of oxides was:

$$10\ Na_2O\ 1\ Al_2O_3\ 60\ SiO_2\ 3000\ H_2O.$$

All gels were prepared by weight to give a total of 400 g and reactions carried out in stirred (300 rpm) 500 cm^3 stainless-steel autoclaves. A series of reactions were carried out at 383, 403 and 423 K with and without aging. Gels were aged in 1 litre polypropylene bottles in a pre-heated oven set at 368 K for 6 days. The small amount of water lost through evaporation during this process was replaced with ultrapure water (368 K) before transferring the gel to the autoclave.

Cleaning of Autoclaves

The autoclaves were cleaned as described in Chapter 2, with the exception that Aristar NaOH was used instead of KOH.

Results and Discussion

Table A-1 shows the results of crystallisations from aged and non-aged reaction mixtures. As expected the only zeolitic phase obtained at the three temperatures investigated was ZSM-5 and the crystallisation rate was significantly decreased as the reaction temperature was decreased. The effect on nucleation was particularly significant.

SEM photomicrographs (not shown) of the products crystallised at 383, 403, and 423 K showed that the crystals were generally oval in shape with rather ill-defined surfaces. As the crystallisation temperature was increased from 383 K to 423 K, the crystal size increased as expected. It is noteworthy that all the SEM's showed the presence of a trace of magadiite which was difficult to detect in the XRPD patterns.

The rate of crystallisation for the aged gels was independent of the aging treatment at all the temperatures investigated, thus at 383, 403 and 423 K the crystallisation took 4, 2 and 1 day respectively (E *act* = 54 kj mol^{-1}). However the onset of crystallisation was significantly perturbed by the aging treatment. At 383 K the onset time was reduced from 14 days to 8 days for aging times at 368 K

Table 8–1: Crystallisation of Na-ZSM-5 from the composition: 10 Na_2O 1 Al_2O_3 60 SiO_2 3000 H_2O with aged and none-aged gels

Run No	Time Aged / d	Cryst$^{n.}$ Time / d		Run Temp / K
		t_{nuc}	$t_{100\%}$	
A1	0	-	1	423
D265	6	2	3	423
D44	6	3	3	423
D6	0	3	5	403
D30	6	4	6	403
D7	6	4	7	403
D21	0	14	18	383
D22	39	8	12	393
D34	6	8	12	393

of 6 days and 39 days. This is consistent with nucleation in the static system at 368 K at a rate similar to that of the stirred system at 383 K. At higher reaction temperatures static aging increased the time to the onset of crystallisation. This was a most unexpected result which is difficult to explain satisfactorily. The 383 K experiments indicate that nuclei do form at 368 K, and hence they must be initially present in the 403 and 423 K experiments. It may be that at higher temperatures some or all of these nuclei are destroyed or other changes in the gel during the aging process slow down further nucleation at the higher temperatures. Alternatively, the gel chemistry may be changed to such an extent that it loses its ability to *detect* seed or organic impurities. Unfortunately neither of these explanations is convincing and further work should be carried out to account for these observations.

Conclusions

Aging the sodium gel at 368 K increased the overall crystallisation time of ZSM-5 at 403 and 423 K. However, the time to the onset of crystallisation is significantly reduced when the gel is crystallised at 383 K. It is clear that gel aging inhibits nucleation. While this can be attribute to a change in gel chemistry, the possibility that the gel loses its ability to detect minute traces of seed or organic impurity, as in the potassium system (Chapter 5) cannot be ruled out.

References

[1] Cronstedt, A.F., *Akad. Handl.*, Stockholm, **17**, 120 (1756)

[2] Murray, J. and Renard, A.F., *Deep Sea Deposits; Scientific Results of the Voyage of H.M.S. Challenger*, 1873-1876, Eyre and Spottiswood, London (1891)

[3] Deville, St. C., *Compt. Rend.*, **54**, 324 (1862)

[4] Breck, D.W., *Zeolite Molecular Sieves*, Wiley, New York (1974)

[5] Morey, G.W. and Ingerson, E., *Econ. Geol.*, **38**, 607 (1937)

[6] Barrer, R.M., *J. Chem. Soc.*, 127 (1948)

[7] Breck, D.W., Eversole, W.G., Milton, R.M., Reed, T.B. and Thomas, T.L., *J. Am. Chem. Soc.*, **78**, 5963 (1956)

[8] Milton, R.M., US Patent 2 882 243 (1959)

[9] Milton, R.M., US Patent 2 882 244 (1959)

[10] Breck, D.W., US Patent 3 130 007 (1964)

[11] Flanigen, E.M., *Proc. 5th Int. Conf. Zeo.*, Rees, L.V.C. (ed.), Heyden, London (1980) p. 760

[12] Wilson, S.T., Lok, B.M., Messina, C.A., Cannan, T.R. and Flanigen, E.M., *J. Am. Chem. Soc.*, **104**, 1146 (1982)

[13] Dyer, A., *An Introduction to Zeolite Molecular Sieves*, Wiley, New York (1989)

[14] McBain, J.W., *The Sorption of Gases and Vapours by Solids*, Rutledge and Sons, London (1932)

[15] Liebau, F., *Zeolites*, **3**, 191 (1983)

[16] Smith, J.V., *Mineralogical Society of America*, Special Paper No.1, 281 (1963)

[17] Smith, J.V., *Zeolites*, **4**, 309 (1984)

[18] Szostak, R., *Molecular Sieves: Principles of Synthesis and Identifiction*, Van Nostrand Reinhold, New York (1989)

[19] Meier, W.M., in *Molecular Sieves*, Soc. Chem. Ind. (ed.), London (1968) p. 10

[20] Meier, W.M. and Olson, D.H., *Atlas of Zeolite Structures*, (2nd edition), Butterworths, London (1987)

[21] Liebau, F., *Structural Chemistry of Silicates: Structure, Bonding and Classification*, Springer-Verlag, Berlin (1985) p. 146

[22] Barrer, R.M., *Hydrothermal Chemistry of Zeolites*, Academic Press, New York (1982)

[23] van Koningsveld, H., *Zeolites*, **12**, 114 (1992)

[24] Barrer, R.M., *J. Soc. Chem. Ind.*, **64**, 130 (1945)

[25] Barrer, R.M., *Brit. Chem. Eng.*, May, 1 (1959)

[26] Jacobs, P.A., Martens, J.A., Weitkamp, J. and Beyer, H.K., *Faraday Disc. Chem. Soc.*, **72**, 353 (1981)

[27] Martens, J.A., Tielen, M., Jacobs, P.A. and Weitkamp, J., *Zeolites*, **4**, 98 (1984)

[28] Jacobs, P.A. and Martens, J.A., in *Synthesis of High-Silica Zeolites*, Delmon, B. and Yates, J.T. (eds.), *Stud. Surf. Sci. Catal.*, , **33** (1987)

[29] Loewenstein, W., *Am. Mineral.*, **39**, 92 (1954)

[30] Barrer, R.M. and Cole, J.F., *J. Chem. Soc., A*, 1516 (1970)

[31] Vaughan, D.E.W., *Chem. Eng. Prog.*, Feb. 25 (1988)

[32] Reference [4] p. 579

[33] Townsend, R., *Chem.Ind.*, 241, (1984)

[34] Townsend, R., *Zeolites*, **4**, 191 (1984)

[35] Flanigen, E.M., *Pure Appl. Chem.*, **52**, 2192 (1980)

[36] Dyer, A., *Chem. Ind.*, 246, (1984)

[37] Dyer, A., *Zeolites*, **4**, 215 (1984)

[38] Barrer, R.M., *J. Soc. Chem. Ind.*, **64**, 130 and 133 (1945)

[39] Barrer, R.M. and Belchety, L., *J. Soc. Chem. Ind.*, **64**, 131 (1945)

[40] Reference [4] p. 640

[41] Breck, D.W., *J. Chem. Educ.*, **41**, 678 (1964)

[42] Wanless, G.J., GB Patent 1 433 416 (1976)

[43] Florack, P.M., Eur. Patent Appl. 6 665 (1980)

[44] Seko, M., Mujake, T. and Indana, K., *Hydrocarbon Processing*, Jan., 133 (1980)

[45] Grose, R.W. and Flanigen, E.M., US Patent 4 061 724 (1977)

[46] Elliot, K.M. and Eastwood, S.C., *Oil Gas J.*, **60**, 142 (1962)

[47] Eastwood, S.C., Plank, C.J. and Weisz, P.B., *8th World Petrol. Congr. Proc.*, **4**, 246 (1971)

[48] Weisz, P.B. and Frilette, V.J., *J. Phys. Chem.*, **64**, 382 (1960)

[49] Csicsery, S.M., *Zeolites*, **4**, 202 (1984)

[50] Weisz, P.B., *Pure Appl. Chem.*, **52**, 2091 (1980)

[51] Chang, C.D. and Silvestri, A.J., *J. Catal.*, **47**, 249 (1977)

[52] Derouane, E.G., Dejaifive, P., Gabelica, Z. and Vedrine, J.C., *Disc. Faraday Soc.*, **72**, 331 (1981)

[53] Haggin, J., *C. & En.*, March 25, 39 (1985)

[54] Derouane, E.G., in *Catalysis by Zeolites*, Imelik, B., Naccache, C., Taarit, Y. Ben., Vedrine, J.C., Coudivier, G. and Praliaud, H., (eds.), Stud. Surf. Sci. Catal., **5**, Elsevier, Amsterdam (1980)

[55] Hoelderich, W.F., in *Zeolites: Facts, Figures, Future*, Jacobs, P.A. and van Santen, R.A. (eds.), Stud. Surf. Sci. Catal., **49 (Part A)**, Elsevier, Amsterdam (1989) p. 69

[56] Rabo, J.A., *Catal. Rev.-Sci. Eng.*, **23 (1&2)**, 293 (1981)

[57] Heinemann, H., *ibid.*, p. 315

[58] Haggin, J., *C. & En.*, Dec. 13, 9 (1982)

[59] Leach, H.F., *Ann. Rep. Progr. Chem. Sect. A*, **68**, 195 (1972)

[60] Naccache, C. and Taarit, Y.B., *Pure Appl. Chem.*, **52**, 2175 (1980)

[61] Weitkamp, J. in *Catalysis and Adsorption by Zeolites*, Ohlmann, G., Pfeifer, H. and Fricke, R. (eds.), Stud. Surf. Sci. Catal., **65**, Elsevier, Amsterdam (1991) p. 21

[62] Flanigen, E.M., *Molecular Sieves*, Meier, W.M. and Uytterhoeven (eds.) A.C.S., **121**, (1973) p. 119

[63] Lok, B.M., Cannan, T.R. and Messina, C.A., *Zeolites*, **3**, 282 (1983)

[64] Barrer, R.M., *Zeolites*, **1**, 130 (1981)

[65] Davis, M.E. and Lobo, R.F., *Chem. Mater.*, **4**, 756 (1992)

[66] Aiello, R. and Barrer, R.M., *J. Chem. Soc., A*, 1470 (1970)

[67] Barrer, R.M. and Denny, P.J., *J. Chem. Soc., A*, 971 (1961)

[68] Barrer, R.M., US Patent 3 308 922 (1967)

[69] Reference [4] p. 308

[70] Kerr, G.T., US Patent 3 314 752 (1967)

[71] Wadlinger, R.L., Kerr, G.T., Rosinski, E.J. and Plank, C.J., US Patent 3 375 205 (1968)

[72] Flanigen, E.M. and Kellberg, E.B., US Patent 4 241 036 (1968)

[73] Wadlinger, R.L., Kerr, G.T. and Rosinski, E.J., US Patent 3 308 069 (1967), reissued: Re-28 341 (1975)

[74] Argauer, R.J. and Landolt, G.R., US Patent 3 702 886 (1972)

[75] Chu, P., US Patent 3 709 979 (1973)

[76] Jablonski, G.A., Sand, L.B. and Gard, J.A., *Zeolites*, **6**, 396 (1986)

[77] Reference [28] p. 113

[78] Kokotailo, G.T. and Meier, W.M., *Prop. and Appl. of Zeolites, Special Publication 33, Chem. Soc.*, London, 133 (1980)

[79] Dwyer, F.G. and Jenkins, E.E., US Patent 3 941 871 (1976)

[80] Flanigen., E.M., Bennett, J.M., Grose, R.W., Cohen, J.P., Patton, R.L., Kirchner, R.M. and Smith, J.V., *Nature*, **271**, 512 (1978)

[81] Bibby, D.M., Milestone, N.B. and Aldridge, L.P., *Nature*, **280**, 664 (1979)

[82] Budiansky, S., *Nature*, **300**, 309 (1982)

[83] Rees, L.V.C., *Nature*, **296**, 491 (1982)

[84] Fyfe, C.A., Gobbi, G.C., Klinowski, J., Thomas, J.M. and Ramdas, S., *Nature*, **296**, 530 (1982)

[85] Uytterhoeven, J.B., *Progr. Colloid and Polymer Sci.*, **65**, 233 (1978)

[86] Marler, B. *Zeolites*, **7**, 393 (1987)

[87] Gies, H. and Gunawardane, R.P., *Zeolites*, **7**, 442 (1987)

[88] Gunawardane, R.P., Gies, H. and Marler, B., *Zeolites*, **8**, 127 (1988)

[89] Franklin, K.R. and Lowe, B.M. in *Zeolites: Facts, Figures, Future*, Jacobs, P.A. and van Santen, R.A. (eds.), Stud. Surf. Sci. Catal., **49 (Part A)**, Elsevier, Amsterdam (1989) p. 179

[90] Liebau, F., *Zeolites*, **6**, 373 (1986)

[91] Gies, H. and Marler, B., *Zeolites*, **12**, 42 (1992)

[92] Perego, G., Bellussi, G., Corno, C., Taramasso, M., Buonomo, F. and Esposito, A. in *New Developments in Zeolite Science and Technology*, Murakami, Y., Iijima, A. and Ward, J.W. (eds.), Stud. Surf. Sci. Catal., **28**, Elsevier, Amsterdam (1986) p. 129

[93] Reference Barrerbook, p. 134

[94] Lowe, B.M. in *Innovation in Zeolite Materials Science*, Grobet, P.J., Mortier, W.J., Vansant, E.F. and Schulz-Elkoff, G. (eds.), Stud. Surf. Sci. Catal., **37**, Elsevier, Amsterdam (1988) p. 1

[95] den Ouden, C.J.J. and Thompson, R.W., *Ind. Eng. Chem. Res.*, **31** 369 (1992)

[96] Casci, J.L. and Lowe, B.M., *Zeolites*, **3**, 186 (1983)

[97] Culfaz, A. and Sand, L.B., in *Molecular Sieves*, 140 (1973)

[98] Zhdanov, S.P. and Samulevich. N.N., in *Proc. 5th Int. Conf. Zeo.*, Rees, L.V.C. (ed.), Heyden, London (1980) p. 75

[99] Freund, E.F., *J. Crystal Growth*, **34**, 11 (1976)

[100] Cournoyer, R.A., Kranich, W.L. and Sand, L.B., *J. Phys. Chem.*, **79**, 1578 (1975)

[101] Reference [22], p. 54

[102] Narita, E., Sato, K., Yatabe, N. and Okabe, T., *Ind. Eng. Chem. Prod. Res. Dev.*, **24**, 507 (1985)

[103] Iler, R., in *The Chemistry of Silica*, Wiley, (1979)

[104] Fajula, F., Vera-Pacheco, M. and Figueras, F., *Zeolites*, **7**, 203 (1987)

[105] Hou, L.Y. and Sand, L.B., in *Proc. 6th Int. Conf. Zeo.*, Olson, D, and Bisio, A. (eds.), Butterworths, London (1984) p. 887

[106] Franklin, K.R. and Lowe, B.M., *Zeolites*, **8**, 501 (1988)

[107] Erdem, A. and Sand, L.B., *J. Catal.*, **60**, 241 (1979)

[108] Chao, K-J., Tasi, T.C., Chen, M-S. and Wang, I., *J. Chem. Soc. Faraday Trans. 1*, **77**, 547 (1981)

[109] Rollmann, L.D., in *Proc. 6th Int. Conf. Zeo.*, Olson, D, and Bisio, A. (eds.), Butterworths, London (1984) p. 109

[110] Araya, A. and Lowe, B.M., *J. Chem. Res., S*, 192 (1985)

[111] Padovan, M., Leofanti, G., Solario, M. and Moretti, E. *Zeolites*, **4**, 295 (1984)

[112] Hogan, P.J., Whittam, T.V., Birtill, J.J. and Stewart, A., *Zeolites*, **4**, 275 (1984)

[113] Hayhurst, D.T., Nastro, A., Aiello, R., Crea, F. and Giordano, G., *Zeolites*, **8**, 416 (1988)

[114] Romannikov, V.N., Mastikhin, V.M., Hocevar, S. and Drzaj, B. *Zeolites*, **3**, 311 (1983)

[115] Fegan, S.G. and Lowe, B.M., *J. Chem. Soc. Faraday Trans. 1*, **82**, 801 (1986)

[116] Lowe, B.M., *Zeolites*, **3**, 300 (1983)

[117] Reference [22] p. 47

[118] Suzuki, K., Kiyozumi, Y., Shin, S., Fujisawa, K., Watanabe, H., Saito, K. and Noguchi, K., *Zeolites*, **6**, 290 (1986)

[119] Lowe, B.M., Mc Gilp, N.A. and Whittam, T.V. in *Proc. 5th Int. Conf. Zeo.*, Rees, L.V.C. (ed.), Heyden, London (1980) p. 85

[120] Mostowicz, R. and Sand, L.B., *Zeolites*, **2**, 143 (1982)

[121] Greenberg, S.A., *J. Phys. Chem.*, **61**, 960 (1957)

[122] Reference [22] p. 239

[123] Dwyer, F.G. and Chu, P., *J. Catal.*, **59**, 263 (1979)

[124] Patel, A.K. and Sand, L.B., *Molecular Sieves-II*, A.C.S. Symp. Ser., Katzer, J.R. (ed.), **40** (1977) p. 207

[125] Whittam, T.V., Brit. Patent 1 450 411 (1976)

[126] Shiralker, V.P., Joshi, P.N., Eapen, M.J. and Rao, B.S., *Zeolites*, **11**, 511 (1991)

[127] Kerr, G.T., *J. Phys. Chem*, **72**, 1385 (1968)

[128] Berak, J.M. and Mostowicz, R., in *Zeolites: Synthesis, Structure, Technology and Application*, Drzaj, B., Hocevar, S. and Pejovnik, S. (eds.), Stud. Surf. Sci. Catal., **24** (1985), p. 47

[129] Breck, D.W. and Flanigen, E.M. in *Molecular Sieves*, Soc. Chem. Ind. (ed.), London (1968) p.47

[130] McNicol, B.D., Pott, G.T., Loos, R.K. and Mulder, N. *Molecular Sieves*, Meier, W.M. and Uytterhoeven (eds.) A.C.S., **121**, (1973) p. 152

[131] Derouane, E.G., Detremmerie, S., Gabelica, Z. and Blom, N., *Appl. Catal.*, **1**, 201 (1981)

[132] Reference [4] p. 340

[133] von Ballmoos, R., in *The* ^{18}*O-Exchange Method in Zeolite Chemistry*, Salle and Sauerlander, Frankfurt am Main (1981)

[134] von Ballmoos, R. and Meier, W.M., *Nature*, **289**, 782 (1981)

[135] Kerr, G.T., *J. Phys. Chem*, **70**, 1047 (1966)

[136] Aiello, R., Barrer, R.M. and Kerr, G.T., *Adv. Chem. Ser.*, **101**, 44 (1970)

[137] Guth, J.L., Caullet, P. and Wey, R. in *Proc. 5th Int. Conf. Zeo.*, Rees, L.V.C. (ed.), Heyden, London (1980) p. 30

[138] Ueda, S., Kageyama, N., Koizumi, M., Kobayashi, S., Fujiurara, Y. and Kyogoku, Y., *J. Phys. Chem*, **88**, 2128 (1984)

[139] Weldes, H.H. and Lange, K.R., *Ind. Eng. Chem.*, **61**, 29 (1969)

[140] Keijsper, J.J. and Post, M.F.M., in *Zeolite Synthesis*, Occelli, M.L. and Robson, H.E. (eds.), ACS Symp. Ser. **398**, Am. Chem. Soc., Washington D.C., 1989, p. 28

[141] Harvey, G. and Dent-Glasser, L., in *Zeolite Synthesis*, Occelli, M.L. and Robson, H.E. (eds.), ACS Symp. Ser. **398**, Am. Chem. Soc., Washington D.C., 1989, p. 49

[142] McCormick, A.V. and Bell, A.T., *Catal. Rev.-Sci. Eng.*, **31 (1&2)**, 97 (1989)

[143] Casci, J.L., *PhD Thesis*, University of Edinburgh (1982)

[144] Reference [22] p. 107

[145] Aiello, R., Crea, F., Nastro, A., Subotic, B. and Testa, F., *Zeolites*, **11**, 767 (1991)

[146] Groenen, E.J.J., Kortbeek, A.G.T.G., Mackay, M. and Sudmeijer, O., *Zeolites*, **6**, 403 (1986)

[147] van Santen, R.A., Keijsper, J., Ooms, G. and Kortbeek, A.G.T.G., in *New Developments in Zeolite Science and Technology*, Murakami, Y., Iijima, A. and Ward, J.W. (eds.), Stud. Surf. Sci. Catal., **28**, Elsevier, Amsterdam (1986) p. 169

[148] Van den Berg, J.P., de Jong-Versloot, P.C., Keijsper, J. and Post, M.F.M., in *Innovation in Zeolite Materials Science*, Grobet, P.J., Mortier, W.J., Vansant, E.F. and Schulz-Elkoff, G. (eds.), Stud. Surf. Sci. Catal., **37**, Elsevier, Amsterdam (1988) p. 85

[149] Englehardt, G. and Michel, D., in *High Resolution Solid State NMR of Silicates and Zeolites*, Wiley, New York (1987) p. 348

[150] Kokotailo, G.T., Lawton, S.L., Olson, D.H. and Meier, W.M., *Nature*, **272**, 437 (1978)

[151] Bibby, D.M., Milestone, N.B. and Aldridge, L.P., *Nature*, **285**, 30 (1980)

[152] Dwyer, F.G. and Chu, P., Eur. Patent Appl. 11 362 (1980)

[153] Nakamoto, H. and Takahashi, H., *Chem. Soc. Jap., Chem. Lett.*, 1739 (1981)

[154] Ghamami, M. and Sand, L.B., *Zeolites*, **3**, 155 (1983)

[155] Araya, A. and Lowe, B.M., *J. Catal.*, **85**, 135 (1984)

[156] Dodwell, G.W., Denkewicz, R.P. and Sand, L.B., *Zeolites*, **5**, 153 (1985)

[157] Hongyuan, L., Juan, L., Muliang, Y. and Baoxiang, L., in *Zeolites: Synthesis, Structure, Technology and Application*, Drzaj, B., Hocevar, S. and Pejovnik, S. (eds.), Stud. Surf. Sci. Catal., **24**, Elsevier, Amsterdam (1985) p. 89

[158] Franklin, K.R. and Lowe, B.M., *Zeolites*, **8**, 495 (1988)

[159] Muller, U., Brenner, A., Reich, A. and Unger, K.K., in *Zeolite Synthesis*, Occelli, M.L. and Robson, H.E. (eds.), ACS Symp. Ser. **398**, Am. Chem. Soc., Washington D.C., 1989, p. 346

[160] Mobil Oil, US Patent 1 581 513 (1980)

[161] Reference [133] p. 73

[162] Reference [28] p. 137

[163] Reference [28] p. 134

[164] Nastro, A. and Sand, L.B., *Zeolites*, **3**, 57 (1983)

[165] Araya, A. and Lowe, B.M., *Zeolites*, **4**, 280 (1984)

[166] Gabelica, Z., Blom, N. and Derouane, E.G., *Appl. Catal.*, **5**, 227 (1983)

[167] Reference [18] p. 73

[168] Rollmann, L.D., in Adv. Chem. Ser., **173**, 387 (1979)

[169] Daniels, R.H., Kerr, G.T. and Rollmann, L.D., *J. Am. Chem. Soc.*, **100**, 3097 (1978)

[170] Occelli, M.L., Innes, R.A., Pollack, S.S. and Sanders, J.V., *Zeolites*, **7**, 265 (1987)

[171] Mate, T.C., *J. Phys. Chem.*, **43**, 2799 (1965)

[172] Price, G.D., Pluth, J.J., Smith, J.V., Bennett, J.M. and Patton, R.L., *J. Am. Chem. Soc.*, **104**, 5971 (1982)

[173] Casci, J.L., Lowe, B.M. and Whittam, T.V., Eur. Patent Appl. (1981)

[174] Zones, S.I., Olmstead, M.M. and Santilli, D.S., *J. Am. Chem. Soc.*, **114**, 4195 (1992)

[175] Reference [22] p. 166

[176] Sieber, W. and Meier, W.M., *Helv. Chim. Acta.*, **57**, 1533 (1974)

[177] Van der Gaag, F.J., Jansen, J.C. and van Bekkum, H., *Appl. Catal.*, **17**, 261 (1985)

[178] Araya, A. and Lowe, B.M., *Zeolites*, **6**, 111 (1986)

[179] Casci, J.L., in *New Developments in Zeolite Science and Technology*, Murakami, Y., Iijima, A. and Ward, J.W. (eds.), Stud. Surf. Sci. Catal., **28**, Elsevier, Amsterdam (1986) p. 215

[180] Valyocsik, E.W. and Rollmann, L.D., *Zeolites*, **5**, 123 (1985)

[181] Gilson, J.P. in *Zeolite Microporous Solids: Synthesis, Structure and Reactivity*, **352**, 19 (1992)

[182] Reference [18] p. 94

[183] Derouane, E.G., *Zeolites*, **2**, 299 (1982)

[184] Li, H., Liang, J., Ying, M. and Liu, B., in *Zeolites: Synthesis, Structure, Technology and Application*, Drzaj, B., Hocevar, S. and Pejovnik, S. (eds.), Stud. Surf. Sci. Catal., **24**, Elsevier, Amsterdam (1985) p. 89

[185] Franklin, K.R. and Lowe, B.M., *Zeolites*, **7**, 433 (1987)

[186] Aiello, R., Nastro, A. and Pellegrino, C., in *New Developments in Zeolite Science and Technology*, Murakami, Y., Iijima, A. and Ward, J.W. (eds.), Stud. Surf. Sci. Catal., **28**, Elsevier, Amsterdam (1986) p. 255

[187] Tianyou, S., Ruren, X., Liyun, L. and Zhaohui, Y., in *New Developments in Zeolite Science and Technology*, Murakami, Y., Iijima, A. and Ward, J.W. (eds.), Stud. Surf. Sci. Catal., **28**, Elsevier, Amsterdam (1986) p. 201

[188] Flanigen, E.M., Patton, R.L. and Wilson, S.T., in *Innovation in Zeolite Materials Science*, Grobet, P.J., Mortier, W.J., Vansant, E.F. and Schulz-Elkoff, G. (eds.), Stud. Surf. Sci. Catal., **37**, Elsevier, Amsterdam (1988) p. 13

[189] Jansen, J.C., in *Introduction to Zeolite Science and Practice*, Delmon, B. and Yates, J.T. (eds.), Stud. Surf. Sci. Catal., **58** (1991) p. 77

[190] Franklin, K.C., *PhD Thesis*, University of Edinburgh (1993)

[191] von Ballmoos, R. and Higgins, J.B., *Zeolites*, **10** 1990

[192] Wu, E.L., Lawton, S.L., Olson, D.H., Rohrman, Jr., A.C. and Kokatailo, G.T., *J. Phys. Chem.*, **83**, 2777 (1979)

[193] Bibby, D.M., Aldridge, L.P. and Milestone, N.B. *J. Catal.*, **72**, 373 (1981)

[194] Pollack, S.S., Adkins, J.W., Wetzel, E.L., and Newbury, D., *Zeolites*, **4**, 181 (1984)

[195] Jacobs, P.A., Derouane, E.G. and Weitkamp, J., *J. Chem. Soc., Chem. Commun.*, 591 (1981)

[196] Pendlebury, R., *Private Communication* (1992)

[197] Hampson, B., *PhD Thesis*, University of Edinburgh (1991)

[198] Franklin, K.R., King, A. and Lowe, B.M., *Thermochimica Acta*, **136**, 307 (1988)

[199] Karge, H.G., Ladebeck, J., Sarbak, Z. and Hatada, K., *Zeolites*, **2**, 94 (1982)

[200] Kaeding, W.W., *J. Catal.*, **95**, 512 (1985)

[201] Sing, K.S.W. in *Colloids and Surfaces*, Elsevier, Amsterdam (1989)

[202] Reference [18] p. 104

[203] Grose, R.W. and Flanigen, E.M., US Patent 4 257 885 (1981)

[204] Dai, F-Y., Suzuki, M., Takahashi, H. and Saito, Y., in *New Developments in Zeolite Science and Technology*, Murakami, Y., Iijima, A. and Ward, J.W. (eds.), Stud. Surf. Sci. Catal., **28**, Elsevier, Amsterdam (1986) p. 223

[205] Dai, F-Y., Deguchi, K., Suzuki, M., Takahashi, H. and Saito, Y., *Chem. Lett.*, 869 (1988)

[206] Dai, F-Y., Suzuki, M., Takahashi, H. and Saito, Y., in *Zeolite Synthesis*, Occelli, M.L. and Robson, H.E. (eds.), ACS Symp. Ser. **398**, Am. Chem. Soc., Washington D.C., 1989, p. 244

[207] Schwieger, W., Bergk, K-H., Freude, D., Hunger, M. and Pfeifer, H. in *Zeolite Synthesis*, Occelli, M.L. and Robson, H.E. (eds.), ACS Symp. Ser. **398**, Am. Chem. Soc., Washington D.C., 1989, p. 274

[208] Shiralkar, V.P. and Clearfield, A., *Zeolites*, **9**, 363 (1989)

[209] Nastro, A., Colella, C. and Aiello, R. in *Zeolites: Synthesis, Structure, Technology and Application*, Drzaj, B., Hocevar, S. and Pejovnik, S. (eds.), Stud. Surf. Sci. Catal., **24**, Elsevier, Amsterdam (1985) p. 39

[210] Aiello, R., Crea, F., Nastro, A. and Pellegrino, C., *Zeolites*, **7**, 549 (1987)

[211] Nastro, A. and Aiello, R. in *Successful Design of Catalysts*, Inui, T. (ed.), Stud. Surf. Sci. Catal., **44** (1988) p. 227

[212] Bellussi, G., Perego, G., Carati, A., Cornaro, U. and Fattore, V. in *Innovation in Zeolite Materials Science*, Grobet, P.J., Mortier, W.J., Vansant, E.F. and Schulz-Elkoff, G. (eds.), Stud. Surf. Sci. Catal., **37**, Elsevier, Amsterdam (1988) p. 37

[213] ASTM X-ray powder diffraction file card no. 16-692

[214] ASTM X-ray powder diffraction file card no. 19-968

[215] ASTM X-ray powder diffraction file card no. 20-1157

[216] Araya, A. and Lowe, B.M., Eur. Patent Appl. 77 624 (1983)

[217] Gordon, J.W., *PhD Thesis*, University of Edinburgh (1985)

[218] Hogan, P.J., Stewart, A. and Whittam, T.V., Eur. Patent Appl. 65 400 (1982)

[219] Reference [22] p. 123

[220] Ueda, S. and Koizumi, M., *Amer. Mineral.*, **64**, 23 (1979)

[221] Edelman, R.D., Kudalkar, D.V., Ong, T., Warzywoda, J. and Thompson, R.W., *Zeolites*, **9**, 496 (1989)

[222] Arika, J., Miyazaki, H., Igawa, K. and Itabashi, K., Eur. Patent Appl. 106 552 (1984)

[223] Franklin, K.R. and Lowe, B.M. *Zeolites*, **7**, 135 (1987)

[224] Franklin, R. *PhD Thesis*, University of Edinburgh (1989)

[225] Golemme, G., Nastro, A., Nagy, J.B., Subotic, B., Crea, F. and Aiello, R., *Zeolites*, **11**, 776 (1991)

[226] le Febre, R.A., Kouwenhoven, H.W. and van Bekkum, H., *Zeolites*, **8**, 60 (1988)

[227] Baerlocher, C. and Meier, W.M., *Helv. Chim. Acta*, **52**, 1853 (1969)

[228] Baerlocher, C. and Meier, W.M., *Helv. Chim. Acta*, **53**, 1285 (1970)

[229] Camblor, M.A. and Perez-Pariente, J., *Zeolites*, **11**, 202 (1991)

[230] Camblor, M.A., Mifsud, A. and Perez-Pariente, J., *Zeolites*, **11**, 792 (1991)

[231] Perez-Pariente, J., Martens, J.A. and Jacobs, P.A., *Appl. Catal.*, **31**, 35 (1987)

[232] Perez-Pariente, J., Martens, J.A. and Jacobs, P.A., *Zeolites*, **8**, 46 (1988)

[233] Caullet, P., Hazm, J., Guth, J.L., Joly, J.F., Lynch, J. and Raatz, F., *Zeolites*, **12**, 240 (1992)

[234] Casci. J.L., *Private Communication* (1992)

[235] Barlow, M.T., Eur. Patent Appl. 162 719 (1985)

[236] Rubin, M.K., Eur. Patent Appl. 166 513 (1986)

[237] Rubin, M.K. and Rosinski, E.J., US Patent 3 699 139 (1972)

[238] Nagy, J.B., Gabelica, Z. and Derouane, E.G., *Zeolites*, **3**, 43 (1983)

[239] Whittam, T.V. and Youll, B., US Patent 4 060 590 (1977)

[240] Newsam, J.M., Treacy, M.M.J., Koetsier, W.T. and de Gruyter, C.B., *Proc. R. Soc. Lond. A*, **420**, 375 (1988)

[241] Millward, G.R., Ramdas, S., Thomas, J.M. and Barlow, M.T., *J. Chem. Soc., Faraday Trans. 2*, **79**, 1075 (1983)

[242] Casci, J.L., Lowe, B.M. and Whittam, T.V., Eur. Patent Appl. 63 436 (1982)

[243] Plank, C.J., Rosinski, E.J. and Rubin, M.K., US Patent 4 076 842 (1978)

[244] Dwyer, F.G., Cormier, W.E. and Chu, P., UK Patent Appl. 2 002 733 (1979)

[245] Olson, D.H., Rollmann, L.D. and Valyocsik, E.W., Eur. Patent Appl. 26 962 (1981)

[246] Olson, D.H. and Valyocsik, E.W., Eur. Patent Appl. 26 963 (1981)

[247] Olson, D.H. and Valyocsik, E.W., Eur. Patent Appl. 197 775 (1986)

[248] Rossin, J.A. and Davis, M.E., *Ind. J. Tech.*, **25**, 621 (1987)

[249] Smith, J.V., Pluth, J.J., Boggs, R.C. and Howard, D.G., *J. Chem. Soc., Chem. Commun.*, 363 (1991)

[250] Charnell, J.F., *J. Crystal Growth*, **3**, 291 (1971)

[251] Sand, L.B., Sacco Jr., A., Thompson, R.W. and Dixon, A. G., *Zeolites*, **7**, 387 (1987)

[252] Scott, G., Thompson, R.W., Dixon, A.G. and Sacco Jr., A., *Zeolites*, **10**, 44 (1990)

[253] Klocke, D.J., Vartuli, J.C. and Kirker, G.W., Eur. Patent Appl. 220, 893 (1987)

[254] Morris, M., Sacco Jr., A., Dixon, A.G. and Thompson, R.W., *Zeolites*, **11**, 178 (1991)

[255] Morris, M., Dixon, A.G., Sacco Jr., A. and Thompson, R.W., *Zeolites*, **13**, 113 (1993)

[256] Franklin, K.R. and Lowe, B.M., *Thermochimica Acta*, **127**, 319 (1988)

[257] Casci, J.L. and Lowe, B.M., *Private Communication* (1990)